Development of Biotin Protein Ligase Inhibitors from *Staphylococcus aureus* as New Antibiotics

Jiage Feng

A thesis submitted in total fulfilment of the requirements for

the degree of Doctor of Philosophy

THE UNIVERSITY *of* ADELAIDE

2016

Department of Chemistry

The University of Adelaide

Table of Contents

_____

Chapter Three

Chapter Four

_____

_____

Chapter Seven

_____

Abstract

Biotin protein ligase (BPL) catalyses the ordered reaction of biotin and ATP to give biotinyl-5'-AMP **1.03**, which then activates a number of biotin dependent enzymes that are critical to cell survival. Research undertaken in this thesis highlights strategies to selectively inhibit *Staphylococcus aureus* biotin protein ligase (*Sa*BPL) over the mammalian equivalent using 1,2,3-triazole and acylsulfonamide isosteres to replace the phosphoroanhydride linker found in biotinyl-5'-AMP **1.03**.

Chapter one describes the structure and catalytic mechanism of the target enzyme *Sa*BPL, along with an overview of chemical analogues of biotin and biotinyl-5'-AMP **1.03** as BPL inhibitors reported to date. Preliminary studies on the utility of a 1,2,3-triazole as a bioisostere of the phosphoroanhydride linker of biotinyl-5'-AMP **1.03** are also discussed.

Chapter two further examines 1,2,3-triazole analogues of lead *Sa*BPL bisubstrate inhibitors **1.22** and **1.23**. Specific chemical modifications were carried out at the ribose of biotinyl-5'-AMP **1.03**, and a new class of purine analogues was developed to mimic the adenine group as in **1.03**. *In silico* docking experiments using our x-ray structure of *Sa*BPL aided in the design of these analogues by predicting optimal binding conformations. A structure activity relationship for the ribose and adenine mimics was developed and this revealed limited improvement in potency against *Sa*BPL on modification at these two sites.

Chapter three reports the first examples of truncated 1,2,3-triazole based BPL inhibitors with a 1-benzyl substituent designed to interact with the ribose binding pocket of *Sa*BPL. *In silico* docking studies using a crystal structure of *Sa*BPL aided in the selection of benzyl groups that present in the ribose-binding pocket of *Sa*BPL. The halogenated benzyl derivatives **3.20**, **3.21**, **3.23** and **3.24** provided the most potent inhibitors of *Sa*BPL with the respective K_i value of 0.28, 0.6, 0.39 and 1.1 µM. These compounds also inhibited the growth of *S. aureus* ATCC49775 (MIC = 4 – 16 µg/ml), while possessing low cytotoxicity against HepG2 cells.

Chapter four builds upon the active 1,2,3-triazole based inhibitors of *Sa*BPL described in chapter two and three with an investigation at C5 of the triazole ring to generate 1,4,5-

_____

trisubstituted 1,2,3-triazoles. A class of 5-iodo 1,2,3-triazoles was synthesised from 1-iodoacetylene **4.02** and azides using CuAAC. Subsequent halogen exchange reaction allowed conversion of iodide to other halogens. 5-Fluoro-1,2,3-triazole **4.07**, the lead compound from this series of inhibitors, proved to be a potent and selective inhibitor of SaBPL (K_i = 0.42 $\pm$ 0.06 µM) and it significantly reduced $S.$ $aureus$ growth with no cell growth apparent at 16 µg/mL.

Chapter five investigates the use of acylsulfonamide as a bioisostere of the phosphoroanhydride linker as in biotinyl-5'-AMP **1.03**. Acylsulfonamide **5.05** was found as the most active and selective inhibitor of SaBPL (K_i = 0.72 x 10^{-3} µM) and MtbBPL (K_i = 0.74 10^{-3} µM) reported to date. Antibacterial studies revealed that **5.05** was active against susceptible $S.$ $aureus$ (MIC = 0.5-1.0 µg/mL), methicillin-resistant $S.$ $aureus$ ((MIC = 0.5-1.0 µg/mL) and $Mycobacterial$ $tuberculosis$ ((MIC = 51 µg/mL). Finally, the x-ray structure **5.05** bound to SaBPL was solved to reveal important molecular interactions critical to the potency of **5.05** and emphasized the acylsulfonamide moiety as an effective bioisostere of phosphoroanhydride linker.

Chapter six discusses the use of in $situ$ click chemistry as an alternative approach for the synthesis of 1,2,3-triazoles. The target enzyme SaBPL was directly involved in the selection of its optimum triazole based inhibitor by catalysing the reaction of biotin acetylene and organic azides without copper as a catalyst. The use of high throughput LC/MS provided improved efficiency and sensitivity of detection of triazole-based inhibitors and allowed the in $situ$ approach to be widely applied to BPLs from other bacteria.

Chapter seven details the experimental procedures for compounds described in chapter 2 – 6, and the chromatographic analysis of in $situ$ click experiments described in chapter 6.

Declaration

This work contains no material which has been accepted for the award of any other degree or diploma in any university or other tertiary institution and to the best of my knowledge and belief, contains no material published or written by another person, except where due reference has been made in the text.

I give my consent for this copy of my thesis, when deposited in the University Library, being made available for loan and photocopying, subject to the provisions of the Copyright Act *1968* (Cth).

The author acknowledges that copyright of published works contained within this thesis resides with the copyright holder(s) of those works.

I also give permission for the digital version of my thesis to be made available on the internet, via the University's digital research repository, the Library catalogue, the Australasian Digital Theses Program (ADTP) and also through internet search engines, unless permission has been granted by the University to restrict access for a period of time.

Jiage Feng

4 August 2017

Date

Acknowledgement

First and foremost, I would like to express my deep and sincere gratitude to Professor Andrew Abell for his supervision and guidance during the whole project. I am deeply grateful for his extensive knowledge, enormous support, enthusiastic view on research and tireless efforts in drafting and revising this thesis.

I would also like to express my gratitude to our collaborators in the BPL project, without them this thesis would not be possible. I would like to thank Ashleigh Susan Paparella, David Heim, Andrew Haye and Dr. Steven Polyak for performing the BPL and antimicrobial assays; Dani Cini and Professor Mathew Wilce for solving the invaluable x-ray crystallographic structures of inhibitors bound to SaBPL; Dr. Mark Blaskovic and Professor Matt Copper for providing priceless chemicals for *in situ* click experiments. Particular mention goes to Professor Grant Booker (co-supervisor) and Dr. Steven Polyak for their support, enthusiasm and tireless efforts throughout my candidature.

I would like to thank all the past and present members of the Abell group for creating a friendly and stimulating working atmosphere. I am grateful to the Post-docs (William Tieu, Sabrina Heng, Beatiz Blanco Rodriguez and more) for the technical advice in the laboratory and having shared many experiences and thoughts with me throughout my candidature. Special thanks to my co-supervisor Dr. William Tieu who kept an eye on the daily progress of my work. He has not only assisted me in the research, but also been a good friend to my personal life.

Last but not least, thank you to my supportive family, my presents Xiaofang and Qiaodi, for the moral support and encouragement even if you are far away in China. I must thank my wife Caiying for understanding the life of a PhD student and always been there supporting me, especially in difficult times.

Abbreviations

AaBPL	*A. aeolicus* biotin protein ligase
ABL	ATP binding loop
AcBPL	*A. calcoaceticus* biotin protein ligase
ACC	Acetyl CoA carboxylase
ACN	Acetonitrile
AcOH	Acetic acid
AMP	Adenosine-5'-monophosphate
ATP	Adenosine-5'-triphosphate
BBL	Biotin binding loop
BCCP	Biotin carboxyl carrier protein
BOC	*tert*-Butoxycarbonyl
BPL	Biotin protein ligase
BSA	Bovine serum albumin
CaBPL	*C. albicans* biotin protein ligase
CDI	1,1' – carbonyldiimidazole
COSY	Correlation spectroscopy
^{13}C NMR	Carbon nuclear magnetic resonance
CA-MRSA	Community acquired methicillin resistant *S. aureus*
Cp*	Pentamethylcyclopentadienyl
CSI	Chlorosulfonyl isocyanate
CuAAC	Copper mediated Alkyne Azide Cycloaddition
DCC	N,N' - Dicyclohexylcarbodiimide
DCM	Dichloromethane
DMAP	Dimethylaminopyridine
DMF	Dimethylformamide
DMSO	Dimethyl sulphoxide
DMP	2,2-Dimethoxypropane
DSC	Disuccinimidyl carbonate
EcBPL	*E. coli* biotin protein ligase
EDA	Ethylenediamine

EtOAc	Ethyl acetate
EtOH	Ethanol
FTIR	Fourier transform infrared spectroscopy
^{19}F NMR	Fluorine nuclear magnetic resonance
^{1}H NMR	Proton nuclear magnetic resonance
HA-MRSA	Hospital acquired methicillin resistant *S. aureus*
HPLC	High-performance liquid chromatography
HRMS	High resolution mass spectrometry
HsBPL	*Homo sapiens* biotin protein ligase
HSQC	Heteronuclear single quantum coherence spectroscopy
IC_{50}	Half maximum inhibitory concentration
iPrOH	isopropanol
K_i	Dissociation constant
*Kp*BPL	*K. pneumoniae* biotin protein ligase
KPhth	potassium phthalimide
Me	Methyl group
MEK	Methyl ethyl ketone (2-butanone)
MeOH	Methanol
MIC	Minimum inhibitory concentration
MRSA	Methicillin resistant *S. aureus*
MSSA	Methicillin sensitive *S. aureus*
MtbBPL	*M. tuberculosis* biotin protein ligase
NaOMe	sodium methoxide
NMO	*N*-methylmorpholin *N*-oxide
NMI	*N*-Iodomorpholine hydriodide
Pd(OAc)$_2$	Palladium(II) acetate
PhBPL	*P. horikoshii* biotin protein ligase
PPh$_3$	triphenylphosphine
p-TsOH	*para*-Toluenesulphonic acid
Py	Pyridine
ROESY	Rotating frame overhauser enhanced spectroscopy
RuAAC	Ruthenium mediated Alkyne Azide cycloaddition
SaBPL	*S. aureus* biotin protein ligase

_____

SAR	Structure activity relationship
t-BuOH	*tert*-butanol
TEA	Triethylamine
TFA	Trifluoroacetic acid
THF	Tetrahydrofuran
TLC	Thin layer chromatography
Ts	4-toluenesulphonyl group
TsCl	tosyl chloride

1.1 The need for new antibiotics

Infectious diseases caused by pathogenic bacteria, such as *Staphylococcus aureus* (*S. aureus)*, are a major threat to human health. The spread of antibiotic resistant *S. aureus*, such as methicillin resistant *S. aureus* (MRSA), is particularly problematic as it has developed resistance to most penicillin-based antibiotics.[1,2] Antibiotic resistance arises in two major subsets of MRSA, hospital acquired MRSA (HA-MRSA) and community acquired MRSA (CA-MRSA). Both have been described over the past decade in the USA[3], UK[4] and Australia amongst other countries.[5] The impact of HA-MRSA and CA-MRSA has become an overwhelming and ongoing problem of increasing difficulty and treatment cost. In the USA alone, the cost to treat HA-MRSA stands at $USD 9.7 billion annually[6], and CA-MRSA accounts for 18% of all MRSA incidents.[3] Overall, these factors have contributed to an increase in the mortality rate due to MRSA infections worldwide.[7] One critical strategy to combat drug resistance in *S. aureus* is to develop new classes of antibiotics with novel mechanisms of action that have no pre-existing target-based resistance.[8] This thesis presents *S. aureus* biotin protein ligase (*Sa*BPL) as one such target and the design of small molecule inhibitors of biotin protein ligase (BPL) for antibacterial discovery.

1.2 Biotin Protein Ligase as a novel antibacterial target

BPL, a vital enzyme present in all organisms, is responsible for the post-translational attachment of biotin **1.01** onto a specific lysine residue present within biotin-dependent enzymes, as shown in Scheme 1.[9,10] *S. aureus* expresses two such enzymes, namely acetyl CoA carboxylase (ACC)[11] and pyruvate carboxylase (PC)[12], that are known to catalyze key reactions in important metabolic pathways. ACC is a critical enzyme for the carboxylation of acetyl-CoA to malonyl-CoA in fatty acid biosynthesis which is essential for cell membrane biogenesis and maintenance.[13] Biotin-activated PC is involved in the conversion of pyruvate to oxaloacetate in the citric acid cycle which is central to a number of key metabolic pathways, such as gluconeogenesis and amino acid biosynthesis.[14] The significance of these pathways to *S. aureus* survival and virulence make BPL a potential new antibacterial drug target. Moreover, genetic knockout studies on various bacteria,

_____

including *S. aureus*[15,16], resulted in no cell growth in the absence of the BPL gene, highlighting that no alternative pathway for protein biotinylation exists in bacteria.

In addition to its pivotal role in the activation of ACC and PC, BPL also acts as a transcriptional repressor.[17-19] In the absence of non-biotinylated biotin-dependent enzymes, *Sa*BPL can form a dimer that is responsive to DNA binding. The *Sa*BPL dimer is a transcriptional repressor that controls the uptake and biosynthesis of biotin by binding a specific DNA sequences in the promoters of the genes encoding these proteins. Therefore, BPL not only utilises biotin, but it also regulates its import and synthesis in responsive to cellular demand. This bifunctional property makes BPL an attractive drug target as it is less likely for bacteria to develop resistance due to multiple pathways.[19]

Step 1
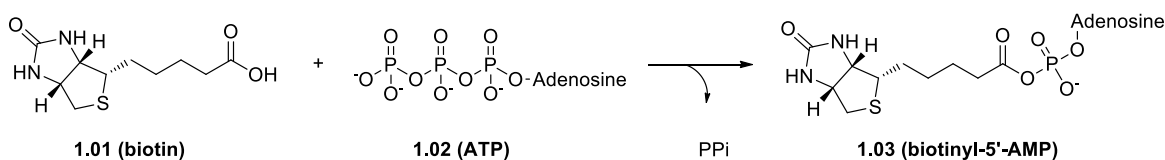
Step 2
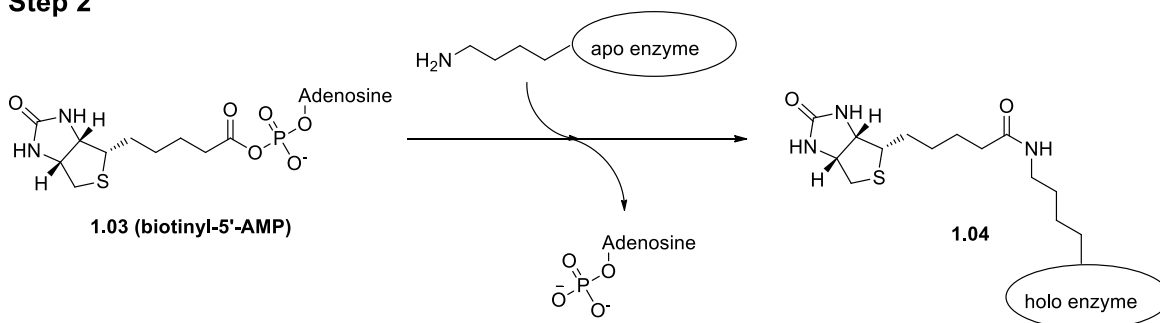
Scheme 1: The catalytic mechanism of biotinylation.

1.2.1 Mechanism of BPL

BPL catalyses protein biotinylation through a two-step reaction as shown in Scheme 1.[10,20] In the first step, BPL catalyses a condensation reaction between biotin **1.01** and ATP **1.02** to form biotinyl-5'-AMP **1.03**, with the release of pyrophosphate (PPi). During this stage, biotin **1.01** binds to the biotin-binding pocket in BPL and, thus, induces ordering of a biotin-binding loop (BBL) within the enzyme (Figure 1). This conformational change in the protein creates the ATP pocket that allows subsequent binding of ATP **1.02**. Reaction of biotin with the α-phosphate of ATP then produces the intermediate biotinyl-5′-AMP

_____

1.03 to complete the first reaction. The complex of BPL with biotinyl-5′-AMP **1.03** then forms a protein: protein interaction with the unliganded biotin dependent enzyme (ie. the apo enzyme in Scheme 1) to allow the second reaction. During this step, the ε-amino group of the target lysine residue present in apo protein provides a positive charge that facilitates a nucleophilic reaction on the carbonyl group of **1.03**, resulting in the transfer of the biotin moiety onto the biotin domain to afford biotinylated ACC or PC (ie. the holo enzyme in Scheme 1), with the release of AMP. This stepwise mechanism (i.e. activation followed by attachment) is conserved in all species, suggesting a high degree of homology amongst different BPL enzymes.[21,22]
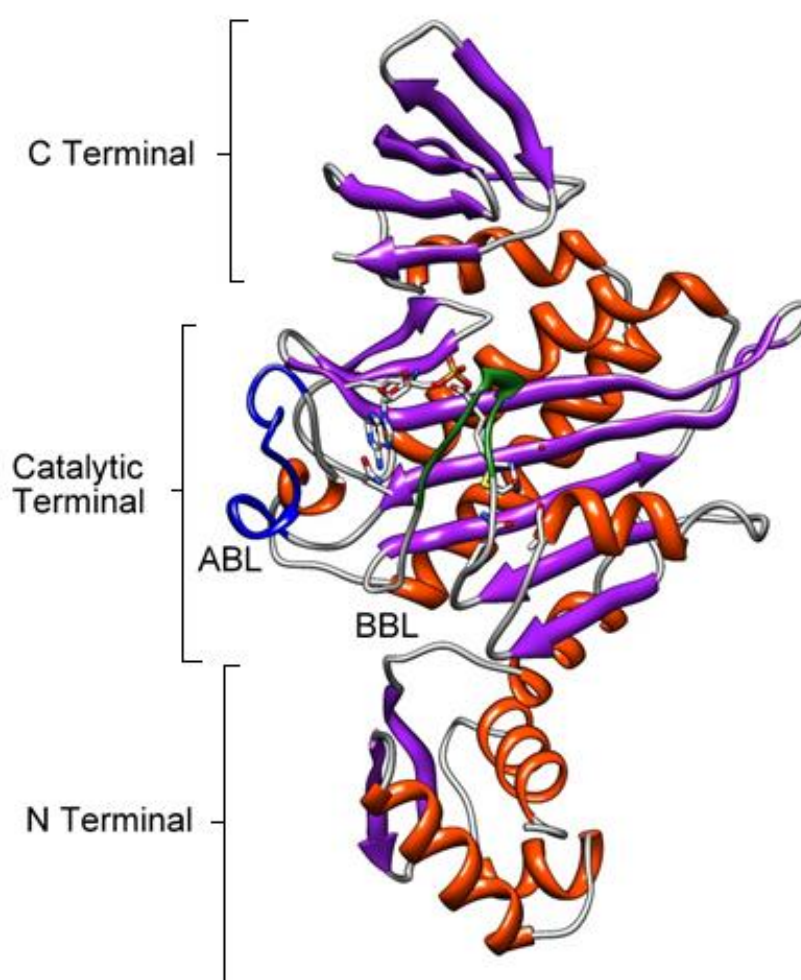
Figure 1: 3D depiction of *Sa*BPL with biotinyl-5'-AMP **1.03** bound (PDB: 3V8L). The β sheets are shown in purple, α helices in orange, biotin binding loop in green and ATP binding loop in blue.

1.2.2 BPL structure

BPL can be divided into three distinct structural classes. Classes I and II include BPLs from Archaea, prokaryotes and plants. Class III contains BPLs from yeast, insects and mammals. All three classes of BPLs contain a conserved catalytic domain and a C-terminal cap domain that are essential for protein biotinylation.[21] Class I BPL, including *Mycobacterium tuberculosis* biotin protein ligase (*Mtb*BPL)[23], consists solely of the conserved catalytic domain and C-terminal domain. Class II BPLs, such as *Sa*BPL and *E. coli* BPL (*Ec*BPL) contain an additional N-terminal domain that facilitates binding to DNA in the regulation of cellular uptake of biotin and biosynthesis of biotin, as described above. Class III BPLs, including *Homo sapiens* BPL (*Hs*BPL)[24], have a larger N-terminal extension that is distinct from the DNA-binding domain of class II enzymes.[24-27] X-ray crystal structures of class I BPLs from *Mycobacterium tuberculosis* (*M. tuberculosis*)[23], *Aquifex aeolicus*[28], and *P. horikoshii*[10] and class II BPL from *S. aureus*[29] and *E. coli*[20] have been reported. Examination of these data reveals that all BPLs adopt a highly conserved protein fold within the catalytic domain via a disordered-to-ordered binding mechanism. An ATP binding loop (highlighted by blue ribbons in Figure 1), and biotin-binding loop (highlighted by green ribbons in Figure 1) are considered responsible for the ordered binding mechanism. A closer examination of these structural features is detailed below with a view to designing inhibitors that can occupy the active site.

1.2.3 Catalytic domain

As mentioned above, the catalytic domain of BPL contains two major ligand-binding pockets for biotin **1.01** and ATP **1.02**. The biotin-binding site consists of two distinct regions, a hydrophobic wall to accommodate the valeric acid chain on biotin and a glycine rich hydrophilic pocket to accommodate the two heterocycles. Multiple hydrogen bonding interactions are formed between the ureido ring of biotin **1.01** and amino acid residues in the hydrophilic region of *Sa*BPL[30], namely Ser92, Thr93, Gln115 and Arg119, as depicted in Figure 2. These residues are highly conserved in BPLs from all species.[31] Sulphur and carbon atoms in the heterocycles of biotin **1.01** form additional hydrophobic interactions with Trp127 and Gly209. The carbon chain on the valeric tail of biotin is orientated to a hydrophobic tunnel consisting of Gly118, Gly209, Gly188, Leu191 and Ile208 by induced fit binding of biotin in the first catalytic step of BPL.[21,22] The overall binding of biotin

_____

results in an ordering of the biotin binding loop which caps the ligand and prevents release from the active site. Sequence analysis reveals a high degree of conservation in the biotin binding pocket of *Sa*BPL[29], *Ec*BPL[20], *Mtb*BPL[32], *Aa*BPL (*Aquifex aeolicus*)[28] and *Ph*BPL (*Pyrococcus horikoshii*)[22] with Figure 2 highlighting the binding mode of biotin structure of biotinyl-5′-AMP **1.03** within this pocket for *Sa*BPL.
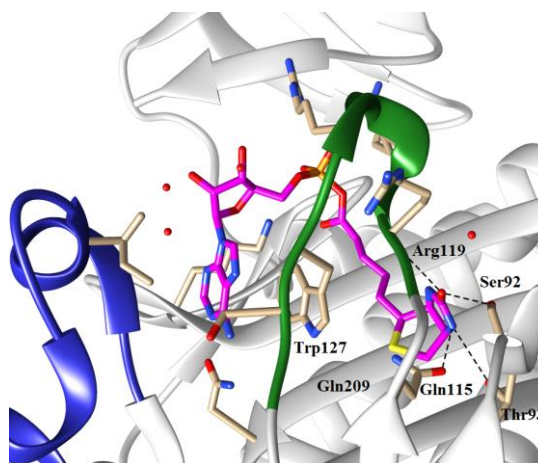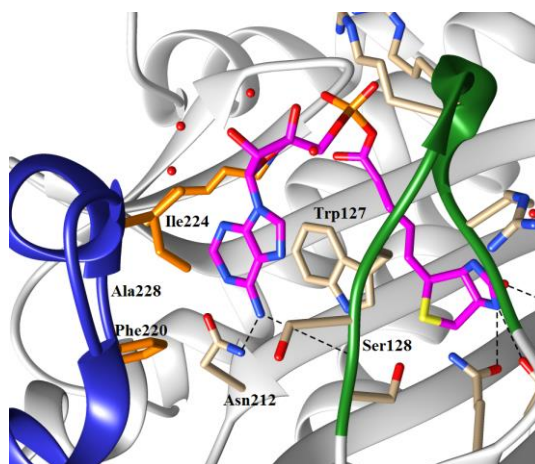

Figure 2: 3D depiction of reaction intermediate biotinyl-5'-AMP **1.03** bound to *Sa*BPL (PDB: 3V8L) with a close examination of biotin binding pocket. Green ribbon highlighting the biotin binding loop and black dashes indicating hydrogen bonding interactions between the ureido ring of biotin and *Sa*BPL.

A phosphate-binding domain is located between the biotin and ATP binding pockets and is found to be highly homologous in all BPLs. A number of hydrogen bonding interactions are observed between the phosphoroanhydride linker of biotinyl-5′-AMP **1.03** and the side chains of Lys187 and Arg125, as well as the backbone of Arg122 (Figure 3).[30] The conserved 'Gly-Arg-Gly-Arg[122]-X' motif present in the biotin-binding loop is critical in stabilising the biotinyl-5′-AMP **1.03** by shielding it from solvent.[20] Of particular note is Arg122, which plays an important role in stabilising the active binding site by assisting the formation of a complex network with a water-mediated hydrogen bond with the side chain of Asp180 (Figure 3).[30,31] This observation is also supported by studies with *E. coli* BPL where a point mutation of the equivalent residue (Arg118) results in dissociation rates enhanced by 100-fold for biotin **1.01** and 400-fold for biotinyl-5′-AMP **1.03**.[31] Mutation of Arg122 to glycine results in a 'leaky phenotype' that has been exploited using *Sa*BPL and applied on *in situ* click chemistry.[33] Details of this work and subsequent improvements are discussed in Chapter 6.
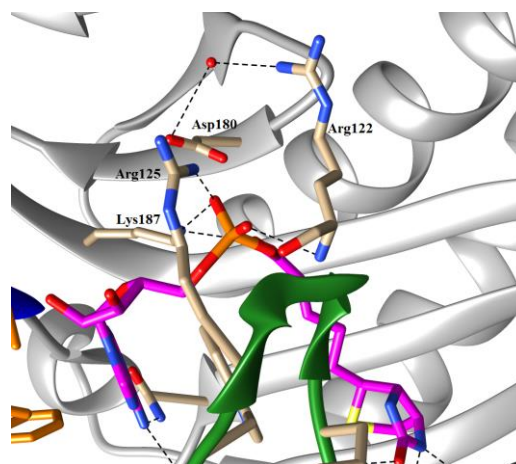
Figure 3: 3D depiction of reaction intermediate biotinyl-5′-AMP **1.03** bound to *Sa*BPL (PDB: 3V8L) with a close examination of phosphate binding pocket. Green ribbon highlights the biotin-binding loop.

The previously mentioned induced-fit binding of the biotin-binding loop (highlighted in green as in Figure 4) orientates the side chain of Trp127 of *Sa*BPL such that it creates a binding pocket for nucleotide binding from ATP. This binding is stabilised by a displaced parallel π interaction between the adenine ring of ATP and the indole ring of Trp127.[31,34] It is noteworthy that this key binding interaction does not occur in the absence of biotin..[10] A number of hydrogen binding interactions are also observed between the adenine ring of ATP and Asn212 and Ser128 at the base of the ATP-binding pocket. Following ATP binding, a condensation reaction occurs between biotin and ATP to give biotinyl-5′-AMP **1.03**.[30] The ATP-binding loop (highlighted in blue in Figure 4) then helps to stabilise the reaction intermediate (**1.03**) via a disordered-to-ordered transition. Here, the ATP binding loop folds over the adenosine moiety of **1.03** and forms hydrophobic interactions with **1.03** through Ile224, Ala228 and Phe220. This structural data provides molecular explanation for the ordered ligand binding mechanism critical for the design of inhibitors.

Figure 4: 3D depiction of reaction intermediate biotinyl-5'-AMP **1.03** bound to *Sa*BPL (PDB: 3V8L) with a close examination of ATP binding pocket. Green ribbon highlighting the biotin binding loop and blue ribbon highlighting the ATP binding loop.[30]

1.3 BPL Inhibitors - Preliminary Data

*Sa*BPL is an attractive novel target for antibiotic development for three main reasons. Firstly, *Sa*BPL is a bi-functional enzyme that regulates biotinylation of ACC and PC of *S. aureus.*[35] Secondly, *Sa*BPL is the only enzyme in *S. aureus* responsible for regulation of biotin biosynthesis on cellular demand. Thus, targeting *Sa*BPL targets the source of biotin and the utility of biotin.[17,18] Thirdly, *Sa*BPL is not the target of antibiotics currently in clinical use, thereby providing a novel mechanism of action. Recent structure-guided approach to the design of small molecule inhibitors against *Sa*BPL has led to the discovery of BPL inhibitors that bind selectively to bacterial BPL over the human homolog.

1.3.1 Biotin 1.01 analogues as antibacterial agents

An effective approach to stop protein biotinylation is to design small molecule inhibitors that bind tightly and specifically to the active site of bacterial BPL, thereby blocking all protein biotinylation. Based on x-ray crystal structure of the biotin binding site, a class of biotin **1.01** analogues was designed with chemical modifications to the ureido and thiophene ring, such as analogues **1.05** and **1.06** as shown in Figure 5.[30] The study revealed that BPLs were highly specific to the natural structure of biotin **1.01** and did not utilise other biotin analogues as substrates.[30] In addition, amino acid sequence alignments
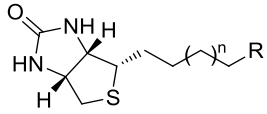
_____

highlight that the biotin-binding pocket is highly conserved amongst BPLs from all species, including human.[29,30,36] This presents a challenge for the design of a selective inhibitor for bacterial BPLs over human BPL. Moreover, analysis of X-ray structure of *Sa*BPL reveals a relatively small biotin-binding pocket, hence providing little space for chemical modifications (Figure 5).
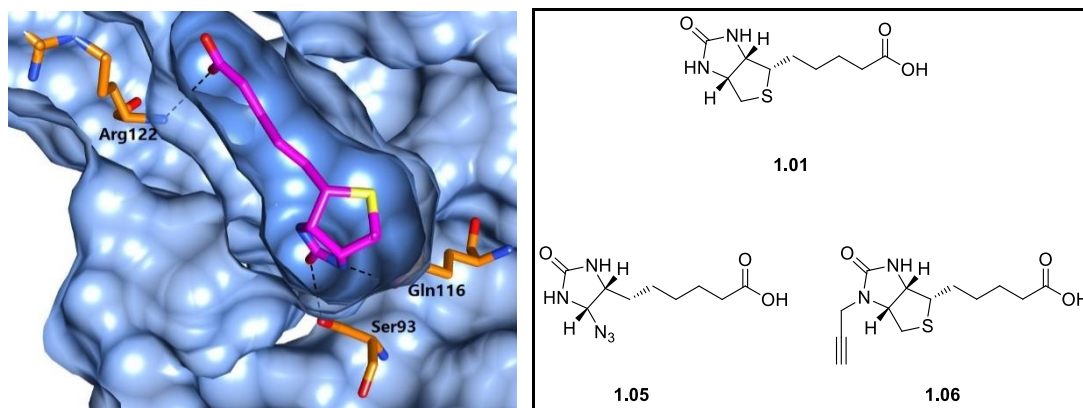
Figure 5: 3D depiction of biotin **1.01** bound to *Sa*BPL (PDB: 3V8K) with a side view of biotin binding pocket (Left); Chemical structures of biotin **1.01** and its analogues **1.05** and **1.06** (Right).[30]

Specific chemical modifications were also recently reported on the carboxyl group of biotin **1.01** to give a series of BPL inhibitors.[30] The analogues **1.07-1.13**, including hydroxyl, alkane and alkyne for the replacement of the carboxyl group of biotin, are listed below in Table 1. These compounds were assayed against *Sa*BPL, *Ec*BPL and *Hs*BPL. The alcohol derivative **1.07** was found to be equally active against *Sa*BPL and *Ec*BPL with $K_i \approx$ 4.0 µM. However, **1.07** lacks selectivity over *Hs*BPL with $K_i \approx$ 9.0 µM. The more hydrophobic analogues **1.09-1.13** showed up to 70-fold higher activity against *Sa*BPL over the alcohol derivative **1.07**. The most active derivative **1.09** in this series also has a 90-fold increasing for *in vitro* potency against *Hs*BPL (K_i = 0.1 µM) compared to **1.07**, suggesting poor selectivity. The x-ray structures of *Sa*BPL in complex with **1.01** revealed a conserved hydrogen bonding interaction between the carboxyl group of **1.01** and the backbone amide of Arg122 (Figure 5). Interestingly, increasing the length of the carbon chain, for example as in **1.11-1.13**, results in reduced potency, presumably due to the disruption of this key bonding interaction. Overall, this study suggests that biotin derivatives with chemical modifications at the biotin heterocycles and the valeric acid moiety are not ideal for achieve optimal potency and selectivity towards *Sa*BPL.

_____

Table 1: biotin analogue series[30]

	n	R	*Sa*BPL K_i (µM)	*Ec*BPL K_i (µM)	*Hs*BPL K_i (µM)
1.07	2	OH	3.4	4.0	9.0
1.08	3	OH	>20	>20	>20
1.09	1	CH$_3$	0.05	1.1	0.1
1.10	2	CH$_3$	0.5	7.3	6.4
1.11	1	C≡C	0.08	0.9	0.2
1.12	2	C≡C	0.3	7.3	3.5
1.13	3	C≡C	2.4	20	12

1.3.2 BPL reaction intermediate analogues as antibacterial agents

As discussed the first step of the BPL reaction is to catalyse the formation of biotinyl-5′-AMP **1.03**. Recent studies have focused on developing mimics of biotinyl-5′-AMP **1.03** with the reactive acyl phosphate group replaced with a more stable bioisostere. The first example of the reaction intermediate mimic, biotinol-5′-AMP **1.14** (Figure 6, below), has the acyl phosphate group of **1.03** replaced with the non-hydrolysable and enzymatically stable bioisosteric phosphodiester linker between the biotin and adenosine components.[37] Importantly, biotinol-5′-AMP **1.14** is a potent inhibitor against *Sa*BPL (K_i = 0.03 µM) and possesses anti-*S. aureus* property with a minimal inhibitory concentration (MIC) of 1 – 8 µg/µL.[38] However, progressing biotinol-5′-AMP **1.14** as drug candidate is limited by its selectivity over *Hs*BPL with K_i = 0.42 µM. Two other phosphonate based isosteres, as in **1.15** and **1.16** respectively, were initially developed by Sittiwong *et al* for investigation of holocarboxylase synthetase (HLCS) inhibitors.[39] HLCS has a similar mechanism to *Sa*BPL in catalyzing the covalent attachment of biotin to biotin dependent enzymes (see section 1.3 for the mechanism of BPL).[39] However, the β-ketophosphonate **1.15** and β-hydroxyphosphonate **1.16** analogues both showed reduced activity (*IC$_{50}$* of 39.7 µM and 203.7 µM, respectively) against HLCS compared to biotinol-5′-AMP **1.14** (*IC$_{50}$* = 7 µM against HLCS).[39]

Brown and co workers[37,40] described a sulfamoyl analogue **1.17** as a structure mimic of natural reaction intermediate **1.03** (Figure 6). However, this analogue is reported to lack potency toward *E. coli* BPL due to its structural instability and rapid decomposition.[23,37] A recent study has identified a sulfonamide analogue, **1.18**, with greater stability than the sulfamoyl linker of **1.17**.[23] Significantly, **1.18** is a competitive inhibitor against *Mtb*BPL with the half maximum inhibitor concentration (IC_{50}) of 135 nM. This analogue also displayed anti-mycobacterial activity against the virulent *M. tuberculosis* strain H37Rv as well as a number of multi-drug resistant *M. tuberculosis* strains, with an MIC ranging from 0.625 to 0.16 µg/mL.[23] However, cytotoxicity was observed in the mammalian Vero cell line for compound **1.16** suggesting potential issue with selectivity for the bacterial BPL over the human homolog.
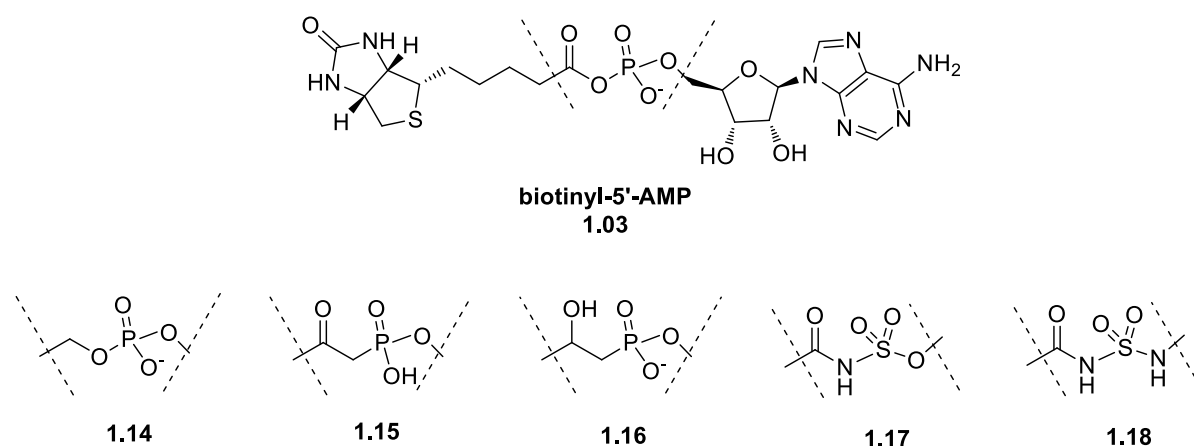
Figure 6: Reaction intermediate biotinyl-5'-AMP **1.03** and its mimics, biotinol-5'-AMP **1.14**, β-ketophosphonate **1.15**, β-hydroxyphosphonate **1.16**, acylsulfamate **1.17**, and acylsulfonamide **1.18**.

1.3.3 1,2,3-Triazole Based Analogues

In an attempt to improve selectivity for *Sa*BPL over *Hs*BPL, Soares da Costa *et al.* identified 1,2,3-triazole as an alternative bioisostere for the labile phosphoanhydride linker in biotinyl-5'-AMP **1.03**.[30] The triazole, as shown below in Figure 7, offers a number of advantages over the natural phosphate linker of **1.03** making it a good bioisostere candidate. It is stable to acid/base hydrolysis, reductive and oxidative conditions, as well as typical physiologically conditions, and therefore resistant to metabolic degradation.[41] In addition, the 1,2,3-triazole motif has three potential hydrogen bond acceptor sites (Figure 7) and an ability to participate in π-π stacking interactions with Trp127 of *Sa*BPL.

_____
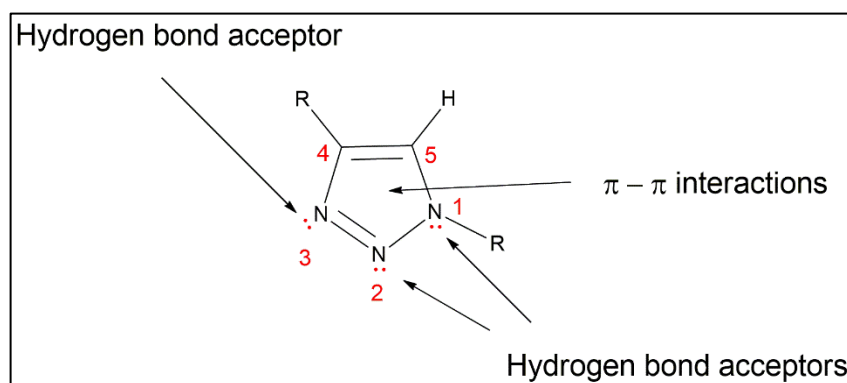
Figure 7: The assignment of 1,2,3-triazole with the potential intermolecular interaction sites.

Synthesis of 1,2,3-triazole

The synthesis of 1,2,3-triazole by reaction of an acetylene with an azide was first reported by Rolf Huisgen in 1963.[42] This chemistry provides a convenient method for the preparation of five membered heterocycles with high atom efficiency and multiple bonds formation from much simpler starting reactants. However, such a formation of 1,2,3-triazole requires high activating energy, such as heat[43] or constraints (intramolecular reactions)[44], and yields both 1,4- and 1,5-triazole isomers, as shown in Scheme 2.
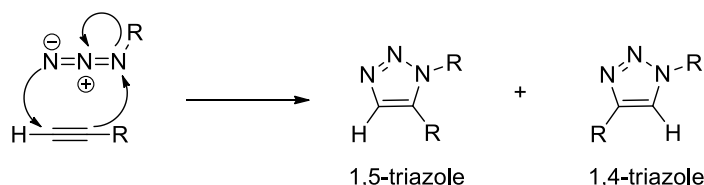
Scheme 2: 1,3-dipolar cycloaddition reaction between alkyne and terminal azide. A simplified mechanism is shown highlighting the routes towards 1,4 and 1,5-triazole configuration[45].

The regioselective synthesis of a 1,4-triazole over a 1,5-triazole was only solved a decade ago, with the advent of copper and ruthenium catalysis of a 1,3 dipolar cycloaddition reaction between acetylene and azide (Scheme 3). The use of copper mediated alkyne azide cycloaddition reaction (CuAAC) allows selective formation of the 1,4-triazole isomer over the 1,5-triazole, with a 10 million fold acceleration in the rate of reaction compared with traditional Huisgen cycloaddition.[46] Therefore, CuAAC results in a facile reaction that can proceed at ambient temperature with high yields, high selectivity (1,4-triazole over the 1,5-triazole), compatability with a wide range of functional groups, and simple product

_____

isolation by crystallisation, distillation or silica gel chromatography. The reliable and facile nature of CuAAC and the associated 1,2,3-triazole has resulted these structures being widely applied as a bioisostere for amides[47,48], olefins[49], disulfides[50,51], phosphomonoesters[52], pyrophosphate[53], phosphodiester[54] and phosphoroanhydride.[55] The ruthenium catalysed synthesis of regioselective 1,5-triazole shown in Scheme 3 was first reported by Zhang and co workers in 2005.[56] The RuAAC reaction complements CuAAC in that it provides a reliable means to produce selective 1,5-triazole with minimal by-products and high tolerance for a variety of functional groups.

Recently, a new approach, namely *in situ* click chemistry, can also be used to synthesise the regioselective 1,4 and 1,5-triazoles.[33,57] Further details about this approach and its applications will be discussed below and in chapter 6.
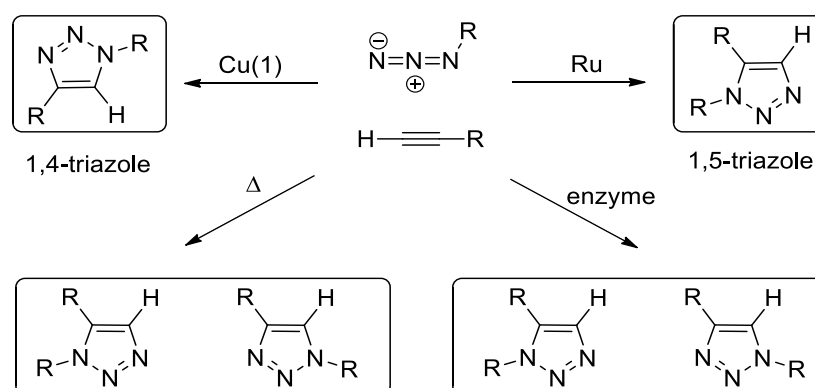

Scheme 3: Four possible synthetic routes to 1,2,3-triazole. Clockwise from top left: Copper alkyne azide cycloaddition (CuAAC), ruthenium alkyne azide cycloaddition (RuAAC), *in situ* click chemistry, 1,3-dipolar cycloaddition.

1,2,3-Triazole based analogues

A series of 1,2,3-triazole based analogues of **1.20-1.23** (see Scheme 4 and Figure 9) was synthesised and tested for inhibitory activity against *Sa*BPL and *Hs*BPL.[30] The first example of a 1,4 disubstituted triazole (**1.20**) was synthesised by reacting biotin acetylene **1.12** and adenosine azide **1.19** *via* CuAAC (Scheme 4). This 1.4-triazole (**1.20**) was found to be active against *Sa*BPL ($K_i = 1.8$ μM) with good selectivity over *Hs*BPL ($K_i > 33$ μM) *in vitro*. Importantly, the 1,4-triazole **1.20** was not toxic against mammalian HepG2 cells in culture, thereby providing the first example of a triazole analogue as a selective *Sa*BPL inhibitor. Importantly for work described in this thesis, the 1,5-triazole regioisomer **1.21**

_____

prepared *via* RuAAC proved to be inactive against *Sa*BPL.[30] X-ray crystallography of *Sa*BPL in complex with **1.20** revealed that the 1,4-triazole also provides the desired U-shape geometry on binding to *Sa*BPL, as observed for biotinyl-5′-AMP **1.03**.[30]
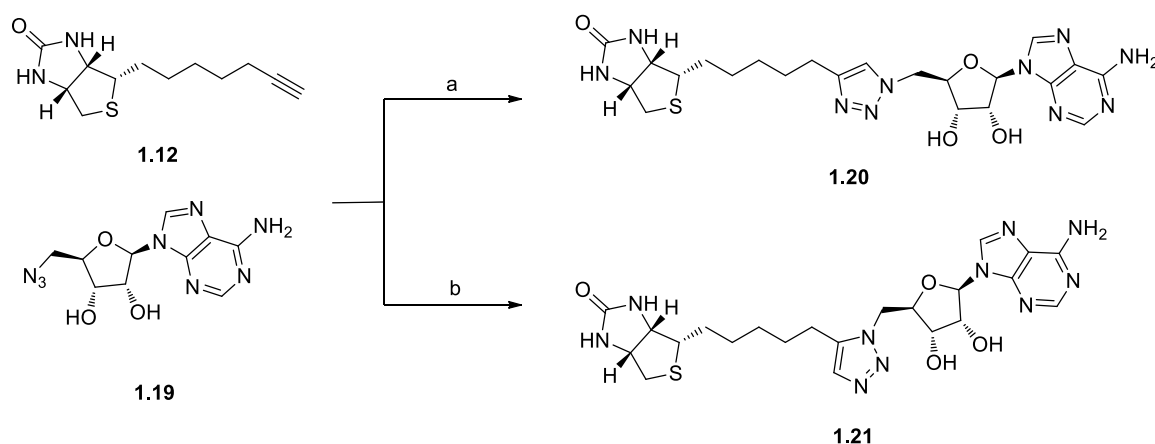
Scheme 4: Synthesis of 1,4-triazole **1.20** and 1,5-triazole **1.21** from biotin acetylene **1.12** and azide **1.19.** Conditions and reagents: a) (i) copper nano powder, 2:1 AcCN/H$_2$O, 4 h, sonication, 35 °C. b) (i) Cp*RuCl(PPh$_3$)$_2$, 1:1 THF/DMF, 4h, 70 °C.

Based on the above assessment, a new generation of *Sa*BPL inhibitors was designed to target the ATP binding site. Analysis of the crystal structure of **1.20** bound to *Sa*BPL revealed no significant hydrogen bonding interactions between the ribose moiety of **1.20** and *Sa*BPL (Figure 9).[30] In support, the 1,4-triazole analogue **1.22**, lacking the ribose group, proved to be more potent than **1.20** against *Sa*BPL with K_i of 0.7 µM.[30] Furthermore, the study identified a series of biotin 1,4-triazole analogues with chemical mimics of the adenine moiety of **1.22** to target the ATP binding pocket. The 1,4-triazole **1.23**, with a 2-benzoxazolone moiety was identified to be the most potent *Sa*BPL inhibitor with a $K_i = 0.09 \pm 0.01$ µM. Significantly, 1,4-triazole **1.23** exhibited over 1100 fold selectivity for *Sa*BPL compared to human BPL. It thus represents the most potent and selective inhibitors of *Sa*BPL reported to date. Bacteriostatic activity was observed for 1,4-triazole **1.23** against *S. aureus* ATCC strain 49775, with the compound effectively reducing *S. aureus* cell growth by 80% at 8 µg/mL. Both 1,4-triazoles **1.22** and **1.23** were not toxic in a cell culture model using HepG2 cells, highlighting these triazoles are excellent hits for further antibiotic development.[30]
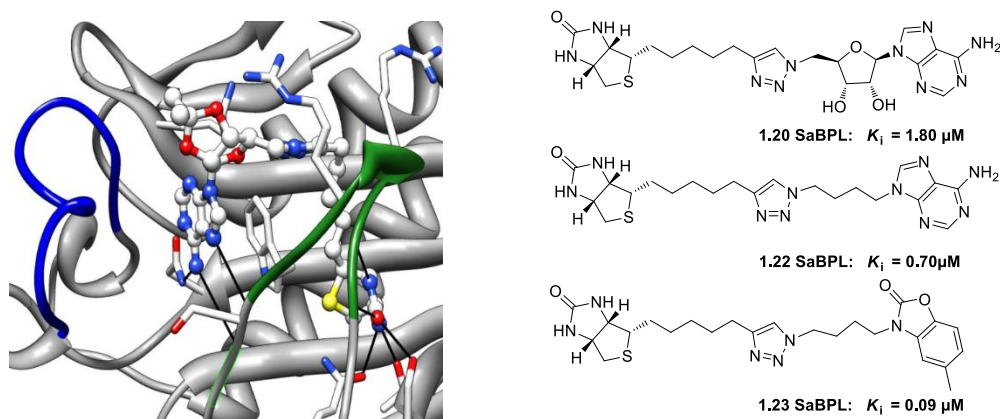
Figure 9: 3D depiction of 1,4-triazole **1.20** bound to *Sa*BPL (PDB: 3V7C) (Left); Chemical structures of 1,2,3-triazole analogues: 1,4-triazole **1.22** and 1,4-triazole **1.23** (Right).

1.3.4 *In situ* click chemistry

In situ click chemistry has recently been investigated as an alternative approach to optimize the biotin triazole series.[57-59] Here the target enzyme is used as a template to identify and bind the optimum azide and acetylene fragments from a library of such structures. Once each azide and acetylene bind to their respective pockets a cycloaddition reaction occurs in the absence of external catalysts (such as copper or ruthenium) to form the 1,2,3-triazole. Moreover, as the biological target is actively involved in selecting its most potent inhibitor from a library of precursor, *in situ* click chemistry is able to circumvent the need to individually synthesise and screen all possible triazole combinations, and the hit identification can be as simple as determining whether a given combination of building blocks has resulted in a product. The subsequent biological testing for determining inhibitory potency, bioavailability, and toxicity can be limited to a small number of enzyme generated products, thus greatly facilitating the discovery of new drug candidates.[60-62]

A recent study reported by William Tieu and co-workers at Adelaide employed the *in situ* click chemistry as an alternative approach for the synthesis of 1,4-triazoles.[33] As mentioned above, 1,4-triazoles **1.22** and **1.23** are known as potent and selective *Sa*BPL inhibitors with K_i = 0.7 µM and 0.09 µM, respectively.[30] An initial *in situ* click reaction was performed between biotin acetylene **1.12** (K_i = 0.3 µM) and adenosine azide **1.19** using wild type *Sa*BPL as a template (Scheme 5). Analysing the crude reaction mixture using standard HPLC or mass spectrometry indicated 1.07 ± 0.1 mol of triazole **1.18**

_____

formed per mol of *Sa*BPL. The triazole formed by *Sa*BPL is presumed to be the 1,4-triazole **1.20** (K_i = 1.18 µM), given that the 1,5-triazole **1.21** (see Scheme 4) was inactive and hence unable to bind *Sa*BPL. Next *in situ* experiment was performed between biotin acetylene **1.12** and a small library of azides (**1.24-1.27**), as shown in Scheme 5. However, in this case triazole products could not be detected by standard HPLC or mass spectrometry above the background level. It is noteworthy that the *in situ* chemistry using wild type *Sa*BPL is difficult to produce multiple round of catalysis due to the resulting compound having high binding affinity for the target enzyme, thereby resulting in a low turnover rate. The before mentioned biotin-binding loop of *Sa*BPL is suspected to be responsible for the low catalytic efficiency, and it achieves such by folding over the active binding site to prevent dissociation of the synthesised triazoles.[30] As discussed above in section 1.2.3, the key amino acid residue Arg122 is responsible for stabilising biotin-binding loop through the intricate hydrogen bonding network.[30,31] Therefore, in the study by Tieu *et al*., Arg122 was substituted by glycine in order to improve dissociation of the triazole inhibitors from the enzyme, hence to increase the enzyme's turnover rate.[33]

Recent efforts in this area have focus on optimising sensitivity of detection using a HPLC associated high resolution electrospray mass spectrometry (LC/HRMS) approach. Compared to the standard HPLC, LC/HRMS allows instantaneous and precise identification of individual products by retention time and high resolution molecular mass. The approach has been used in a number of *in situ* click chemistry to detect triazole products produced by native enzymes, such as acetylcholinesterase[60,63] and HIV-1 protease.[64] The work described in this thesis proposed to use LC/HRMS as an alternative solution to detect the low level of triazole products generated by only using wild type *Sa*BPL as the template. Details about this work will be discussed in Chapter 6.
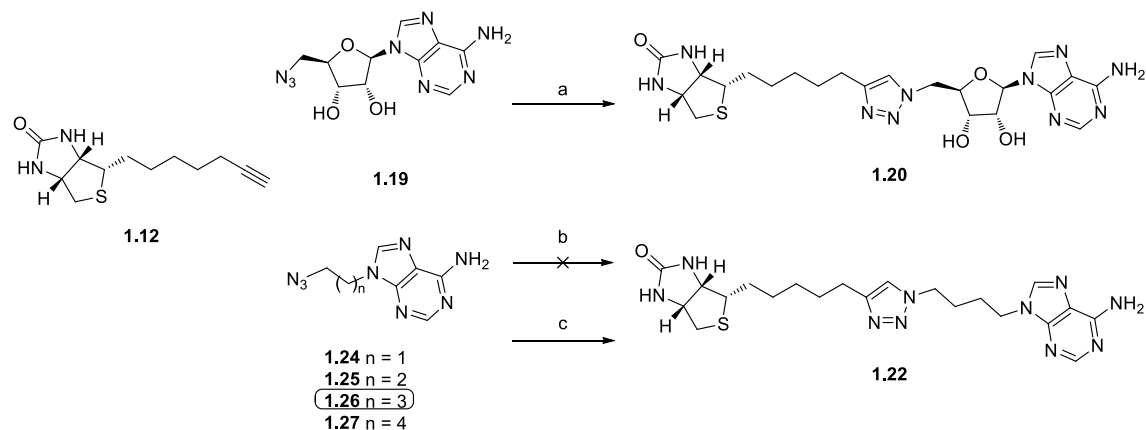
Scheme 5: a) *In situ* click reactions of acetylene **1.12** with azides **1.19** In the presence of wild type *Sa*BPL, 1,4-triazole **1.20** was confirmed by HPLC; b) *In situ* click reactions of

_____

acetylene **1.12** with azides **1.24-1.27** in the presence of wild type *Sa*BPL, no triazole products were observed by HPLC; c) *In situ* click reactions of acetylene **1.12** with azides **1.24-1.27** in the presence of *Sa*BPL Arg122-Gly, 1,4-triazole **1.22** was confirmed by HPLC.

1.4 Research described in this thesis

This thesis reports new classes of BPL inhibitors that have improved potency and selectivity towards *Sa*BPL and *Mtb*BP. Chapter 1 describes the structure and catalytic mechanism of *Sa*BPL and preliminary data with a novel class of BPL inhibitors that 1) has a new mode of antibacterial action; 2) has unique selectivity for the bacterial BPL target over the human isozyme; 3) has antimicrobial activity against *S. aureus*; and 4) does not show toxicity against a human cell line in tissue culture or in an animal model. Chapter 2 elaborates on the potent inhibitors **1.22** and **1.23** with chemical modifications carried out at the tether area between the triazole ring and adenine as in **1.22** or 2-benzoxazolone as in **1.23**. Chapter 3 describes the design, synthesis, and biological assay of a new series of 1,4-triazole analogues with small benzylic components towards the ATP binding pocket of *Sa*BPL. Chapter 4 builds on the active 1,2,3-triazole analogues developed in chapters 2 and 3 with chemical modifications carried out on the triazole ring itself and development of a novel class of 1,4,5-trisubstituted triazole inhibitors. Chapter 5 focuses on design of acyl sulfonamide as a bioisosteric analogue of the phosphoroanhydride linker of biotinyl-5'-AMP **1.03** and investigates a novel class of *Sa*BPL inhibitors with improved potency and selectivity. Finally, chapter 6 elaborates on our previously published *in situ* click chemistry and investigates the use of high throughput LC/MS as a new detection method with improved sensitivity and reliability.

1.5 References for Chapter One

(1)   Boucher, H. W.; Talbot, G. H.; Bradley, J. S.; Edwards, J. E.; Gilbert, D.; Rice, L. B.; Scheld, M.; Spellberg, B.; Bartlett, J. *Clinical Infectious Diseases* **2009**, *48*, 1-12.

(2)   Lewis, K. *Nature* **2012**, *485*, 439-440.

(3)   Kallen, A. J.; Mu, Y.; Bulens, S.; Reingold, A.; Petit, S.; Gershman, K.; Ray, S. M.; Harrison, L. H.; Lynfield, R.; Dumyati, G.; Townes, J. M.; Schaffner, W.; Patel, P. R.; Fridkin, S. K. *JAMA: The Journal of the American Medical Association* **2010**, *304*, 641-647.

(4)   Pearson, A.; Chronias, A.; Murray, M. *Journal of Antimicrobial Chemotherapy* **2009**, *64*, i11-i17.

(5)   Ferguson, J. *Healthcare Infection* **2007**, *12*, 60-66.

(6)   Klein, E.; Smith, D.; Laxminarayan, R. *Emerging Infectious Diseases journal* **2007** *13*, 1840-1846.

(7)   Holmes, N. E.; Turnidge, J. D.; Munckhof, W. J.; Robinson, J. O.; Korman, T. M.; O'Sullivan, M. V.; Anderson, T. L.; Roberts, S. A.; Gao, W.; Christiansen, K. J. *Journal of Infectious Diseases* **2011**, *204*, 340-347.

(8)   Fischbach, M. A.; Walsh, C. T. *Science* **2009**, *325*, 1089-1093.

(9)   Samols, D.; Thornton, C. G.; Murtif, V. L.; Kumar, G. K.; Haase, F. C.; Wood, H. G. *Journal of Biological Chemistry* **1988**, *263*, 6461-6464.

(10)   Bagautdinov, B.; Kuroishi, C.; Sugahara, M.; Kunishima, N. *Journal of Molecular Biology* **2005**, *353*, 322-333.

(11)   Nenortas, E.; Beckett, D. *Journal of Biological Chemistry* **1996**, *271*, 7559-7567.

(12)   Paul V, A. *The International Journal of Biochemistry & Cell Biology* **1995**, *27*, 231-249.

(13)   Bloch, K.; Vance, D. *Annual Review of Biochemistry* **1977**, *46*, 263-298.

(14)   Wallace, J. C.; Jitrapakdee, S.; Chapman-Smith, A. *The International Journal of Biochemistry & Cell Biology* **1998**, *30*, 1-5.

_____

(15)   Payne, D. J.; Gwynn, M. N.; Holmes, D. J.; Pompliano, D. L. *Nature Reviews Drug Discovery* **2007**, *6*, 29-40.

(16)   Forsyth, R.; Haselbeck, R. J.; Ohlsen, K. L.; Yamamoto, R. T.; Xu, H.; Trawick, J. D.; Wall, D.; Wang, L.; Brown‐Driver, V.; Froelich, J. M. *Molecular Microbiology* **2002**, *43*, 1387-1400.

(17)   Abbott, J.; Beckett, D. *Biochemistry* **1993**, *32*, 9649-9656.

(18)   Rodionov, D. A.; Mironov, A. A.; Gelfand, M. S. *Genome Research* **2002**, *12*, 1507-1516.

(19)   Beckett, D. *The Journal of Nutrition* **2009**, *139*, 167-170.

(20)   Wood, Z. A.; Weaver, L. H.; Brown, P. H.; Beckett, D.; Matthews, B. W. *Journal of Molecular Biology* **2006**, *357*, 509-523.

(21)   Chapman-Smith, A.; Cronan Jr, J. E. *Biomolecular Engineering* **1999**, *16*, 119-125.

(22)   Bagautdinov, B.; Matsuura, Y.; Bagautdinova, S.; Kunishima, N. *Journal of Biological Chemistry* **2008**, *283*, 14739-14750.

(23)   Duckworth, B. P.; Geders, T. W.; Tiwari, D.; Boshoff, H. I.; Sibbald, P. A.; Barry, C. E., 3rd; Schnappinger, D.; Finzel, B. C.; Aldrich, C. C. *Chemistry & Biology* **2011**, *18*, 1432-1441.

(24)   Campeau, E.; Gravel, R. A. *Journal of Biological Chemistry* **2001**, *276*, 12310-12316.

(25)   Mayende, L.; Swift, R. D.; Bailey, L. M.; Da Costa, T. P. S.; Wallace, J. C.; Booker, G. W.; Polyak, S. W. *Journal of Molecular Medicine* **2012**, *90*, 81-88.

(26)   Polyak, S. W.; Chapman-Smith, A.; Brautigan, P. J.; Wallace, J. C. *Journal of Biological Chemistry* **1999**, *274*, 32847-32854.

(27)   Pendini, N. R.; Bailey, L. M.; Booker, G. W.; Wilce, M. C.; Wallace, J. C.; Polyak, S. W. *Archives of Biochemistry and Biophysics* **2008**, *479*, 163-169.

(28)   Tron, C. M.; McNae, I. W.; Nutley, M.; Clarke, D. J.; Cooper, A.; Walkinshaw, M. D.; Baxter, R. L.; Campopiano, D. J. *Journal of Molecular Biology* **2009**, *387*, 129-146.

(29)   Pendini, N. R.; Yap, M. Y.; Polyak, S. W.; Cowieson, N. P.; Abell, A.; Booker, G. W.; Wallace, J. C.; Wilce, J. A.; Wilce, M. C. *Protein Science* **2013**, *22*, 762-773.

_____

(30)   Soares da Costa, T. P.; Tieu, W.; Yap, M. Y.; Zvarec, O.; Bell, J. M.; Turnidge, J. D.; Wallace, J. C.; Booker, G. W.; Wilce, M. C.; Abell, A. D. *ACS Medicinal Chemistry Letters* **2012**, *3*, 509-514.

(31)   Kwon, K.; Beckett, D. *Protein Science* **2000**, *9*, 1530-1539.

(32)   Purushothaman, S.; Gupta, G.; Srivastava, R.; Ramu, V. G.; Surolia, A. *PLoS ONE* **2008**, *3*, e2320.

(33)   Tieu, W.; da Costa, T. P. S.; Yap, M. Y.; Keeling, K. L.; Wilce, M. C.; Wallace, J. C.; Booker, G. W.; Polyak, S. W.; Abell, A. D. *Chemical Science* **2013**, *4*, 3533-3537.

(34)   Naganathan, S.; Beckett, D. *Journal of Molecular Biology* **2007**, *373*, 96-111.

(35)   Rozwarski, D. A.; Vilchèze, C.; Sugantino, M.; Bittman, R.; Sacchettini, J. C. *Journal of Biological Chemistry* **1999**, *274*, 15582-15589.

(36)   Chapman-Smith, A.; Cronan, J. E. *Trends in Biochemical Sciences* **1999**, *24*, 359-363.

(37)   Brown, P. H.; Cronan, J. E.; Grøtli, M.; Beckett, D. *Journal of Molecular Biology* **2004**, *337*, 857-869.

(38)   Tieu, W.; Polyak, S. W.; Paparella, A. S.; Yap, M. Y.; Soares da Costa, T. P.; Ng, B.; Wang, G.; Lumb, R.; Bell, J. M.; Turnidge, J. D. *ACS Medicinal Chemistry Letters* **2014**, *6*, 216-220.

(39)   Sittiwong, W.; Cordonier, E. L.; Zempleni, J.; Dussault, P. H. *Bioorganic & Medicinal Chemistry Letters* **2014**, *24*, 5568-5571.

(40)   Brown, P. H.; Beckett, D. *Biochemistry* **2005**, *44*, 3112-3121.

(41)   Rostovtsev, V. V.; Green, L. G.; Fokin, V. V.; Sharpless, K. B. *Angewandte Chemie* **2002**, *114*, 2708-2711.

(42)   Huisgen, R. *Angewandte Chemie International Edition in English* **1963**, *2*, 565-598.

(43)   Hlasta, D. J.; Ackerman, J. H. *The Journal of Organic Chemistry* **1994**, *59*, 6184-6189.

(44)   Li, R.; Jansen, D. J.; Datta, A. *Organic & Biomolecular Chemistry* **2009**, *7*, 1921-1930.

(45)   Hassner, A. *Synthesis of heterocycles via cycloadditions*; Springer, 2008.

(46)   Meldal, M.; Tornøe, C. W. *Chemical Reviews* **2008**, *108*, 2952-3015.

_____

(47)   Monceaux, C. J.; Hirata-Fukae, C.; Lam, P. C. H.; Totrov, M. M.; Matsuoka, Y.; Carlier, P. R. *Bioorganic & Medicinal Chemistry Letters* **2011**, *21*, 3992-3996.

(48)   Brik, A.; Alexandratos, J.; Lin, Y.-C.; Elder, J. H.; Olson, A. J.; Wlodawer, A.; Goodsell, D. S.; Wong, C.-H. *ChemBioChem* **2005**, *6*, 1167-1169.

(49)   Mesenzani, O.; Massarotti, A.; Giustiniano, M.; Pirali, T.; Bevilacqua, V.; Caldarelli, A.; Canonico, P.; Sorba, G.; Novellino, E.; Genazzani, A. A.; Tron, G. C. *Bioorganic & Medicinal Chemistry Letters* **2011**, *21*, 764-768.

(50)   Empting, M.; Avrutina, O.; Meusinger, R.; Fabritz, S.; Reinwarth, M.; Biesalski, M.; Voigt, S.; Buntkowsky, G.; Kolmar, H. *Angewandte Chemie International Edition* **2011**, *50*, 5207-5211.

(51)   Holland-Nell, K.; Meldal, M. *Angewandte Chemie International Edition* **2011**, *50*, 5204-5206.

(52)   Byun, Y.; Vogel, S. R.; Phipps, A. J.; Carnrot, C.; Eriksson, S.; Tiwari, R.; Tjarks, W. *Nucleosides, Nucleotides and Nucleic Acids* **2008**, *27*, 244-260.

(53)   Chen, L.; Wilson, D. J.; Xu, Y.; Aldrich, C. C.; Felczak, K.; Sham, Y. Y.; Pankiewicz, K. W. *Journal of Medicinal Chemistry* **2010**, *53*, 4768-4778.

(54)   El-Sagheer, A. H.; Brown, T. *Chemical Society Reviews* **2010**, *39*, 1388-1405.

(55)   Somu, R. V.; Boshoff, H.; Qiao, C.; Bennett, E. M.; Barry, C. E.; Aldrich, C. C. *Journal of Medicinal Chemistry* **2005**, *49*, 31-34.

(56)   Zhang, L.; Chen, X.; Xue, P.; Sun, H. H. Y.; Williams, I. D.; Sharpless, K. B.; Fokin, V. V.; Jia, G. *Journal of the American Chemical Society* **2005**, *127*, 15998-15999.

(57)   Mamidyala, S. K.; Finn, M. G. *Chemical Society Reviews* **2010**, *39*, 1252-1261.

(58)   Sharpless, K. B.; Manetsch, R. *Expert Opinion on Drug Discovery* **2006**, *1*, 525-538.

(59)   Thirumurugan, P.; Matosiuk, D.; Jozwiak, K. *Chemical Reviews* **2013**, *113*, 4905-4979.

(60)   Krasiński, A.; Radić, Z.; Manetsch, R.; Raushel, J.; Taylor, P.; Sharpless, K. B.; Kolb, H. C. *Journal of the American Chemical Society* **2005**, *127*, 6686-6692.

(61)   Mocharla, V. P.; Colasson, B.; Lee, L. V.; Röper, S.; Sharpless, K. B.; Wong, C.-H.; Kolb, H. C. *Angewandte Chemie International Edition* **2005**, *44*, 116-120.

_____

(62)   Hirose, T.; Sunazuka, T.; Sugawara, A.; Endo, A.; Iguchi, K.; Yamamoto, T.; Ui, H.; Shiomi, K.; Watanabe, T.; Sharpless, K. B.; Omura, S. *J Antibiot* **2009**, *62*, 277-282.

(63)   Manetsch, R.; Krasinski, A.; Radic, Z.; Raushel, J.; Taylor, P.; Sharpless, K. B.; Kolb, H. C. *Journal of the American Chemical Society* **2004**, *126*, 12809-12818.

(64)   Whiting, M.; Muldoon, J.; Lin, Y. C.; Silverman, S. M.; Lindstrom, W.; Olson, A. J.; Kolb, H. C.; Finn, M.; Sharpless, K. B.; Elder, J. H. *Angewandte Chemie International Edition* **2006**, *45*, 1435-1439.

2.1 Introduction

As discussed previously in chapter 1, the first step of the biotin protein ligase (BPL) reaction is to catalyse the formation of the acyl-adenylate intermediate **1.03**.[1-3] Similar reactions are also present in the aminoacyl-tRNA synthetases and lipoyl ligases, where an adenylated intermediate is also formed.[4,5] Studies targeting aminoacyl-tRNA synthetases provided initial proof of concept that the labile phosphoanhydride linker as in **1.03** can be replaced with more stable bioisosteres.[6-8] This approach provides a route to design small molecule inhibitors of *Sa*BPL by mimicking the acyl-adenylate intermediate **1.03**. Soares da Costa *et al.* in Abell research group, Adelaide, reported on the use of 1,4-disubstituted 1,2,3-triazole as an alternative bioisostere for the labile phosphoanhydride as in **1.03** (Figure 1).[9] 1,2,3-Triazole **1.20**, as shown in Figure 1, is a direct chemical analogue to the natural reaction intermediate **1.03** formed by replacing the phosphoanhydride group with the triazole ring.[9] Triazole **1.20** was a potent and selective inhibitor of *Sa*BPL ($K_i = 1.2$ µM) devoid of activity against human BPL, thereby making it the first triazole based analogue that is a selective BPL inhibitor.[9] In addition, Tieu *et al.* reported that 1,2,3-triazole **1.22** that lacks the ribose group of **1.18** was a more potent inhibitor of *Sa*BPL ($K_i = 0.7$ µM) than **1.20** ($K_i = 1.2$ µM).[9] This compound (**1.22**) also exhibited similar potency against *Mtb*BPL with a K_i of 0.6 µM and no activity against the human isoform, making it the current leading *Mtb*BPL inhibitor.[9]
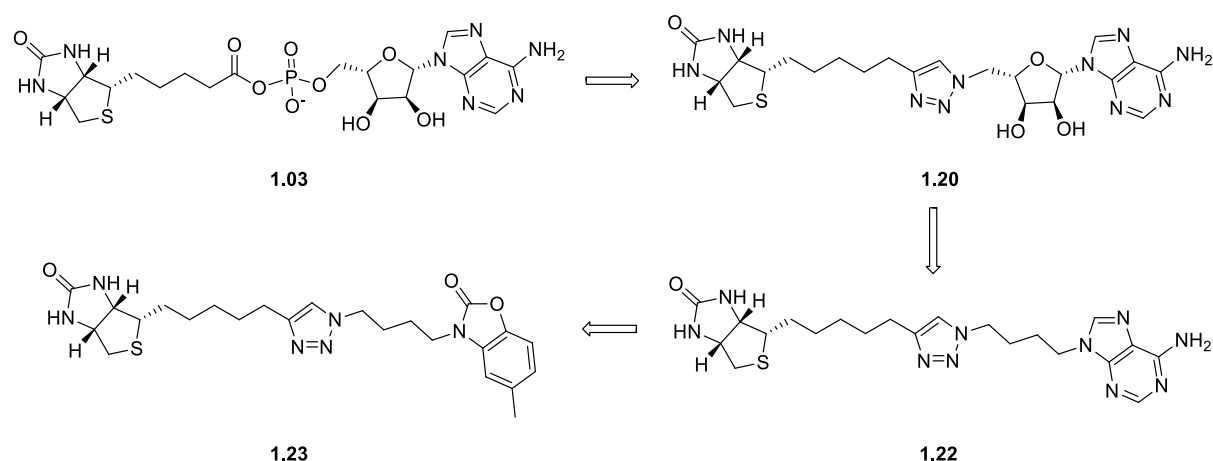
Figure 1: Natural reaction intermediate biotinyl-5'-monophosphate adenosine **1.03**, first generation BPL inhibitor with 1,2,3-triazole in place of acyl phosphate **1.20**, current leading *Mtb*BPL inhibitor **1.22**, with an acyclic chain replacing the ribose group as in **1.20**, current leading *Sa*BPL inhibitor **1.23**, with 2-benzoxazolone in place of adenine as in **1.22**.

_____

Tieu and co-workers in Abell research group, Adelaide, also identified a 2-benzoxazolone moiety of **1.23** (Figure 1) as a structural mimic of adenine group of **1.22**.[9] 2-Benzoxazolone triazole **1.23** is a potent and selective inhibitor against *Sa*BPL with a $K_i = 0.09 \pm 0.01$ µM, which is over 11-fold more potent than **1.22** ($K_i = 0.7$ µM against *Sa*BPL). It also exhibited >1100-fold selectivity over the human isoform (*Hs*BPL) and is inactive against *Mtb*BPL, making 1,2,3-triazole **1.23** the most potent and selective *Sa*BPL inhibitor identified to date.[9] In addition, bacteriostatic activity was observed, where **1.23** prevented cell growth of *S. aureus* ATCC 49775 by 80% at 8 µg/ml.[9] *In vivo* study of triazole **1.23** was also conducted in mice for preliminary pharmacokinetic assessment and efficacy.[9,10] When administered subcutaneously (dose 30 mg/kg) the maximum serum concentration (C_{MAX}) of **1.23** was 3 µg/ml, which was 2-fold below the MIC (8 µg/ml).[9,10] In order to obtain *in vivo* efficacy in the infection model, an ideal compound should yield a C_{MAX} in excess of the MIC. Both triazoles **1.22** and **1.23** were nontoxic in a human HepG2 cell culture model making them attractive hits for further development.

Given the limitations of triazole **1.23** in animal trials, presumably due to its low aqueous solubility, specific chemical modifications are required to improve its drug-like properties. Towards this goal, previous modifications of the biotin site of the triazole based analogues (highlighted in green, Figure 2A) and understanding of the biotin-binding site from x-ray crystallography of *Sa*BPL (Figure 2B) addressed a number of limitations for modifying biotin structure.[11-14] An overview of these limitations is listed below.
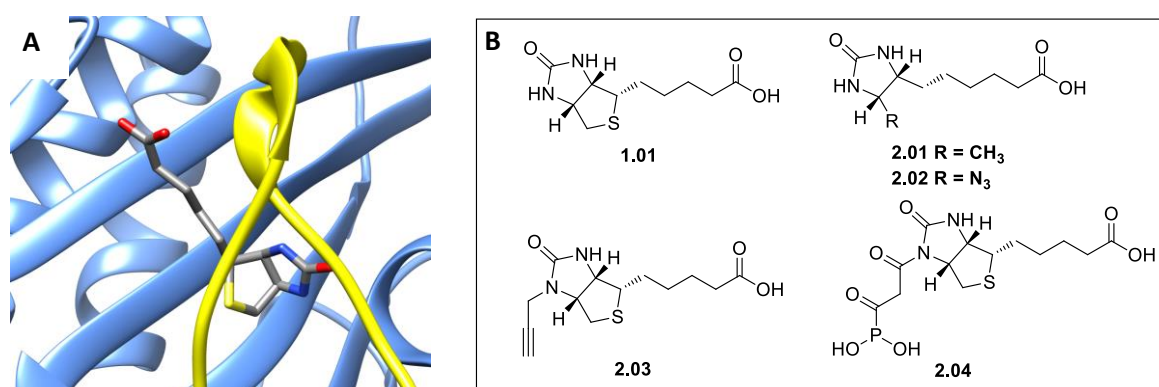

Figure 2: (A) X-ray structure of *Sa*BPL in complex with biotin **1.01** PDB 3V8K.[9,11] (B) Chemical structures of biotin **1.01** and its analogues α-methyldethiobiotin **2.01**[14], dethiobiotin azide **2.02**[13], propargyl biotin **2.03**[13], biotin phosphonacetate **2.04**.[12]

1. Chemical modifications upon the ureido and thiophane rings of biotin **1.01**, such as α-methyldethiobiotin **2.01** and dethiobiotin azide **2.02** (Figure 2B), were carried out by

_____

Hanka *et al*[14] and Slavoff *et al*[11,13] respectively. These compounds displayed limited activity against BPLs in a variety of species (e.g. *S. aureus, E. coli* and *Homo sapiens*) suggesting that chemical modifications upon biotin rings were not tolerated. In addition, the x-ray crystallographic data and primary sequence analysis indicated that the biotin-binding pocket is highly conserved amongst BPL.[9] Therefore, modifying biotin rings is not favourable for the development of selective BPL inhibitors over the human counterpart.

2. The x-ray crystallography of *Sa*BPL in complex with biotin **1.01** indicated a relatively small biotin-binding pocket (Figure 2A).[9] Biotin analogues, such as propargyl biotin **2.03**[13] and biotin phosphonacetate **2.04** (Figure 2B)[12], resulted in no inhibition against bacterial BPLs. These results, together with the x-ray crystallography of *Sa*BPL in complex with biotin **1.01** (Figure 2A)[11,13], indicated a relatively small biotin-binding pocket, hence restricting the opportunity to extend from the biotin rings.

3. Likewise, the hydrophobic tunnel in the biotin-binding pocket that accommodates the hydrogen carbon chain between 1,2,3-triazole and the biotin rings is relatively narrow, limiting modifications that can be made to this area.[9,11]

Given the limited scope for modifying the biotin site of triazole, the proposed triazole analogues described in this chapter retain the biotin, adenine or benzoxazolone and triazole components which are suggested to be necessary for binding. This chapter builds on preliminary results as described above with the design, synthesis and assay of more 1,2,3-triazole based inhibitors towards *Sa*BPL and *Mtb*BPL in an attempt to achieve improved potency, selectivity, and *in vitro* antibacterial activity. Specific chemical modifications were conducted in two areas of the leading inhibitors **1.22** and **1.23** (highlighted in Figure 3), as described below:
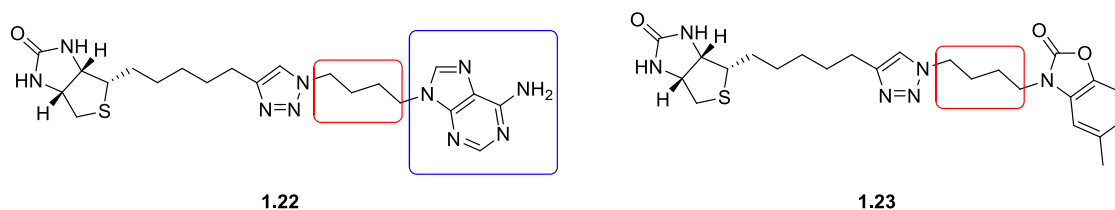
Figure 3: Current leading *Mtb*BPL inhibitor, **1.22** (Right); current leading *Sa*BPL inhibitor **1.23** (Left). Red square represents the tether area with chemical modifications discussed in this chapter section 2.2; Blue square represents the adenine moiety with modifications discussed in this chapter section 2.3.

_____

1. Chemical modifications and extensions were conducted in the tether area between the 1,2,3-triazole ring and adenine (**1.22**) motif or benzoxazolone (**1.23**) motif (highlighted in red, Figure 3). The 3D structures of triazole **1.22** and **1.23** bound to *Sa*BPL (Figure 4) suggest a relatively open environment at the tether area which allows more room for chemical modifications.[9] The design, synthesis and assay results of these triazoles are discussed below in section 2.2.

2. Direct analogues to the adenine bicyclic ring system of **1.22** (highlighted in blue, Figure 3) were investigated and are discussed below in section 2.3. From the x-ray crystallography data of *Sa*BPL, in complex with **1.22** (Figure 4), amino acid residues Asn212 and Ser128 are involved in hydrogen bonding interactions with the adenine motif of **1.22**.[9] Trp127 participates in a $\pi - \pi$ stacking with adenine rings. In addition to these interactions, the ATP binding pocket contains a number of amino acid residues adjacent to the adenine motif, such as Arg227 and Lys187.[9] These amino acids provide additional hydrogen bonding sites allowing more interactions to form. Thus, targeting the ATP binding pocket by modifying the adenine rings was anticipated to provide opportunities for improving potency and selectivity against bacterial BPLs (e.g. *Sa*BPL and *Mtb*BPL).
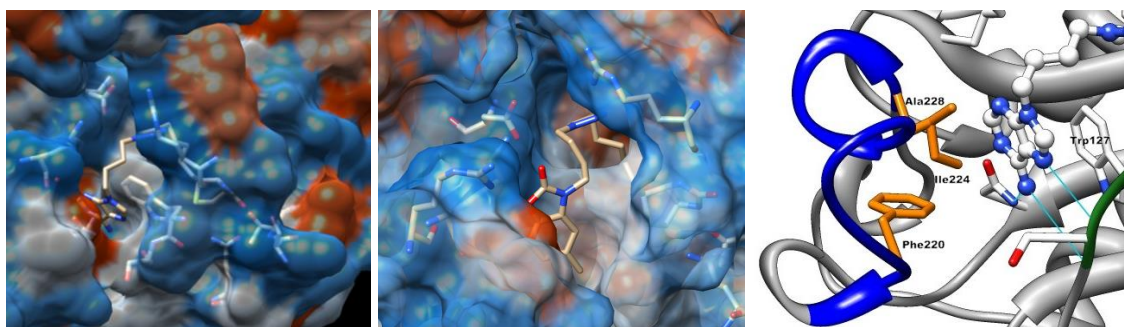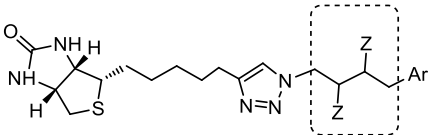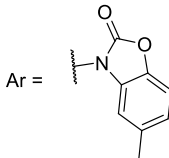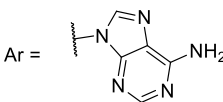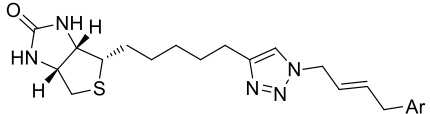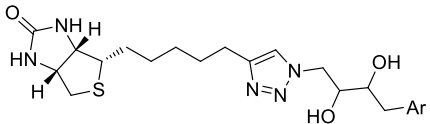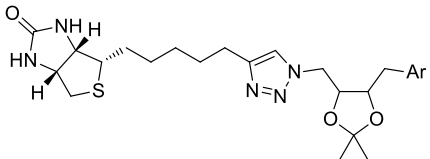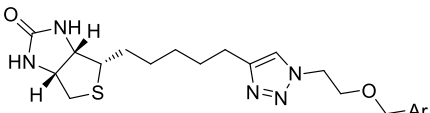

Figure 4: 3D depictions of *Sa*BPL surface with triazole **1.22** PDB 3V7R[9] (Left) and **1.23** PDB 3V7S[9] (Middle); The zoomed depiction of ATP binding pocket of *Sa*BPL in complex with **1.22** (Right).

2.2 Design, synthesis and assay of tether analogues

The design of triazole inhibitors, shown in Table 1 and discussed in this chapter, was based on the reported X-ray crystal structures of triazole **1.22** and **1.23** bound to *Sa*BPL[9] (Figure 4). Docking studies of the proposed triazole **2.05-2.12** with *Sa*BPL were performed, and are discussed below in section 2.2.1, in order to predict and visualise the binding modes of these triazoles. The features of proposed triazoles are summarised and discussed below.

Table 1: Leading inhibitors **1.22** and **1.23**, and the proposed triazole analogues **2.02-2.09**

	1.23 (Z = H)	**1.22** (Z = H)
	2.05	**2.09**
	2.06	**2.10**
	2.07	**2.11**
	2.08	**2.12**

1. 1,2,3-Triazoles **2.05** and **2.09**, containing constrained double bonds in the tether, provide the starting points for the synthesis of 1,2,3-triazoles **2.07-2.10**. More importantly, a number of studies have stated that an increased protein-ligand binding affinity may accompany the introduction of conformational constraints into flexible ligands.[15-18] Thus, these modifications with constrained double bonds were encouraged by these reports and presumably are more favoured for binding to BPLs.

_____

2. 1,2,3-Triazoles **2.06** and **2.10**, containing di-hydroxyl groups at the tether area, provide additional hydrogen bond accepting and donating sites which allow more potential hydrogen bonding interactions to form. Increased polarity due to these hydroxyl groups also potentially improves improved aqueous solubilities.

3. Protecting the di-hydroxyl groups of **2.06** and **2.10** as an acetonide, as shown in **2.07** and **2.11,** mimics the original ribose ring as found in the native reaction intermediate **1.03**. Such modifications were designed to rationalise the potency and selectivity upon the ribose analogues. Also, these modifications restrict flexibility of the hydroxyl groups to form more rigid structures. This leads to a potential beneficial entropic contribution to binding which may enhance binding affinity to BPLs.

4. Replacing the saturated hydrogen carbon chain between triazole and adenine of **1.22** and benzoxazolone of **1.23** with a glycol tether, as shown in **2.08** and **2.12,** provides an additional hydrogen bonding site for more potential hydrogen bonding in this area. These glycol type tethers also potentially increase the overall polarity of the compounds, hence improving aqueous solubility, while maintaining the same tether length (four atoms) allows the proposed triazoles **2.08** and **2.12** to achieve optimal binding.

2.2.1 Docking

All these structures and the bound ligands of the protein 3V7S and 3V7R were docked by using the software AutoDockTools 1.5.6 and binding affinities were predicted. All molecules were drawn using ChemBio3D Ultra 12.0 with energy minimised before loading to the AutoDockTools.[19]

The protein for docking was taken from RCSB protein data bank: *Staphylococcus aureus* 3V7S.[9] The original bound ligand was removed and all water molecules were also removed from the original Protein Data Bank file. Polar hydrogen atoms were added and the protein was set as a rigid conformation for docking. Each docking ligand was prepared by setting to the fewest number of active torsions for rotating during docking.

Docking was performed using the Lamarkian genetic algorithm. Each docking experiment was performed 10 times, yielding 10 docked conformations. Parameters for the docking were as follows: population size of 150; random starting position and conformation;

_____

mutation rate of 0.02; crossover rate of 0.80; and elitism value of 1. Simulations were performed with a maximum of 250,000 energy evaluations and a maximum of 27,000 iterations.
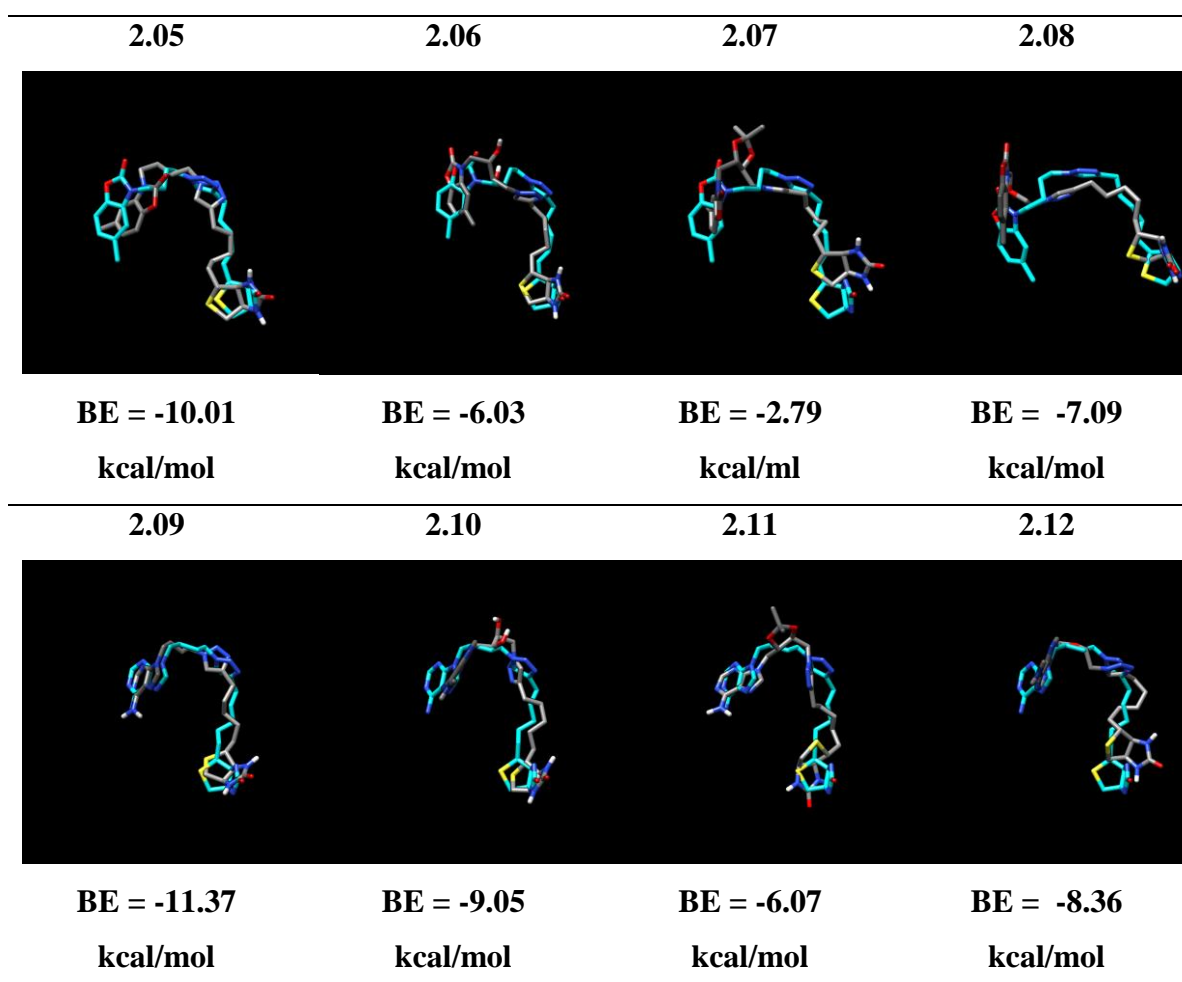
Before docking the proposed molecules into the binding site, the docking protocol was validated by removing the 3V7S bound ligand (**1.23**, Figure 5 Left) and the 3V7S bound ligand (**1.22**, Figure 5 Right) from their active sites and docking back into the same binding sites.[9] As shown in Figure 5, the predicted binding conformation of **1.23** (left grey stick) and **1.22** (right grey stick) represented conformational superposition with the obtained ligand from the x-ray crystallography (purple sticks), suggesting the reasonable docking parameters that can be performed for the proposed triazoles.
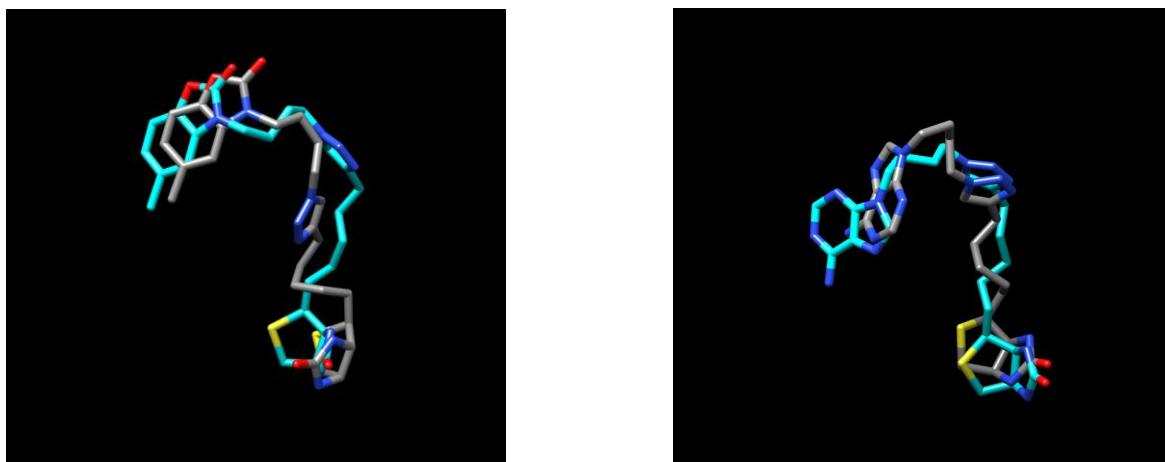
Figure 5: (Left) A superimposed image of the predicted binding conformation of **1.23** (grey stick) with the original 3V7S[9] bound ligand (cyan stick); (Right) A superimposed image of the predicted binding conformation of **1.22** (grey stick) with the original 3V7R[9] bound ligand (cyan stick).

_____

Final docked conformations were ranked by binding energy and the conformation with the highest ranking was selected to compare and overlay with the original bound ligands **1.22** and **1.23**, respectively. The overlayed images are listed below in Figure 6 with the corresponding binding energy (BE) shown therein.

2.05	2.06	2.07	2.08

BE = -10.01 kcal/mol	BE = -6.03 kcal/mol	BE = -2.79 kcal/ml	BE = -7.09 kcal/mol

2.09	2.10	2.11	2.12

BE = -11.37 kcal/mol	BE = -9.05 kcal/mol	BE = -6.07 kcal/mol	BE = -8.36 kcal/mol

Figure 6: Superimposed images of the proposed triazoles **2.05-2.12** with the original bound ligands and their corresponding bonding energies. (Top): 2-Benzoxazolone triazoles (grey sticks) overlayed with the bound ligand **1.23** of 3V7S (cyan sticks); (Bottom): Adenine triazoles (grey sticks) overlayed with the bound ligand **1.22** of 3V7R (cyan sticks).

All docked molecules interacted the same binding mode and U-shape geometrical orientation as observed with crystallised ligand (**1.22**) of 3V7R and ligand (**1.23**) of 3V7S, suggesting that the proposed triazoles **2.05-2.12** can bind to the binding pockets of *Sa*BPL, hence potentially can be developed as potent inhibitors. Docking scores for benzoxazolone analogues (**2.05**- **2.08**) varied from -2.79 to -10.01 kcal/mol, while a score range between -6.07 and -11.37 kcal/mol was obtained for adenine analogues (**2.09-2.12**). Adenine analogues had a higher average score than that of benzoxazolone analogues, indicating that adenine analogues may be more active than the benzoxazolone series. Furthermore, the

constrained tether analogues (**2.05** and **2.09**) yielded the highest dock scores (-10.01 and -11.37 kcal/mol) in their corresponding categories, suggesting that these two analogues may be developed as the most active inhibitors of this series.

2.2.2 Building blocks for triazole 2.05-2.12

The synthesis of triazoles **2.05-2.12** utilises the building blocks azides **2.13-2.20** (shown in Figure 7A) and biotin acetylene **2.21** (shown in Figure 7B) and involves the optimised copper mediated alkyne azide cycloaddition reaction (CuAAC) condition for coupling, as reported by Tieu *et al.*[9,11]
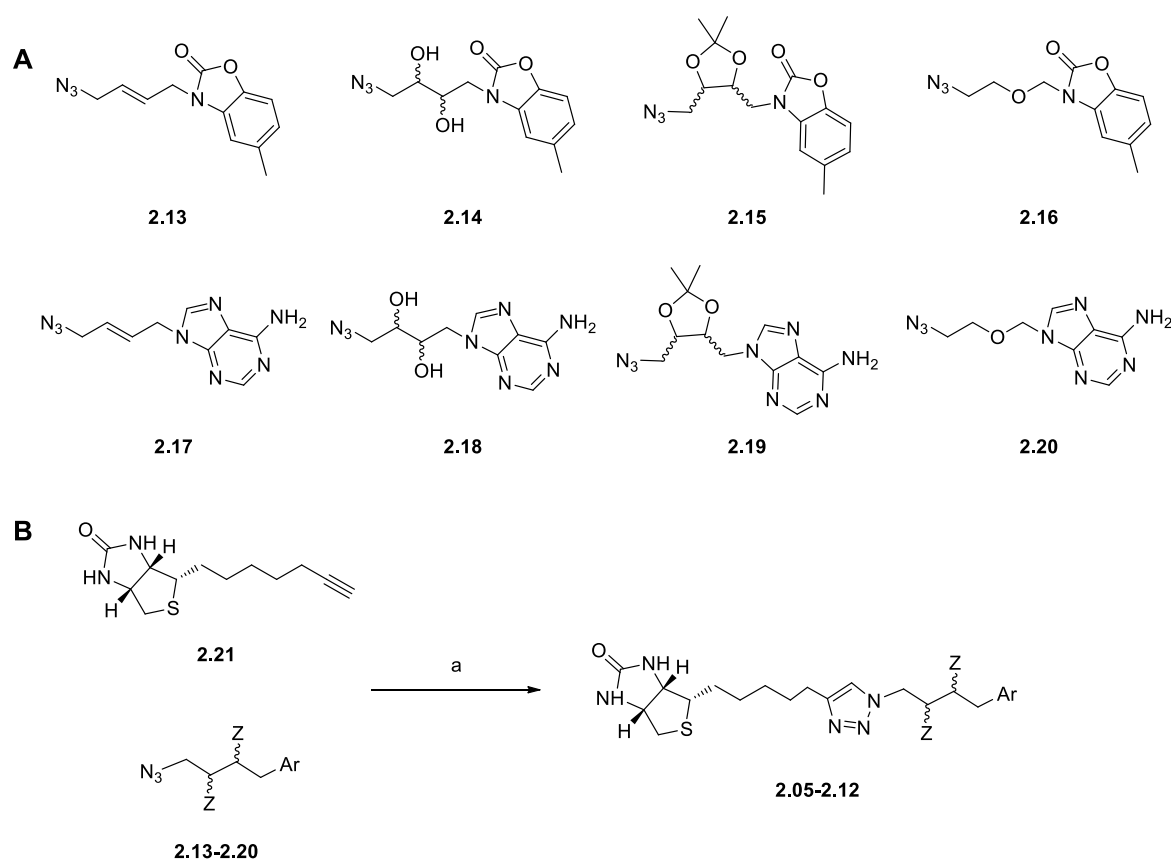
Figure 7: (A) Precursors for the synthesis of triazole **2.05-2.12**. (B) CuAAC reaction between biotin acetylene **2.21** and purine azide **2.13-2.20** to give 1,4-triazole **2.05-2.12** a) 20 mol% Cu nano-powder, 2:1 AcCN/H_2O, 12h, rt.

_____

Biotin acetylene 2.21

The synthesis of the key biotin acetylene **2.21** was achieved according to the reported procedure by Tieu *et al* and depicted in Scheme 1.[11]
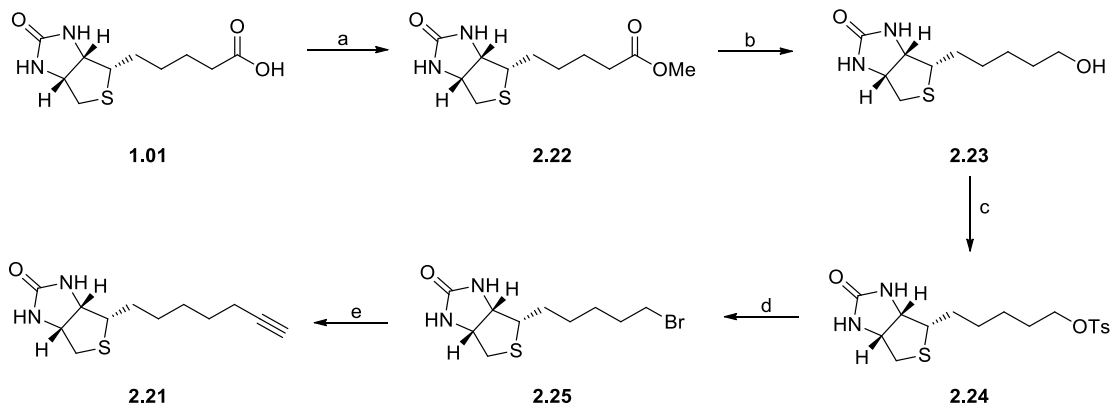
Scheme 1: a) SOCl$_2$, MeOH, 90 min; b) LiAlH$_4$, THF, 12h; c) TsCl, Py, 5 °C, 12h; d) LiBr, MEK. 80 °C, 3 h; e) Li-acetylide EDA complex, DMSO, 15 °C, 3h;

Biotin **1.01** was firstly treated with thionyl chloride in methanol to give the methyl ester **2.22** in quantitative yield. The subsequent reduction of methyl ester **2.22** using LiAlH$_4$ gave biotinol **2.23** in 90% yield. Biotinol **2.23** was obtained in >95% purity (judged by HPLC) by simply adding Na$_2$SO$_4$ and isolating the resulting solid by vacuum filtration that was used without further purification. Biotinol **2.23** was then tosylated by reacting tosyl chloride, in dry pyridine, at 5 °C, to give tosylate **2.24**. The tosylate **2.24** was unstable and decomposed on silica gel chromatography, it was thus used in the next synthetic step without purification. The crude tosylate **2.24** was treated with lithium bromide in 2-butanone (MEK), under reflux, to give biotin bromide **2.25** in 55% yield over two steps. Treatment of **3.19** with lithium acetylide ethylene diamine complex (EDA), in DMSO at ambient temperature, gave biotin acetylene **2.21** in a yield of 80%.

00

Alkene azides 2.13 and 2.17

Following the reported conditions as described by Tieu *et al*[20], treating 2-amino-cresol **2.26** with CDI in DCM gave 2-benzoxazolone **2.27** in 96% yield and over 95% purity as judged by ^{1}H NMR. **2.27** was then used for the synthesis of 2-benzoxazolone bromide **2.28** without further purification. Treating **2.27** with potassium carbonate and di-bromobutene in DMF at 50 °C for 12 h gave **2.28** in yield of 65% after purification by flash

_____

chromatography. The 2-benzoxazolone bromide **2.28** was then reacted with sodium azide in DMF to give the corresponding azide **2.13** in 83% yield after purification by flash chromatography (Scheme 2).
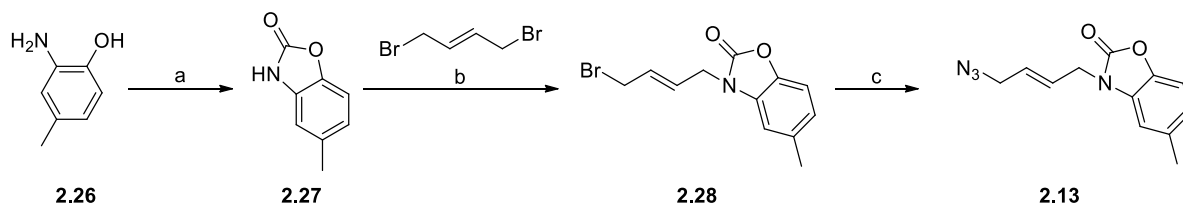
Scheme 2: a) CDI, DCM, rt, 45 min; b) $Br(CH_2)_2(CH)_2Br$, K_2CO_3, DMF, 50 °C, 12h; c) NaN_3, DMF, rt, 12h.

Following the same conditions for the preparation of **2.13**, adenine **2.29** was initially alkylated with di-bromobutene in DMF at 50 °C to give adenine bromide **2.30** (Scheme 3, entry 1) in a low yield of 10% after purification by flash chromatography. In order to improve the yield of **2.30**, alternative conditions were investigated as outlined in Table 2.
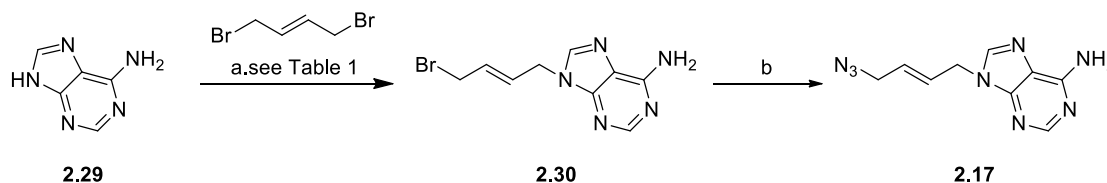
Scheme 3: a) see Table 2; b) NaN_3, DMF

Table 2ª: Optimisation of 2.30

Entry	Solvent	Base[a]	Temp (°C)	Time	Yield[b] (%)
1	DMF	K_2CO_3	50 °C	12 h	10
2	DMF	K_2CO_3	rt	12 h	30
3	DMF	NaH	-78 °C to rt	6 h	5
4	DMF	Cs_2CO_3	rt	4 h	55%

[a] All reactions were conducted with 1.5 equiv of base and monitored by TLC (1: 9 MeOH/DCM); [b] isolated yield of **2.30** after column chromatography (1: 9 MeOH/DCM).

_____

The key observation to the initial condition as described in entry 1 was that the starting material **2.29** was all consumed, suggesting that the poor yield of **2.30** might be due to the instability of **2.30** under the thermal conditions. The reaction was thus repeated at room temperature (entry 2) instead of 50 °C (entry 1) to give an improved yield of 30% (entry 2). Replacing potassium carbonate with sodium hydride and performing the reaction under -78 °C gave a reduced yield of 5% (entry 3). Finally, caesium carbonate was used and the reaction was repeated at room temperature. The TLC monitoring indicated that all starting material was consumed after 4 h and purification of the crude product by column chromatography gave an improved yield of 55% (entry 4). Finally, bromide **2.30** was reacted with sodium azide in DMF to give the corresponding azide **2.17** in 83% yield.

Diol azides 2.14, 2.18 and acetonide azides 2.15, 2.19

The synthesis of 2-benzoxazolone diol azide **2.14** was attempted using a variety of conditions as listed in Table 3 and discussed below. The subsequent 2-benzoxazolone acetonide azides **2.14** was synthesised by protecting the dihydroxyl groups of **2.14** with 2,2-dimethoxypropane as described in Scheme 4.
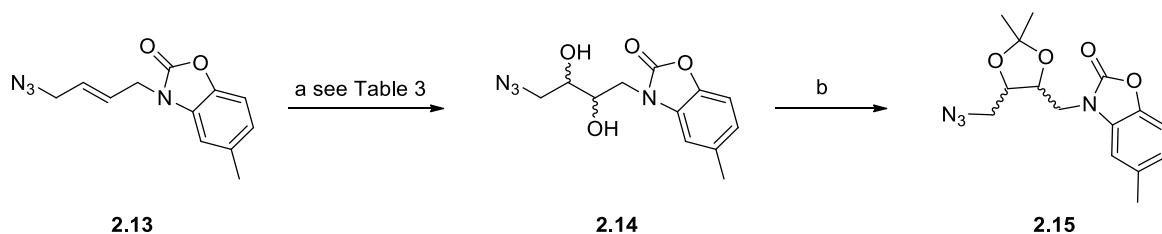
Scheme 4: a) see Table 3; b) DMP/(CH$_3$)$_2$CO (1:1), pTsOH$_{(cat)}$, rt, 12h.

Table 3^a: Synthesis of 2-benzoxazolone diol azide 2.14

| Entry	catalyst	Solvent	Temp	Yield^e (%)
1^a	AD-mix α^c	t-BuOH: water (1: 1)	0 °C to rt	0
2^a	AD-mix β^c	t-BuOH: water (1: 1)	0 °C to rt	0
3^b	OsO$_4$^{d}	Acetone: water (10: 1)	rt	46

^{a} Reactions in entries 1 and 2 were carried out at 0 °C for 15 min, followed by stirring at room temperature for 12 h. ^{b} Reactions in entries 3 were carried out at room temperature

_____

for 12 h. [c] 1.5 equivalent of AD-mix was added to each entry. [d] 5 mol % of OsO$_4$, NMO. [e] isolated yield after flash chromatography (9: 1 DCM/MeOH).

The dihydroxylation reaction of alkene azide **2.13** to give **2.14** was initially attempted following a general protocol developed for Sharpless dihydroxylation in order to prepare the enantioselective diols.[21,22] Conditions for asymmetrical dihydroxylation, using 1.5 equivalents of commercially available AD-mix α (pre-packaged mixtures containing: K$_2$OsO$_2$(OH)$_4$, K$_2$CO$_3$, K$_3$Fe(CN)$_6$, (DHQD)$_2$PHAL) in a *t*-BuOH/water (1:1) mixture) were initially investigated.[21,22] The desired diol product **2.14** was not observed or isolated under these conditions (Table 3, entry 1), rather the starting material **2.13** was simply recovered. Replacing AD-mix α with AD-mix β (pre-packaged mixtures containing: K$_2$OsO$_2$(OH)$_4$, K$_2$CO$_3$, K$_3$Fe(CN)$_6$, (DHQ)$_2$PHAL) gave the same result as observed in entry 1, where only the starting material **2.13** was recovered. Indeed, it has been previously reported that the rate of the asymmetric dihydroxylation of electron-deficient olefins, such as **2.13**, can be very low.[23] Moreover, the ligand prepacked in the AD-mix α ((DHQD)$_2$PHAL) or AD-mix β ((DHQ)$_2$PHAL) may not be ideal for the dihydroxylation reaction of alkene azide **2.13**.

Given the limited scope of asymmetric hydroxylation of **2.13**, a *syn*-selective preparation of 2-benzoxazolone diol azide **2.14** using the Upjohn dihydroxylation was then performed[24] (Table 3, entry 3). The 2-benzoxazolone alkene azide **2.13** was treated with osmium tetroxide and *N*-methylmorpholin *N*-oxide (NMO) as the cooxidant in a solvent mixture of acetone/water (10:1).[24] The crude material was purified by flash column chromatography to give the desired product **2.14** in 46% yield. Importantly, the reaction was carried out in the absence of chiral ligands ((DHQD)$_2$PHAL) and (DHQ)$_2$PHAL)) which would result in the formation of a racemic mixture of diol azide **2.14**.[24] The ratio of each enantiomer of **2.14** was determined to be 1:1 using chiral-HPLC (see section 2.2.4 for details). An enantioselective synthesis of 2-benzoxazolone diol azides of **2.14** was not further investigated as the final 2-benzoxazolone diol triazoles **2.07** and **2.08** were found to be inactive against *Sa*BPL (discussed in section 2.2.5). With the racemic mixture of 2-benzoxazolon diol azides **2.14** in hand, protection of the di-hydroxyl groups was accomplished by reacting **2.14** with a mixture of 2,2-dimethoxypropane/acetone (1:1) in the presence of *p*-toluenesulfonic acid monohydrate to give the corresponding acetonide **2.15** as the racemic mixture in 58% yield after purification by flash chromatography.

The synthesis of adenine diol azide **2.18** was achieved using the optimised condition for the preparation of 2-benzoxazolon diol azides **2.14** as described in Table 3, entry 3. As shown below in Scheme 5, adenine alkene azide **2.17** was treated with NMO and osmium tetroxide in acetone/water (10:1) mixture to give **2.18** in 43% yield after purified by flash chromatography. Protection of the di-hydroxyl group of **2.18**, on treatment with a mixture of 2,2-dimethoxypropane/acetone (1:1) in the presence of *p*-toluenesulfonic acid monohydrate, gave adenine acetonide **2.19** in 29% yield after purification by flash chromatography (Scheme 5).
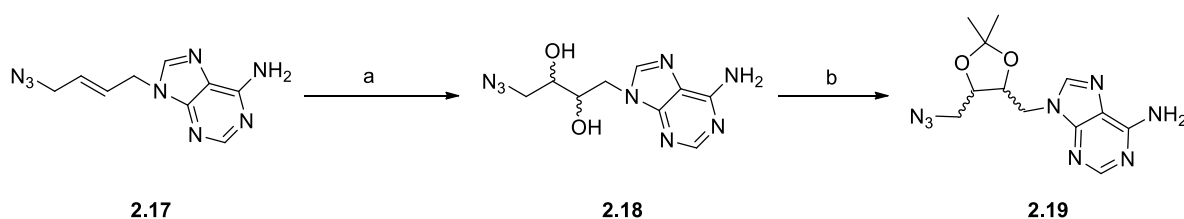
Scheme 5: a) OsO_4, NMO, $(CH_3)_2CO/H_2O$ (10:1), rt, 12h; b) DMP/$(CH_3)_2CO$ (1:1), pTsOH$_{(cat)}$, rt, 12h.

The racemic diol azides **2.14**, **2.18** and acetonide azides **2.15**, **2.19** were analysed by HPLC using a chiral column and results are discussed in section 2.2.4. The racemic azides was used for preparation of triazoles **2.07-2.10** via CuAAC without separation.

_____

Glycol azides 2.16 and 2.20

The preparation of glycol azides **2.16** and **2.29** required a four step synthesis starting with the respective alkylation of 2-benzoxazolone **2.27** and adenine **2.29** with 2-(bromomethoxy) ethyl acetate **2.31**, as described in Schemes 6 and 7, respectively.
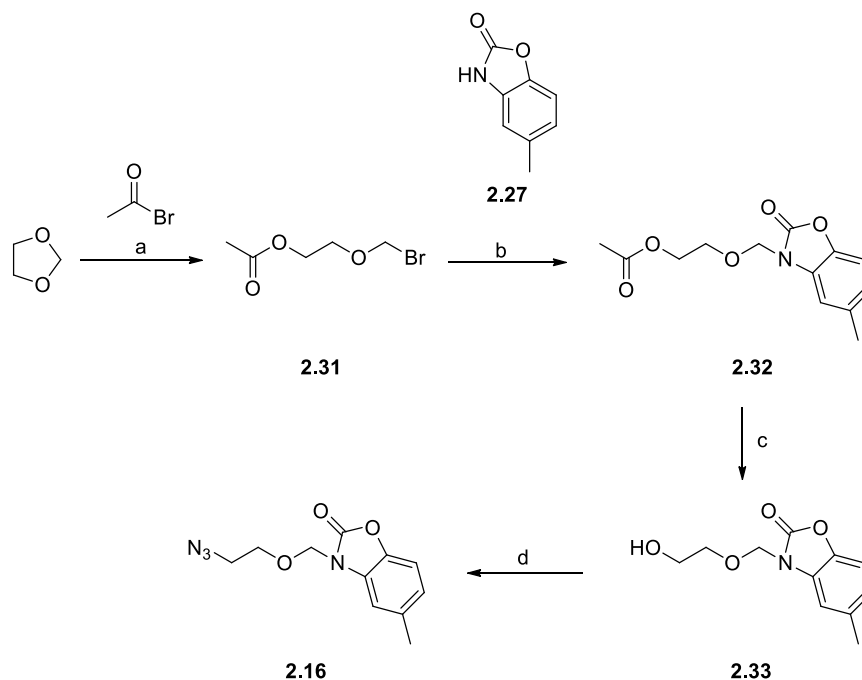
Scheme 6: a) 60 °C, 3 h; b) K_2CO_3, DMF, 50 °C, 30 min; c) LiOH (1.0 M), MeOH, THF, rt, 1h; d) CCl_4, NaN_3, TEA, DMF, 80 °C, 1.5h;

The key reagent, 2-(bromomethoxy) ethyl acetate **2.31**, was synthesised according to the reported procedure by Kai *et al.*[25] Treating acetyl bromide with 1,3-dioxolane at 60 °C for 3 h and the following removal of excess starting materials under reduced pressure, gave **2.31** that was used without further purification. The bromide **2.31** was then attached to 2-benzoxazolone **2.27** in the presence of potassium carbonate to give the corresponding ester **2.32** in 83% yield. The resulting glycol ester **2.32** was then hydrolysed to the corresponding alcohol **2.33** on reaction with lithium hydroxide and methanol in THF with an isolated yield of 32% after purification by flash chromatography. Following the modified Appel reaction[26], alcohol **2.33** was treated with carbon tetrachloride, sodium azide and triethylamine in anhydrous DMF to give its corresponding azide **2.16** in a moderate yield of 67% after purification by flash chromatography.

_____

The preparation of adenine glycol azide **2.20** was similar to the synthesis of **2.16** and shown below in Scheme 7. However, the alkylation of adenine **2.29** with 2-(bromomethoxy) ethyl acetate **2.31** was accomplished at room temperature in the presence of caesium carbonate to give **2.34** in 83% yield after purified by flash chromatography. The resulting adenine glycol ester **2.34** was hydrolysed to the corresponding alcohol **2.35** in 48% yield. Finally, **2.35** was converted to the azide **2.20** in 13% yield after purified by column chromatography.
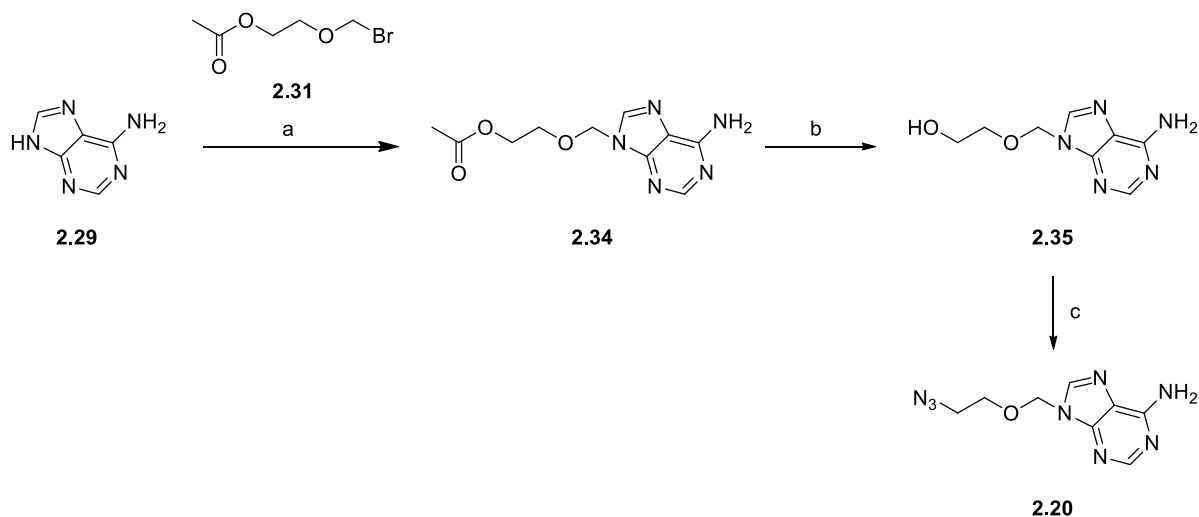
Scheme 7: a) Cs$_2$CO$_3$, DMF, rt, 12h; b) LiOH (1.0 M), MeOH, THF, rt, 1h; c) CCl$_4$, NaN$_3$, TEA, DMF, 80 °C, 1.5h.

2.2.3 Synthesis of 1,4-triazole 2.05-2.12 via CuAAC

Triazole analogues were synthesised according to optimised reaction conditions, as discussed by Tieu *et al.*[9] The appropriate azide **2.13-2.20** and biotin acetylene **2.21** were dissolved in acetonitrile and water mixture (2:1) and treated with 20 mol% copper nano powder, sonicated for 15 min, followed by stirring at room temperature for 12 h. The resulting triazoles **2.05-2.12** were isolated and purified by flash chromatography in yields reported in Table 4. The stereochemistry of diol triazoles **2.06** and **2.10**, acetonide triazoles **2.07** and **2.11** were confirmed by ^{13}C NMR and chiral HPLC experiments and discussed in section 2.2.4.

_____

Table 4: CuAAC between acetylene **2.21** and azides **2.13-2.20**

Azide (reactant)	Ar (product)	Yield[b]	Azide (reactant)	Ar (product)	Yield[b]
2.13	**2.05**	75%	**2.17**	**2.09**	53%
2.14	**2.06**	33%	**2.18**	**2.10**	32%
2.15	**2.07**	43%	**2.19**	**2.11**	44%
2.16	**2.08**	77%	**2.20**	**2.12**	75%

[a] Conditions: copper nano powder, 2:1 AcCN/H_2O, 12 h, sonication, 35 °C;

[b] isolated yields after flash chromatography.

2D ROESY NMR spectra of **2.05-2.12** indicated through space coupling between protons H_A and H_B with H_A and H_C which is consistent with a 1,4-disubstituted rather than 1,5-disubstituted triazole, see Figure 8. This is the expected result based on the CuAAC reaction conditions used in their preparation.[9,27]

2.05
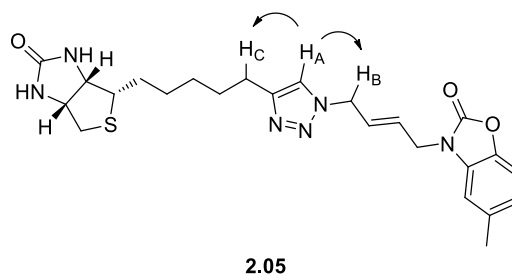
Figure 8: A depiction of through space interactions with arrows indicating interactions observed in ROESY 2D ^{1}H NMR experiment. Triazole **2.05** is shown as a representative example.

2.2.4 Discussion of diastereochemistry of diol triazole 2.06, 2.10 and acetonide triazole 2.07, 2.11

Upjohn dihydroxylation allows *syn*-selective preparation of diols from alkenes.[24] It was difficult to discriminate the diasterioisomers of triazoles **2.06**, **2.07**, **2.10** and **2.11** by ^{1}H NMR, and as such these samples (and precursor azides **2.14**, **2.15**, **2.18**, **2.19**) were further analysed by ^{13}C NMR and HPLC using chiral column (Phenomenex Lux Cellulose-2 3 µM (50 x 2 mm)). HPLC traces and NMR spectra of azide **2.14** and its corresponding triazole **2.06** are shown below in Figures 9 and 10 as representative examples.

The dihydroxylation of 2-benzoxazolone alkene azide **2.13** would be expected to produce a mixture of 2-benzoxazolone (*2R,3R*)-dihydroxybutyl azide **2.14a** and 2-benzoxazolone (*2S,3S*)-dihydroxybutyl azide **2.14b** (Figure 9A). An analytical HPLC trace using reverse phase C18 column of the reaction mixture indicated a single peak at 16 min (Figure 9B), which is consistent with a single diastereoisomer. However, analysis of the same sample with the chiral cellulose-2 column resulted in two peaks at 6.2 and 7.6 min, respectively (Figure 9C). This is consistent with the two *syn* enantiomers 2.14a and 2.14b shown
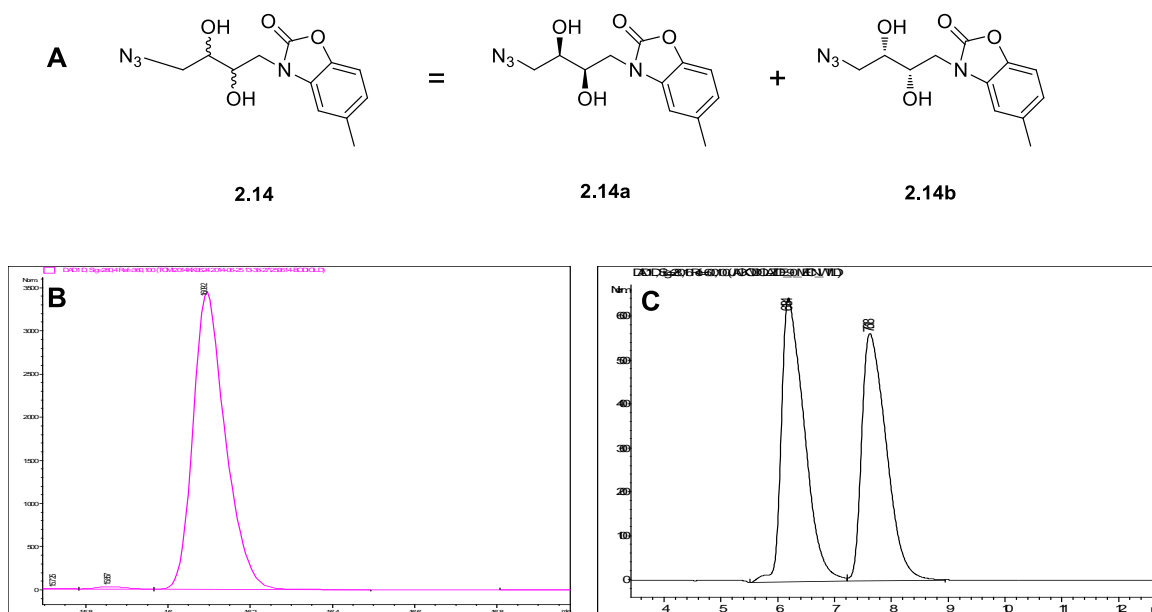
Figure 9: **(A)** A schematic representative of 2-benzoxazolone diol azide **2.14** as a racemic mixture of (*R,R*)-isomer **2.14a** and (*S,S*)-isomer **2.14b**; **(B)** HPLC trace of azide **2.14** using reverse phase C18 column (Phenomenex Luna C18 10 µM (50 x 10 mm)); **(C)** HPLC trace of azide **2.14** using chiral column (Phenomenex Lux cellulose-2 3 µM (50 x 2 mm));

A ^{13}C NMR spectrum of the triazole **2.06** indicated a mixture of diasereoisomers (**2.06a** and **2.06b**) based on doubling of some resonances (Figure 10A). The assignment through 2D HSQC ^{1}H-^{13}C NMR confirmed that: 1) two resonances at 70.2 ppm and 68.8 ppm were due to chiral centres C23 and C24 (Figure 10B); 2) two resonances at 52.7 ppm and 44.8 ppm were due to allylic C20 and C25 (Figure 10C); 3) two resonances at 28.7 ppm and 25.1 ppm were due to the hydrogen carbon chain (C1-C5) from the biotin region (Figure 10D). The evenly split signal of each doublet suggetsted a mixture of two diastereoisomers in a ratio of 1:1. Additionally, the HPLC trace of triazole **2.06** using a reverse phase C18 column indicated a single signal at 10.2 min (Figure 10E). In contrast, HPLC analysis of triazole **2.03** using chiral column revealed two signals with retention time of 13.2 min and 13.8 min (Figure 10F), presumably due to the presence of the two diastereoisomers **2.06a** and **2.06b**.
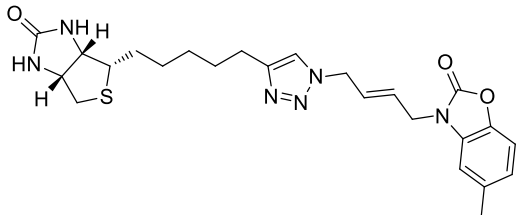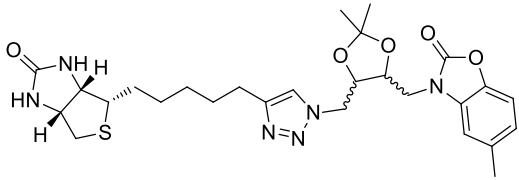
A
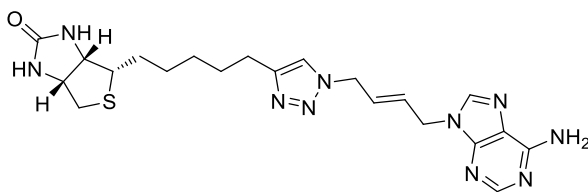

2.06

=

2.06a

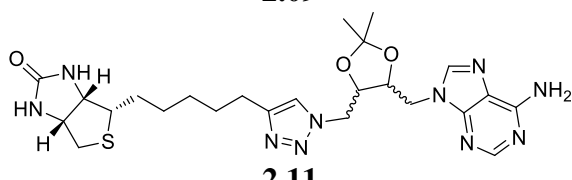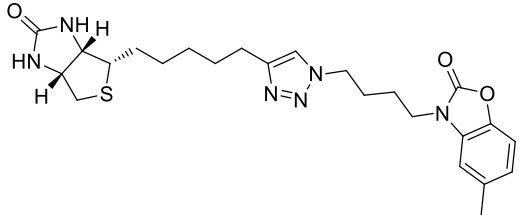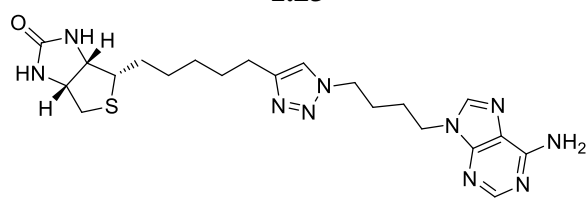+

2.06b

B

C
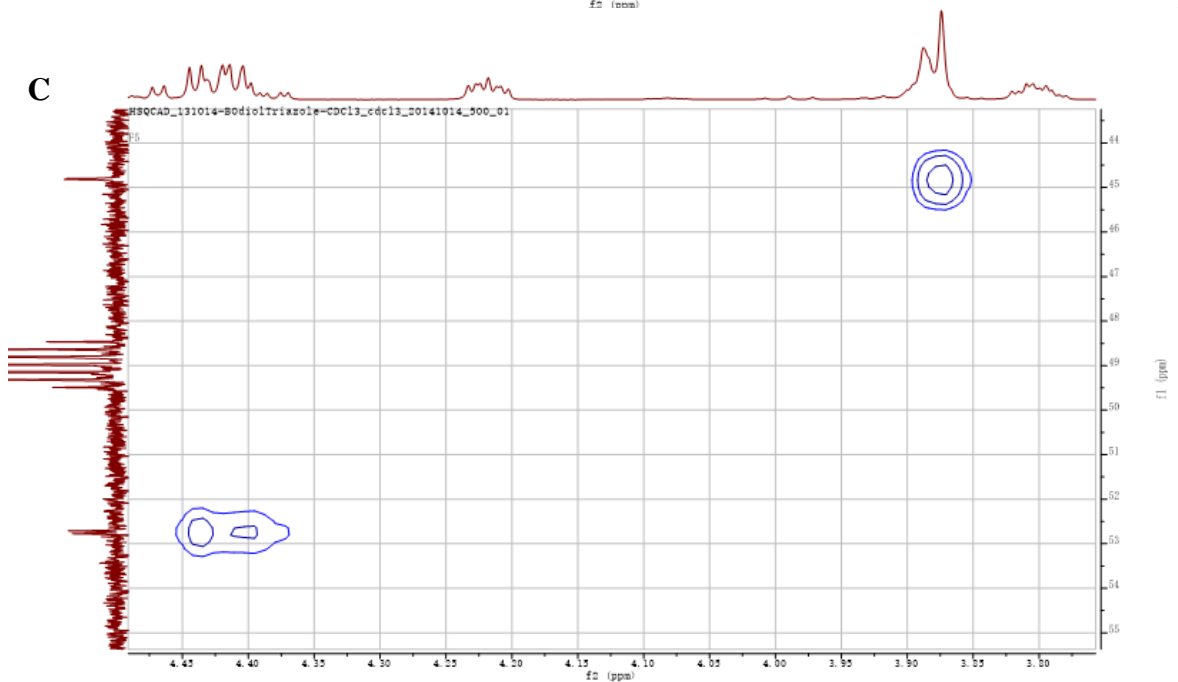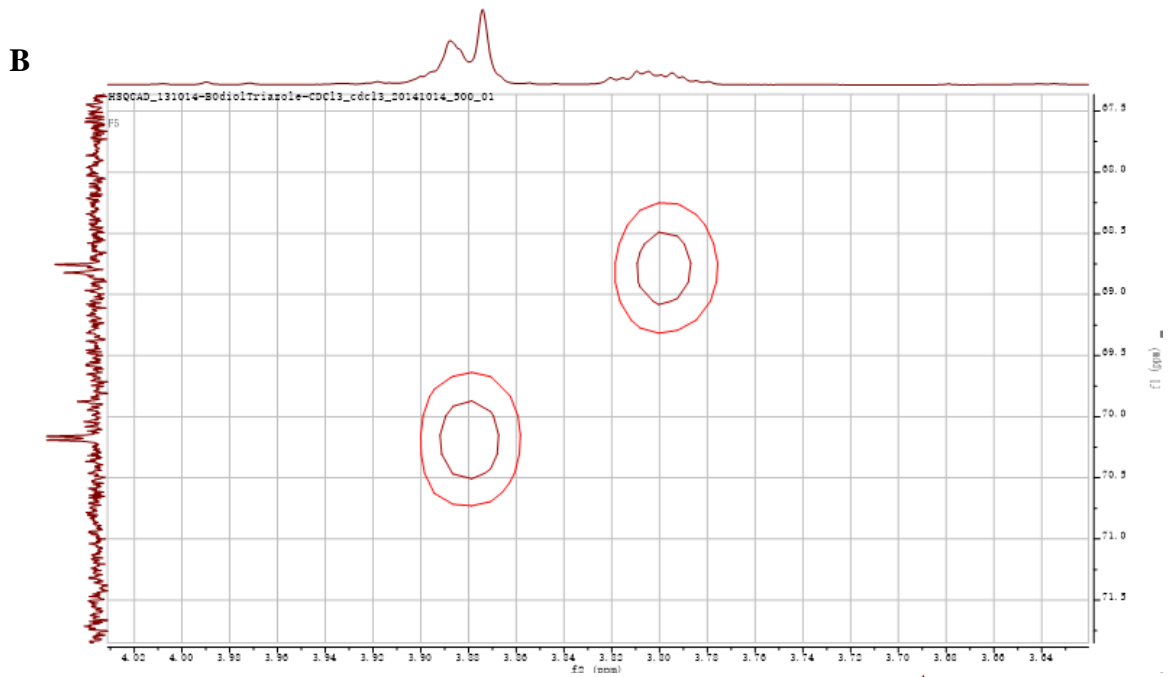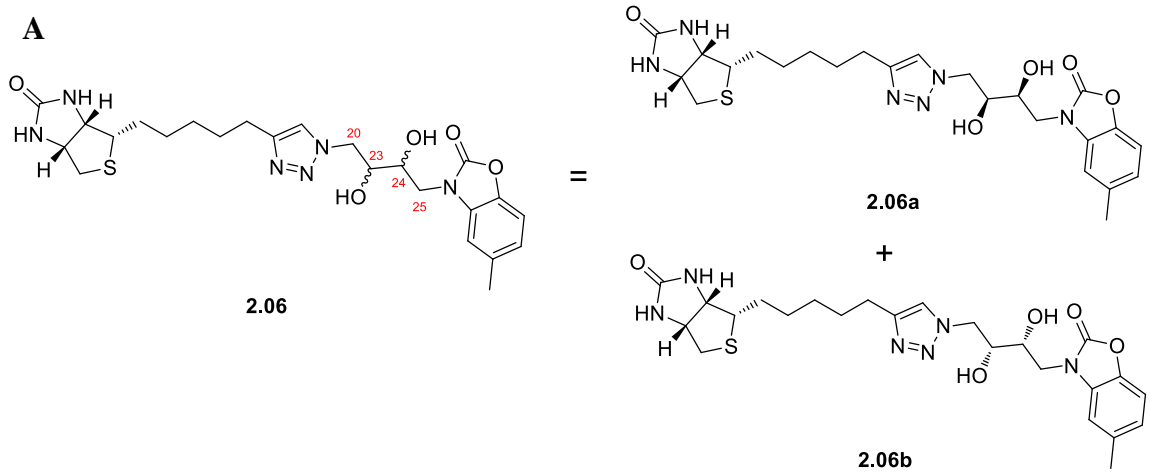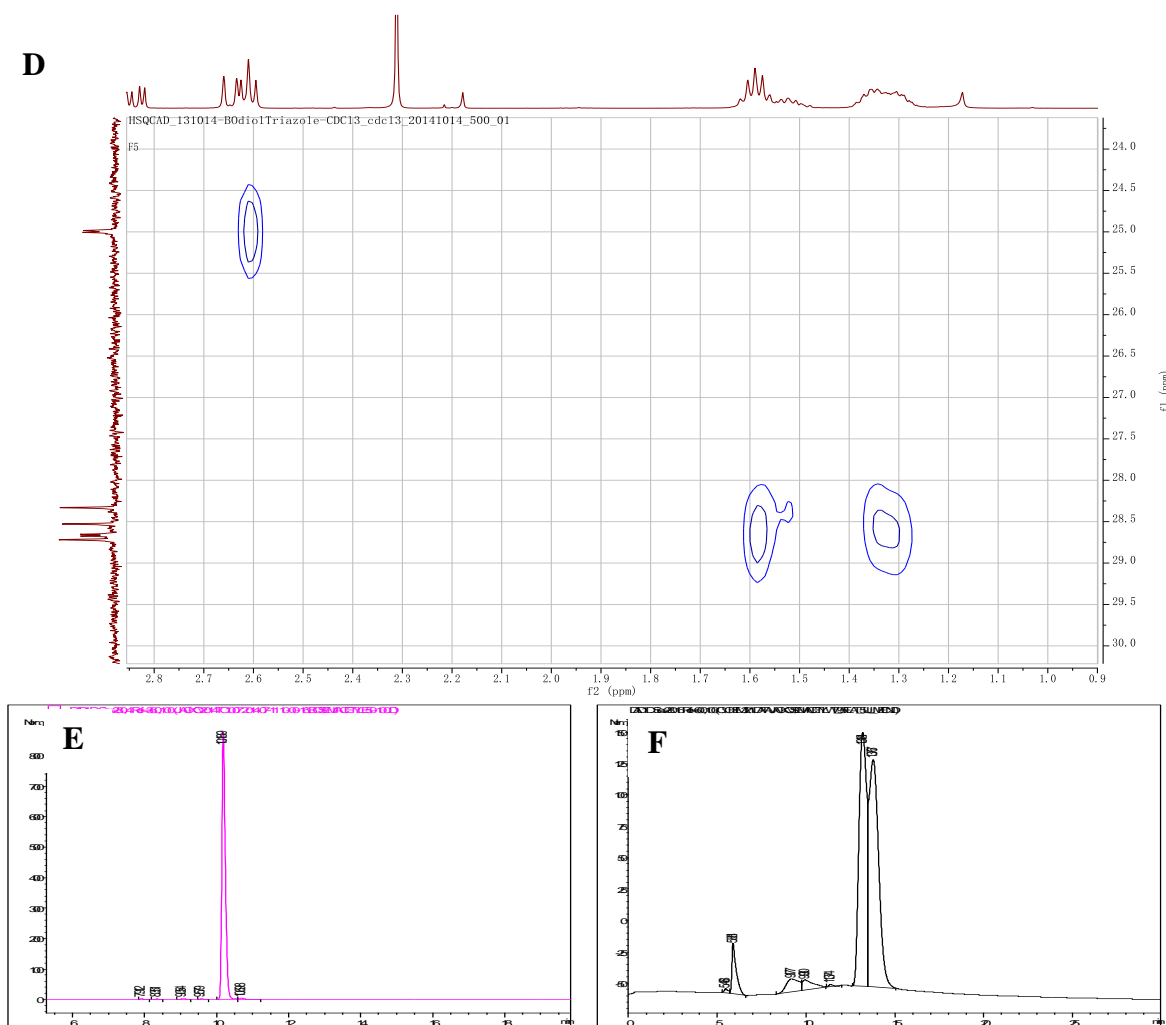
Figure 10: (A) A schematic representative of 2-benzoxazolone diol triazole **2.06** as a diastereoisomer mixture of (*R,R*)-isomer **2.06a** and (*S,S*)-isomer **2.06b**; (B) 2D HSQC ^{1}H-^{13}C NMR spectrum of **2.06** with the duplicated signals zommed at 70.2 ppm and 68.8 ppm; (C) 2D HSQC ^{1}H-^{13}C NMR spectrum of **2.06** with the duplicated signals zommed at 52.7 ppm and 44.8 ppm; (D) 2D HSQC ^{1}H-^{13}C NMR spectrum of **2.06** with the duplicated signals zommed at 28.7 ppm and 25.1 ppm; (E) HPLC trace of **2.06** using reverse phase C18 column (Phenomenex Luna C18 10 µM (50 x 10 mm)); (F) HPLC trace of **2.06** using chiral column (Phenomenex Lux cellulose-2 3 µM (50 x 2 mm))

2.2.5 BPL inhibition and antimicrobial assay results

The 1,4-triazole **2.05-2.12** were assayed against *Sa*BPL, *Mtb*BPL and *Hs*BPL and results are shown in Table 5. The assay was performed by collaborators at Molecular Life Science, University of Adelaide, following the method described by Chapman-Smith and co workers.[28] The IC$_{50}$ value of each compound (or isomeric mixture) was determined from a

dose-response curve by varying inhibitor concentration under the same enzyme concentration.

Table 5: Inhibition of triazole **2.05, 2.07, 2.09** and parent inhibitors **1.22** and **1.23** against *Sa*BPL, *Mtb*BPL and *Hs*BPL.

Compound	*Sa*BPL IC_{50} (µM)	*Mtb*BPL IC_{50} (µM)	*Hs*BPL IC_{50} (µM)
2.05	> 200	> 200	> 200
2.07	5	>200	> 200
2.09	10	10	> 200
2.11	>200	>200	> 200
1.23	0.53 ± 0.01	>200	>200
1.22	4.0 ± 0.9	3.9 ± 0.8	>200

In vitro biotinylation assays were carried out using 6.25 nM of enzyme.

_____

Triazole **2.05**, the direct triazole analogue of benzoxazolone triazole **1.23** (IC_{50} = 0.53 ± 0.01 µM against SaBPL), showed no inhibitory activity against SaBPL under 200 µM. Interestingly, adenine alkene triazole **2.09** was found to show inhibitory activities when assay concentration was over 10 µM, which was at least 2-fold less active than its parent lead structure **1.22** which contains the same adenine group (IC_{50} = 4.0 ± 0.9 µM against SaBPL, IC_{50} = 3.9 ± 0.8 µM against MtbBPL). These observations suggest that flexibility of tether between the triazole and 2-benzoxazolone or adenine groups is critical for inhibitory activity towards SaBPL and MtbBPL.

Interestingly, triazoles **2.07** with an acetonide group in the tether region was found to be a good inhibitor of SaBPL with IC_{50} = 4.0 µM with at least a 50-fold selectivity over MtbBPL and HsBPL. While **2.07** is less potent than the parent lead structure **1.23** (8 fold decrease), the retained selectivity towards SaBPL highlights the importance of the 1,2,3-triazole ring for selectivity and allows exploration of more analogues based on the 1,2,3-triazole bioisostere (see Chapter 3). Moreover, the adenine acetonide analogue **2.11** completely lost the activity compared with the parent structure **1.22**, supporting the observation that the 2-benzoxazolone group provides improved activity against SaBPL compared to the adenine group.[9]

2.3 Design of purine triazole analogues

The limited activity of triazoles **2.05-2.12** towards *Sa*BPL and *Mtb*BPL, as discussed in section 2.2, demonstrates that chemical changes upon the tether areas between 1,2,3-triazole and adenine or benzoxazolone were not well tolerated. Previous work has shown that the length of the tether between the triazole ring and ATP pocket binding moieties is important with 4 atoms being optimum.[9] Therefore, further modifications of tether length were not investigated.

This section moves on and discusses the design, synthesis and assay of 1,2,3-triazole analogues formed by modifying the adenine component of **1.22**. The analogues (**2.36-2.43**) proposed in Figure 11 retain the original saturated hydrogen carbon chain of **1.22** and mimic the adenine ring system by a number of purine analogues.


1.22

| 2.36 R = Cl | 2.38 | 2.31 | 2.40 R = CH | 2.42 R = H |
| 2.37 R = OMe | | | 2.41 R = N | 2.43 R = Br |
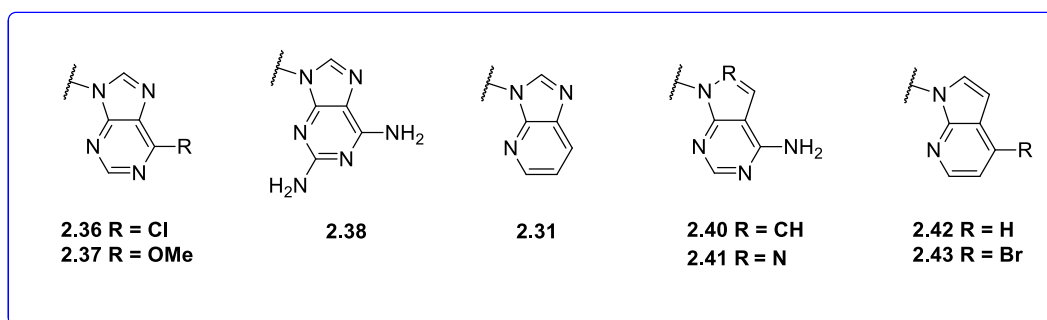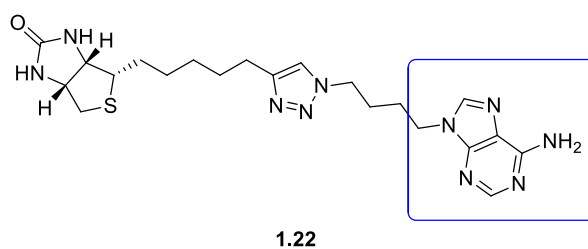
Figure 11: The leading inhibitor **1.22** and proposed analogues **2.36-2.43.**

The choice of adenine analogues found in **2.36-2.43** (Figure 8) were guided by the crystal structures of triazole **1.22** bound to *Sa*BPL (Figure 12) to reveal key characteristics relevant to the design, as follows[9]:

1. The ATP binding pocket in *Sa*BPL is dominated by Trp127 which is involved in a parallel π interaction with the adenine ring of triazole **1.22**. It is therefore critical to maintain the adenine ring system in the inhibitor design.

2. The ATP binding pocket is dominated by hydrophobic residues found within the ATP binding loop (Figure 12, highlighted in blue). Leu224, Ala228 and Phe220 define a

_____

hydrophobic region within the ATP binding loop that presents to the plane of the adenine ring as seen with triazole **1.22**.[9]

3. In addition to the dominated hydrophobic residues, a number of hydrogen bonding interactions were observed between the adenine of **1.22** and the ATP binding pocket of *Sa*BPL (Figure 12). As shown in Figure 12, the lone pair electrons of N1 and the amine at C6 of the adenine ring hydrogen bond to Asn212 with distance of 2.88 Å and 2.96 Å. The lone pair electrons of N9 and the amine group participate in the hydrogen bonding interactions with Ser128 of *Sa*BPL with distance of 2.92 Å and 3.16 Å.

4. Additionally, the C8 of the adenine ring is 3.33 Å away from His126, and the distance between the C2 and Lys187 is 3.96 Å. The adenine moiety of **1.22** is also surrounded by these amino acid residues that provide potential sites for alternative hydrogen bonding interactions.
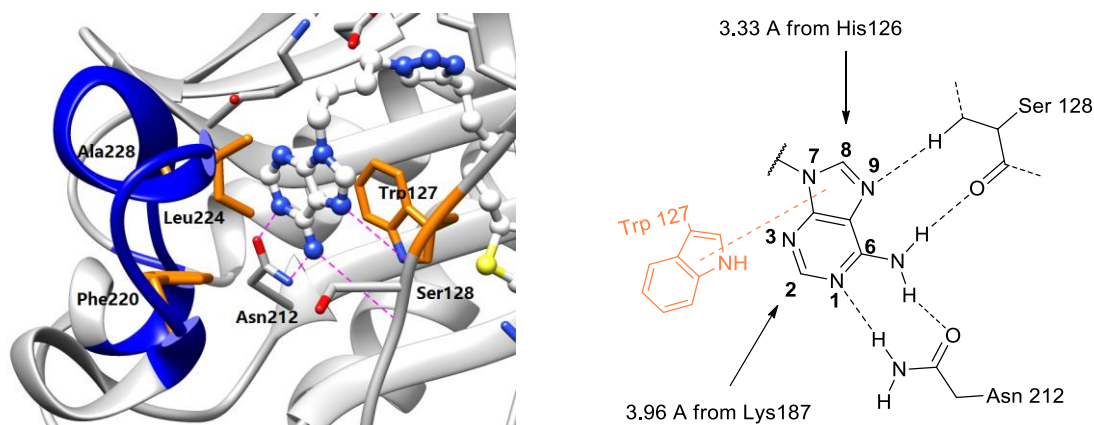
Figure 12: 3D depiction of triazole **1.22** bound to *Sa*BPL (PDB 3V7R) with hydrogen bonding interactions shown in magenta dashes (left). 2D depiction of the adenine component of **1.22** bound to the ATP binding pocket of *Sa*BPL with hydrogen bonding interactions shown in black dashes (right). π – π interaction between Trp127 (orange) and adenine ring are shown in magenta dash (right). The arrows indicate proposed hydrogen bonding interactions (right).

_____

2.3.1 Synthesis of azide building blocks 2.44-2.51

The synthesis of purine triazoles **2.36-2.43** was performed by coupling purine azides **2.44-2.51** (shown in Figure 13A) to the biotin acetylene **2.21** using the optimised CuAAC conditions[9] (shown in Figure 13B).
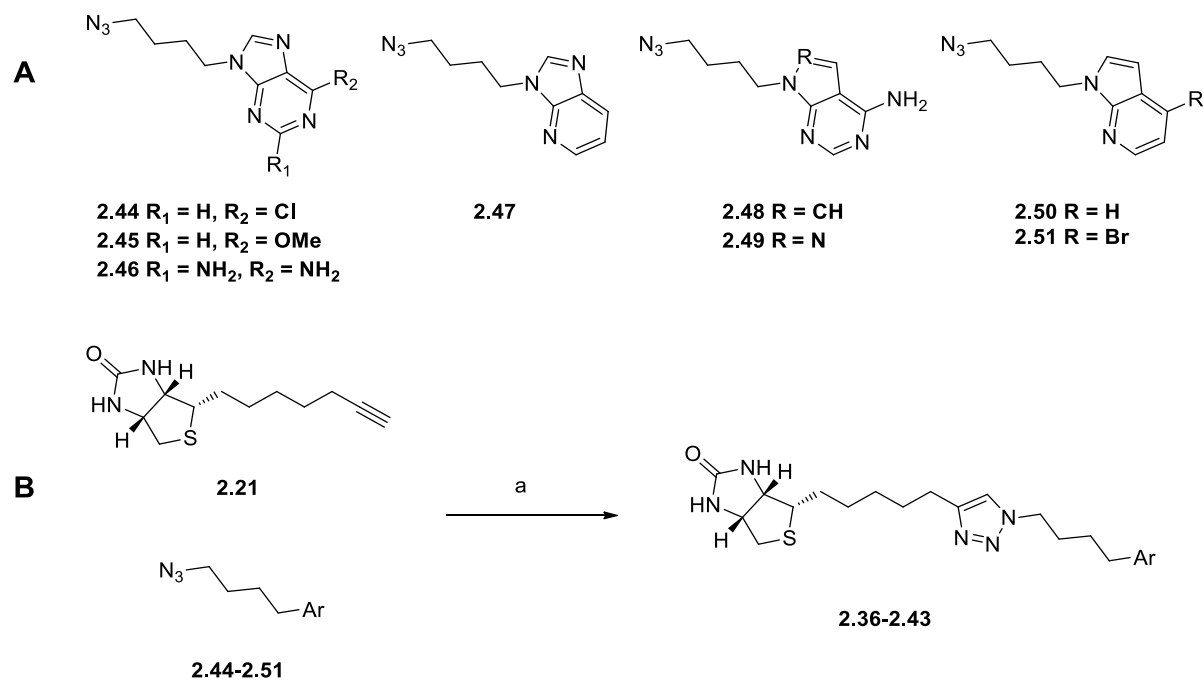

Figure 13: (A) Precursors for the synthesis of triazole **2.36-2.43**. B) CuAAC reaction between biotin acetylene **2.21** and purine azide **2.44-2.51**; (B) 20 mol% copper nano powder, 2:1 AcCN/H$_2$O;

Commercially available purine precursors **2.52**, **2.53**, **2.56**, **2.58**, **2.59**, **2.62** and **2.63** were initially treated with caesium carbonate and the resulting aminoxide was separately alkylated with dibromobutane to give the corresponding purine bromide **2.54**, **2.55**, **2.57**, **2.60**, **2.61**, **2.64** and **2.65** with yields ranging from 23% to 83% as shown in Scheme 8. The bromides were then reacted with sodium azide in DMF to give corresponding azides **2.44** and **2.46-2.51** with the respective yield as shown in Scheme 8. The 6-methoxypurine azide **2.45** was synthesized separately from 6-chloropurine azide **2.44**, as presented below in Scheme 8.
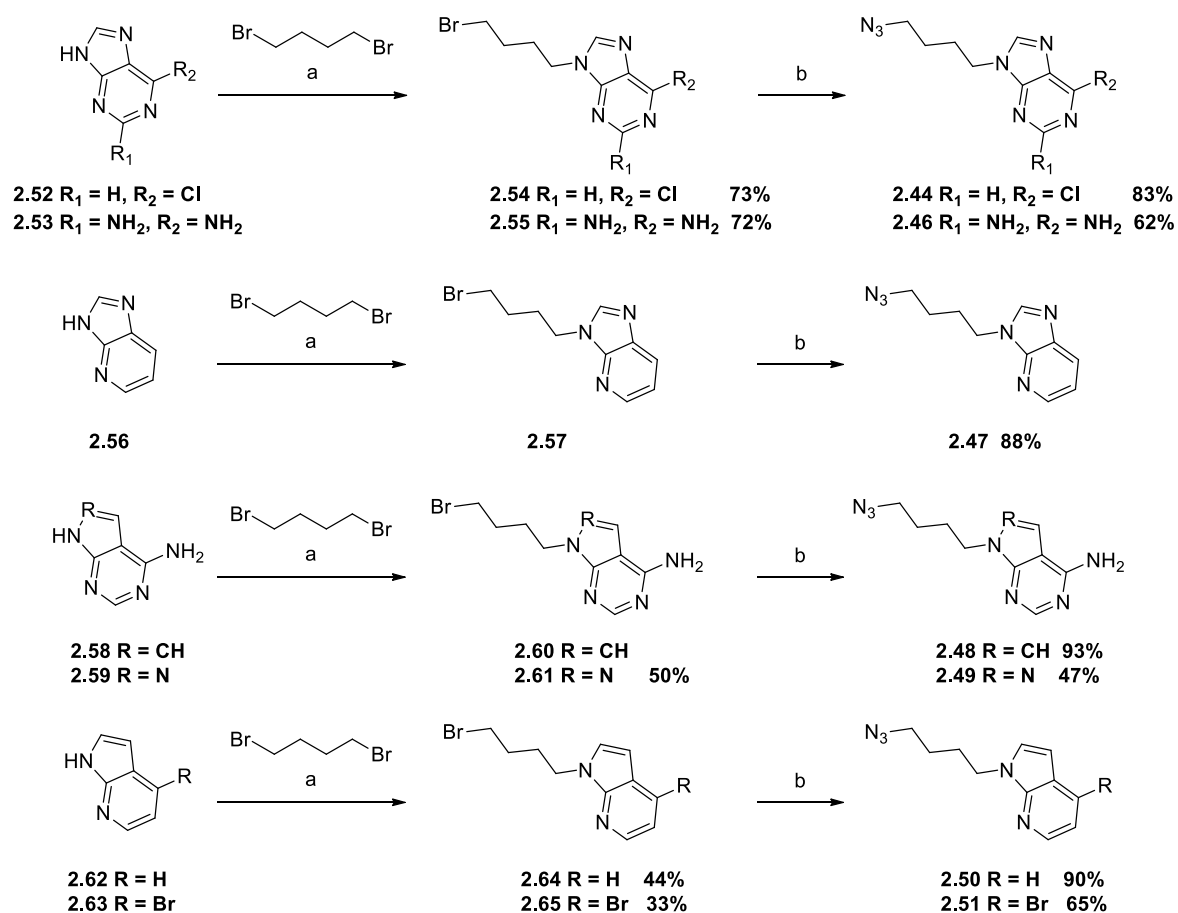
Scheme 8: a) Br(CH$_2$)$_4$Br, Cs$_2$CO$_3$, DMF, rt, 12h; b) NaN$_3$, DMF, rt, 12h

The 6-methoxypurine azide **2.45** was synthesised by stirring 6-chloro-purine azide **2.44** with sodium methoxide in methanol at room temperature for 3 hours. The reaction mixture was purified by flash chromatography to give **2.45** as white solid in 88% yield.
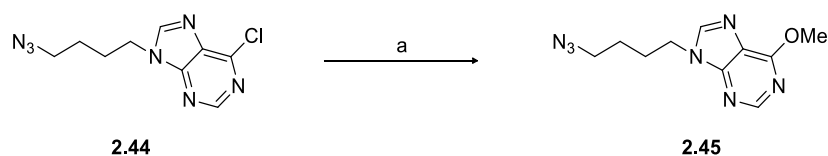

Scheme 9: a) NaOMe, MeOH, rt, 3h.

2.3.2 Synthesis of 1,2,3-triazoles 2.36-2.43 via CuAAC

The synthesis of triazoles **2.36-2.43** was accomplished by separated treatment of azides **2.44-2.51** with biotin acetylene **2.21** in the presence of copper nano powder (20 mol%) in 2:1 acetonitrile/water, sonicated for 15 min and stirred at 35 ºC for 12 h (see Table 6). The

resulting triazoles **2.36-2.43** were isolated and purified by flash chromatography with yields reported in Table 6.

Table 6ᵃ: CuAAC between acetylene **2.21** and azides **2.44-2.51**
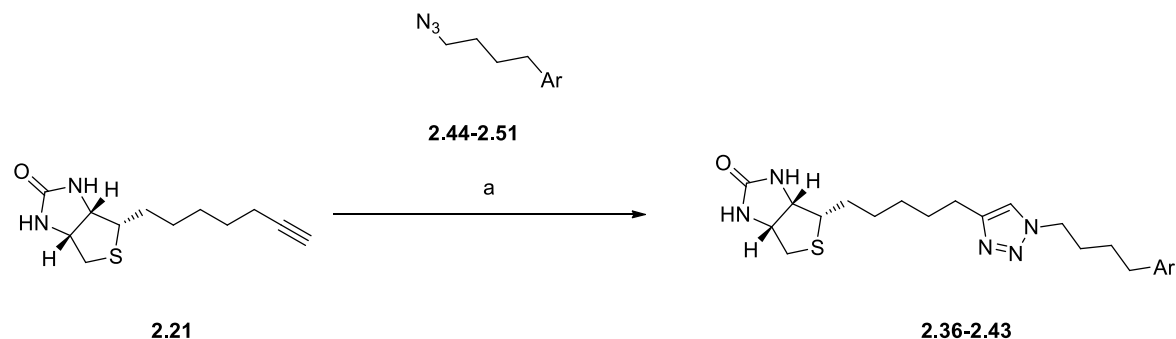
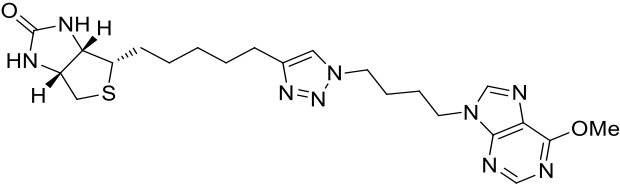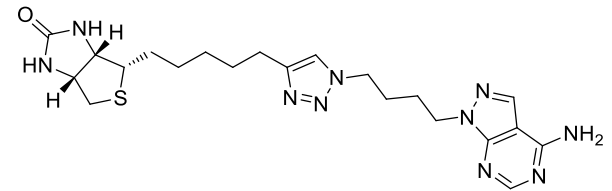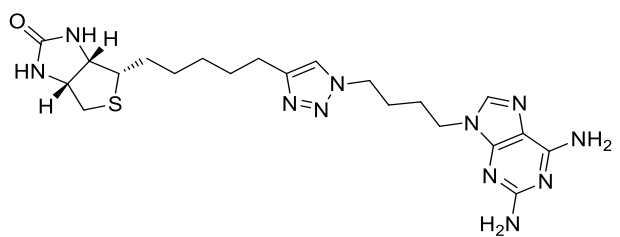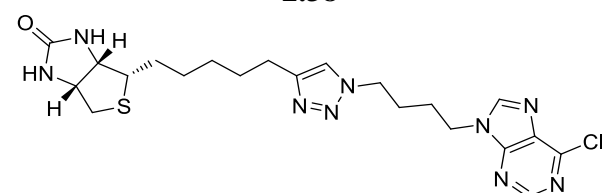| Azide (reactant)	Ar (product)	Yield[b]	Azide (reactant)	R (product)	Yield[b]
2.44	**2.36**	83%	**2.48**	**2.40**	73%
2.45	**2.37**	88%	**2.49**	**2.41**	58%
2.46	**2.38**	43%	**2.50**	**2.42**	77%
2.47	**2.39**	63%	**2.51**	**2.43**	75%
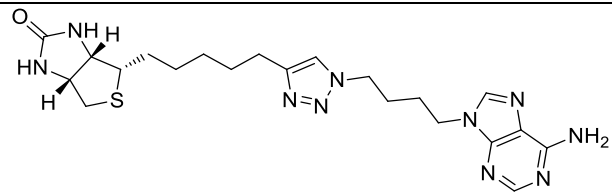
ᵃ Conditions: copper nano powder, 2:1 AcCN/H$_2$O, 12 h, sonication, 35 °C;

ᵇ isolated yields after flash chromatography.

_____

2.3.3 BPL inhibition and antimicrobial assay

1,2,3-Triazoles **2.36-2.43** were assayed for inhibitor potency against *Sa*BPL, *Mtb*BPL and *Hs*BPL and results are shown in Table 7 The assays were performed by collaborators at Molecular Life Science, University of Adelaide, following the method described by Chapman-Smith and coworkers[28]. The IC$_{50}$ value of each compound was determined from a dose-response curve by varying inhibitor concentration under the same enzyme concentration.

Table 7: Inhibition of triazole **2.36-2.38**, **2.41** and **2.43** against *Sa*BPL, *Mtb*BPL and *Hs*BPL.

Compound	*Sa*BPL IC$_{50}$ (µM)	*Mtb*BPL IC$_{50}$ (µM)	*Hs*BPL IC$_{50}$ (µM)
1.22	0.66 + 0.05	0.64 + 0.14	>200
2.37	100	5.0	>200
2.41	100	5.0	>200
2.38	>200	>200	>200
2.36	>200	>200	>200

_____

| | >200 | >200 | >200 |

2.43
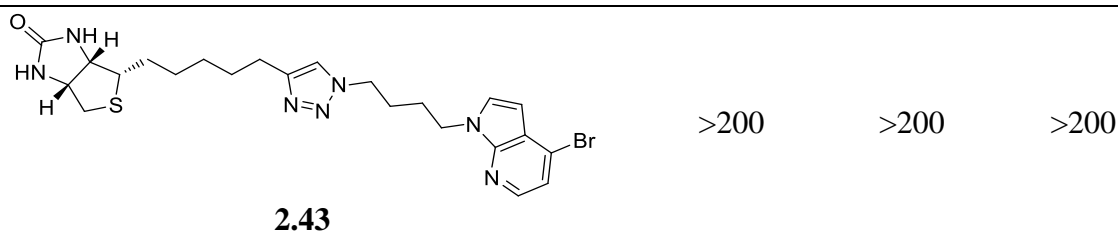
In vitro biotinylation assays were carried out using 6.25 nM of enzyme.

As shown in Table 7, two purine analogues (**2.37** and **2.41**) exhibited potency against *Mtb*BPL (*IC$_{50}$* = 5.0 µM), whilst these triazoles were approximately 3-fold less active than the lead adenine triazole **1.22** (*K$_i$* = 0.64 ± 0.14 µM).[9] Interestingly, for the first time, triazoles **2.37** and **2.41** exhibited selectivity where these triazoles were found to have at least 20-fold less activity against *Sa*BPL (*IC$_{50}$* > 100 µM). Similar to **1.22**, these triazoles were found to be non-active against *Hs*BPL at the highest compound concentration (i.e, *IC$_{50}$* > 200 µM). Interestingly, the 2,6-diamino adenine **2.38** showed no measurable *IC$_{50}$* value against *Sa*BPL, *Mtb*BPL and *Hs*BPL (*IC$_{50}$* > 200 µM), suggesting an extra amine group at position 2 is not well tolerated. The study of mono-substituted adenine derivatives at position 6 (**2.36** and **2.43**) showed no significant inhibitory activities against both *Sa*BPL and *Mtb*BPL. Therefore, halogen substitution at this position was not tolerated by BPLs.

These results indicate very steep SAR for adenine derivatives that: 1) additional hydrogen substrate binding sites are not well tolerated within the ATP binding pocket of BPLs; 2) hydrogen bonding interactions within the ATP binding pocket may have a limited role in binding affinity; 3) the ATP binding pocket is highly restricted to the physiological ligand adenine as changes in nitrogen amounts and positions around adenine derivatives resulted in decreased or non-activity against BPLs.

_____

2.4 Conclusion

This chapter reported on chemical modifications conducted in two areas of the current lead *Mtb*BPL inhibitor **1.22** and *Sa*BPL inhibitor **1.23**. For the tether between 1,2,3-triazole and adenine ring of **1.22** or benzoxazolone of **1.23**, triazoles **2.05-2.12** were successfully synthesised using CuAAC with yields of 34 –67%. The stereochemistry of diol triazoles **2.06**, **2.07** and acetonide triazoles **2.10**, **2.11**, as well as their azide building blocks **2.14**, **2.15**, **2.18** and **2.19**, was confirmed using a combination of chiral HPLC and ^{13}C NMR. Enzyme inhibition assay against *Sa*BPL, *Mtb*BPL and *Hs*BPL revealed that only triazole **2.07** was an active inhibitor of *Sa*BPL with IC_{50} = 4.0 µM, while it was about 8-fold less active than its parent lead inhibitor **1.23** (IC_{50} = 0.53 ± 0.01 µM). This suggests that chemical modifications, such as introducing additional polar functional groups, were not well tolerated by *Sa*BPL and *Mtb*BPL.

The second area, 1,2,3-triazoles **2.36-2.43** as analogues of the adenine bicyclic ring system of **1.22** were synthesised using CuAAC with yields of 34–74%. The inhibition assay results of these adenine analogues revealed limited activity against *Sa*BPL, *Mtb*BPL and *Hs*BPL, suggesting there is limited scope for modifying the bicyclic ring of adenine. Thus, no further investigations were undertaken upon the adenine ring.

_____

2.5 References for Chapter Two

(1)   Bagautdinov, B.; Matsuura, Y.; Bagautdinova, S.; Kunishima, N. *Journal of Biological Chemistry* **2008**, *283*, 14739-14750.

(2)   Tron, C. M.; McNae, I. W.; Nutley, M.; Clarke, D. J.; Cooper, A.; Walkinshaw, M. D.; Baxter, R. L.; Campopiano, D. J. *Journal of Molecular Biology* **2009**, *387*, 129-146.

(3)   Xu, Y.; Beckett, D. *Biochemistry* **1994**, *33*, 7354-7360.

(4)   Artymiuk, P. J.; Rice, D. W.; Poirrette, A. R.; Willet, P. *Nature Structural & Molecular Biology* **1994**, *1*, 758-760.

(5)   Reche, P. A. *Protein Science* **2000**, *9*, 1922-1929.

(6)   Bernier, S.; Akochy, P.-M.; Lapointe, J.; Chênevert, R. *Bioorganic & Medicinal Chemistry* **2005**, *13*, 69-75.

(7)   Böttcher, C.; Dennis, E. G.; Booker, G. W.; Polyak, S. W.; Boss, P. K.; Davies, C. *PloS one* **2012**, *7*.

(8)   Lee, J.; Kang, S. U.; Kang, M. K.; Chun, M. W.; Jo, Y. J.; Kkwak, J. H.; Kim, S. *Bioorganic & Medicinal Chemistry Letters* **1999**, *9*, 1365-1370.

(9)   Soares da Costa, T. P.; Tieu, W.; Yap, M. Y.; Pendini, N. R.; Polyak, S. W.; Sejer Pedersen, D.; Morona, R.; Turnidge, J. D.; Wallace, J. C.; Wilce, M. C.; Booker, G. W.; Abell, A. D. *Journal of Biological Chemistry* **2012**, *287*, 17823-17832.

(10)   S Paparella, A.; P Soares da Costa, T.; Y Yap, M.; Tieu, W.; CJ Wilce, M.; W Booker, G.; D Abell, A.; W Polyak, S. *Current Topics in Medicinal Chemistry* **2014**, *14*, 4-20.

(11)   Soares da Costa, T. P.; Tieu, W.; Yap, M. Y.; Zvarec, O.; Bell, J. M.; Turnidge, J. D.; Wallace, J. C.; Booker, G. W.; Wilce, M. C.; Abell, A. D. *ACS Medicinal Chemistry Letters* **2012**, *3*, 509-514.

(12)   Blanchard, C. Z.; Amspacher, D.; Strongin, R.; Waldrop, G. L. *Biochemical and Biophysical Research Communications* **1999**, *266*, 466-471.

(13)   Slavoff, S. A.; Chen, I.; Choi, Y.-A.; Ting, A. Y. *Journal of the American Chemical Society* **2008**, *130*, 1160-1162.

(14)   Hanka, L.; Martin, D.; Reineke, L. *Antimicrobial Agents and Chemotherapy* **1972**, *1*, 135-138.

(15)   Shi, Y.; Zhu, C. Z.; Martin, S. F.; Ren, P. *J Phys Chem B* **2012**, *116*, 1716-1727.

_____

(16)   Harrison, B. A.; Gierasch, T. M.; Neilan, C.; Pasternak, G. W.; Verdine, G. L. *Journal of the American Chemical Society* **2002**, *124*, 13352-13353.

(17)   Smith, W. W.; Bartlett, P. A. *Journal of the American Chemical Society* **1998**, *120*, 4622-4628.

(18)   Khan, A. R.; Parrish, J. C.; Fraser, M. E.; Smith, W. W.; Bartlett, P. A.; James, M. N. *Biochemistry* **1998**, *37*, 16839-16845.

(19)   Morris, G. M.; Goodsell, D. S.; Halliday, R. S.; Huey, R.; Hart, W. E.; Belew, R. K.; Olson, A. J. *Journal of Computational Chemistry* **1998**, *19*, 1639-1662.

(20)   Tieu, W.; Jarrad, A. M.; Paparella, A. S.; Keeling, K. A.; Soares da Costa, T. P.; Wallace, J. C.; Booker, G. W.; Polyak, S. W.; Abell, A. D. *Bioorganic & Medicinal Chemistry Letters* **2014**, *24*, 4689-4693.

(21)   Hartmuth C. Kolb; Michael S. VanNieuwenhze; Sharpless, K. B. *American Chemical Society* **1994**, *94*, 2483-2547.

(22)   Junttila, M. H.; Hormi, O. E. *The Journal of Organic Chemistry* **2004**, *69*, 4816-4820.

(23)   K. Barry Sharpless; Willi Amberg; Matthias Beller; Hou Chen; Jens Hartung; Yasuhiro Kawanami; Doris Lubben; Eric Manoury; Yasukazu Ogino; Tomoyuki Shibata; Ukita, T. *The Journal of Organic Chemistry* **1991**, *56*.

(24)   Molander, G. A.; Figueroa, R. *Organic Letters* **2006**, *8*, 75-78.

(25)   Kai, K.; Fujii, H.; Ikenaka, R.; Akagawa, M.; Hayashi, H. *Chemical Communications* **2014**, *50*, 8586-8589.

(26)   Newman, S. G.; Bryan, C. S.; Perez, D.; Lautens, M. *Synthesis* **2011**, *2011*, 342-346.

(27)   Himo, F.; Lovell, T.; Hilgraf, R.; Rostovtsev, V. V.; Noodleman, L.; Sharpless, K. B.; Fokin, V. V. *Journal of the American Chemical Society* **2005**, *127*, 210-216.

(28)   Chapman-Smith, A.; Cronan, J. E. *Trends in Biochemical Sciences* **1999**, *24*, 359-363.

A new series of BPL inhibitors to probe the ribose-binding pocket of *Staphylococcus aureus* biotin protein ligase

Jiage Feng,[‡,‡] Ashleigh S. Paparella,[§] William Tieu,[‡,▼] David Heim,[§] Sarah Clark,[‡,◊] Andrew Hayes,[§] Grant W. Booker,[§] Steven W. Polyak[§] and Andrew D. Abell

[‡]*Department of Chemistry, University of Adelaide, Adelaide, South Australia 5005, Australia*

[§]*Department of Molecular and Cellular Biology, University of Adelaide, South Australia 5005, Australia*

[‡]*Centre for Nanoscale BioPhotonics (CNBP), University of Adelaide, Adelaide, South Australia 5005, Australia*

(Prepared in publication format "text in manuscript")

3.1   Introduction: Design of benzylic triazole analogues.

Biotin protein ligase (BPL) catalyses the reaction of biotin **1.01** and ATP **1.02** to give biotinyl-5′-AMP **1.03**, which then biotinylates and activates essential metabolic enzymes required for fatty acid biosynthesis and gluconeogenesis, specifically acetyl CoA carboxylase and pyruvate carboxylase (Figure 1).[1-5] A number of analogues of biotinyl-5′-AMP **1.03** have recently been reported as inhibitors of BPL as shown in Figure 2. Some of these compounds have demonstrated potential as antibacterial agents by inhibiting BPL from clinically important pathogens such as *Staphylococcus aureus,*[6] *Escherichia coli* [5,7,8] and *Mycobacterium tuberculosis*.[9,10] A range of bioisosteres have been investigated as replacements for the labile phosphoanhydride of biotinyl-5′-AMP **1.03**, including phosphodiester **1.14**,[11-13] hydroxyphosphonate **1.15**,[14] ketophosphonate **1.16**,[14] acylsulfamate **1.17**,[4] sulfamylamide **1.18**[9,10] (Figure 2). We have also reported biotin triazoles as a novel class of BPL inhibitor that selectively target BPL from the clinically important bacterial pathogen *Staphylococcus aureus* over the human homologue, for example **1.20**.[15-17]
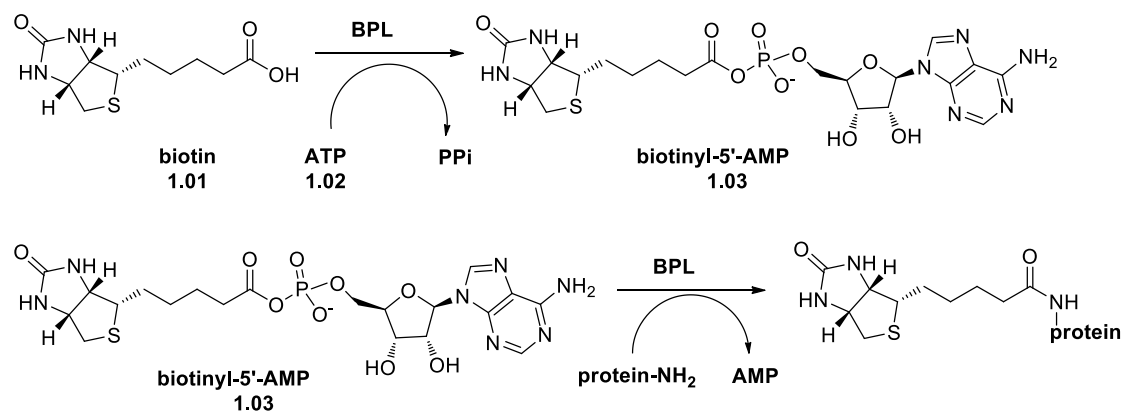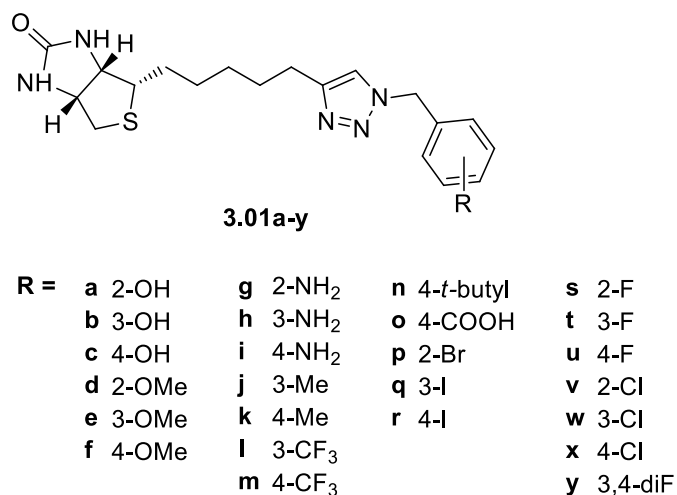

**Figure 1.** General mechanism of BPL catalyzed biotinylation
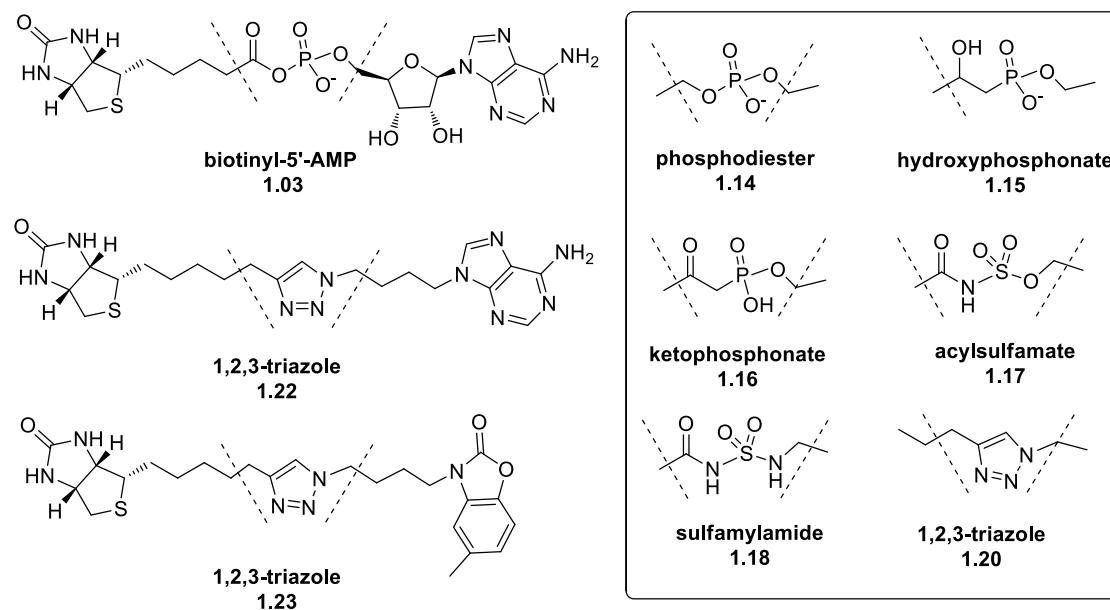
Figure 2. Reported biotinyl-5'-AMP **1.03** analogues of biotin protein ligase.

Without exception, all isostere-based BPL inhibitors reported to date contain both a biotin and adenine group, or analogue thereof, as discussed above and as shown in Figure 2. These two groups occupy well-defined binding pockets in the enzyme as per biotinyl-5′-AMP **1.03**, as supported by x-ray crystallographic and mutagenesis studies.[15,18] The ribose group of the triazole series can be removed as in **1.20** and the adenine can be also modified as in **1.23**, which has improved stability and >1000-fold specificity for the BPL from *S. aureus* over the human homologue.[15] We now report the first examples of truncated 1,2,3-triazole-based BPL inhibitors with a 1-benzyl substituent designed to interact with the ribose binding pocket of *S. aureus* BPL (*Sa*BPL), see **3.01a-y** Figure 3. These derivatives are the first examples of isostere-based BPL inhibitors lacking an appended adenine analogue and the associated tether as discussed above. The ribose-binding pocket is composed of amino acids that provide potential hydrogen bonding sites, specifically through the side chains of K187, R122, R125 and R227 as well as the backbone peptide atoms from H126 and S128 (Figure 3). This series of inhibitors provides an important new starting point for further medicinal chemistry-based optimization.

3.01a-y

R =
a	2-OH	**g**	2-NH$_2$	**n**	4-*t*-butyl	**s**	2-F	
b	3-OH	**h**	3-NH$_2$	**o**	4-COOH	**t**	3-F	
c	4-OH	**i**	4-NH$_2$	**p**	2-Br	**u**	4-F	
d	2-OMe	**j**	3-Me	**q**	3-I	**v**	2-Cl	
e	3-OMe	**k**	4-Me	**r**	4-I	**w**	3-Cl	
f	4-OMe	**l**	3-CF$_3$			**x**	4-Cl	
		m	4-CF$_3$			**y**	3,4-diF	

Figure 3. Benzyl substituted 1,2,3-triazole analogues.

In silico docking experiments were carried out in order to explore possible binding modes by which this series of benzyl analogues might occupy the active site of *Sa*BPL. Flexible ligand docking was carried out using AutoDockTools (version 1.5.6). The docking protocol was first validated by removing compound **1.23** from its co-crystal structure with *S. aureus* BPL (PDB 3V7S) and then re-docking. This occurred with a high degree of commonality as revealed by superimposition of the docked and crystallised ligands in the active site. We next docked the target benzylated triazoles **3.01a-c** (Figure 3) into *Sa*BPL. Each of these structures contains a single hydroxyl substituent on the benzyl ring capable of forming a hydrogen bond as per the diol in the ribose of biotinyl-5′-AMP **1.03**. Gratifyingly, the top ranking poses of all three analogues placed the hydroxyl group in the site occupied by the ribose diol of **1.03** (Figure 4a). Rotation around the alkyl linker connecting the triazole and benzyl moieties produced subtly different posses with regards to the ribose-binding site (Figure 4b). These binding modes minimised steric clashes with the protein and facilitated hydrogen bonding between the alcohol group and R122 for **3.01a** and R227 for **3.01b** and **3.01c**. This data reflects an apparent openness of the solvent exposed pocket, and suggests that this site could accommodate a variety of functional groups. Hence, we designed an extended series of benzyl analogues (Scheme 1) to further probe binding within the ribose pocket.
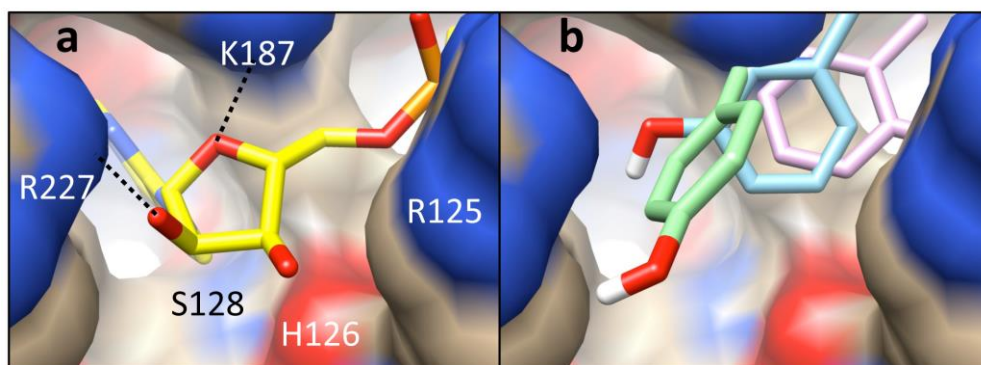
Figure 4. a) X-ray structure of the *Sa*BPL active site with biotinyl-5′-AMP **1.03** (yellow) bound PDBID 3RIR.[10] Amino acids that encompass the ribose-binding pocket are shown. Dashed lines represent hydrogen bonds. b). *In silico* docking poses for biotin triazole analogues **3.01a**, **3.01b** & **3.01c** with a hydroxyl at C2- (pink), C3- (blue) and C4- (green), respectively.

3.2   Synthesis of 1,2,3-triazole 3.01a-y

The synthesis of the 1,2,3-triazoles **3.01a-y** was carried out as summarized in Scheme 1. The key benzyl azides **3.03a-y** were prepared from commercially available benzyl derivatives alcohols (**3.02a-i** & **3.02n**) and halides (**3.04j-m** & **3.04o-y**). Specifically, commercially available benzyl alcohols **3.02a-i** and **3.02n** were converted directly into the corresponding azides **3.03a-i** and **3.03n** on reaction with triphenylphosphine, in the presence of carbon tetrachloride and sodium azide at ambient temperature.[19] The second series of benzyl azides (**3.03j-m** and **3.03o-y**) was prepared from commercially available benzyl halides **3.04j-m** and **3.04o-y** on reaction with sodium azide in DMF as shown. Huisgen cycloaddition of biotin alkyne **2.21** [20] with each of the benzyl azides **3.03a-y**, in the presence of copper sulfate and sodium ascorbate, [15] then gave the corresponding 1,2,3-triazole **3.01a-y**.
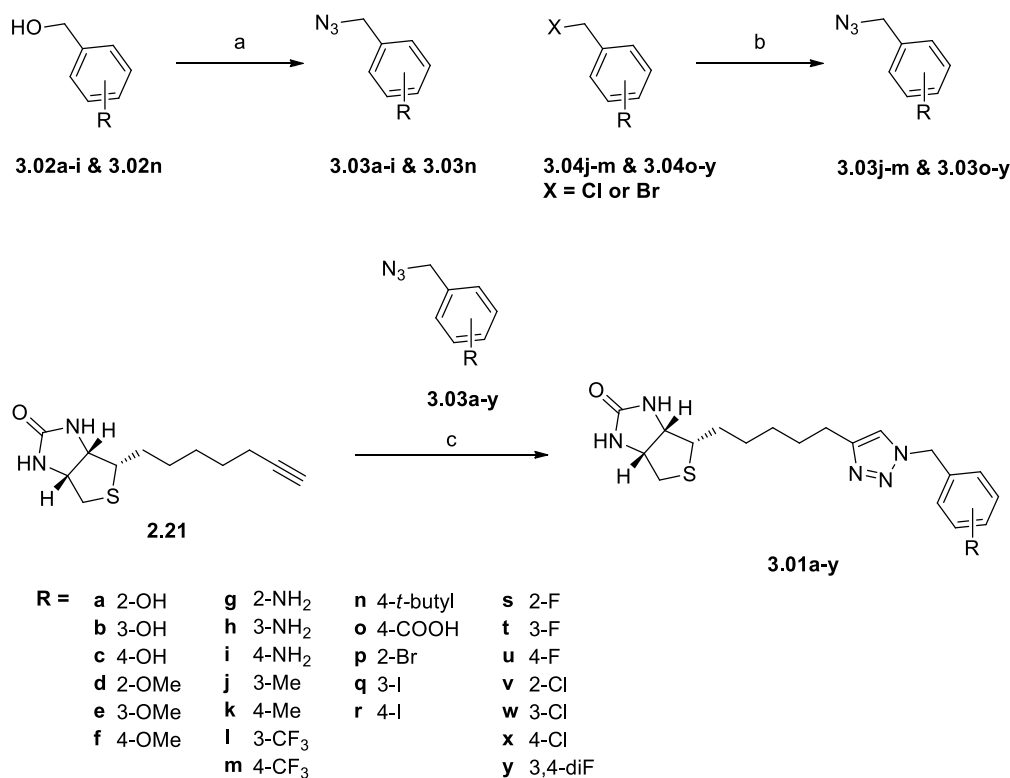
Scheme 1. Conditions and reagents: (a) (i) PPh$_3$, CCl$_4$, DMF, (ii) NaN$_3$, DMF, rt; (b) NaN$_3$, DMF, rt; (c) Cu$_2$SO$_4$ Ascorbate, DMSO/H$_2$O, rt, 12h (give **3.01a-y** (18%-55%))

3.3 BPL inhibition and antimicrobial activity of 1,2,3-triazole 3.01a-y

The complete activity profiles of 1,2,3-triazoles **3.01a-y** were determined using established biochemical and microbiological assay protocols.[15,21] Compounds with selective inhibitory activity against *Sa*BPL and cytotoxic activity against bacteria, but not mammalian cells, provide important candidates for further antibiotic development. The *in vitro* potency and selectivity of the 1,2,3-triazoles **3.01a-y** were first measured using recombinant BPLs from *S. aureus* and *Homo sapiens.* Here the enzymatic incorporation of radiolabelled biotin onto an acceptor protein was measured in the presence of varying concentrations of compound with the results shown in Tables 1 and 2. Previous enzymology and X-ray crystallography studies have demonstrated that the biotin triazoles are competitive inhibitors against biotin,[15,17,18] and as such inhibitory constants (K_i) were calculated from IC_{50} values using the known K_M for biotin as previously described.[22] The antibacterial activity of the compounds was also determined using *S. aureus* strain ATCC 49775.[20] Growth of the bacteria 20 hours post treatment was measured spectrophotometrically at 600 nm. Finally, selected

_____

compounds were assessed for potential toxicity using a cytotoxicity assay with cultured mammalian HepG2 cells (ATCC HB-8065). [15]

Table 1. *In vitro* biotinylation and antibacterial assay results for benzyl triazole series 1.

ID	R	K_i *Sa*BPL (μM)	K_i Human BPL (μM)	Anti-S. aureus activity
3.01a	2-OH	>10	>10	-
3.01b	3-OH	>10	>10	-
3.01c	4-OH	1.59 ± 0.08	>10	-
3.01d	2-OMe	0.53 ±0.05	>10	-
3.01e	3-OMe	1.17 ± 0.1	>10	-
3.01f	4-OMe	>10	>10	-
3.01g	2-NH$_2$	1.48 ± 0.14	>10	+
3.01h	3-NH$_2$	>10	>10	-
3.01i	4-NH$_2$	>10	>10	-
3.01j	3-Me	0.71 ± 0.04	>10	+
3.01k	4-Me	>10	>10	-
3.01l	3-CF$_3$	>10	>10	-
3.01m	4-CF$_3$	>10	>10	-
3.01n	4-tBu	1.22 ± 0.07	>10	+
3.01o	4-COOH	0.67 ± 0.06	>10	-
3.01p	4-Br	0.96 ± 0.13	>10	+
3.01q	3-I	>10	>10	-
3.01r	4-I	0.56 ± 0.06	>10	+

In vitro biotinylation assays were carried out using 6.25 nM of enzyme.

+ = inhibited growth observed,

 - = compound did not inhibit bacterial growth

The initial series of alcohol analogues **3.01a-c** (initially synthesised and characterized by Dr William Tieu) docked against *Sa*BPL were first assayed against the enzyme (Table 1) with the compound containing a C4 hydroxyl group (**3.01c**) showing modest activity (K_i = 1.59 μM). The C2 and C3 hydroxylated derivatives (**3.01a** and **3.01b**) were devoid of activity. It thus appears that the ribose pocket is sensitive to the position of the hydroxyl group and more so than predicted by the modeling. This observation is supported on analysis of other substituents, although there is little consistency regarding which position is most favored. Specifically, derivatives with a methoxy group at C2 and C3 were both active (**3.01d**, K_i = 0.53 μM and **3.01e**, K_i = 1.1 μM respectively), while the C4 analogue (**3.01f**) was inactive. For an amino substituent **3.01g-i** (synthesised and characterized by Dr

William Tieu), C2 is active (**3.01g,** K_i = 1.49 µM) while both C3 (**3.01h**) and C4 (**3.01i**) were inactive. Of the other derivatives initially tested, C3 methyl (**3.01j**, K_i = 0.71 µM, synthesised by Sarah Clark), C4 carboxyl and tertiary butyl (**3.01o**, K_i = 0.67 µM and **3.01n**, K_i = 1.1 µM respectively) were all active. A strongly electron withdrawing trifluoromethyl group at C3 and C4, resulted in compounds (**3.01l** and **3.01m**) devoid of activity against *Sa*BPL.

The 2-bromo and 4-iodo derivatives **3.01p** and **3.01r** proved to be particularly important in that both were particularly active against *S. aureus* BPL (K_i = 0.96 µM and 0.56 µM, respectively) while also displaying anti-*S. aureus* activity, see Table 1. These two derivatives provided an important starting point for an expanded series of halogenated compounds as discussed in detail below. All of the biotin triazoles tested were inactive against human BPL. This is an important finding as it demonstrates that benzyl truncated triazoles retain the selectivity profile (ie active against *S. aureus* but not human BPL) of the earlier and more complex triazoles.[15,17]

All compounds were assayed for antibacterial activity against *S. aureus* ATCC 49775 (Table 1). Compounds were designated as antibacterial if they reduced the optical density of the culture by >40% relative to the non-treated controls. Of the eighteen compounds produced in the first series, only 5 (bearing amine, methyl, tertiary butyl bromo and iodo substituents) were active in the whole cell assays, namely **3.01g**, **3.01j**, **3.01n**, **3.01p** and **3.01r** (Figure 5). The fact that these compounds were also inhibitors in the enzyme assays, is consistent with the mechanism of antibacterial action being through the BPL target. It is possible that those BPL inhibitors devoid of whole cell activity, namely **3.01c-e**, **3.01g**, **3.01j** and **3.01p,** are unable to penetrate the bacterial membrane, a problem often encountered in antibacterial discovery.[23]

Table 2: *. In vitro* biotinylation and antibacterial assay results for benzyl triazole series 2.

ID	R	K_i SaBPL (μM)	K_i Human BPL (μM)	Anti-S. aureus activity	Cytotox HepG2*
3.01s	2-F	>10	>10	-	N/D
3.01t	3-F	0.28 ± 0.02	>10	+	>40
3.01u	4-F	0.6 ±0.1	>10	+	>40
3.01v	2-Cl	>10	>10	-	N/D
3.01w	3-Cl	0.39 ± 0.04	>10	+	>40
3.01x	4-Cl	1.1 ± 0.07	>10	+	>40
3.01y	3,4-diF	>10	>10	-	N/D

In vitro biotinylation assays were carried out using 6.25 nM of enzyme.

+ = inhibited growth observed,

_____

- = compound did not inhibit bacterial growth

* Compounds were assayed at 40 µg/ml.

Based on the encouraging results for **3.01p** and **3.01r**, a further series of halogenated derivatives was also investigated, see **3.01s-x** in Table 2. Four of these compounds displayed potent activity against *S. aureus* BPL, see **3.01t**, **3.01u** and **3.01w** and **3.01x** which had K_i values of 0.28, 0.6, 0.39 and 1.1 µM respectively. A 3-halo substituent was optimum in these cases for activity, with both chloro and iodo being favored at this position, see **3.01t** and **3.01w**. The inhibition constants were 2 and 3 fold lower for the 3-*vs* 4- halogenated analogs **3.01t/3.01u** and **3.01w/3.01x** respectively. The smaller 3-fluoro substituent (**3.01t**) provided the most potent compound in the series with a K_i = 0.28 µM. In comparison, the incorporation of a halogen at C2 removed all activity, see **3.01s** and **3.01v** as did the introduction of a second fluoro substituent as in **3.01y**. Again all active compounds in this series showed excellent selectivity for *S. aureus* BPL over the human homologue.

Further microbiological assays revealed **3.01u** and **3.01x** to be bacteriostatic against *S. aureus*. Viable cell counts were measured after treating the bacteria for 24 hours at the concentration that had the greatest effect upon cell growth measured spectrophotometrically, that is, **3.01u** at 16 µg/ml or **3.01x** at 4 µg/ml, respectively. Both compounds reduced the number of live cells relative to a non-treated control by 410-fold for **3.01u** and 300-fold for **3.01x**, consistent with a bacteriostatic agent. Finally, cytotoxicity was assessed using mammalian HepG2 cells at a single concentration of 40 µg/ml for compound **3.01t**, **3.01u**, **3.01w**, and **3.01x** (Figure 5). None of these compounds showed cytotoxic activity.

Figure 5: Inhibition of *S. aureus* growth *in vitro*. Compounds **3.01g** (□), **3.01j** (♦), **3.01p** (○), **3.01r** (△), **3.01t** (■), **3.01u** (●), **3.01w** (▼) and **3.01x** (▲) were tested against *S. aureus* strain ATCC 49775.

3.4 Conclusion

The 1-benzyl substituted 1,2,3-triazoles reported here represent a new class of BPL inhibitors that lack the adenine group, or analogue thereof, found in all other isostere-based BPL inhibitors. Of these, the halogenated benzyl analogs are promising lead structures for further development of new antibacterial compounds. Importantly our biochemical and microbiological data provide a clear relationship between the *in vitro* inhibition of BPL and anti-*S. aureus* activity, with our most potent enzyme inhibitors also providing our most promising antibacterial. In antibiotic drug discovery this is not always the case as a number of external factors contribute to bioactivity, such as cell permeability and susceptibility to efflux and metabolic degradation. Our SAR data provides us with confidence that optimization of *in vitro* inhibition will lead to improved antibacterial activity. Our *in silico* docking supports a proposed binding mechanism where the halogenated benzyl group binds within the ribose pocket of *Sa*BPL. The C4 fluoro and chloro substituted benzyl triazoles **3.01u** and **3.01x** provide important new scaffolds suitable for further chemical modification and activity optimization, specifically to interact with the adjacent adenyl-binding site in the enzyme. Such studies are currently underway.

3.5   References for Chapter Three

(1)   Polyak, S. W.; Chapman-Smith, A. In *Encyclopedia of Biological Chemistry*; 2nd ed.; Lennarz, W. J., Lane, M. D., Eds.; Elsevier: Oxford, 2013; Vol. 1, p 221-225.

(2)   Pendini, N. R.; Bailey, L. M.; Booker, G. W.; Wilce, M. C.; Wallace, J. C.; Polyak, S. W. *Biochim. Biophys. Acta.* **2008**, *1784*, 973-82.

(3)   Polyak, S.; Abell, A.; Wilce, M.; Zhang, L.; Booker, G. *Applied Microbiology and Biotechnology*, **2012**, *93*, 983.

(4)   Brown, P. H.; Cronan, J. E.; Grøtli, M.; Beckett, D. *Journal of Molecular Biology* **2004**, *337*, 857-869.

(5)   Brown, P. H.; Beckett, D. *Biochemistry* **2005**, *44*, 3112-3121.

(6)   Paparella, A. S.; Soares da Costa, T. P.; Yap, M. Y.; Tieu, W.; Wilce, M. C.; Booker, G. W.; Abell, A. D.; Polyak, S. W. *Current Topics in Medicinal Chemistry* **2014**, *14*, 4-20.

(7)   Xu, Y.; Beckett, D. *Biochemistry* **1994**, *33*, 7354-7360.

(8)   Xu, Y.; Beckett, D. *Methods Enzymol.* **1997**, *279*, 405.

(9)   Duckworth, B. P.; Nelson, K. M.; Aldrich, C. C. *Current Topics in Medicinal Chemistry* **2012**, *12*, 766.

(10)   Duckworth, B. P.; Geders, T. W.; Tiwari, D.; Boshoff, H. I.; Sibbald, P. A.; Barry, C. E., 3rd; Schnappinger, D.; Finzel, B. C.; Aldrich, C. C. *Chemistry & Biology* **2011**, *18*, 1432-41.

(11)   Brown, P. H.; Cronan, J. E.; Grotli, M.; Beckett, D. *Journal of Molecular Biology* **2004**, *337*, 857-869.

(12)   Tieu, W.; Polyak, S. W.; Paparella, A. S.; Yap, M. Y.; Soares da Costa, T. P.; Ng, B.; Wang, G.; Lumb, R.; Bell, J. M.; Turnidge, J. D.; Wilce, M. C.; Booker, G. W.; Abell, A. D. *ACS Medicinal Chemistry Letters* **2015**, *6*, 216-220.

(13)   Xu, Z.; Yin, W.; Martinelli, L. K.; Evans, J.; Chen, J.; Yu, Y.; Wilson, D. J.; Mizrahi, V.; Qiao, C.; Aldrich, C. C. *Bioorganic & Medicinal Chemistry* **2014**, *22*, 1726-1735.

(14)   Sittiwong, W.; Cordonier, E. L.; Zempleni, J.; Dussault, P. H. *Bioorganic & Medicinal Chemistry* **2014**, *24*, 5568-5571.

(15)   Soares da Costa, T. P.; Tieu, W.; Yap, M. Y.; Pendini, N. R.; Polyak, S. W.; Sejer Pedersen, D.; Morona, R.; Turnidge, J. D.; Wallace, J. C.; Wilce, M. C.; Booker, G. W.; Abell, A. D. *The Journal of Biological Chemistry* **2012**, *287*, 17823-32.

_____

(16)   Tieu, W.; Jarrad, A. M.; Paparella, A. S.; Keeling, K. A.; Soares da Costa, T. P.; Wallace, J. C.; Booker, G. W.; Polyak, S. W.; Abell, A. D. *Bioorganic & Medicinal Chemistry Letters* **2014**, *24*, 4689-93.

(17)   Tieu, W.; Soares da Costa, T. P.; Yap, M. Y.; Keeling, K. L.; Wilce, M. C. J.; Wallace, J. C.; Booker, G. W.; Polyak, S. W.; Abell, A. D. *Chemical Science* **2013**, *4*, 3533-3537.

(18)   Pendini, N. R.; Yap, M. Y.; Polyak, S. W.; Cowieson, N. P.; Abell, A.; Booker, G. W.; Wallace, J. C.; Wilce, J. A.; Wilce, M. C. *Protein Science* **2013**, *22*, 762-773.

(19)   Koziara, A. *Journal of Chemical Research (S)* **1989**, 296-297.

(20)   Soares da Costa, T. P.; Tieu, W.; Yap, M. Y.; Zvarec, O.; Bell, J. M.; Turnidge, J. D.; Wallace, J. C.; Booker, G. W.; Wilce, M. C.; Abell, A. D.; Polyak, S. W. *ACS Medicinal Chemistry Letters* **2012**, *3*, 509-514.

(21)   Polyak, S. W.; Chapman-Smith, A.; Brautigan, P. J.; Wallace, J. C. *The Journal of Biological Chemistry* **1999**, *274*, 32847-32854.

(22)   Cheng, Y.; Prusoff, W. H. *Biochem Pharmacol* **1973**, *22*, 3099-3108.

(23)   Tommasi, R.; Brown, D. G.; Walkup, G. K.; Manchester, J. I.; Miller, A. A. *Nature reviews. Drug discovery* **2015**, *14*, 529-542.

4.1 Introduction

Chapter 2 revealed 1,2,3-triazole **1.22** as the leading *Mtb*BPL inhibitor with a K_i of 0.6 µM, and 1,2,3-triazole **1.23** as the leading *Sa*BPL inhibitor with K_i of 0.09 µM[1,2] (see Figure 1). Specific structural modifications were carried out upon two areas of these two leading inhibitors in attempt to probe ATP binding pocket of BPLs (*Sa*BPL and *Mtb*BPL). Examples of such chemical modifications are depicted in Figure 1 and the biological activities are summarised below:

1. Chemical modifications were carried on the tether between the triazole and adenine group of **1.22** or benzoxazolone group of **1.23** (highlighted in blue in Figure 1). Functional groups such as di-hydroxyl were introduced the tether area and resulted in triazoles **2.06** and **2.10** with reduced potency ($K_i > 33$ µM) against both *Sa*BPL and *Mtb*BPL.

2. Structural mimics of the adenine ring of **1.22** (highlighted in purple in Figure 1) was discussed in section 2.3. However, the adenine ring mimics such as analogues **2.36** and **2.37** resulted in reduced potency and selectivity ($K_i \approx 10$ µM) against *Sa*BPL and *Mtb*BPL.
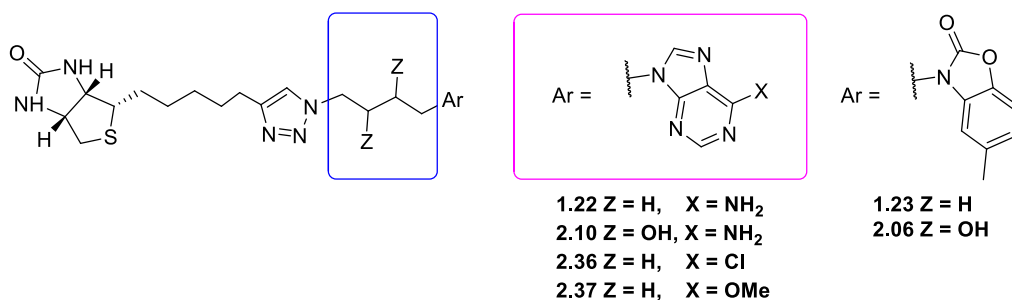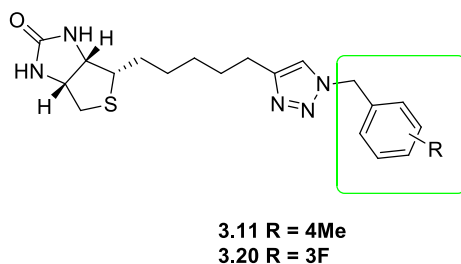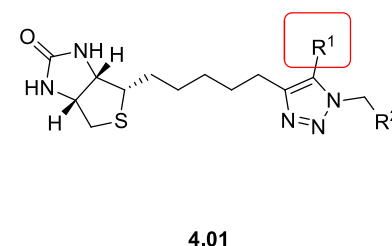
Figure 1: Overview of Chapters 2, 3 and 4. Chapter 2 investigated modifications upon the tether area and adenine analogues highlighted in blue. Chapter 3 investigated the benzylic

_____

analogues highlighted in green. Chapter 4 investigates the 5-position of the triazole ring, highlighted in red with the general structure **4.01**.

Chapter 3 introduced a novel class of triazoles with smaller and more drug-like benzylic substituents at N1 of the triazole ring (see Figure 1). These analogues were designed to specifically bind into the biotin and ribose binding pockets of *Sa*BPL. 1,2,3-Triazole **3.01t**, with a *meta* fluoro substituent, was identified as a potent *Sa*BPL inhibitor with $K_i = 0.25$ µM and possessed good antibacterial properties against *S. aureus*. Triazole **3.01k** with a *para* methyl group was found to be weakly active against *Sa*BPL with $K_i \approx 10$ µM. Although this class of triazoles possessed less activity against *Sa*BPL and *Mtb*BPL compared to the parent compounds (**1.22** and **1.23**), the simpler structures and less molecular weight would potentially improve the drug-like properties, such as aqueous solubility, making this class of triazoles as good drug candidates for further investigation.

As summarised above, chapter 2 and 3 report the use of copper-catalysed azide-alkyne cycloaddition reaction (CuAAC) and its associated triazole linkage as a powerful method to assemble diverse azides and terminal acetylenes. The practical simplicity and robust nature of 1,2,3-triazole products have allowed to rationalise a large library of 1,4-disubstituted triazole analogues.[1,3-5] However, the reduced activities of these triazole based BPL inhibitors as discussed in chapter 2 and 3 suggested that there was limited scope to achieve optimal potency by targeting the ATP binding site of *Sa*BPL. It is therefore suggested that there is a need to discover a new area for further modifications in order to achieve the optimal potency and selectivity.

Recently, a number of studies have turned attention to explore the regioselective synthesis of fully-decorated 1,2,3-triazoles with diverse functionalities on C5 of the triazole ring.[6-8] These studies suggest a number of approaches for expanding the 1,2,3-triazole from its C5 position, which provides additional room for further chemical modifications. The work discussed in this chapter is inspired by these studies with the design, synthesis and assay of 1,4,5-trisubstituted triazole analogues based on the general structure **4.01** (Figure 1). The potent *Sa*BPL inhibitors identified in chapter 2 (**1.22** and **1.23**) and chapter 3 (**3.01k** and **3.01t**) were selected for the investigation of their fully substituted triazole analogues. The proposed synthetic strategy was discussed below in section 4.2

_____

4.2   Proposed synthesis of 1,4,5-trisubstituted triazoles

A number of useful approaches have been developed for synthesis of 1,4,5-trisubstituted triazoles. The specific 1,3-dipolar cycloaddition between 1-iodoacetylene **4.02** and organic azides is particularly interesting.[9,10] One approach reported by Brady Worrell *et al.*[6] provides an efficient and reliable means to generate 5-iodo-1,2,3-triazoles which can not only be used as precursors for direct functionalisation by palladium-catalysed reactions[11,12], but also for the introduction of other halides by halogen exchange reactions.[7,9] Following the reported procedure, the synthetic route to the general structure of 1,4,5-trisubstituted triazole **4.01** was proposed and is depicted in Scheme 1.
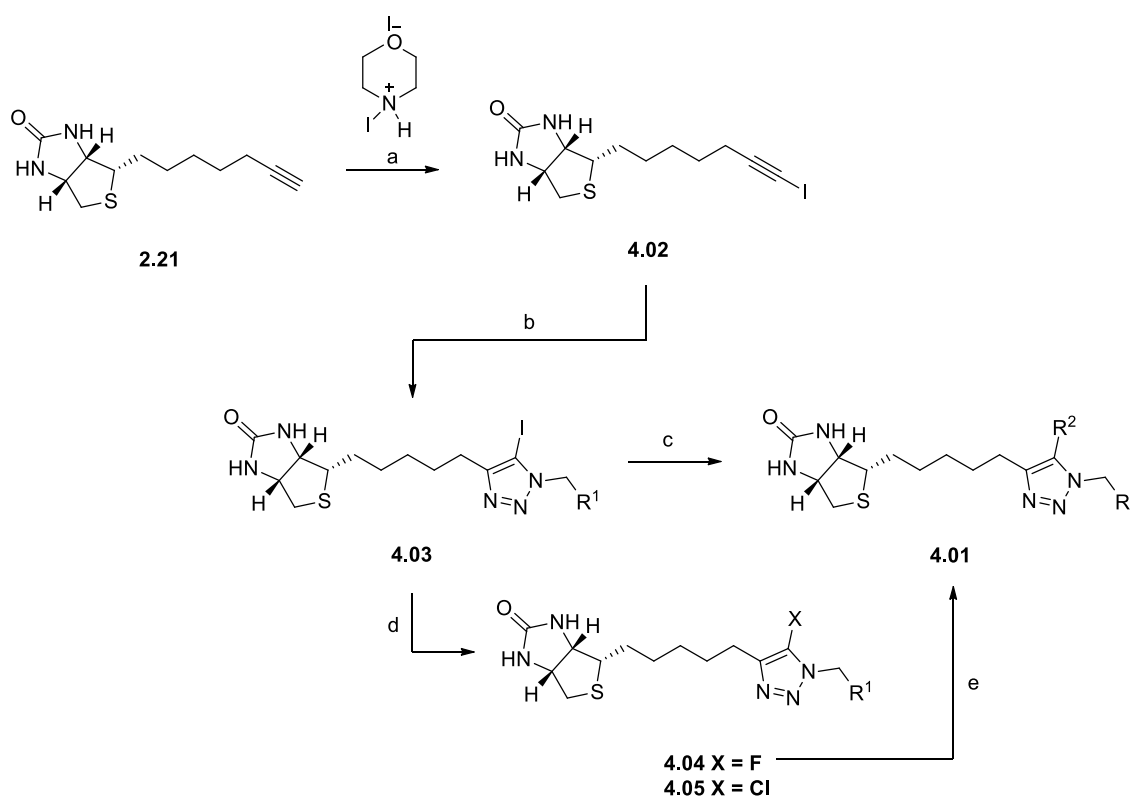
Scheme 1: a) THF, CuI, rt, 3h; b) R^1N_3, THF, CuI, TEA, rt, 12h; c) Pd(OAc), TEA, $R^2B(OH)_2$, THF, 60 °C, 12h; d) KX, MeCN/H_2O (1:1), 180 °C, 10min, mw; e) R^2H, NaH, THF, 3h, 70 °C

The proposed approach involved the synthesis of 1-iodoacetylene **4.02** by treating terminal biotin acetylene **2.21** with *N*-iodomorpholine hydriodide (NMI) and CuI in THF. As per conventional CuAAC reactions, the azide-iodoacetylene cycloaddition can be accomplished by reacting 1-iodoacetylene **4.02** with an azide in the presence of triethylamine (TEA) and CuI to give 5-iodotrizole **4.03**. It was envisaged that this 5-

iodotrizole **4.03** could be further functionalised to 1,4,5-trisubstituted triazole **4.01** by palladium-catalysed cross-coupling with an appropriate boronic acid. Alternatively, according to the reported halogen exchange reaction by Brady Worrell *et al.*[7], the 5-iodotrizoles **4.03** could be converted to 5-fluorotriazole **4.04** or 5-chlorotriazole **4.05** by reacting with potassium halide (such as KF or KCl) under microwave environment (180 °C, 250 psi). The 5-fluorotriazole **4.04** would then undergo a nucleophilic substitution reaction (S$_N$Ar), in which the fluorine could be replaced with nucleophiles to generate the fully substituted triazole **4.01**.

4.3 Design and synthesis of 1,4,5-trisubstituted triazoles

1,4-Triazoles **1.22**, **1.23**, **3.01k** and **3.01t**, as discussed above, were selected as structural models for investigating their 1,4,5-trisubstituted triazole analogues. Based on the proposed synthetic route described in Scheme 1, halogenated 1,4,5-trisubstituted triazoles **4.06-415** were proposed (Figure 2). Specifically, 5-iodotriazoles (**4.06**, **4.09**, **4.12**, and **4.14**) served as versatile synthetic precursors for the synthesis of 5-fluorotriazoles (**4.07**, **4.10**, **4.13**, and **4.15**) and 5-chlorotriazoles (**4.08** and **4.11**).

1.23 X = H
4.06 X = I
4.07 X = F
4.08 X = Cl

1.22 X = H
4.09 X = I
4.10 X = F
4.11 X = Cl

3.01k R = 4Me, X = H
3.01t R = 3F, X = H
4.12 R = 4Me, X = I
4.13 R = 4Me, X = F
4.14 R = 3F, X = I
4.15 R = 3F, X = F

4.16 R = OMe
4.17 R = OH
4.18 R = Ph
4.19 R = *iso*-butyl
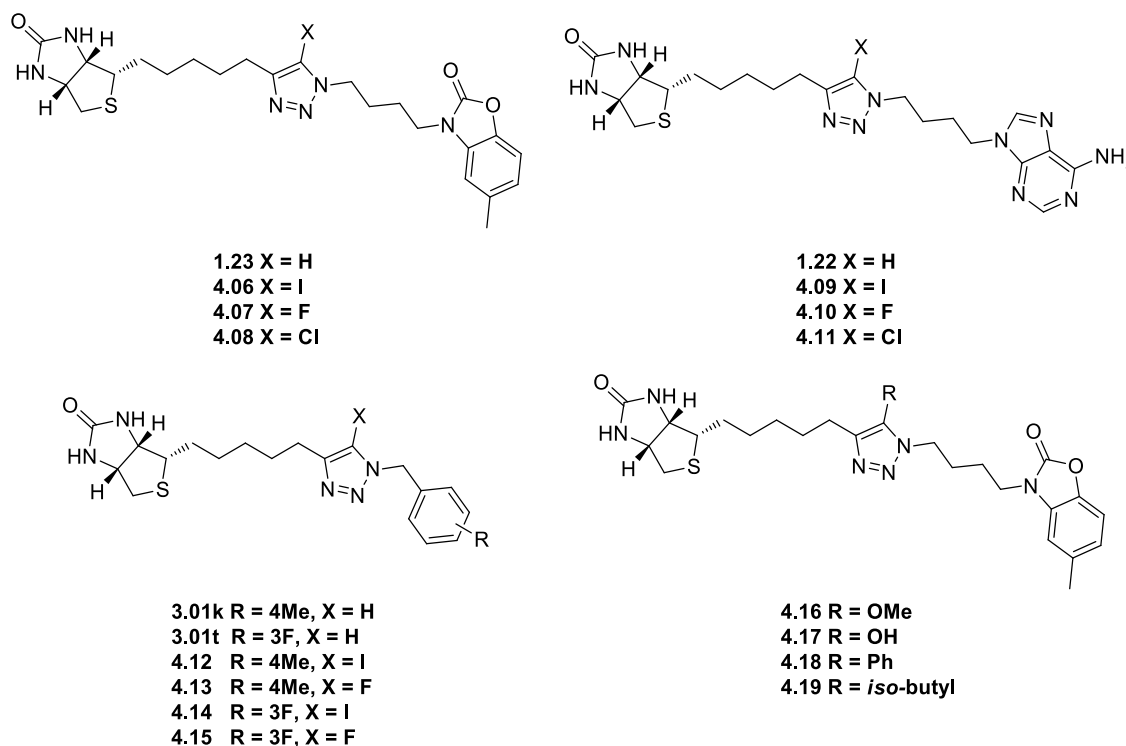
Figure 2: Active *Sa*BPL inhibitors 1,4-triazoles **1.22**, **1.23**, **3.01k** and **3.01t**. The proposed 1,4,5-trisubstituted triazoles **4.06-4.19**.

Subsequent modifications at the C5 of 1,4-triazoles involved S_NAr-type reactions and palladium-catalysed cross-coupling reactions as depicted in Scheme 1. 1,4,5-Trisubstituted triazoles **4.18** and **4.19** with a phenyl and *iso*-butyl group on C5 of the triazole ring were designed to investigate the palladium-catalysed arylation (sp^2) and alkylation (sp^3) cross-coupling.[11] Moreover, such extensions with larger functional groups provide an opportunity to explore potential interactions within the deeper space of the drug binding site in *Sa*BPL.

1,4,5-Trisubstituted-triazoles **4.16** with a methoxide group at C5 of the 1,2,3-triazole ring was proposed as a study model for the S_NAr-type reaction. The methoxide group was considered as a strong nucleophile and related reaction of this nucleophile with a 5-fluoro-triazole has been reported by Brady Worrell *et al.*[7] The design of 1,4,5-Trisubstituted-triazoles **4.17** with a hydroxyl group attached at C5 of triazole was guided by the crystal structure of 1,4-triazole **1.23** bound to *Sa*BPL.[1] The study revealed key features of this functional group within the triazole binding pocket of *Sa*BPL. These features are summarised below with the associated images of **4.17** docked to *Sa*BPL shown in Figure 3.

1. X-ray structure of **1.23** bound to *Sa*BPL reveals that the triazole C5 hydrogen is 3.43 Å and 3.59 Å removed from two carboxylate oxygens of Asp180. In addition it is 4.27 Å away from the amine group of Lys187.[1,2] (Figure 3). These distances are slightly larger than the ideal hydrogen bond distance (2.7Å – 3.2Å).[13] the introduction of a hydrogen-bonding group, such as hydroxyl, at C5 of the triazole would provide an opportunity for further hydrogen bonding.

2. As observed from the X-ray structure of biotinol-5'-AMP **1.05** bound to *Sa*BPL (Figure 3)[14,15], the phosphate oxygens of biotinol-5'-AMP **1.05** form an intricate hydrogen bonding network with two water molecules and the adjacent amino acid residues (Lys187, Asp180, Arg122 and Arg125) of *Sa*BPL. Introducing the hydroxyl group onto the triazole ring mimics the phosphate oxygens and presumably allow to form such hydrogen bonding network.

_____
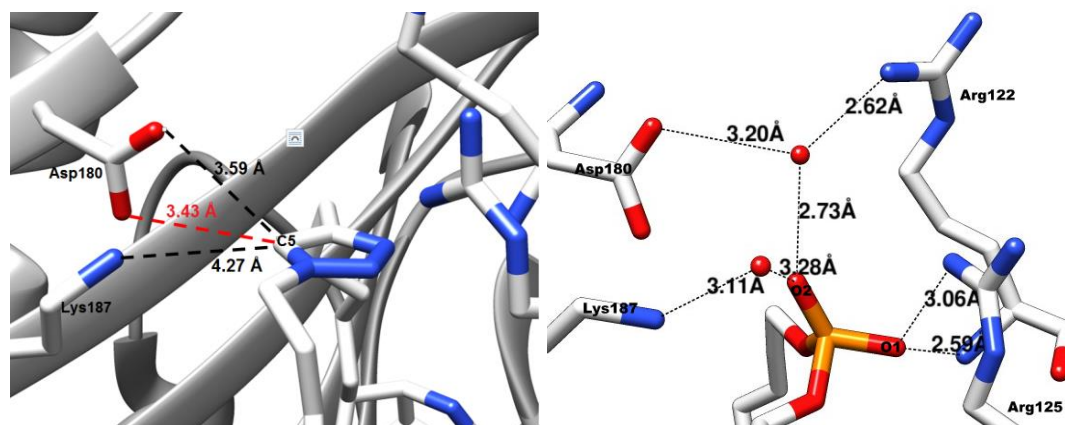
Figure 3: Reported 3D depiction of 1,2,3-triazole **1.23** bound to *Sa*BPL obtained from PDB: 3V7S (left) and biotinol-5'-AMP **1.05** bound to *Sa*BPL obtained from PDB: 4DQ2 (right). The hydrogen bonding interactions are represented with black dashes.

3. In addition to hydrogen bonding interactions, While the hydroxyl group of 1,2,3-triazole **4.17** provides an additional site for hydrogen bonding, it also increases hydrophilicity with a calculated cLogP value of 0.83, compared to the parent triazole inhibitor **1.23** (cLogP = 1.08). This suggests that **4.17** should have improved water solubility.

4. The hydroxyl group in **4.17** also provides a chemical handle, allowing further functionalisation.

4.3.1 Synthesis of 1-iodoacetylene 4.02 and azide building blocks 4.20 and 4.21

Synthesis of the key building block, 1-iodoacetylene **4.02**, was based on the general synthetic procedure described in Scheme 1 with a series of conditions investigated for optimisation, as outlined in Table 1.
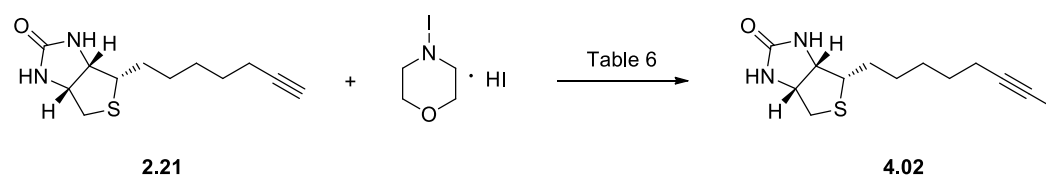
Scheme 2: a) see Table 6

_____

Table 1[a]: Synthesis of 1-iodoalkyne **2.36** using CuI[b]

Entry	Quant of NMI	Solvent	Time	Conversion (%)[b]
1	2 equiv.	THF	3 h	33
2	4 equiv.	THF	12 h	33
3	2 equiv.	THF:DMF (1:1)	3 h	80
4	2 equiv.	DMF	1 h	> 99

[a] Conditions: reactions were carried out in the presence of 20 mol% CuI at room temperature under anhydrous conditions. [b] conversion of 1-protoacetylene **2.21** to 1-iodoacetylene **4.02**, percentage judged by ^{1}H NMR of crude product.

Following conditions reported by Worrell *et al.[6]* and outlined in Table 1 entry 1, biotin acetylene **2.21** was treated with two equivalents of NMI in the presence 20 mol% CuI in anhydrous THF at ambient temperature. It is noteworthy that the starting material **2.21** and the product **4.02** shared similar polarities, thereby TLC failed to monitor reaction progress. The reaction was thus monitored using ^{1}H NMR of the crude mixture sampled every 1 h. It was demonstrated that approximately 33% of biotin acetylene **2.21** was converted to the product **4.02** after 3 h reaction (entry 1). Increasing the reaction time to 12 h with four equivalents of NMI did not improve conversion to **4.02** (entry 2). A key observation was that the starting material **2.21** was not completely soluble in THF.

In an attempt to overcome poor solubility of biotin acetylene **2.21** in THF, a mixture solvent of THF and DMF (1:1) was used, and two equivalents of NMI was added to the reaction (see entry 3 Table 1). ^{1}H NMR of the crude material after 3 h confirmed an approximate 80% conversion from biotin acetylene **2.21** to 1-iodoacetylene **4.02** after 3 h (entry 3). Full conversion (> 99% in entry 4) was achieved when the solvent was changed to DMF only and the reaction was complete within 1 h as judged by ^{1}H NMR (entry 4). The reaction mixture was filtered through neutral aluminium oxide, washed with MeOH/DCM (1:9) mixture, and dried *in vacuo* to give **4.02** as a pale yellow solid, which was used for CuAAC without further purification.

_____

The preparation of azide building blocks **4.20** and **4.21** was reported by Tieu *et al.*[1] and repeated herein. 2-Benzoxazolone **2.27** obtained from chapter 2 was initially treated with potassium carbonate, followed by reaction with dibromobutane in DMF to give bromide **4.22** in 93% yield. Bromide was converted to 2-benzoxazolone azide **4.20** on reaction with sodium azide in DMF, as shown in Scheme 3, with a yield of 91% after purification by column chromatography.
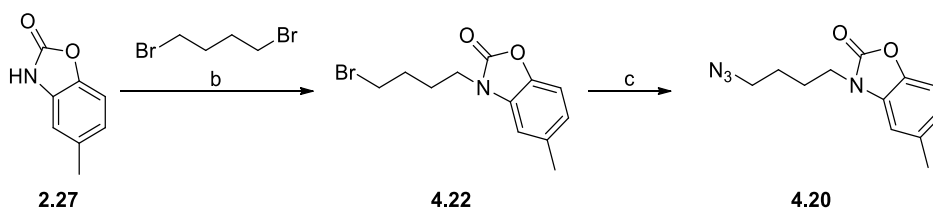
Scheme 3: a) K_2CO_3, DMF, 50 °C, 3h; b) NaN_3, DMF, 12h.

Synthesis of the adenine azide **4.21** was accomplished by first treating adenine **2.29** with caesium carbonate and dibromobutane in DMF. The resulting adenine bromide **4.23** was then treated with sodium azide in DMF, as shown in Scheme 4, to give the corresponding azide **4.21** in total yield of 50% over two steps.
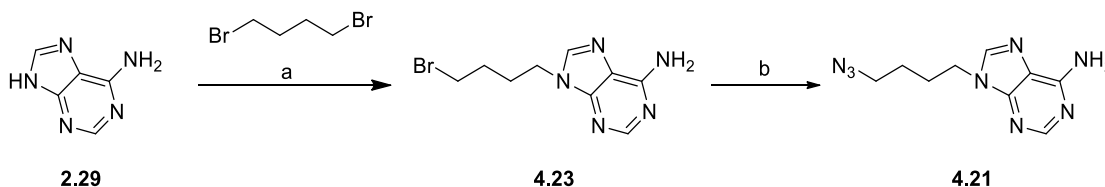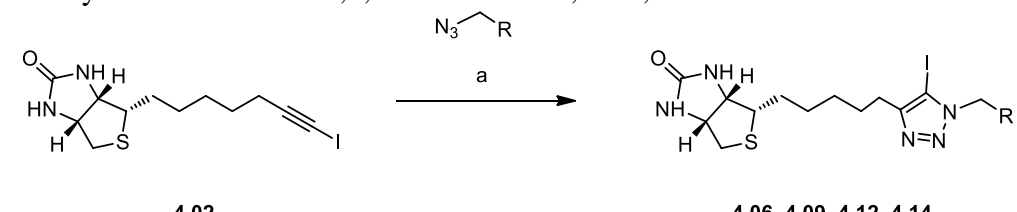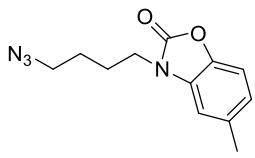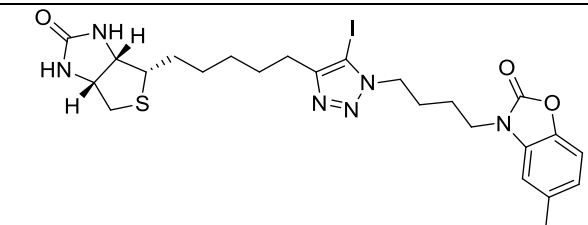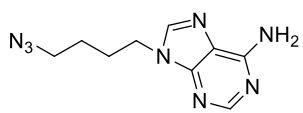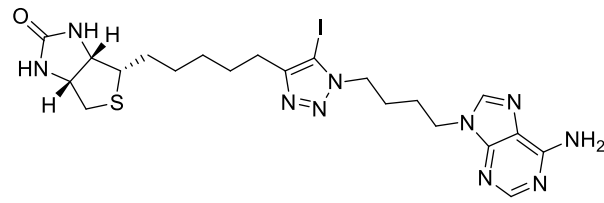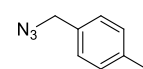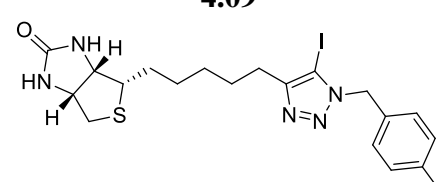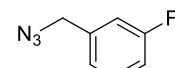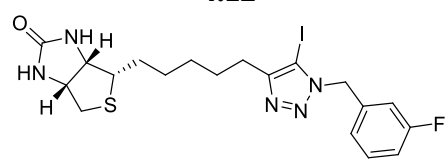
Scheme 4: a) Cs_2CO_3, DMF, rt, 12 h; b) NaN_3, DMF, rt, 12h.

4.3.2 Synthesis of 5-iodo-1,2,3-triazoles 4.06, 4.09, 4.12 and 4.14

With the key building block 1-iodoacetylene **4.02** in hand, the 5-iodo-1,2,3-triazoles **4.06**, **4.09**, **4.12** and **4.14** were synthesised according to the general procedure outlined in Table 2 1.[9] It was learned from the previous reaction (Scheme 2) that the solubility of **4.02** in THF was poor, thus anhydrous DMF was used. As summarised in Table 2, azides **4.20** and **4.21** and benzylic azides **3.01k** and **3.01t** (described in chapter 3) were separately treated with 1-iodoacetylene **4.02** in the presence of CuI and stoichiometric amount of triethylamine (TEA) in anhydrous DMF. The resulting 5-iodo-1,2,3-triazoles were isolated

_____

and purified using flash chromatography to give **4.06, 4.09, 4.12** and **4.11** in yields of 36%, 66%, 44% and 55%, respectively.

Table 2ª: Synthesis of 5-iodo-1,2,3-triazoles **4.20**, **4.21**, **4.12** and **4.14**

Azide (reactant)	Triazole (product)	Yield[b] (%)
4.20	**4.06**	36
4.21	**4.09**	66
3.03k	**4.12**	44
3.03t	**4.14**	55

[a] Conditions: CuI, DMF, TEA, 12 h, Rt; [b] isolated yields after flash chromatography

___

4.3.3 Halogen exchange reaction of 5-iodo-1,2,3-triazoles 4.06 and 4.09

Following the optimised conditions developed by Fokin's group, 5-iodo-1,2,3-triazole **4.06** was converted to 5-fluoro-1,2,3-triazole **4.07** and 5-chloro-1,2,3-triazole **4.08** by halogen exchange as shown in Scheme 5[7].
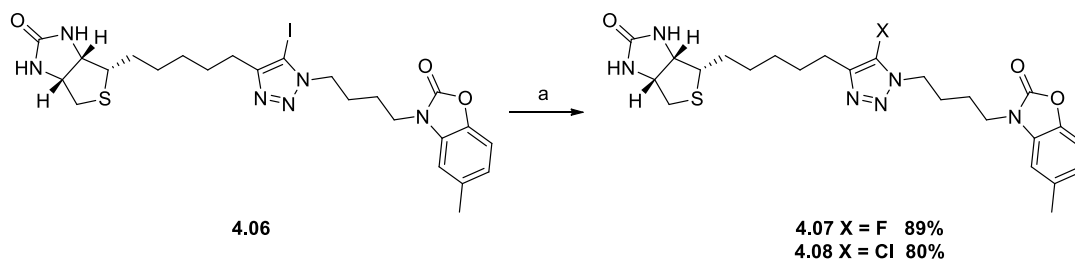
Scheme 5: a) KX (X = F, X = Cl), MeCN/H$_2$O (1:1), 180 $^{\circ}$C, 10 min, mw.

In an appropriate sized round-bottomed microwave vial, 5-iodo-1,2,3-triazole **4.06** was treated with five equivalents of potassium fluoride or potassium chloride in MeCN/H$_2$O (1:1) mixture. Vials were placed into the microwave reactor and allowed to stir at 180 $^{\circ}$C under a pressure of 250 psi for 10 min. The resulting reaction mixtures were concentrated and purified by flash chromatography to give 5-fluoro-1,2,3-triazole **4.07** and 5-chloro-1,2,3-triazole **4.08** in good yields, as reported in Scheme 5.

The synthesis of adenine analogues of 5-fluoro-1,2,3-triazole **4.10** and 5-chloro-1,2,3-triazole **4.11** were attempted with a number of conditions, as listed in Table 3 and discussed below.
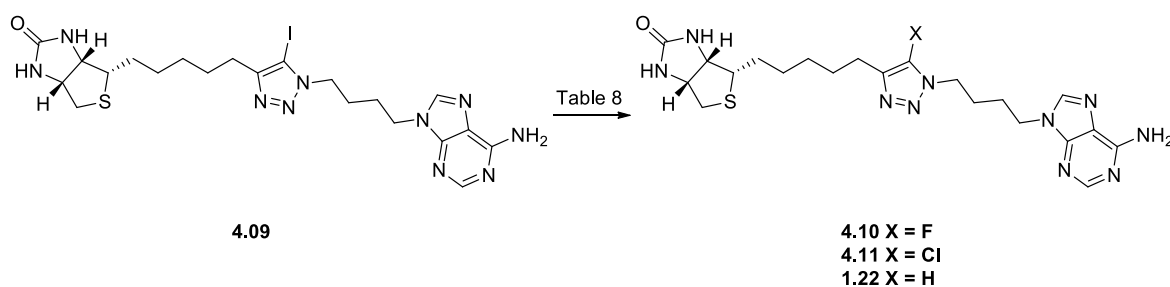
Scheme 6: See Table 3.

_____

Table 3ª: Attempted synthesis of 5-Halogen-1,2,3-triazole **4.10** and **4.11**

Entry	reagent	Solvent	Time	4.09/4.10/1.22[b]
1	KF	MeCN/H$_2$O (1:1)	10 min	1:0:0
2	KF	MeCN/H$_2$O (1:1)	30 min	1:0:0
3	KF	THF	10 min	0:0:1
4	KF	DMF	10 min	-
				4.09/4.11/1.22[c]
5	KCl	MeCN/H$_2$O (1:1)	10 min	1:0:0
6	KCl	MeCN/H$_2$O (1:1)	30 min	1:0:0
7	KCl	THF	10 min	0:0:1
8	KCl	DMF	10 min	-

[a] Conditions: reactions were carried out using microwave reactor with temperature of 18 °C and pressure of 250 psi; [b] isolated material after flash chromatography (DCM/MeOH 9:1) with ratio of starting material **4.09** : 5-fluorotriazole, **4.10** : 5-prototriazole **1.22**; [c] isolated material after flash chromatography (DCM/MeOH 9:1) with ratio of starting material **4.09** : 5-chlorotriazole, **4.11** : 5-prototriazole **1.22**.

The reaction was initially attempted following the same conditions as for preparation of **4.07** and **4.08** depicted in Scheme 5.[7] As shown in Scheme 6, the 5-iodo-1,2,3-triazole **4.09** was treated with potassium fluoride (entry 1) or potassium chloride (entry 5) in the solvent mixture of MeCN/H$_2$O (1:1). The suspension was then placed in the microwave for 10 min to give only starting material recovered. Increasing the reaction time to 30 min had no effect (entry 2 and 6). Alternative solvent systems, such as THF (Table 3, entry 3 and 7) and DMF (Table 3, entry 4 and 8), were used to overcome poor solubility of **4.09** in MeCN/H$_2$O (1:1). However, using THF resulted in the production of 5-proto-1,2,3-triazole **1.22** as the main by-product (Table 3, entries 3 and 7). This presumably formed as a result of reductive dehalogenation reaction[9], where the 5-iodo-1,2,3-triazole **4.06** was converted to the corresponding 5-proto-1,2,3-triazole **1.22**. Finally, reactions using DMF resulted in a complex mixture, suggesting decomposition of the starting material **4.06**. No further

conditions were investigated as the approach described above was limited by low solubility and instability of adenine 5-iodo-1,2,3-triazole **4.09**.

4.12 R = 4Me
4.14 R = 3F

4.13 R = 4Me
4.15 R = 3F
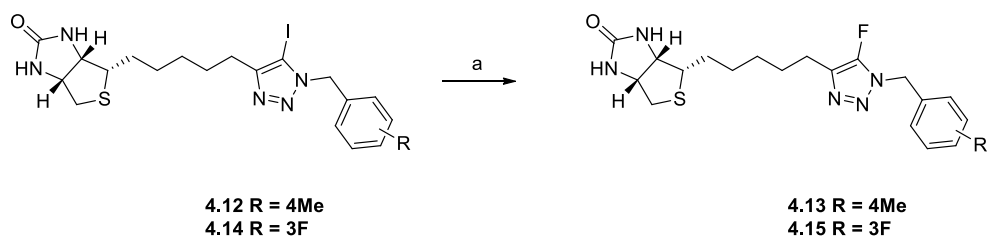
Scheme 7: a) KF, MeCN/H_2O (1:1), 180 °C, 10 min, mw.

Synthesis of 5-fluoro-1,2,3-triazoles **4.13** and **4.15** were accomplished using the same conditions as for preparation of **4.07** described in Scheme 5. As shown in Scheme 6, the 5-iodo-1,2,3-triazoles **4.12** and **4.13** were separately treated with potassium fluoride in THF and reacted in the microwave for 10 min. Reaction mixtures were purified by flash chromatography to give the corresponding 5-fluoro-1,2,3-triazoles **4.13** and **4.15** in 43% and 33%, respectively.

4.3.4 Nucleophilic substitution reaction of 5-fluoro-1,2,3-triazoles 4.07

The S_NAr-type reaction of **4.07** to yield fully substituted 1,2,3-triazoles **4.16** and **4.17** were examined and shown in Scheme 8 using a range of conditions as outlined in Table 4.

4.07

Table 4

4.16 R = OMe
4.17 R = OH
1.23 R = H
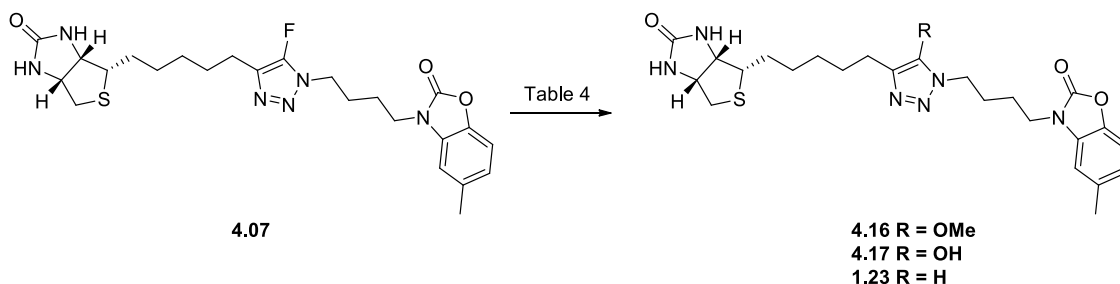
Scheme 8: see Table 4

Table 4: Attempted synthesis of **4.16** and **4.17**

Entry[a]	Nucleophile (2.0 equiv)	Base	Solvent	Temp (°C)	Time	Yield%
1	NaOMe	NaH (1.5 equiv)	THF	reflux	3 h	0
2	NaOMe	NaH (3 equiv)	THF	reflux	3 h	0
3	NaOMe	K_2CO_3 (1.5 equiv)	THF	reflux	3 h	0
4	NaOMe	Cs_2CO_3 (1.5 equiv)	THF	reflux	3 h	0
5	NaOMe	NaH (1.5 equiv)	DMF	80	3 h	0
6	NaOMe	NaH (1.5 equiv)	DMF	130	12 h	55[d]
7[b]	NaOMe	NaH (1.5 equiv)	DMF	80	10 min	0[e]
8	NaOH	NaH (1.5 equiv)	THF	reflux	3 h	0

[a] Conditions: reactions were carried out at the corresponding temperature under nitrogen atmosphere; [b] the reaction was carried out in the microwave reactor at 80 °C with pressure of 250 psi; [c] traces judged by TLC; [d] yield of by-product **1.23** isolated after flash chromatography (DCM/MeOH 9:1); [e] unidentified complex mixture.

Following reported conditions described by Fokin *et al.*[7], 5-fluoro-1,2,3-triazole **4.07** was initially treated with 2.0 equivalents of sodium methoxide and 1.5 equivalents of sodium hydride in THF at reflux condition for 3 h. The reaction failed to give **4.16** as determined by TLC (Table 4, entry 1). Increasing the quantity of sodium methoxide from 1.5 to 3 equivalents gave no trace of desired product **4.16** (Table 9, entry 2). Alternatively, treating 5-fluoro-1,2,3-triazole **4.07** with a different base such as K_2CO_3 and Cs_2CO_3 resulted in recovery of starting material **4.07** only (Table 9, entries 3 and 4).

A key observation for the reactions carried out in entries 1 to 4 was that the starting material **4.07** and sodium methoxide were not fully soluble in THF. Alternative solvent systems, such as DMF and a mixture of THF and DMF, were investigated in order to improve reagent solubility. As described in entry 5, the reaction was repeated using dry DMF in place of THF and heated at 80 °C for 3 h. This resulted in only returned starting material **4.07** as determined by ^{1}H NMR. Increasing the reaction temperature from 80 °C to 130 °C and extending reaction time to 12 h resulted in a complex mixture (see entry 6

_____

Table 4). The crude product was purified by flash chromatography to give the corresponding 5-proto-1,2,3-triazole **1.23** based on ^{1}H NMR and HRMS (Table 4, entry 6). This suggest that at high temperature, reductive dehalogenation of 5-fluoro-1,2,3-triazole **4.07** occurred to give generated 5-proto-1,2,3-triazole **1.23**. Given the instability of 5-fluoro-1,2,3-triazole **1.23** at high temperature, a microwave reaction was attempted with the temperature set to 80 °C and pressure at 250 psi for 10 min (Table 4, entry 7). The crude reaction mixture was isolated and shown to be a complex and unidentifiable mixtures based on ^{1}H NMR. Finally, the synthesis of 5-hydroxy-1,2,3-triazole **4.17** was attempted following the reported condition as described in Table 4 entry 8[9], whilst sodium hydroxide was used as the reagent instead of sodium methoxide. Again, **4.17** was not observed, with only starting material (**4.07**) was present as determined by ^{1}H NMR and HRMS. Additional conditions were not investigated for the synthesis of triazole **4.17** in this study.

Similar S_NAr reactions of S, O, and N based nucleophiles with 5-chlorotriazoles have been described. However, these reactions require electro-withdrawing substituents, such as esters and amides, at C4 of the triazole ring and do not proceed with non-activated triazoles.[7,16-18] 5-Iodo-1,2,3-triazole **4.06** and 5-chloro-1,2,3-triazole **4.08** did not react with sodium methoxide under the general S_NAr reaction conditions (Scheme 9), with only starting material recovered.

4.06 X = I
4.08 X = Cl
4.17
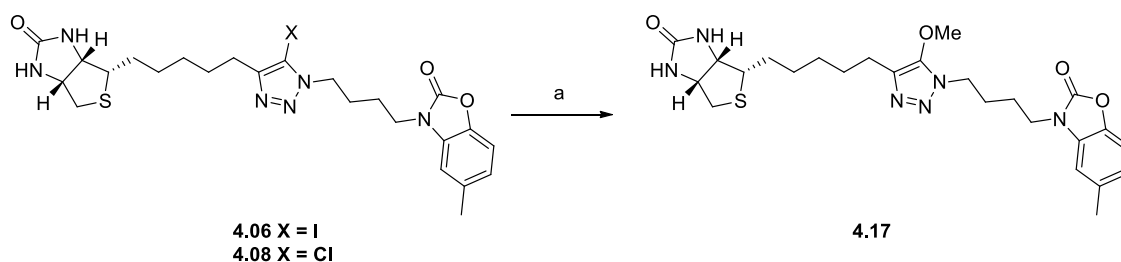
Scheme 9: a) NaOMe, NaH, THF, 70 °C, N_2, 12 h

Given poor stability and solubility of halogenated triazoles **4.06-4.08** in the nucleophilic substitution reactions, use of other conditions for S_NAr reactions of 5-fluoro-1,2,3-triazole **4.07** was not investigated. As such, an alternative palladium-catalysed coupling reaction was devised and is described in section 4.3.5 for the functionalisation of 5-iodo-1,2,3-triazole **4.06**.

4.3.5 Palladium-catalysed reaction of 5-iodo-1,2,3-triazoles 4.06

The palladium-catalysed coupling reactions described in this section involve sp^2 arylation and sp^3 alkylation of 5-iodo-1,2,3-triazole **4.06.** as depicted below in Schemes 10 and 11.[11,19] The reaction conditions attempted here are summarised in Tables 5 and 6, respectively.

Palladium-catalysed sp^2 arylation
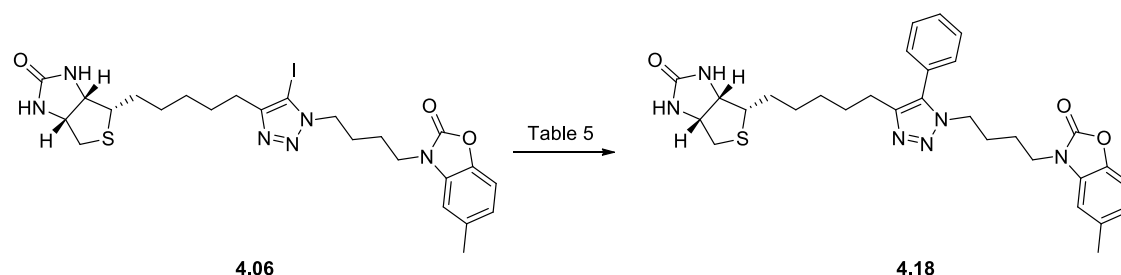
Scheme 10^a: see Table 15

Table 5: Optimisation of Palladium-catalysed sp^2 arylation of 4.06

Entry	Solvent	Temp (^{o}C)	Time	Yield^b (%)
1	DMF	Rt	12 h	Trace^c
2	DMF	150	3 h	63^d
3	THF	70	12 h	41

^{a} General reaction conditions: **4.06** (1 equiv), PhB(OH)$_2$ (1.5 equiv), PdCl$_2$(PPh)$_3$ (5 mol%), K$_2$CO$_3$ (1.5 equiv). ^{b} isolated yield after flash chromatography. ^{c} trace amount of target product detected by TLC. ^{d} 5-proton-triazole **1.23** in yielding of 63%.

Coupling 5-iodo-1,2,3-triazole **4.06** and phenylboronic acid in the presence of 1.5 equivalents of potassium carbonate and a catalytic amount of PdCl$_2$(PPh)$_3$ in dry DMF for 12 h gave only trace quantities of **4.18** as judged by TLC (Table 5, entry 1). Heating the reaction to 150 ^{o}C resulted in reductive dehalogenation of **4.06** to give its corresponding 5-prototriazole **1.23**. This was isolated and purified by flash chromatography in a yield of 63% (Table 5, entry 2). This unexpected reductive dehalogenation reaction, which also occurred in halogen exchange (see section 4.3.3) and S$_N$Ar reactions (see section 4.3.4),

suggests that the 5-halogen-triazole was not stable in polar solvent, such as DMF, at high temperature (> 130 $^{\circ}$C). Therefore, less solvent THF was used and the reaction was repeated at 70 $^{\circ}$C for 12 h to give 5-phenyl-triazole **4.18** in 41% yield after purification by flash chromatography (Table 5, entry 3).

Palladium-catalysed sp³ alkylation
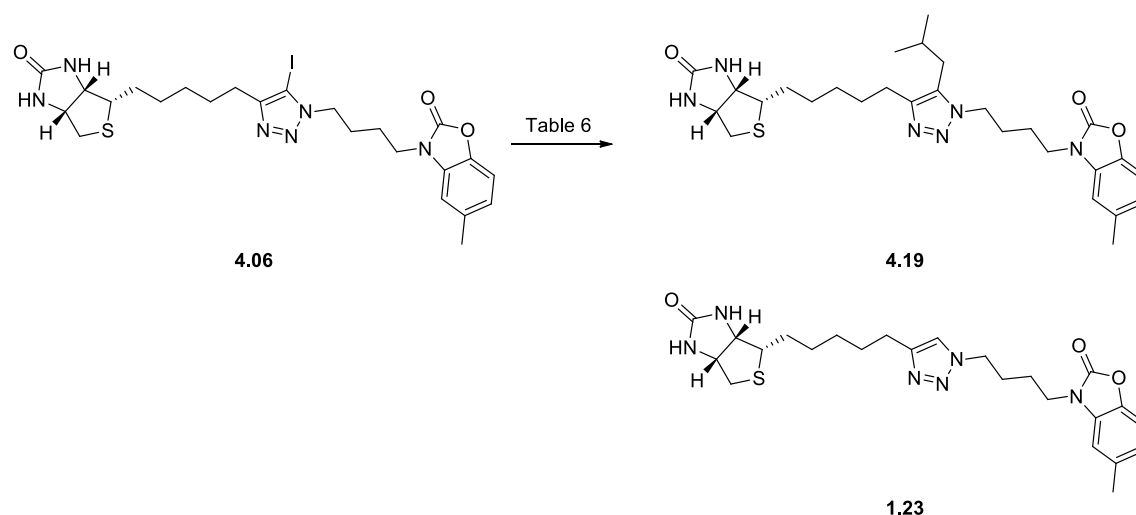
Scheme 11: see Table 6

Table 6ᵃ: Optimisation of Palladium-catalysed sp3 acylation of 4.06

Entry	Catalyst	Base	Solvent	Activation source	additives	4.06/4.19/1.23ᵇ
1	PdCl₂(PPh)₃	K₂CO₃	THF	reflux	-	1 : 0 : 0
2	Pd(OAc)₂	K₂CO₃	THF	reflux	-	3 : 0 : 5
3	Pd(OAc)₂	K₂CO₃	THF	reflux	PPh₃	1 : 0 : 7

ᵃ General reaction conditions: **4.06** (1 equiv), isobuylboronic acid (1.5 equiv), PdCl₂(PPh)₃ (5 mol%), K₂CO₃ (1.5 equiv). ᵇ ratio of the starting material **4.06**, product **4.19** and by-product **1.23**, judged by ¹H NMR.
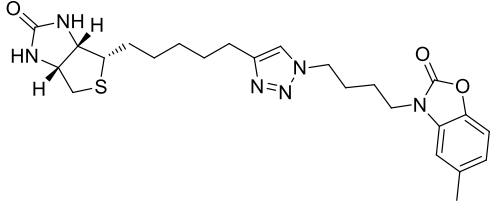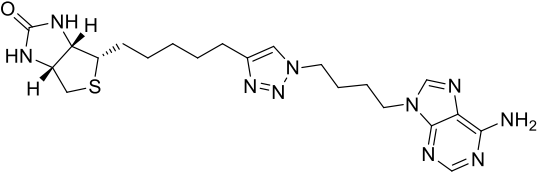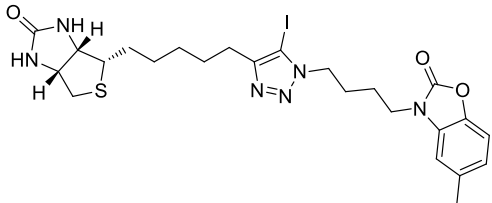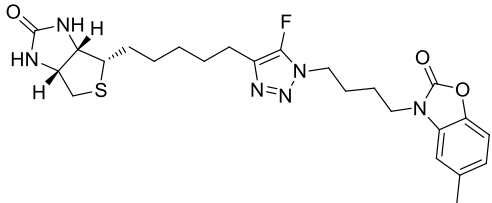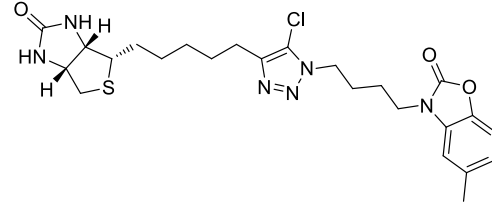
Given the successful synthesis of fully substituted triazole **4.18** by palladium-catalysed *sp²* arylation of **4.06**, a palladium catalysed *sp³* alkylation of **4.06** was proposed as shown in Scheme 11. The optimised conditions for the synthesis of 5-phenyl-1,2,3-triazole **4.18** (Table 5, entry 3) were initially attempted. However, treating 5-Iodo-1,2,3-triazole **4.06** with isobutylboronic acid in the presence of potassium carbonate and PdCl₂(PPh)₃ in THF

failed to give the desired product **4.19** (Table 6, entry 1) and only the starting material **4.06** was recovered. Alternatively, using Pd(OAc)$_2$ instead of PdCl$_2$(PPh)$_3$ resulted in dehalogenation of **4.06** to give a mixture of 5-proto-1,2,3-triazole **1.23** and 5-iodo-1,2,3-triazole **4.06** in a ratio of 5:3 as determined by ^{1}H NMR (Table 6, entry 2). Phosphine ligands have been reported as reducing agents to convert Pd(II) of Pd(OAc)$_2$ to the activated Pd(0) during the reaction.[20] Therefore, the reaction described in entry 2 was repeated but with addition of 0.1 equivalent of PPh$_3$. This resulted in a mixture of 5-iodo-1,2,3-triazole **4.06** and 5-proto-1,2,3-triazole **1.23** with a ratio of 1:7 (**4.06 : 1.23**). Given the difficulties encountered in the attempted activation of much more inert sp^3 C-H bonds compared to the well-known sp^2 C-H activation, further attempts of palladium catalysed alkylation of 5-iodo-1,2,3-triazole **4.06** were held for future investigation.

_____
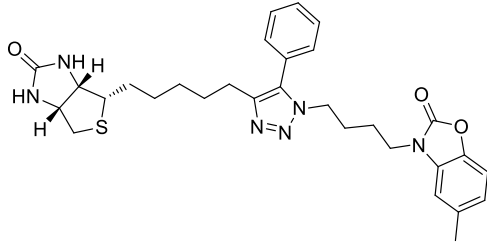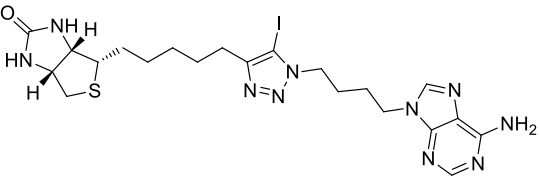
4.4   Enzyme and microbial assay

Compounds **4.06-4.09**, **4.12-4.15** and **4.18** were assayed against *Sa*BPL, *Mtb*BPL and *Hs*BPL by collaborators at Biological Sciences, University of Adelaide, using an *in vitro* biotinylation assay described by Chapman-Smith and co-workers.[21] The results are summarised in Table 7 & 8. Inhibition constant (K_i) values were determined for each compound from a dose-response curve by varying inhibitor concentration under the same enzyme concentration

Table 7: Enzyme assay of triazoles **4.06-4.09** and **4.18** against *Sa*BPL, *Mtb*BPL, and *Hs*BPL

Compound	*Sa*BPL K_i (µM)	*Mtb*BPL K_i (µM)	*Hs*BPL K_i (µM)
1.23	0.09 ± 0.02	> 33	> 33
1.22	0.66 ± 0.15	0.64 ± 0.14	> 33
4.06	0.41 ± 0.02	> 33	> 33
4.07	0.42 ± 0.06	> 33	> 33
4.08	0.90 ± 0.11	> 33	> 33

_____

4.18   0.78 ± 0.17   > 33   > 33

4.09   > 17   0.34 ± 0.03   > 33

In vitro biotinylation assays were carried out using 6.25 nM of enzyme.

As shown in Table 7, four benzoxazolone 1,4,5-trisubstituted triazoles (**4.06-4.09** and **4.18**) were potent and selective against *Sa*BPL over the human homologue. 5-Iodo-1,2,3-triazole **4.06** and 5-fluoro-1,2,3-triazole **4.07** exhibited equal potency against *Sa*BPL with $K_i = 0.41 \pm 0.02$ µM and $K_i = 0.42 \pm 0.06$ µM, respectively. These were 4.6 fold less potent than the parent lead triazole **1.23** ($K_i = 0.09 \pm 0.06$ µM).[1] 5-Chloro-1,2,3-triazole **4.08** was also found to be active against *Sa*BPL with $K_i = 0.90 \pm 0.11$ µM, which is 10 fold less potent compared to triazole **1.23**.
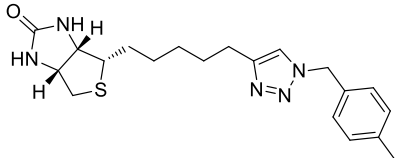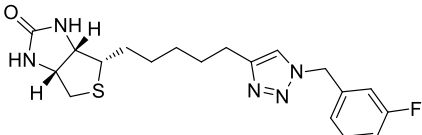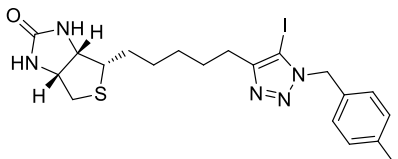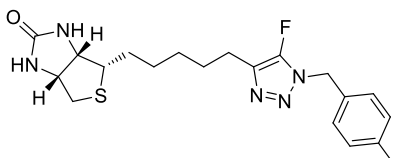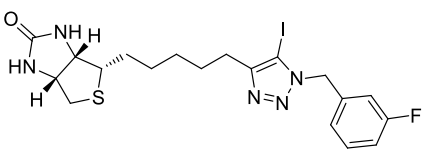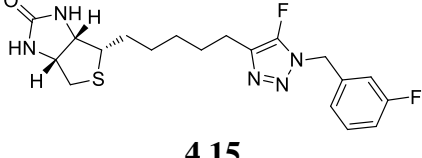
Finally, 1,2,3-triazole **4.18** with a phenyl group on the fifth position of the triazole ring was found to inhibit *Sa*BPL with $K_i = 0.78 \pm 0.17$ µM and was 8.7 fold less potent than proton triazole **1.23**. Consistent with the parent compound **1.23**, the 1,4,5-trisubstituted triazoles **4.06-4.09** and **4.18** showed no inhibitory activity against *Hs*BPL ($K_i > 33$ µM).

Adenine 5-iodo-1,2,3-triazole **4.09** was found to be potent towards *Mtb*BPL with $K_i = 0.34 \pm 0.03$ µM, which was 2 fold more potent compared to the parent adenine 5-proto-1,2,3-triazole **1.22** ($K_i = 0.64 \pm 0.04$ µM). Significantly, this compound (**4.09**) showed high selectivity for *Mtb*BPL over *Sa*BPL. **4.09** was found to be bioactive against *Sa*BPL at a concentration of 100 µM during the enzyme kinetic assay, whilst the parent adenine 5-proto-1,2,3-triazole **1.22** was reported to have $K_i = 0.66 \pm 0.05$ µM towards *Sa*BPL.[1] Finally, 5-iodo-1,2,3-triazole **4.09** showed no activity against *Hs*BPL ($K_i > 33$ µM).

As shown blow in Table 8, benzylic 5-iodo-1,2,3-triazole **4.12** was found to inhibit *Sa*BPL with $Ki = 0.55$µM with at least 60-fold selectivity over *Mtb*BPL ($K_i > 33$ µM) and *Hs*BPL ($K_i > 33$ µM). Importantly, the inhibitor was over 20 fold more potent toward *Sa*BPL

compared to its parent 5-proto-1,2,3-triazole **3.10** (K_i > 10 μM). Interestingly, the fluorinated 1,4,5-trisubstituted triazole **4.13** was found inactive against SaBPL (K_i > 33 μM). Benzylic 5-iodo-1,2,3-triazole **4.14** and 5-fluoro-1,2,3-triazole **4.15** were also found inactive against SaBPL (K_i > 33 μM), whereas the parent 5-proto-1,2,3-triazole **3.01t** was found to be the most active compound (Ki = 0.27 μM) in this class of inhibitors (see Chapter 3). These unexpected results require further investigation, such as solving their x-ray crystal structures in SaBPL.

Table 8: Enzyme assay of triazoles **4.12-4.15** against SaBPL, MtbBPL, and HsBPL

Compound	SaBPL K_i (μM)	MtbBPL K_i (μM)	HsBPL K_i (μM)
3.01k	> 10	> 33	> 33
3.01t	0.28 ± 0.02	> 33	> 33
4.12	0.55	> 33	> 33
4.13	> 33	> 33	> 33
4.14	> 33	> 33	> 33
4.15	> 33	> 33	> 33

In vitro biotinylation assays were carried out using 6.25 nM of enzyme.

_____

Antibacterial activities of parent compound **1.23** and 5-fluoro-1,2,3-triazole **4.07** were investigated by collaborators at Biological Science, University of Adelaide, using a micro broth dilution antibacterial susceptibility assay with *S. aureus* strain ATCC49775.[1] As shown below in Figure 4, **1.23** inhibited growth in a concentration dependent manner with maximum activity at 4 µg/ml.[1] However, an MIC value could not be calculated given that the compound did not completely reduce cell growth. In contrast, compound **4.07** significantly reduce cell growth with no growth apparent at 16 µg/ml. The difference in antibacterial activity between **1.23** and **4.07** is possibly due to improved cellular penetration or reduced efflux or metabolism inside *S. aureus.*[22] The bioactivity of **4.07** in the microbiology assay is an important finding essential for an antibacterial discovery program.
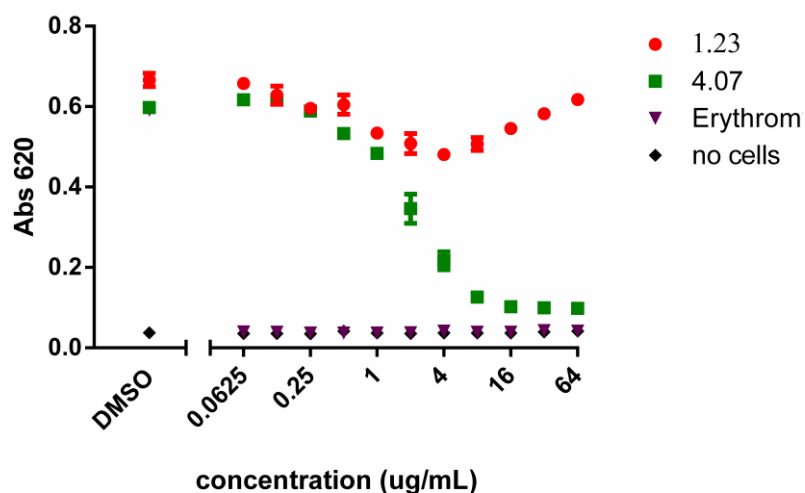
Figure 4: Inhibition of *S. aureus* growth in vitro. Compounds **1.23** (●red), **4.07** (■green), positive control erythromycin (▼purple), negative control no cells (♦black).

4.5   Conclusion

This chapter demonstrated the design, synthesis and assay of fully substituted 1,2,3-triazoles **4.06-4.09**, **4.12-4.14** and **4.18**. Two approaches were proposed and investigated for the synthesis of these triazoles. 5-Iodo-1,2,3-triazoles **4.06**, **4.09**, **4.12**, and **4.14** were successfully synthesised using copper catalysed cycloaddition between azides and 1-iodoacetylene in yields of 36%-66%. The halogen exchange approach efficiently converted 5-iodo-1,2,3-triazoles (**4.06**, **4.12** and **4.14**) to 5-fluoro-1,2,3-triazoles (**4.07**, **4.13** and **4.15**) and 5-chloro-1,2,3-triazole (**4.08**) by reacting simple salts such as potassium fluoride and potassium chloride. This reaction proceeded rapidly in the microwave reactor (10 min) and gave bench stable products with moderate to quantitative yields of 64%-88%. However, the subsequent S_NAr-type reaction of 5-fluoro-1,2,3-triazole **4.07** failed to give the desired triazoles and often resulted in the reductive dehalogenation reaction that converted 5-fluoro-1,2,3-triazole **4.07** to 5-proto-1,2,3-triazole **4.23**. An alternative palladium-catalysed coupling approach of 5-iodo-1,2,3-triazole **4.06** with phenylbronic acid was examined and this gave 5-pheny-1,2,3-ltriazole **4.18** in good yield of 85%.. In contrast to the sp^2 coupling of 5-phenyl-1,2,3-triazole **4.18**, a palladium-catalysed sp^3 coupling reaction with isobutylboronic acid failed to give the desired product **4.19**. This was presumably due to low reactivity of the triazole ring and as this type of reaction often requires electro-withdrawing substituents at the 4-position of the triazole ring.

The 1,4,5-trisubstituted triazoles **4.06-4.09**, **4.12-4.15** and **4.18** were assayed against a library of BPLs (*Sa*BPL, *Mtb*BPL and *Hs*BPL). Triazoles **4.06-4.08** and **4.18** were shown to be moderate *Sa*BPL inhibitors with K_i of 0.41 to 0.90 μM, and triazole **4.09** was found for the first time to be an active and selective *Mtb*BPL inhibitor with a $K_i = 0.34 \pm 0.03$ μM (cf. *Sa*BPL with $K_i > 17$ μM and *Hs*BPL with $K_i > 33$ μM). Significantly, the new active triazole analogue **4.07** displayed bacterisostatic activity against *S. aureus* ATCC 49755. At 16 μg/ml inhibition concentration *S. aureus* growth was completely suspended for compound **4.07**, as compared to the parent leading inhibitor **1.23** which inhibited *S. aureus* growth with maximum activity at 4 μg/ml, but did not completely reduce cell growth at the highest assayed concentration (64 μg/ml). These results are encouraging and validate the fully substituted 1,2,3-triazoles, in particular the 5-fluoro-1,2,3-triazole **4.07**, as promising candidates that have potential to be developed as antibiotics.

4.6 Reference for Chapter Four

(1)   Soares da Costa, T. P.; Tieu, W.; Yap, M. Y.; Pendini, N. R.; Polyak, S. W.; Sejer Pedersen, D.; Morona, R.; Turnidge, J. D.; Wallace, J. C.; Wilce, M. C.; Booker, G. W.; Abell, A. D. *Journal of Biological Chemistry* **2012**, *287*, 17823-32.

(2)   S Paparella, A.; P Soares da Costa, T.; Y Yap, M.; Tieu, W.; CJ Wilce, M.; W Booker, G.; D Abell, A.; W Polyak, S. *Current Topics in Medicinal Chemistry* **2014**, *14*, 4-20.

(3)   Meldal, M.; Tornøe, C. W. *Chemical Reviews* **2008**, *108*, 2952-3015.

(4)   Rostovtsev, V. V.; Green, L. G.; Fokin, V. V.; Sharpless, K. B. *Angewandte Chemie* **2002**, *114*, 2708-2711.

(5)   Whiting, M.; Muldoon, J.; Lin, Y. C.; Silverman, S. M.; Lindstrom, W.; Olson, A. J.; Kolb, H. C.; Finn, M.; Sharpless, K. B.; Elder, J. H. *Angewandte Chemie International Edition in English* **2006**, *45*, 1435-1439.

(6)   Worrell, B. T.; Ellery, S. P.; Fokin, V. V. *Angewandte Chemie International Edition in English* **2013**, *52*, 13037-41.

(7)   Worrell, B. T.; Hein, J. E.; Fokin, V. V. *Angewandte Chemie International Edition in English* **2012**, *51*, 11791-4.

(8)   Worrell, B. T.; Malik, J. A.; Fokin, V. V. *Science* **2013**, *340*, 457-60.

(9)   Hein, J. E.; Tripp, J. C.; Krasnova, L. B.; Sharpless, K. B.; Fokin, V. V. *Angewandte Chemie International Edition in English* **2009**, *48*, 8018-21.

(10)   Ackermann, L.; Potukuchi, H. K. *Organic & Biomolecular Chemistry* **2010**, *8*, 4503-13.

(11)   Deng, J.; Wu, Y.-M.; Chen, Q.-Y. *Synthesis* **2005**, 2730-2738.

(12)   Takizawa, K.; Nulwala, H.; Thibault, R. J.; Lowenhielm, P.; Yoshinaga, K.; Wooley, K. L.; Hawker, C. J. *Journal of Polymer Science Part A: Polymer Chemistry* **2008**, *46*, 2897-2912.

(13)   Jeffrey, G. A.; Jeffrey, G. A. *An introduction to hydrogen bonding*; Oxford university press New York, 1997; Vol. 12.

(14)   Brown, P. H.; Cronan, J. E.; Grøtli, M.; Beckett, D. *Journal of Molecular Biology* **2004**, *337*, 857-869.

(15)   Brown, P. H.; Beckett, D. *Biochemistry* **2005**, *44*, 3112-3121.

(16)   L'abbé, G.; Beenaerts, L. *Tetrahedron* **1989**, *45*, 749-756.

_____

(17)   Buckle, D. R.; Outred, D. J.; Rockell, C. J.; Smith, H.; Spicer, B. A. *Journal of Medicinal Chemistry* **1983**, *26*, 251-254.

(18)   Buckle, D. R.; Rockell, C. J. *Journal of the Chemical Society, Perkin Transactions 1* **1982**, 627-630.

(19)   Suzuki, A. *Journal of Organometallic Chemistry* **1999**, *576*, 147-168.

(20)   De Meijere, A.; Meyer, F. E. *Angewandte Chemie International Edition in English* **1995**, *33*, 2379-2411.

(21)   Chapman-Smith, A.; Cronan, J. E. *Trends in Biochemical Sciences* **1999**, *24*, 359-363.

(22)   Lu, Y.; Liu, Y.; Xu, Z.; Li, H.; Liu, H.; Zhu, W. *Expert Opinion on Drug Discovery* **2012**, *7*, 375-383.

_____

5.1   Introduction

The facile and reliable CuAAC reaction was utilised extensively in design and development of *Sa*BPL and *Mtb*BPL inhibitors described in chapters 2 and 3. As already discussed, this reaction involves copper catalysed reaction of an acetylene with an azide to give a 1,4-disubstituted 1,2,3-triazole, providing an efficient and reliable means to explore the substituents on the triazole ring.[1-3] Chapter 2 discussed chemical modification of the linker (see Figure 1 highlighted in blue) between the triazole ring and adenine or analogue moieties (i.e. adenine as in **1.22** and benzoxazolone as in **1.23**). The introduction of a diol (**2.06** and **2.10** Figure 1) resulted in reduced potency towards *Sa*BPL and *Mtb*BPL. Chapter 3 presented a novel class of 1,2,3-triazole inhibitor where the ATP analogue groups of **1.22** and **1.23** were replaced with smaller benzylic groups (Figure 1, highlighted in green). From this work, 1,2,3-triazole **3.01t** was identified as a moderately active *Sa*BPL inhibitor ($K_i = 0.25$ µM) with interesting antibacterial activity. Chapter 4 investigated substitution at C5 of the 1,2,3-triazole ring to generated a library of 1,4,5-trisubstituted 1,2,3-triazoles (Figure 1, highlighted in red). From this work, 5-fluorotriazole **4.07** was found to be a potent *Sa*BPL inhibitor with a $K_i = 0.25$ µM and this exhibited antibacterial activity with MIC = 16 µg/mL.[4,5]
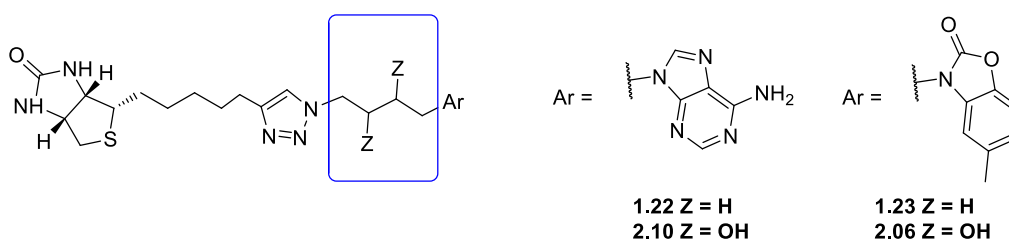
chapter 2

chapter 3
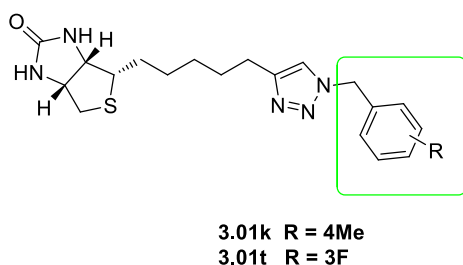
chapter 4
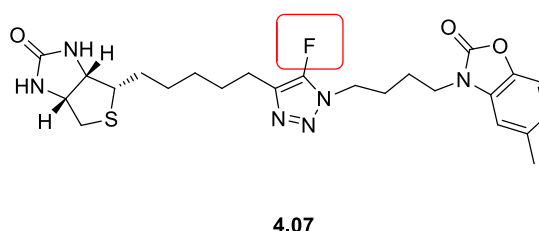
Figure 1: An overview of chapter 2, 3 and 4. Blue square highlights the linker discussed in chapter 2. Green square highlights benzylic analogues discussed in chapter 3. Red square highlights the 5-position of the triazole ring discussed in chapter 4.

_____

While the 1,2,3-triazole of these *Sa*BPL inhibitors provides a good bioisostere of the phosphoanhydride group of biotinyl-5'-AMP **1.03** (see Figure 3 below), it does present some limitations moving forward. Firstly, the triazole contains two less hydrogen bonding sites compared to the phosphate group of biotinyl-5'-AMP **1.03**, thus presenting less opportunity for hydrogen bonding interactions within the phosphate binding domain of *Sa*BPL. Secondly, as previously discussed in chapter 4, the expansion of 1,2,3-triazole series to explore other possible binding interactions within *Sa*BPL is somewhat limited in scope.

An overview of these two key issues follows:

1. **Hydrogen bonds within the phosphate binding domain**

   Biotinol-5'-AMP **1.14** has the unstable phosphoanhydride group of biotinyl-5'-AMP **1.03** replaced with an enzymatically stable bioisostere phosphodiester group. This compound was extremely potent against *Sa*BPL with $K_i = 0.03$ µM, but it is also active against human homolog of BPL.[6,7] The x-ray structure of **1.14** bound to *Sa*BPL[8], depicted in Figure 2, reveals that the phosphodiester group of **1.14** is involved in an intricate network of hydrogen bonds with Arg122, Arg125, Lys187 and two water molecules. This network is central to binding and likely contributes significantly to the high potency of **1.14** toward *Sa*BPL. The 1,2,3-triazole **1.23** (see Figure 1) is the most selective *Sa*BPL inhibitor with $K_i = 0.09$ µM towards *Sa*BPL and importantly it is inactive against both *Mtb*BPL and *Hs*BPL.[8] A crystal structure of **1.23** bound to *Sa*BPL[8] reveals three hydrogen bonding interactions between the triazole ring and Asp180, Arg122 and Arg125 within the active site (see Figure 2). The reduced hydrogen bonding found with the triazole of **1.23** might explain its approximate 4-fold reduced activity against *Sa*BPL as compared to biotinol-5'-AMP **1.14**. This observation suggests that the hydrogen bonding network of biotinol-5'-AMP **1.14** with the phosphate binding domain of *Sa*BPL is likely a contributing factor to binding and hence activity against *Sa*BPL. However it is important to note that the triazole improves selectivity for *Sa*BPL over *Hs*BPL.
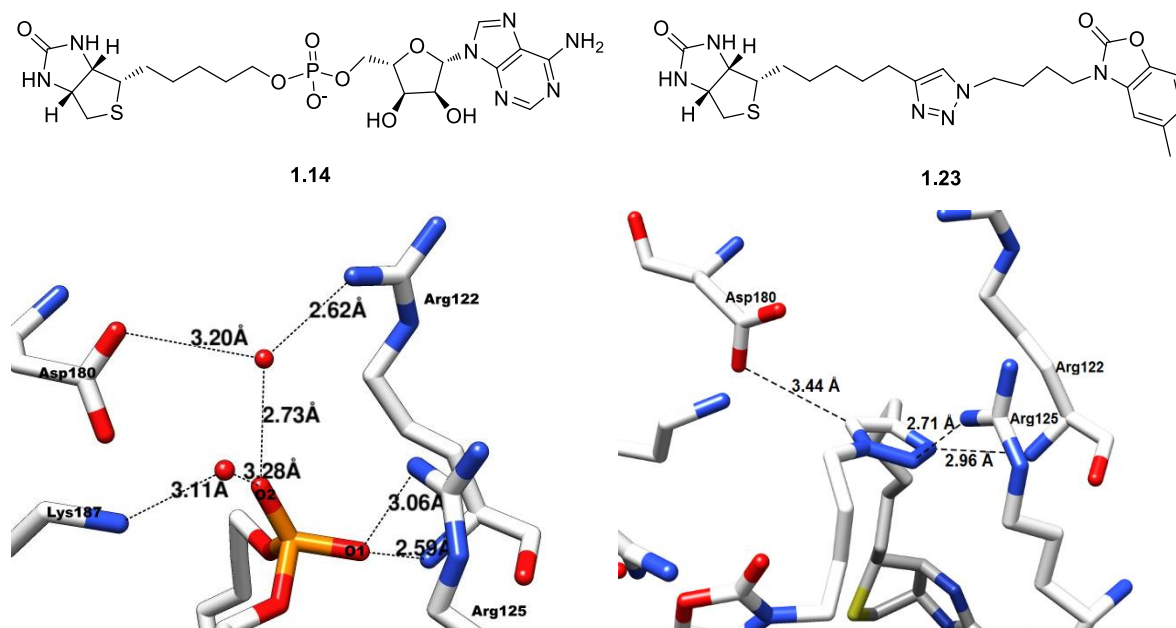
Figure 2: 3D depiction of biotinol-5'-AMP **1.14** (PDB: 4DQ2) and triazole **1.23** (PDB: 3V7S) bound to SaBPL. Black dashes denote hydrogen bonding interaction between respective linkers and Arg122, Arg125, Asp180 and Lys187 of *Sa*BPL.

2. Functionalisation of 1,2,3-triazole

Chapter 4 discussed a number of approaches to functionalise C5 of the triazole ring based on literature chemistry.[9-12] As shown in Scheme 1, the synthesis of the key 5-iodotriazole **4.03** was accomplished by copper catalysed cycloaddition between 1-iodoacetylene **4.02** and azides. Subsequent halogen exchange reactions of **4.03** gave the 5-fluorotriazole **4.04** and 5-chlorotriazole **4.05**. However, further functionalisation of these 5-halogenated triazoles, using nucleophilic substitution reactions and palladium catalysed cross coupling reactions, failed to introduce alternative substituents onto the 1,2,3-triazole. Rather, dehalogenation occurred, with the 5-prototriazole derivative being isolated as the only product. It has been reported that an electron-withdrawing substituent (e.g. ester or amide) on N4 of the triazole is required for such reactions to proceed.[10,13]
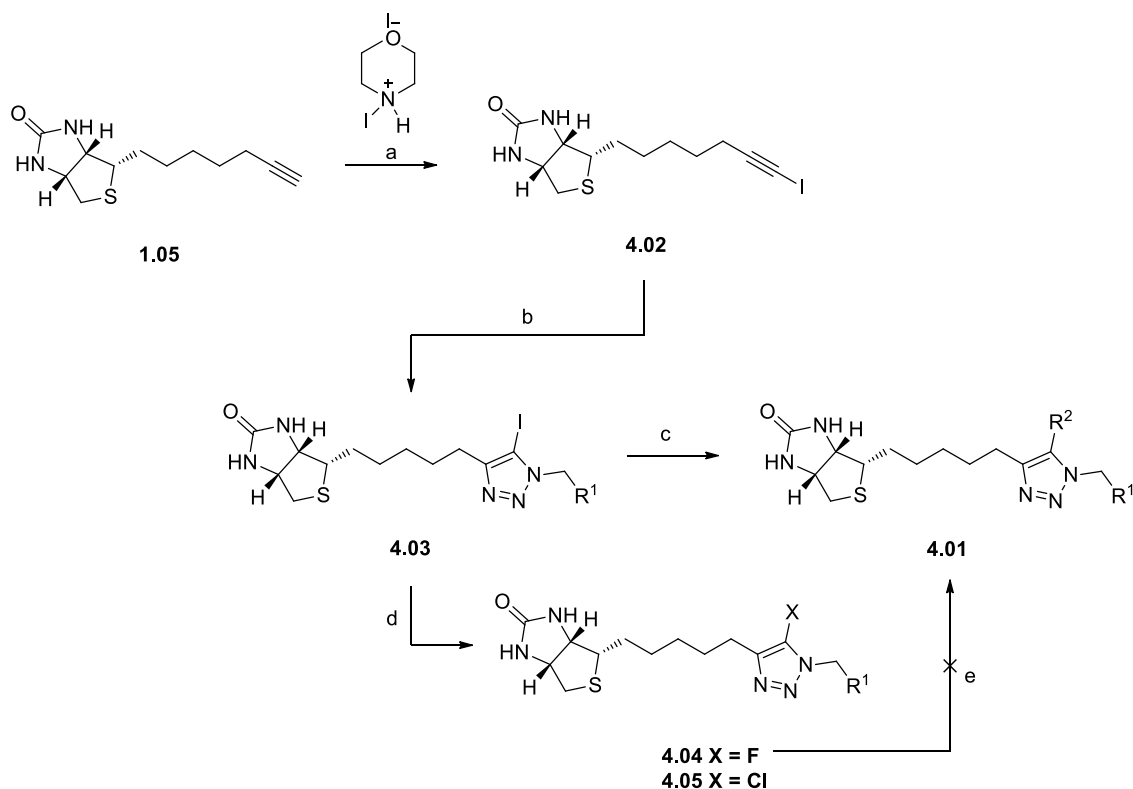
Scheme 1: a) THF, CuI, rt, 3h; b) R^1N_3, THF, CuI, TEA, rt, 12h; c) Pd(OAc), TEA, $R^2B(OH)_2$, THF, 60 °C, 12h; d) KX, MeCN/H_2O (1:1), 180 °C, 10min, mw; e) R^2H, NaH, THF, 3h, 70 °C

5.1.1 The need for a new bioisostere

Given the limitations of 1,2,3-triazole discussed above, the development of a further bioisostere was deemed appropriate in order to achieve improved potency, selectivity and drug-like property of *Sa*BPL inhibitors. As previously mentioned in chapter 1, an alternative analogue **1.17** with the acylsulfamate linker has also been reported by Brown and co-workers.[6] However, **1.17** was found to be chemically unstable, decomposing to *N*-biotinylsulfamic acid **5.01** and 3, 5'-cyclo-5'-deoxyadenosine **5.02** (Figure 3B). Recently, an acylsulfonamide analogue **1.18** was developed where the 5'-oxygen of the acylsulfamate group of **1.17** is replaced with a nitrogen atom to give the acylsulfonamide **1.18**. This derivative was reported to be more stable than **1.17** and it did not undergo cyclonucleoside formation.[14] More importantly, sulfonamide analogue **1.18** exhibited excellent inhibitory activity against *Mtb*BPL with a IC_{50} of 0.14 µM.[14] Interestingly, it was found to be inactive against *Sa*BPL. However, **1.18** did display promising antimycobacterial activity against the laboratory virulent strain *M. tuberculosis* H37Rv and a number of multi-drug resistant and

extensively-drug resistant *M. tuberculosis* strains with minimum inhibition concentrations (MICs) ranging from 0.16 to 0.625 μM.[14]
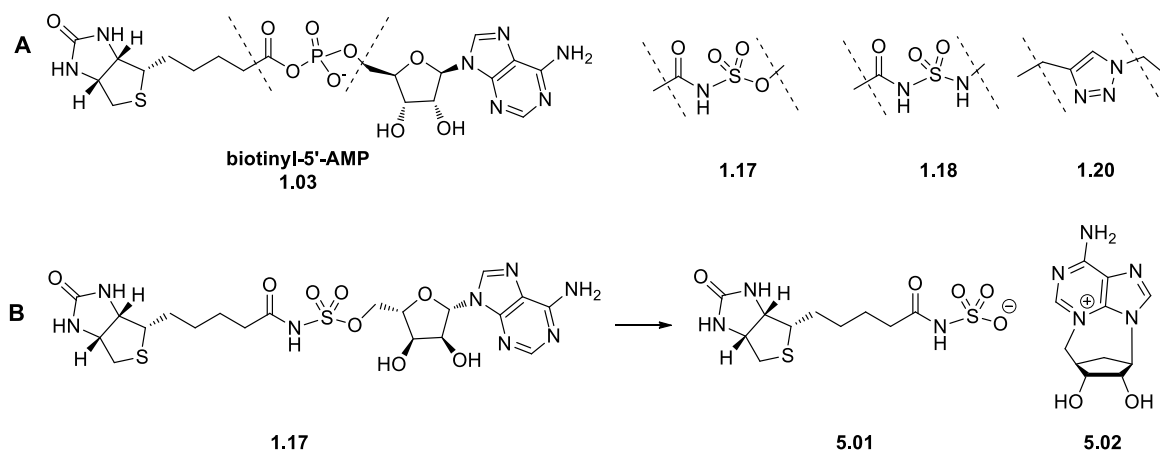
Figure 3: (A) Reaction intermediate biotinyl-5'-AMP **1.03** and its mimics, acylsulfamate **1.17**, acylsulfonamide **1.18** and 1,2,3-triazole **1.20**. (B) Reaction of acylsulfamate **1.17** to give *N*-biotinylsulfamic acid **5.01** and 3, 5'-cyclo-5'-deoxyadenosine **5.02**.

5.1.2 Acylsulfonamide bioisostere

The acylsulfonamide bioisostere of **1.18** displays a number of key features that make it an ideal candidate for further exploration. These features are summarised below:

1. **Hydrogen bonding network**

    As discussed above, the phosphodiester linkage of **1.14** forms a water mediated network of hydrogen bonds with amino acid residues Arg122, Arg125 and Lys187 when bound to *Sa*BPL (Figure 4A). This network is considered a contributing factor to the high potency of **1.14** against *Sa*BPL.[6] An x-ray structure of acylsulfonamide **1.16** bound to *Mtb*BPL was recently solved by Duckworth *et al.*[14] (see Figure 4C) to reveal hydrogen bonding between the sulfonamide group of **1.18** and amino acid residues Arg69, Arg72, and Lys138 (as numbered in *Mtb*BPL). Additional hydrogen bonds are apparent between the sulfonamide group of **1.18** and Asn130, making a total of eight hydrogen bonds.. Compared with the phosphodiester linkage of **1.14** (4 hydrogen bonds) and the triazole ring of **1.20** (3 hydrogen bonds, as shown in Figure 4C), the acylsulfonamide group is considered a good candidate bioisostere for further development of potent inhibitors against bacterial BPLs (ie. *Sa*BPL, *Mtb*BPL).

_____
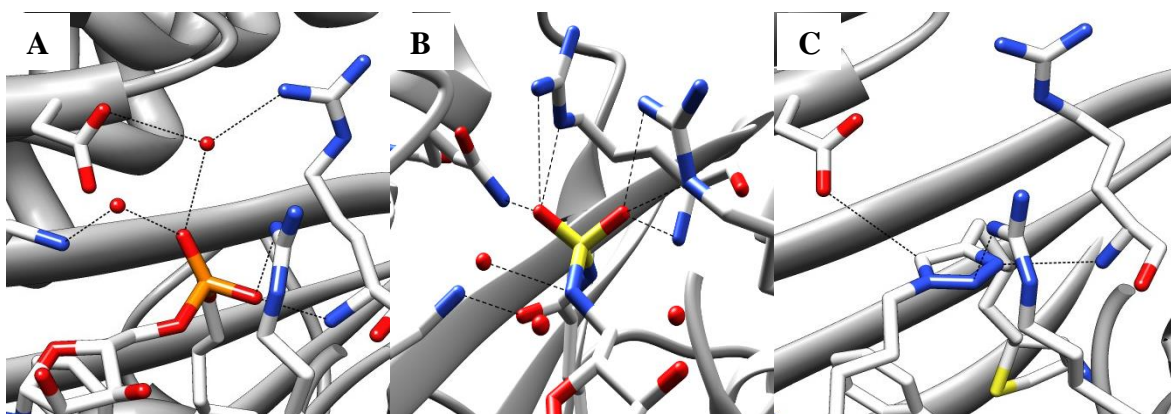
Figure 4: 3D depiction of x-ray structures of (A) biotinol-5'-AMP **1.14** bound to *Sa*BPL; (B) acylsulfonamide **1.18** bound to *Mtb*BPL; (C) 1,2,3-triazole **1.20** bound to *Sa*BPL. The black dashes denote hydrogen bonding interaction of respective linkers.

2. Conformation

The crystal structure of biotinyl-5'-AMP **1.03** bound to *Sa*BPL reveals that it adopts a U-shaped conformation on active site binding binding. [8] This conformation is the result of binding of the biotin and adenosine groups into their respective pockets, as shown in Figure 5. The reported x-ray structure of **1.18** bound to *Mtb*BPL displays a similar U-shape conformation, with the biotin and adenosine groups again occupying these binding pockets of *Mtb*BPL. As for biotinyl-5'-AMP bound *Sa*BPL, hydrogen bonds are observed between adenosine and biotin groups of **1.18** and *Mtb*BPL.[14] The adenosine moiety of **1.18** adopts hydrogen bonds between a side chain of Asn158 and backbone of Ala75. Consistent with the x-ray structure of biotinyl-5'-AMP **1.03** bound to *Sa*BPL, π-π stacking interactions are found between residue Trp74 and the adenine ring of **1.18**. The urea moiety of biotin, as found in **1.18**, is involved in hydrogen bonds to the backbone carbonyl and amide of Arg67, hydroxyl of Ser38, side-chain amide of Gln63 and hydroxyl of Thr39.
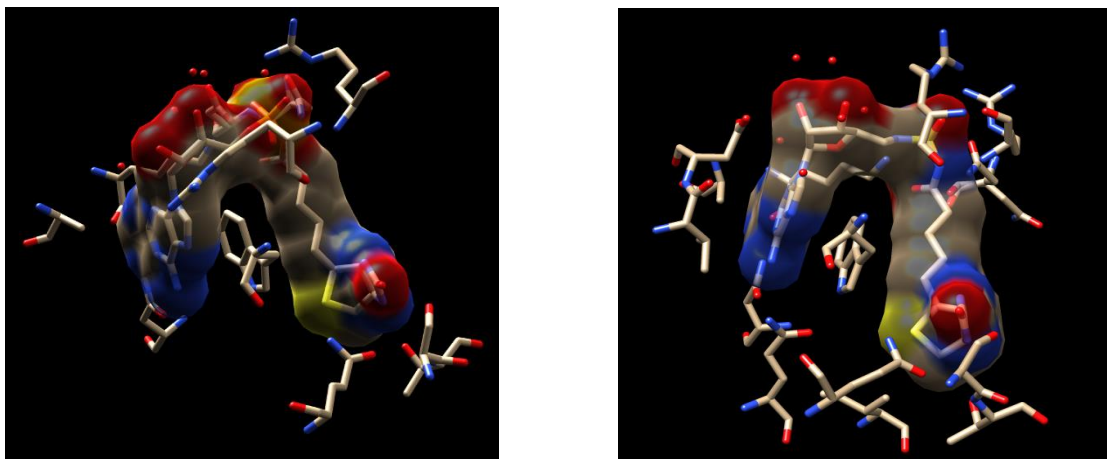
Figure 5: 3D depiction of the natural intermediate biotinyl-5'-AMP **1.03** bound to *Sa*BPL, PDB 3V8L (Left). 3D depiction of the reported acylsulfonamide analogue **1.18** bound to *Mtb*BPL, PDB 3RUX (Right).[14]

5.2   Design and synthesis of acylsulfonamide based analogues

The acylsulfonamide analogues **5.03-5.06** as shown in Figure 6 were initially designed based on the parent 1,2,3-triazole analogues (**3.01k**, **3.01t**, **1.22** and **1.23**), where the 1,2,3-triazole rings are replaced with an acylsulfonamide. Details of the design of the acylsulfonamides **5.06-5.09** are summarised below:

1. A *meta* fluoro substituent as in triazole **3.01t** provided the most potent *Sa*BPL inhibitor in the series, with a K_i of 0.28 µM. While the triazole **3.01k** was less active towards *Sa*BPL (K_i of 10 µM) its structural simplicity made it as an attractive starting compound for investigating the acylsulfonamide series.

2. The adenine containing triazole **1.22** is a potent inhibitor of both *Sa*BPL and *Mtb*BPL with K_i values of 0.66 and 0.64 µM, respectively.[15] Replacement of this adenine group, as discussed in chapter 2, resulted in reduced potency, suggesting that the adenine group should be retained as in the acylsulfonamide **5.05**.

3. The 2-benzoxazolone containing triazole **1.23** is the most active and selective *Sa*BPL inhibitor reported to date with a $K_i = 0.09$ µM.[8] Modification of this 2-benzoxazolone group, to probe the ATP binding pocket of *Sa*BPL, resulted in reduced potency towards *Sa*BPL,[16] suggesting that this group is the best of those studied to date.

4. The ribose ring of **1.20** does not appear to be involved in the binding with *Sa*BPL. Triazole **1.22** (lacking this group) was 4 fold more active towards *Sa*BPL. In support, the reported acylsulfonamide **1.18** (containing the ribose) was devoid inhibition towards

_____

*Sa*BPL,[14] suggesting target compounds (**5.05** and **5.06**) should lack this ribose group.

5. The key biotin group was retained in the design of acylsulfonamide **5.03-5.06**, where this group is critical to potency against *Sa*BPL.[8]
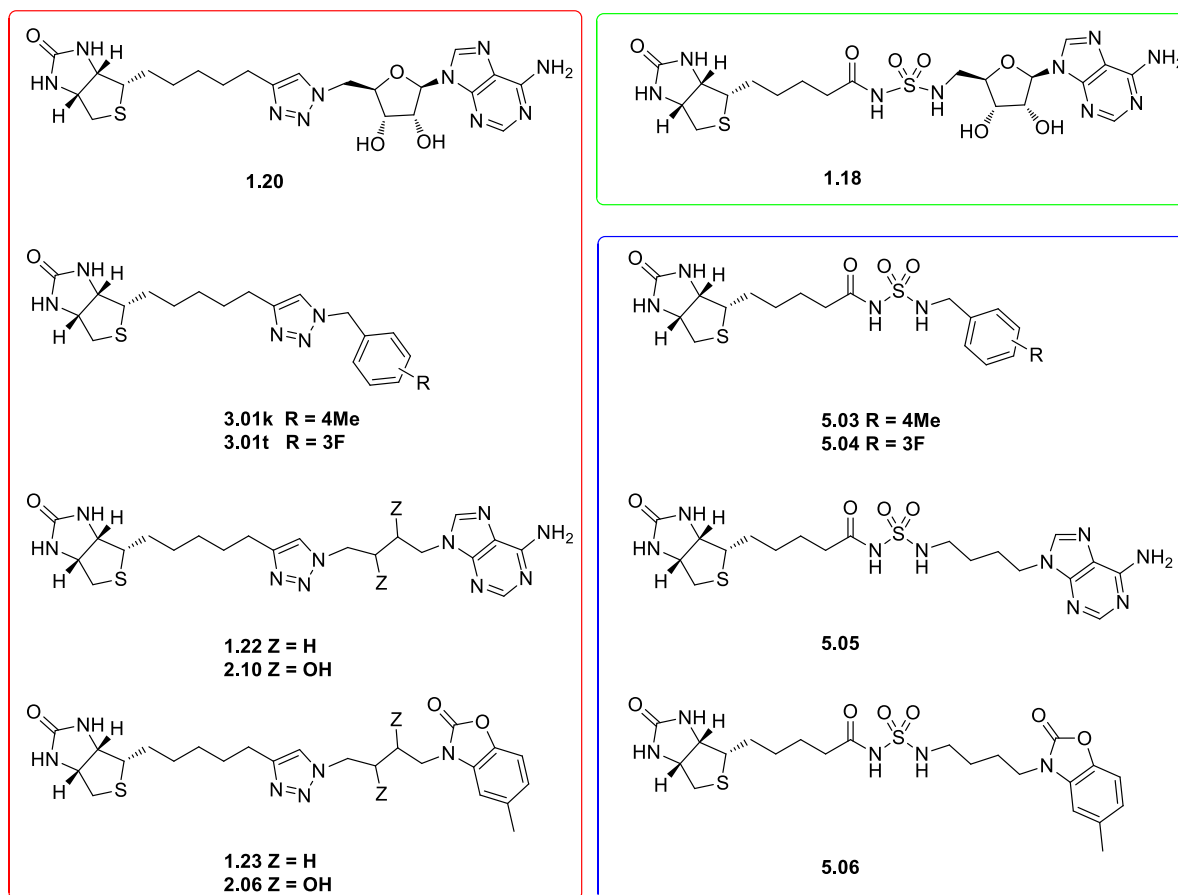
Figure 6: Red box denotes the triazole analogues **1.20**, **3.01k**, **3.01t**, **1.22**, **1.23**, **2.06** and **2.10**. Green denotes reported acylsulfonamide analogue **1.18**[14] and blue the proposed acylsulfonamide analogues **5.03-5.06** discussed in this chapter.

5.2.1 Building blocks for synthesis of acylsulfonamides 5.03-5.06

The proposed synthesis of acylsulfonamides **5.03-5.06** involves coupling biotin succinimidyl ester **5.07** with sulfonyl amine **5.08-5.11** (Figure 7A) in the presence of Cs_2CO_3 and DMF, as shown in Figure 7B.
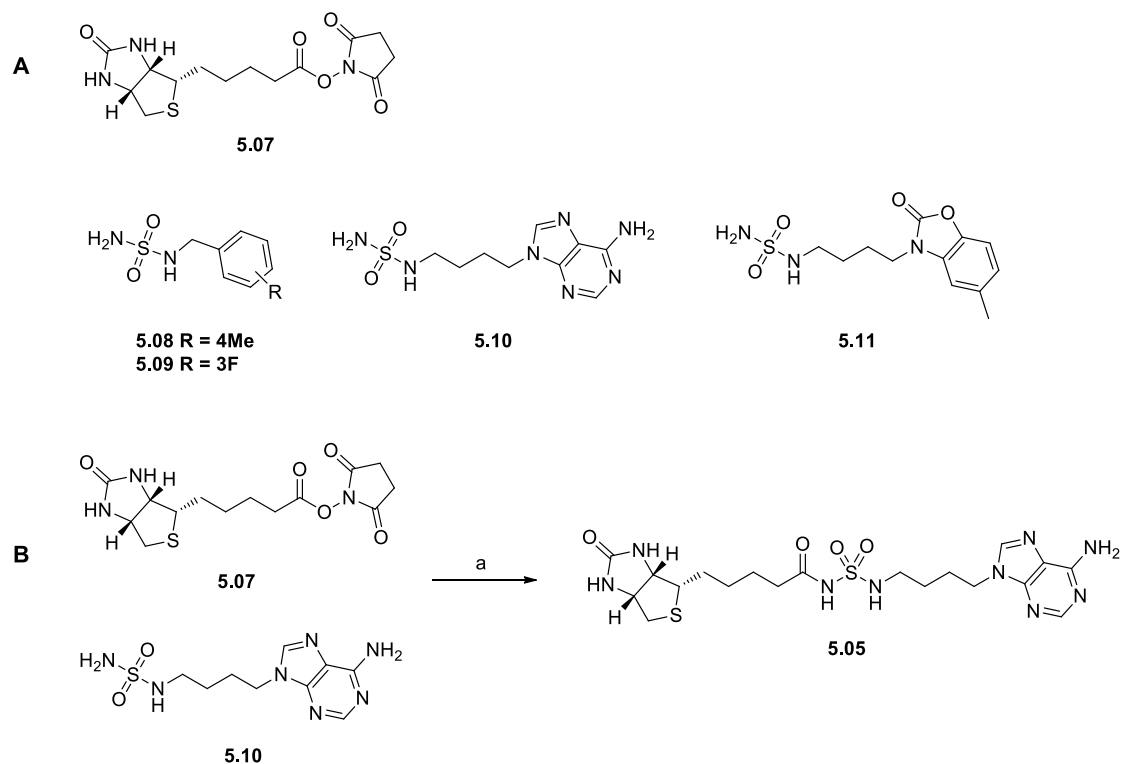
Figure 7: A) Precursors for the synthesis of sulfonamide analogues **5.07-5.11**: B) a) Cs_2CO_3, DMF, rt, 12 h.

The preparation of biotin succinimidyl ester **5.07** was accomplished by reacting biotin carboxylic acid **1.01** with disuccinimidyl carbonate (DSC) and triethylamine (TEA) in DMF.[14,17] The reaction mixture was quenched with PBS buffer and the precipitate extracted by extraction with ethyl acetate to give biotin succinimidyl ester **5.07** as a white solid in 57% yield (Scheme 2).
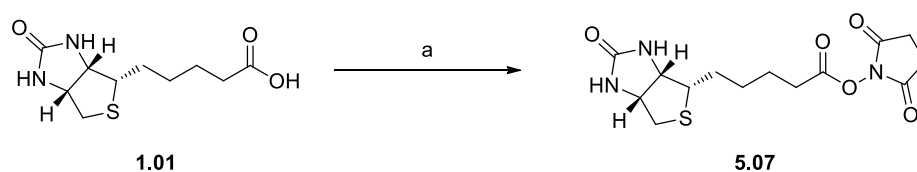
Scheme 2: a) DSC, TEA, DMF, rt, 12h.

Synthesis of benzyl sulfamide building blocks 5.08 and 5.09

The benzyl sulfamide building blocks **5.08** and **5.09** were prepared according to the reported procedure shown in Scheme 3.[14,18] In brief, the key step involves reaction of benzyl amines **5.12** and **5.13** with sulfamoylating agent **5.15** to give boc protected sulfamide **5.16** and **5.17**.
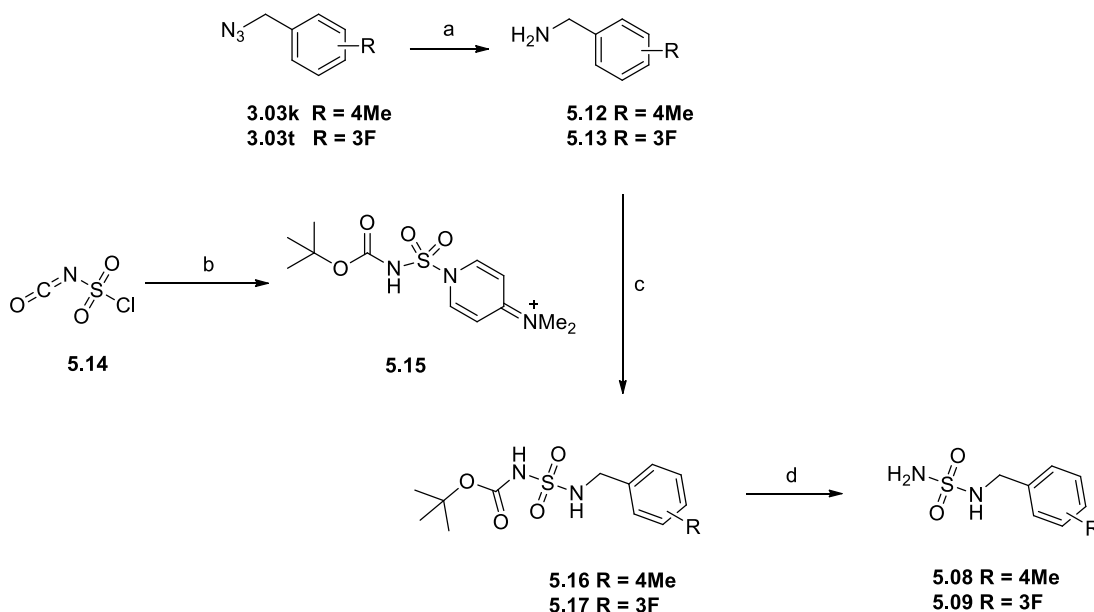
Scheme 3: Conditions and reagents: a) PPh₃, THF, 80 °C, 1h; b) *t*BuOH, CH₂Cl₂, DMAP, rt, 1h; c) DCM, TEA, rt, 12h; d) 10% TFA, DCM, 12h

The benzyl amines **5.12** and **5.13** were prepared from the corresponding azides **3.03k** and **3.03t** by Staudinger reduction as shown in Scheme 2.[19] Benzyl azides **3.103k** and **3.03t** (preparation described in chapter 3) were separately reacted with triphenylphosphine (PPh₃) in THF to give corresponding amines **5.12** and **5.13**, which were used without further purification. The sulfamoylating agent **5.15** was prepared by treating chlorosulfonyl isocyanate (CSI) **5.14** with a cold solution of *tert*-butyl alcohol in anhydrous methylene chloride, followed by addition of (dimethylamino)pridine (DMAP).[18] With sulfamoylating agent **5.15** in hand, the free amine of benzyl derivatives **5.12** and **5.13** were converted to boc-protected sulfamides **5.16** and **5.17** in yields of 43% and 45% respectively, after purification by flash chromatography (Scheme 3). The boc group of **5.16** and **5.17** was then removed on reaction with 10% TFA in DCM to give desired benzyl sulfamide building blocks **5.08** and **5.09** in 63% and 75% yield, respectively.

___

Synthesis of adenine sulfamide building block 5.10

The synthesis of adenine sulfamide build block **5.10** was initially accomplished by Dr William Tieu in Abell group as depicted in Scheme 4.[15]
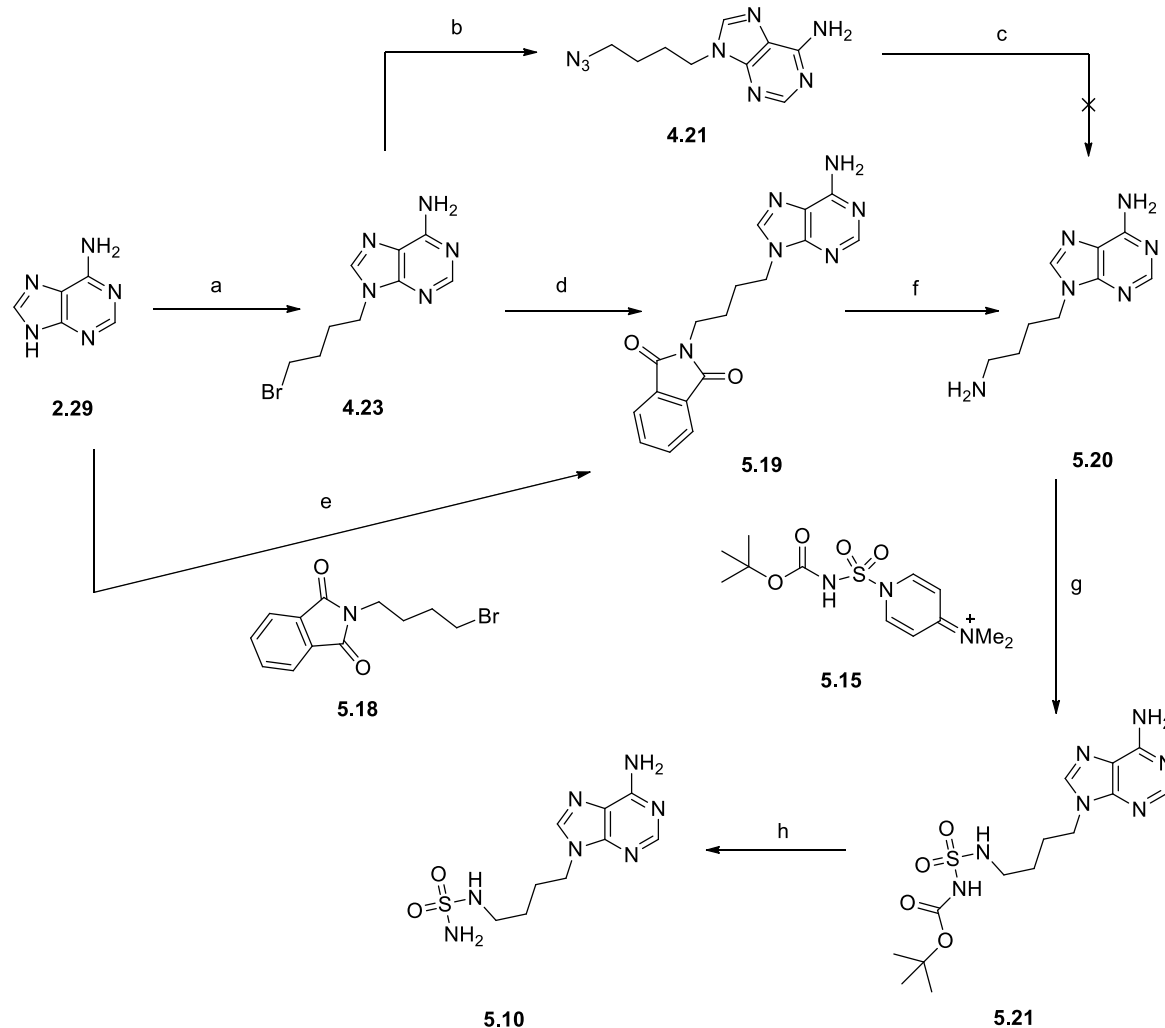
Scheme 4: a) Br(CH₂)₄Br, Cs₂CO₃, DMF, rt, 12h; b) NaN₃, DMF, rt, 12h; c) PPh₃, THF, 80 °C, 1h; ; d) KPhth, K₂CO₃, DMF, rt, 12h; e) K₂CO₃, DMF, 70 °C, 12h; f) NH₂NH₂.H₂O, EtOH, reflux, 12h; g) DCM, TEA, rt, 12h; h) 10% TFA, DCM, 12h

The approach used to prepare benzyl sulfamide building blocks **5.08** and **5.09** was initially attempted for the preparation of adenine sulfamide **5.10** as shown in Scheme 4. Here the key intermediate adenine azide **4.21** was prepared from adenine **2.29** via adenine bromide **4.23** as previously discussed in chapter 4. Subsequent hydrogenation of the azide of **4.21** with PPh₃ and water only give a trace of adenine amine **5.20** as judged by TLC and ¹H NMR of the crude product. Only starting material **4.21** was isolated after purification of the crude product flash chromatography. A key observation was that the adenine azide was not completely dissolved in THF. Reaction using more polar solvent DMSO or DMF gave a

complex of mixture with no trace of **5.20** was identified by TLC or ^{1}H NMR.

An alternative approach was therefore examined for the synthesis of adenine amine **5.20** as shown in Scheme 4. The adenine bromide **4.23** was coupled with potassium phthalimide in the presence of K_2CO_3 in DMF to give adenine phthalimide **5.19** in 48% yield after purification by flash chromatography. Adenine phthalimide **5.19** was also prepared in an improved yield of 67% by alkylation of N-(4-bromobutyl)phthalimide **5.18** with adenine **2.29** in the presence of K_2CO_3 in DMF. The subsequent reduction of adenine phthalimide **5.19** with hydrazine in ethanol gave adenine amine **5.20** in 67% yield as a colorless solid. The adenine amine **5.20** was then coupled with the sulfamoylating agent **5.15** in DCM to give boc-protected adenine sulfamide **5.21** in 23% yield after purification by flash chromatography. Boc deprotection on treatment with 10% TFA in DCM gave the adenine sulfamide building block **5.10** as a white solid.

Synthesis of 2-benzoxazolone sulfamide building block 5.11

The attempted synthesis of the 2-benzoxazolone sulfamide building block **5.11** is summarised in Scheme 5.
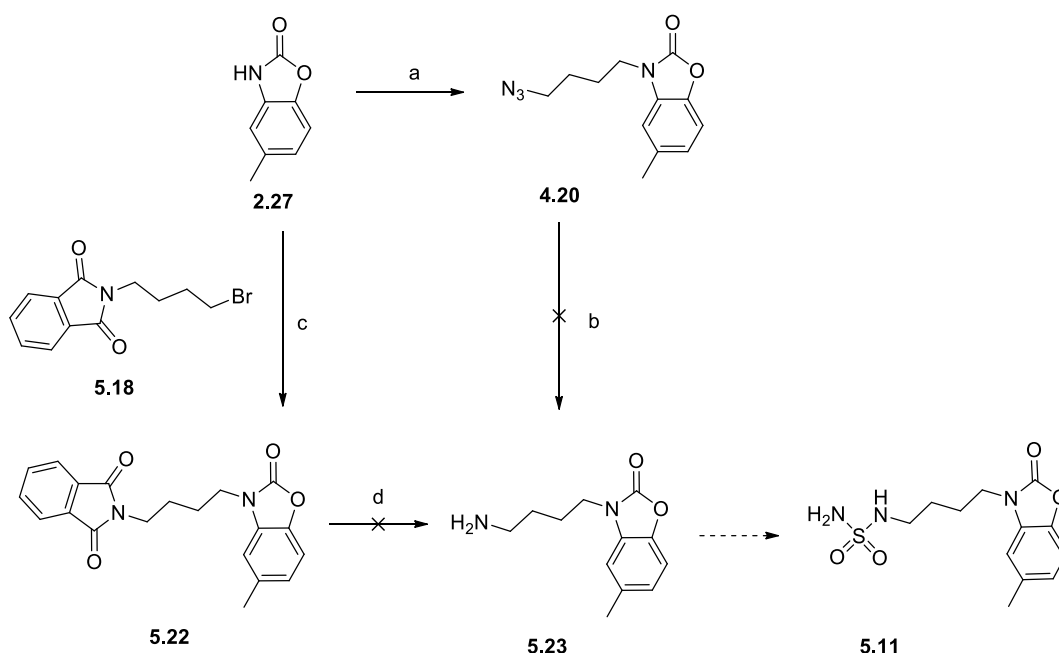
Scheme 5: Conditions and reagents: a) i Br(CH$_2$)$_4$Br, K$_2$CO$_3$, DMF, rt, 12h; ii NaN$_3$, DMF, rt, 12h; b) PPh$_3$, THF, 80 ^{o}C, 1h, c) K$_2$CO$_3$, DMF, rt, 12h; d) NH$_2$NH$_2$.H$_2$O, EtOH, reflux, 12h;

Preparation of the key precursor, 2-benzoxazolone amine **5.23**, was initially attempted from 2-benzoxazolone azide **4.20** as per the synthesis of adenine amine **5.20** (Scheme 5). However, attempted hydrogenation of 2-benzoxazolone azide **4.20** with PPh_3 and water resulted in a complex mixture without the formation of the desired amine **5.23** as judged by ^{1}H NMR and TLC.

An alternative route to 2-benzoxazolone amine **5.23** was then attempted as shown in Scheme 5. 2-Benzoxazolone **2.27** prepared in chapter 2 was treated with N-(4-bromobutyl)phthalimide **5.18** and K_2CO_3 to give 2-benzoxazolone phthalimide **5.22** in a moderate yield of 53% after purification by flash chromatography. However, subsequent treatment of **5.22** with hydrazine in ethanol failed to give 2-benzoxazolone amine **5.23**, despite the starting material **5.22** being consumed as shown by TLC and ^{1}H NMR. This observation suggested that the benzoxazolone moiety decomposed under reductive conditions. Therefore, synthesis of benzoxazolone sulfamide **5.11** and the subsequent sulfonamide derivative **5.06** was not pursued further.

5.2.2 Synthesis of acylsulfonamide derivatives 5.03-5.05

The sulfonamides **5.03-5.04** were synthesised from biotin succinimidyl ester **5.07** and sulfonyl amine **5.08-5.10** as shown in Scheme 6.[14] Biotin succinimidyl ester **5.07** was separately coupled to the sulfamide amine building blocks **5.08-5.10** in the presence of Cs_2CO_3 in DMF to give designed acylsulfonamides **5.03-5.05** in respective yielding of 53%, 63% and 35%.
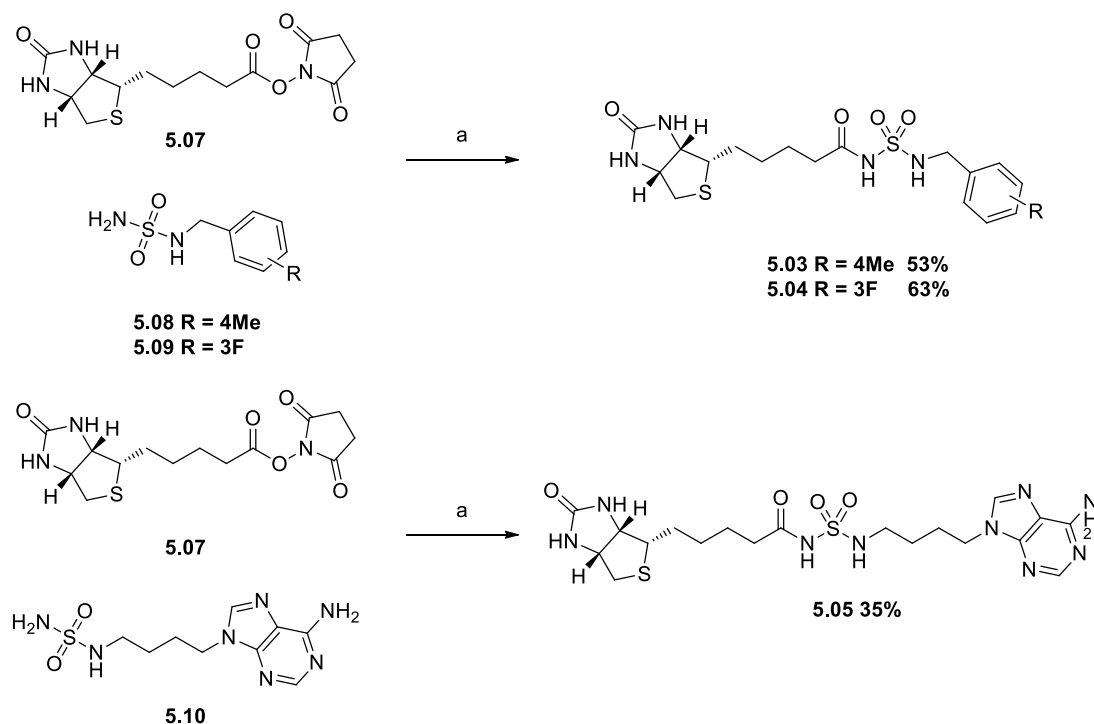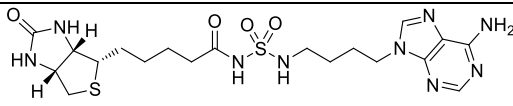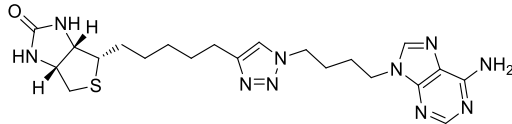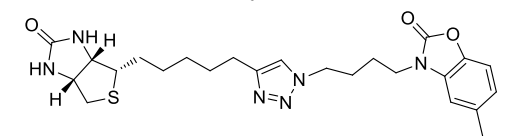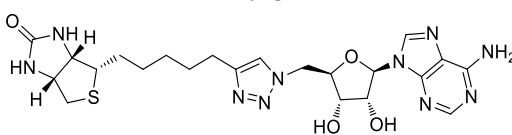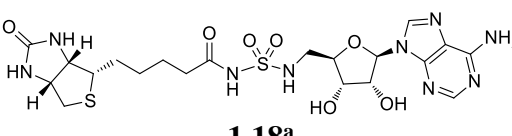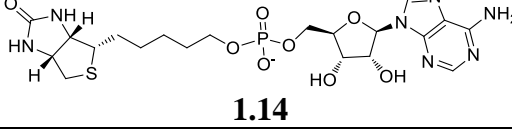
Scheme 6: a) Cs_2CO_3, DMF, rt, 12h.

5.3 BPL inhibition and antimicrobial activity of sulfonamide derivatives

Acylsulfonamide derivatives **5.03-5.05** were assayed against *S. aureus* biotin protein ligase (*Sa*BPL), *M. tuberculosis* biotin protein ligase (*Mtb*BPL) and *H. sapiens* biotin protein ligase (*Hs*BPL). The assay was performed by collaborators at Molecular Life Science, University of Adelaide, using an *in vitro* biotinylation assay described by Chapman-Smith and co-workers[20] and the results are summarised in Table 1 and 2. *IC$_{50}$* values were determined for each compound from a dose-response curve using a range of inhibitor concentrations and a fixed concentration of enzyme.

Table 1: Enzyme assay of acylsulfonamide **5.05** against *Sa*BPL, *Mtb*BPL, and *Hs*BPL

Compounds	*Sa*BPL K_i (µM)	*Mtb*BPL		*Hs*BPL K_i (µM)
		IC$_{50}$ (µM)	K_i (µM)	
5.05	0.72×10^{-3}	8.10×10^{-3}	0.74×10^{-3}	Ni

Compound				
1.22	0.66	7.04	0.64	Ni
1.23	0.09	Ni	Ni	Ni
1.20	1.17	-	-	Ni
1.18[a]	-	0.14	-	-
1.14	0.03	-	-	1.25

[a] IC_{50} of **1.18** towards MtbBPL was reported by Duckworth et al.[14]

Ni = no inhibition at highest compound concentration assayed (200 μM).

- = Compounds were not assayed.

As highlighted in Table 1, adenine acylsulfonamide **5.05** was highly potent towards SaBPL with $K_i = 0.72$ x 10^{-3} μM and also MtbBPL with $K_i = 0.74$ x 10^{-3} μM ($IC_{50} = 8.1$ x 10^{-3} μM against MtbBPL). This compound is approximately 1,000 fold more potent than the parent adenine triazole analogue **1.22** ($K_i = 0.66$ μM against SaBPL and $K_i = 0.64$ μM against MtbBPL). In addition, acylsulfonamide **5.08** was 21 fold more potent toward SaBPL than the leading 1,2,3-triazole inhibitor **1.23** ($K_i = 0.09$ μM).[8] Moreover, 1,2,3-triazole **1.23** was devoid of activity towards MtbBPL whilst acylsulfonamide **5.05** was equally potent against both SaBPL and MtbBPL.
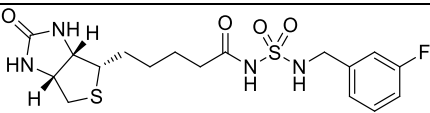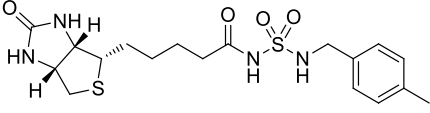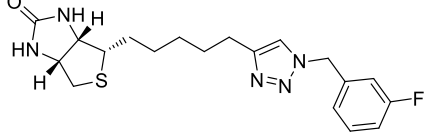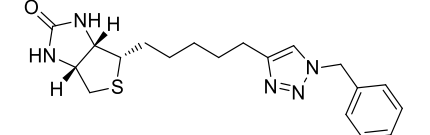
As discussed above, the adenosine ribose (as in triazole **1.20**) is not critical for activity against SaBPL. In fact, the triazole **1.22** ($K_i = 0.66$ μM) that lacks this ribose group is 2 fold more potent than triazole **1.20** ($K_i = 1.17$ μM) towards SaBPL.[8] Likewise, the acylsulfonamide **1.18** containing the ribose sugar is reported to be potent for MtbBPL with $IC_{50} = 0.14$ μM but inactive against $S.aureus$ (MIC > 400 μM) in the whole cell assay.[14] In comparison, acylsulfonamide **5.05** (lacking the ribose sugar) is equally active against SaBPL ($K_i = 0.72$ x 10^{-3} μM) and MtbBPL ($K_i = 0.74$ x 10^{-3} μM). The results suggested that particular selectivity for MtbBPL seems to be obtained with the inclusion of the ribose, see compounds

5.05 and **1.18**.

Finally and importantly, compared to the first generation *Sa*BPL inhibitor, biotinol-5'-AMP **1.14** (K_i = 0.03 µM against *Sa*BPL and K_i = 1.25 µM against *Hs*BPL), the acylsulfonamide **5.05** was 34 fold more active toward *Sa*BPL (K_i = 0.72 x 10^{-3} µM) and showed no inhibition against *Hs*BPL under the highest assayed concentration (200 µM).

Surprisingly, the benzylic acylsulfonamides **5.03** and **5.04** were inactive against *Sa*BPL, *Mtb*BPL and *Hs*BPL, whilst their triazole analogues **3.01k** and **3.01t** (as discussed in chapter 3) were potent *Sa*BPL inhibitors with K_i values of 10 µM and 0.28 µM, respectively. One possible explanation is that benzylic groups of **5.03** and **5.04** are unable to interact with the ATP binding pocket of *Sa*BPL because of the shorter tether length between the acylsulfonamide and benzylic groups. Moreover, compared to the rigid 5-membered triazole rings of **3.01k** and **3.01t**, acylsulfonamide linker is considered to be more flexible and results in different binding modes which might not be favored by *Sa*BPL.

Table 2: Enzyme assay of acylsulfonamide **5.03** and **5.04** against *Sa*BPL, *Mtb*BPL, and *Hs*BPL

Compounds	*Sa*BPL K_i (µM)	*Mtb*BPL K_i (µM)	*Hs*BPL K_i (µM)
5.03	> 33	> 33	> 33
5.04	> 33	> 33	> 33
3.01t	0.28	> 33	> 33
3.01k	1.0	> 33	> 33

___

Antimicrobial assay

The antimicrobial activity of the acylsulfonamide **5.05** and also positive controls (vancomycin, amoxicillin, methicillin and erythromycin) was investigated, with results shown in Figure 8 below. The assays were carried out by collaborators at Molecular Life Science, University of Adelaide, using a micro broth dilution antibacterial susceptibility assay with *S. aureus* strain ATCC 49775.[21]
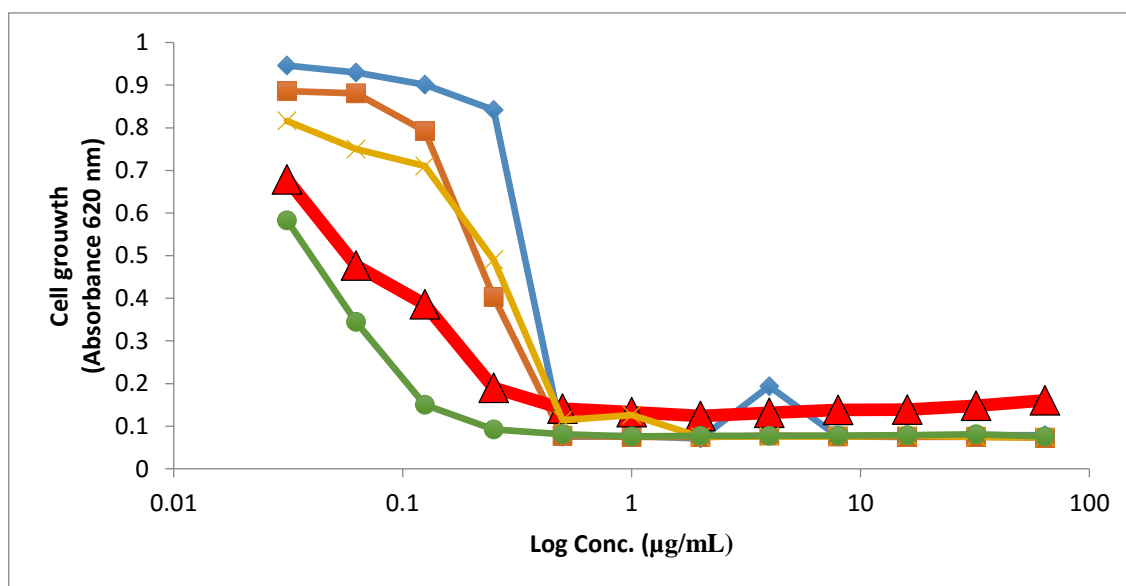
Figure 8: Inhibition of *S. aureus* growth *in vitro*. Acylsulfonamide **5.05** (▲ red), vancomycin (♦ blue), amoxicillin (■ orange), methicillin (× yellow), erythromycin (● green).

The activity of **5.05** significantly reduced cell growth such that the bacteria showed no growth at 0.5-1.0 µg/mL. This result was competitive with positive controls of antibiotics on the market (vancomycin, amoxicillin, methicillin, and erythromycin) which had the same minimum inhibition concentration (MIC) ranging from 0.5-1.0 µg/mL (as determined from Figure 8).

As summarised below in Table 3, the antimicrobial property of **5.05** was also tested towards a library of gram negative and gram positive microbes, namely methicillin-resistant *S. aureus* (MRSA), *M. tuberculosis, Enterococcus faecalis* (*E. faecalis*), *Enterococcus faecium* (*E. faecium*) and *Escherichia coli* (*E. coli*). The acylsulfonamide **5.05** gave equivalent MIC values (ranging from 0.5 to 1.0 µg/mL) for susceptible *S. aureus* and a phenotypically characterised methicillin-resistant *S. aureus* (MRSA). Interestingly, **5.05** was found to have anti-*M. tuberculosis* activity with MIC = 51 µg/mL, which was 50-100 fold lower than the MIC value towards *S. aureus*. The difference of antimicrobial activity of **5.05** between *S.*

aureus and *M. tuberculosis* likely reflects differences in cellular penetration and efflux since **5.05** is equal potency against *Sa*BPL and *Mtb*BPL. Remarkably, **5.05** was inactive in antimicrobial assays for a panel of gram-positive bacteria (*Enterococcus faecalis* (*E. faecalis*) and *Enterococcus faecium* (*E. faecium*)) and gram-negative bacteria (*Escherichia coli* (*E. coli*)) at the highest tested concentration (MIC > 128 µg/mL), suggesting high antimicrobial specificity towards *S. aureus* and *M. tuberculosis*. Finally, the cytotoxicity of **5.05** was evaluated against two mammalian cell lines, HepG2 human liver cells and Hek293 human kidney cells. Importantly, **5.05** exhibited no toxicity to both cells. These results concur with the lack of activity of **5.05** toward *Hs*BPL (*Ki* > 33 µM).

Table 3: Antimicrobial activity and selectivity of acylsulfonamide **5.05**

Strain/Cell Line	Classification	MIC (µg/mL)
S. aureus	Gram-positive	0.5-1.0
Methicillin-resistant S. aureus (MRSA)	Gram-positive	0.5-1.0
M. tuberculosis	-	51
E. faecium	Gram- positive	>128
E. faecalis	Gram- positive	>128
E. coli	Gram-negative	>128
HepG2	Mammalian	-
Hek293	Mammalian	-

5.4 X-ray crystal structure of acylsulfonamide 5.05 bound to *Sa*BPL

A structure of acylsulfonamide analogue **5.05** bound to *Sa*BPL was determined by our collaborators at Monash University, Australia using the method prescribed by Pendini and coworkers to give a final resolution of 2.72 Å.[22] Consistent with the design, sulfonamide **5.05** adopted a U shape conformation when bound to *Sa*BPL (shown in Figure 9). This conformation is defined by binding of biotin and adenine moieties of **5.05** to the respective binding pockets of *Sa*BPL as per the reaction intermediate biotinyl-5'-AMP **1.03** and the 1,2,3-triazole inhibitors such as **1.22**. The adenine group of **5.05** forms hydrogen bonds with Asn212 and Ser128, while the biotin group forms hydrogen bonds with residues Arg120, Ser93, Thr94 and Gln116. The same hydrogen bonding interactions were found within the reported crystal structures of biotinyl-5'-AMP **1.03** and 1,2,3-triazole **1.22** bound to *Sa*BPL.[8] As expected, the acylsulfonamide group of **5.05** interacts with amino acid residues in the phosphate bonding domain of *Sa*BPL. A focus on this domain with a list of interactions is discussed below.
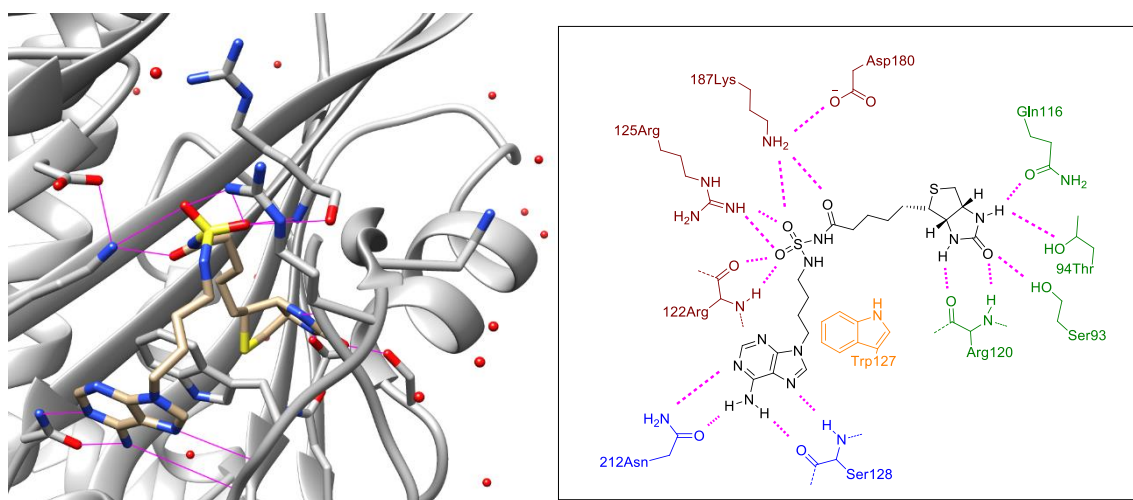
Figure 9: A 3D depiction of acylsulfonamide **5.05** bound to *Sa*BPL with hydrogen bonds shown in purple (Left). 2D depiction of acylsulfonamide **5.05** bound to *Sa*BPL with hydrogen bonding interactions shown in purple dashes (Right: The amino acid residues (blue) denote hydrogen bonding interactions b the adenine group; Trp127 (yellow) denotes π-π stacking with the adenine group; amino acid residues (brown) form hydrogen bonds with acylsulfonamide group; and amino acids (green) denote the hydrogen bonds with biotin heterocycles of **5.05**.

Phosphate binding domain

Figure 10 shows a comparison of hydrogen bonding interactions of **5.05** with the phosphate binding site of *Sa*BPL and similarly **1.18** with *Mtb*BPL.[14] The key observations are summarised as below:

1. For the crystal structure of *Sa*BPL in complex of **5.05**, the terminal amine of Lys187 forms a hydrogen bonding network with the amide oxygen of the acylsulfonamide linker at 3.33 Å, one sulfamide oxygen at 3.41 Å and the carboxylate of Asp180 at 2.72 Å apart. Similar hydrogen bonding interactions are observed for the crystal structure of *Mtb*BPL in complex **1.18** between the conserved Lys138 (*Mtb*BPL numbering) and the acylsulfonamide group of **1.18**.[14](Figure 10B)

2. The guanidium group of Arg125 in *Sa*BPL forms hydrogen bonds with both sulfamide oxygens of **5.05** at a separation of 3.72 Å and 3.78 Å apart, respectively. The side chain of Arg122 forms hydrogen bonds with one sulfamide oxygen of the acylsulfonamide linker of **5.05** at 3.40 Å and 2.54 Å apart, respectively. These two amino acids are conserved in *Mtb*BPL (named as Arg69 and Arg72) and form four hydrogen bonds with the acylsulfonamide group of **1.18**.[14](Figure 10B)

3. A unique hydrogen bonding interaction is observed between the side chain of Asn130 in *Mtb*BPL and the acylsulfonamide group of **1.18**.[14](Figure 10B) The analogue **5.05** lacking such interaction with *Sa*BPL, however, formed indirect bonding with Asp180 through the side chain of Lys187 (Figure 10A).
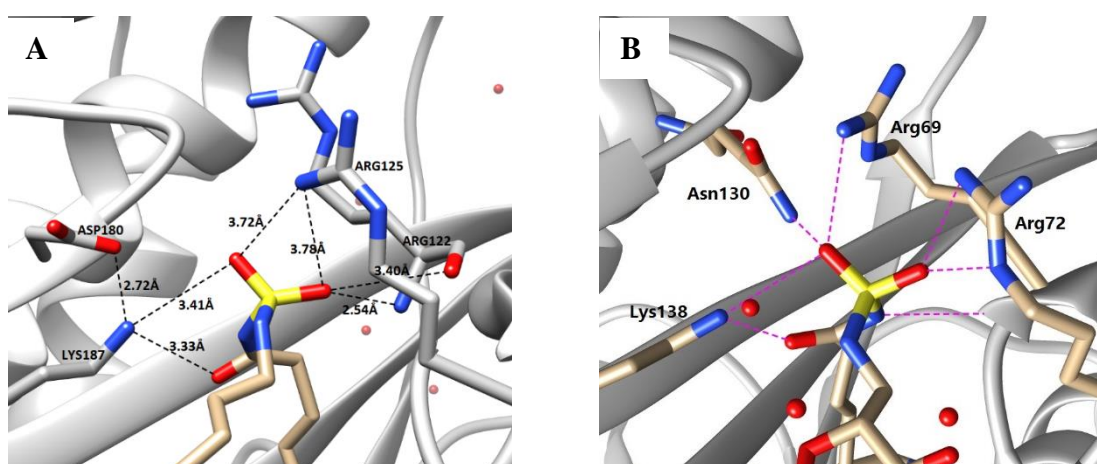
Figure 10: (A) 3D depiction of acylsulfonamide **5.05** looking down into the phosphate binding pocket of *Sa*BPL. Hydrogen bonds are depicted by black dashes with distances shown therein. (B) 3D depiction of acylsulfonamide **1.18** looking down into the phosphate binding pocket of *Mtb*BPL (PDB 3RUX).[14] Hydrogen bonds are depicted by magenta dashes.

As discussed above in section 5.1, the 1,2,3-triazole ring of **1.22** forms three hydrogen bonding interactions with Asp180, Arg122, and Arg125 of *Sa*BPL (Figure 11A). In comparison, the acylsulfonamide group of **5.05** does not hydrogen bond with Asp180, but retains hydrogen bonds with Arg122 and Arg125 and adopts two additional interactions with Lys187 and indirect interactions with Asp180 through Lys187 (Figure 11C). Compared to the natural reaction intermediate, biotinyl-5'-AMP (Figure 11B), the acylsulfonamide of **5.05** again retains all the hydrogen bonding interactions with Lys187, Arg122 and Arg125. These crystallography data support that the acylsulfonamide of **5.05** is a validated bioisostere of both the 1,2,3-triazole and phosphoroanhydride groups found in **1.22** and **1.03**. The key interactions between *Sa*BPL and **5.05**, **1.03** and **1.22** are shown in Figure 11.
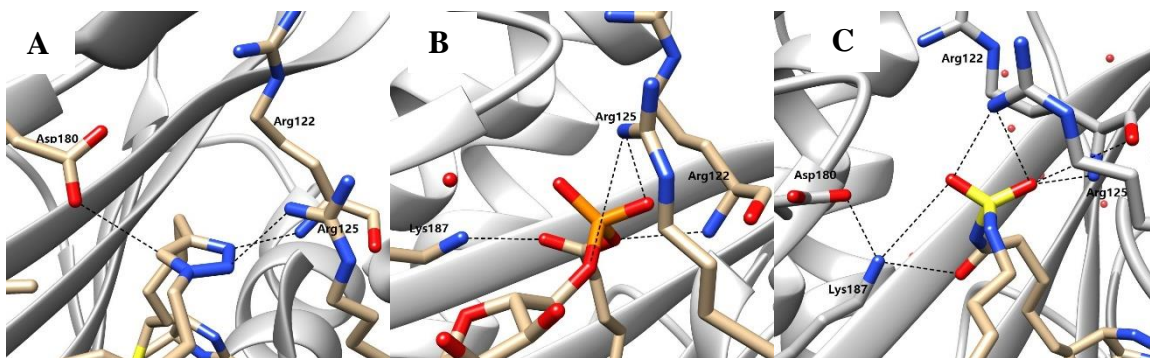
Figure 11: 3D depiction of (A) 1,2,3-triazole **1.22**, (B) biotinyl-5'-AMP 1.**03** and (C) acylsulfonamide **5.05** bound to *Sa*BPL. The black dashes demonstrate the hydrogen bonding interactions between their respective linkers and Arg122, Arg125, Asp180 and Lys187 of *Sa*BPL.

Ribose binding region

As previously discussed, while the acylsulfonamide analogue **5.05** lacks the ribose ring it is highly potent towards *Sa*BPL ($K_i = 0.72$ x 10^{-3} μM) and *Mtb*BPL ($K_i = 0.74$ x 10^{-3} μM). In comparison, analogue **1.18** which contains the ribose ring is inactive against *Sa*BPL and significantly less active against *Mtb*BPL ($K_i = 0.14$ μM). The crystal structure of acylsulfonamide **5.05** bound to *Sa*BPL supports this observation in that hydrogen bonds are not observed between **5.05** and the ribose binding region of *Sa*BPL (Figure 12A. Duckworth et al. reported a unique hydrogen bonding interaction to *Mtb*BPL between Asp167 and the 2'-hydroxyl of the ribose ring of **1.18**[14](Figure 12B). The enhanced potency of **5.05** towards

_____

*Mtb*BPL relative to **1.18**, suggests that this hydrogen bonding interaction might not contribute to the overall binding affinity of *Mtb*BPL.
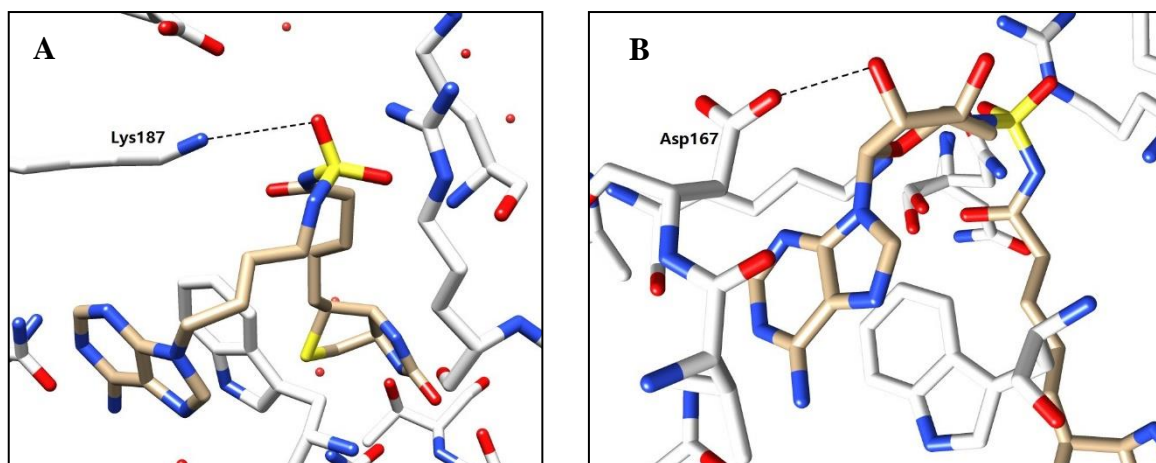
Figure 12: 3D depiction of (A) acylsulfonamide **5.05** bound to *Sa*BPL. No hydrogen bonding interactions are observed between the ribose ring and *Sa*BPL. No hydrogen bonding interactions are observed between the ribose ring and *Sa*BPL; (B) acylsulfonamide **1.18** bound to *Mtb*BPL (PDB 3RUX). The hydrogen bonding interactions between the ribose ring and *Mtb*BPL.

5.5   Conclusion

The three sulfonamides **5.03**-**5.05** were prepared and assayed against a library of BPLs (*Sa*BPL, *Mtb*BPL and *Hs*BPL). Analogues **5.03** and **5.04** were inactive against all three BPLs, whereas their parent triazole analogues **3.01k** and **3.01t** were potent *Sa*BPL inhibitors as discussed in chapter 3. This suggest that for small benzylic analogues with the more flexible acylsulfonamide linkage presents the smaller benzylic groups differently to BPLs as compared to the more structurally rigid 1,2,3-triazole ring as in **3.01k** and **3.01t**.

The acylsulfonamide **5.05** was highly potent against both *Sa*BPL ($K_i = 0.72 \times 10^{-3}$ µM) and *Mtb*BPL ($K_i = 0.74 \times 10^{-3}$ µM). This compares to the parent 1,2,3-triazole analogue **1.22** that is active against *Sa*BPL with a $K_i = 0.66$ µM and *Mtb*BPL with a $K_i = 0.64$ µM. This new acylsulfonamide **5.05** is >900 fold more activity than **1.22** against *Sa*BPL and *Mtb*BPL. Additionally, **5.05** was also found to be 125 fold more active towards *Sa*BPL than the current leading *Sa*BPL inhibitor triazole **1.23** ($K_i = 0.09$ µM) and critically it exhibited at least 1,000-fold selectivity over *Hs*BPL ($K_i > 33$ µM). These combined results make acylsulfonamide **5.05** the most active and selective *Sa*BPL and *Mtb*BPL inhibitor identified to date. Critically,

___

5.05 also displays excellent bacterialisostatic activity against *S. aureus* with MIC = 0.25 – 0.5 µg/ml and *M. tuberculosis* with MIC = 51 µg/ml. It also displays bacterialisostatic activity against methicillin-resistant *S. aureus* (MRSA). Finally, **5.05** is devoid of activity in cell culture models using human HepG2 or HEK293. Thus, body of work described validates the acylsulfonamide **5.05** as an important inhibitor of *Sa*BPL and *Mtb*BPL that can be further developed as a clinical candidate.

The x-ray structure of **5.05** bound to *Sa*BPL confirms that it binds in a U shape conformation whereby the adenine and biotin groups bind to their respective pockets as per the natural reaction intermediate **1.03**. An extensive series of hydrogen bonds were observed between the acylsulfonamide group of **5.05** and Arg122, Arg125, Lys187 and Asp180 suggesting that the acylsulfonamide group is a suitable bioisostere for replacement of the phosphate group as in **1.03** and the 1,2,3-triazole as in **1.22** and **1.23**. Compared to The acylsulfonamide analogue **5.05** lacks the ribose between the acylsulfonamide linker and adenine group was found 17 fold more active against *Mtb*BPL ($IC_{50} = 8.1 \times 10^{-3}$ µM) and equally potent against *Sa*BPL. This compares to the ribose containg analogue **1.18** which is active against *Mtb*BPL ($IC_{50} = 0.14$ µM) against *Mtb*BPL but inactive against *Sa*BPL,[14] This is supported by the observation that limited hydrogen bonding interactions are present between the ribose of **1.18** and *Mtb*BPL, and that no interactions are present between the ribose binding region of **5.05** and *Sa*BPL. Thus the ribose ring is not involved in molecular recognition with *Sa*BPL.

5.6 References for Chapter Five

(1)   Rostovtsev, V. V.; Green, L. G.; Fokin, V. V.; Sharpless, K. B. *Angewandte Chemie* **2002**, *114*, 2708-2711.

(2)   Whiting, M.; Muldoon, J.; Lin, Y. C.; Silverman, S. M.; Lindstrom, W.; Olson, A. J.; Kolb, H. C.; Finn, M.; Sharpless, K. B.; Elder, J. H. *Angewandte Chemie International Edition* **2006**, *45*, 1435-1439.

(3)   Meldal, M.; Tornøe, C. W. *Chemical Reviews* **2008**, *108*, 2952-3015.

(4)   Soares da Costa, T. P.; Tieu, W.; Yap, M. Y.; Pendini, N. R.; Polyak, S. W.; Sejer Pedersen, D.; Morona, R.; Turnidge, J. D.; Wallace, J. C.; Wilce, M. C.; Booker, G. W.; Abell, A. D. *Journal of Biological Chemistry* **2012**, *287*, 17823-32.

(5)   S Paparella, A.; P Soares da Costa, T.; Y Yap, M.; Tieu, W.; CJ Wilce, M.; W Booker, G.; D Abell, A.; W Polyak, S. *Current Topics in Medicinal Chemistry* **2014**, *14*, 4-20.

(6)   Brown, P. H.; Cronan, J. E.; Grøtli, M.; Beckett, D. *Journal of Molecular Biology* **2004**, *337*, 857-869.

(7)   Brown, P. H.; Beckett, D. *Biochemistry* **2005**, *44*, 3112-3121.

(8)   Soares da Costa, T. P.; Tieu, W.; Yap, M. Y.; Zvarec, O.; Bell, J. M.; Turnidge, J. D.; Wallace, J. C.; Booker, G. W.; Wilce, M. C.; Abell, A. D. *ACS Medicinal Chemistry Letters* **2012**, *3*, 509-514.

(9)   Deng, J.; Wu, Y.-M.; Chen, Q.-Y. *Synthesis* **2005**, 2730-2738.

(10)   Worrell, B. T.; Hein, J. E.; Fokin, V. V. *Angewandte Chemie International Edition* **2012**, *51*, 11791-4.

(11)   Hein, J. E.; Tripp, J. C.; Krasnova, L. B.; Sharpless, K. B.; Fokin, V. V. *Angewandte Chemie International Edition* **2009**, *48*, 8018-21.

(12)   Cai, Q.; Yan, J.; Ding, K. *Organic Letters* **2012**, *14*, 3332-3335.

(13)   L'abbé, G.; Beenaerts, L. *Tetrahedron* **1989**, *45*, 749-756.

(14)   Duckworth, B. P.; Geders, T. W.; Tiwari, D.; Boshoff, H. I.; Sibbald, P. A.; Barry, C. E., 3rd; Schnappinger, D.; Finzel, B. C.; Aldrich, C. C. *Chemistry & Biology* **2011**, *18*, 1432-41.

(15)   Tieu, W.; da Costa, T. P. S.; Yap, M. Y.; Keeling, K. L.; Wilce, M. C.; Wallace, J. C.; Booker, G. W.; Polyak, S. W.; Abell, A. D. *Chemical Science* **2013**, *4*, 3533-3537.

_____

(16)   Tieu, W.; Jarrad, A. M.; Paparella, A. S.; Keeling, K. A.; da Costa, T. P. S.; Wallace, J. C.; Booker, G. W.; Polyak, S. W.; Abell, A. D. *Bioorganic & Medicinal Chemistry Letters* **2014**, *24*, 4689-4693.

(17)   Lu, X.; Zhang, H.; Tonge, P. J.; Tan, D. S. *Bioorganic & Medicinal Chemistry Letters* **2008**, *18*, 5963-5966.

(18)   Winum, J.-Y.; Toupet, L.; Barragan, V.; Dewynter, G.; Montero, J.-L. *Organic Letters* **2001**, *3*, 2241-2243.

(19)   Lin, F. L.; Hoyt, H. M.; Van Halbeek, H.; Bergman, R. G.; Bertozzi, C. R. *Journal of the American Chemical Society* **2005**, *127*, 2686-2695.

(20)   Chapman-Smith, A.; Cronan, J. E. *Trends in Biochemical Sciences* **1999**, *24*, 359-363.

(21)   Jorgensen, J. H. *Methods for dilution antimicrobial susceptibility tests for bacteria that grow aerobically: approved standard: NCCLS document M7-A3*; Nccls, **1993**.

(22)   Pendini, N. R.; Polyak, S. W.; Booker, G. W.; Wallace, J. C.; Wilce, M. C. *Acta Crystallographica Section F: Structural Biology and Crystallization Communications* **2008**, *64*, 520-523.

6.1 Introduction

Chapters 2-5 discussed the identification and optimisation of lead *Sa*BPL inhibitor **1.22** (structure refers to Figure 1A) using conventional lead discovery and parallel synthesis.[1,2] Libraries of building blocks (i.e. acetylenes, azides, and sulfonamides) were synthesised and coupled to build a large number of new compounds based on a bifunctional scaffold designed to interact with both the biotin an adenine binding pockets of BPL. These compounds required complete purification and characterization before subjecting them to high-throughput screening assays.[3] Identification of the hit compounds required biological testing of each individual compound. These approaches are often accompanied by challenges related to the efficiency of library synthesis and purity and also the biological testing of the compound library.[4,5] Although researchers have placed considerable effort on optimising such discovery approaches, they have been disappointed by the declining rate of submission and introduction of new drug candidates. The effectiveness of existing approaches to drug discovery has been questioned recently.[3] In the last two decades, novel means of lead discovery approaches have been investigated where the biological target is actively involved in the synthesis of its own inhibitory compound.[6,7] This target guided synthesis (TGS) provides an alternative approach to lead discovery and optimisation by combining the synthesis and screening of libraries of low molecular weight compounds in a single step. Of all the approaches, *in situ* click chemistry using the Huisgen cycloaddition between azides and acetylenes has proved to be one of the better examples of TGS.[8-10]

As previously mentioned in chapter 1, a recent study by William Tieu and co-workers in the Abell research group reported the use of biotin protein ligase (BPL) as a template for *in situ* click chemistry.[11] The initial *in situ* experiment was performed using wild-type *Sa*BPL as a template to catalyse the Huisgen cycloaddition of biotin acetylene **2.21** and adenine azide **4.21** to give the potent triazole **1.22** ($K_i = 0.66\,\mu M$ against *Sa*BPL), as shown in Figure 1A.[11] However, the desired triazole product **1.22** was not readily detected above the background level by HPLC analysis due to poor overall conversion.[11] One explanation is that the biotin-binding loop (Figure 1B, highlighted in green) closes over the active site of *Sa*BPL to prevent release of the substrate, thereby resulting in low turnover rate.[12] This hypothesis is supported by the crystal structure of **1.22** bound to *Sa*BPL, where the substrate is stabilised by a hydrogen bonding network between the 1,2,3-triazole ring of **1.22** and Arg122, Asp180, Arg125 and water molecules (Figure 1C).[11,12] Arg122 is particularly important for stabilising the network by not only forming a hydrogen bond with N3 of 1,2,3-triazole ring, but also

_____

connecting with Asp180 *via* a water molecule (Figure 1C). Arg122 was then selectively mutated to smaller Gly122 and this mutation prevents the biotin-binding loop from closing over the active site, and thereby increases the dissociation rate of substrates from the active binding site.[11] A subsequent *in situ* click experiment using *Sa*BPL mutated in this loop (*Sa*BPL-R122G) successfully produced triazole product **1.22** that could be detected by HPLC.[11] One of the limitations of this study was that the regioselectivity of the product could not be resolved instantaneously, thus requiring additional structural information, particularly by NMR analysis. It also required the use of a mutant enzyme rather than the wild type.

A
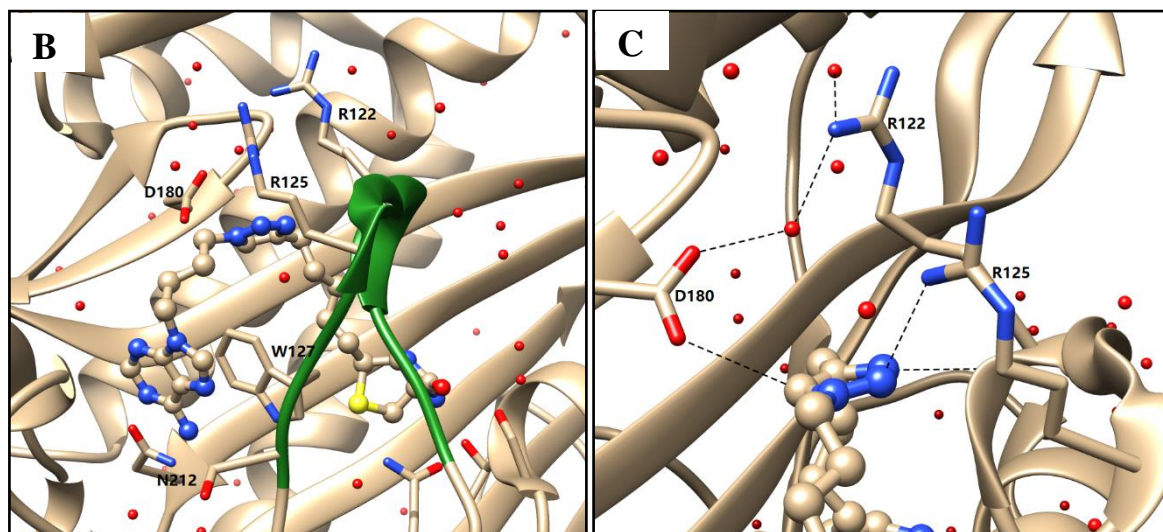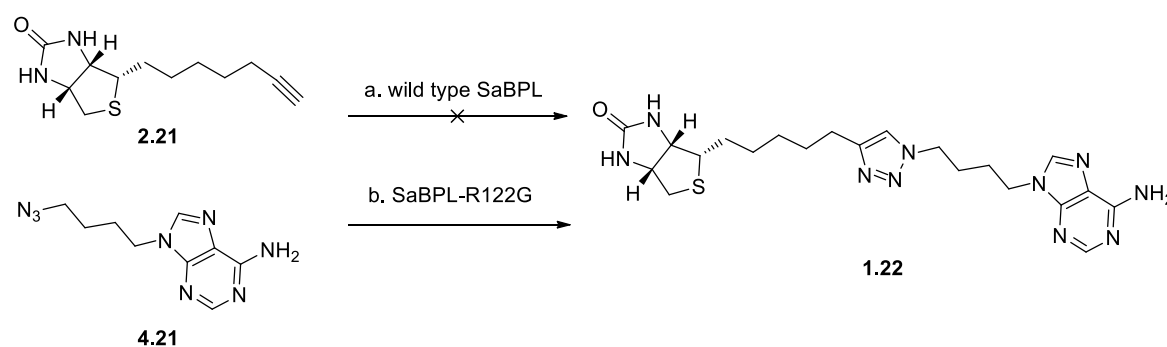
Figure 1: (A) BPL templated *in situ* reactions of 1,4-triazole **1.22** between biotin acetylene **2.21** with adenine azide **4.21**.[11] (a) In the presence of wild type *Sa*BPL. (b) In the presence of *Sa*BPL-R122G. (B) A close up view of the active site of the x-ray crystal structure of 1,4-triazole **1.22** bound to wild type *Sa*BPL (PDB 3V7R). (C) Detailed hydrogen bonding interactions between *Sa*BPL and the 1,2,3-triazole ring (black dashes), specifically between R122, H$_2$O, and D180.

An advance in this area requires an alternative method for analysing the *in situ* click chemistry reaction mixtures with improved sensitivity and accuracy.[13,14] In this chapter the products of the in situ generated library are analysed by HPLC and high resolution electrospray mass spectrometry (LC/HRMS), rather than simply by analytical HPLC. The HPLC analysis performed previously involved monitoring product by absorbance at 280 nm.[11] This is problematic when compounds have similar retention times. For the purpose of *in situ* click chemistry, LC/HRMS allows instantaneous and precise identification of individual products using a combination of retention time and high resolution molecular mass. Potential also exists to assign the regioselectivity of the *in situ* generated di-substituted triazole product (1,4 vs 1,5) by comparing retention times of each regioisomer.[13,15] Therefore, the LC/HRMS approach is more versatile, while also reducing analysis times from days to hours. Additionally, chromatographic removal of compounds that might otherwise obscure the mass spectrum of products allows dramatic increase of the resolution of mass spectra.[13] Most importantly, the improved sensitivity should allow detection of *in situ* products that might not be observed by analytical HPLC. For example, the previously mentioned low level of triazole **1.22** produced by native *Sa*BPL might be detected by LC/HRMS.

6.2 In situ click chemistry using native BPLs

6.2.1 Experiment 1: Proof of concept and determination of substitution of 1,4-triazole 1.22

The first study involved determining whether or not LC/HRMS is able to detect triazole products generated by the native *Sa*BPL. The previously reported *in situ* click reaction of biotin acetylene **2.21** and azide **4.21**, as presented in Scheme 1, was used in this study.[11] The *in situ* reaction mixture was prepared by mixing biotin acetylene **1.22** (500 µM) and adenine azide **4.21** (500 µM) in phosphate buffered saline (pH 7.4) in the absence of copper using wild type *Sa*BPL (2 µM). Two control experiments were carried out in parallel, whereby *Sa*BPL was replaced with either bovine serum albumin (BSA) (2 µM) or water (2 µM) in order to demonstrate that the Click reaction does not proceed in the absence of BPL or with an unrelated protein, BSA. All three reaction mixtures were incubated at 37°C for 48 h. Each reaction mixture was then analysed by LC/HRMS in positive mode with selective ion monitoring of triazole **1.22** (M+H$^+$ = 471.2398 Da). The LC/MS traces of the three *in situ*

experiments are shown in Figure 2 with the corresponding retention time of triazole product depicted therein.
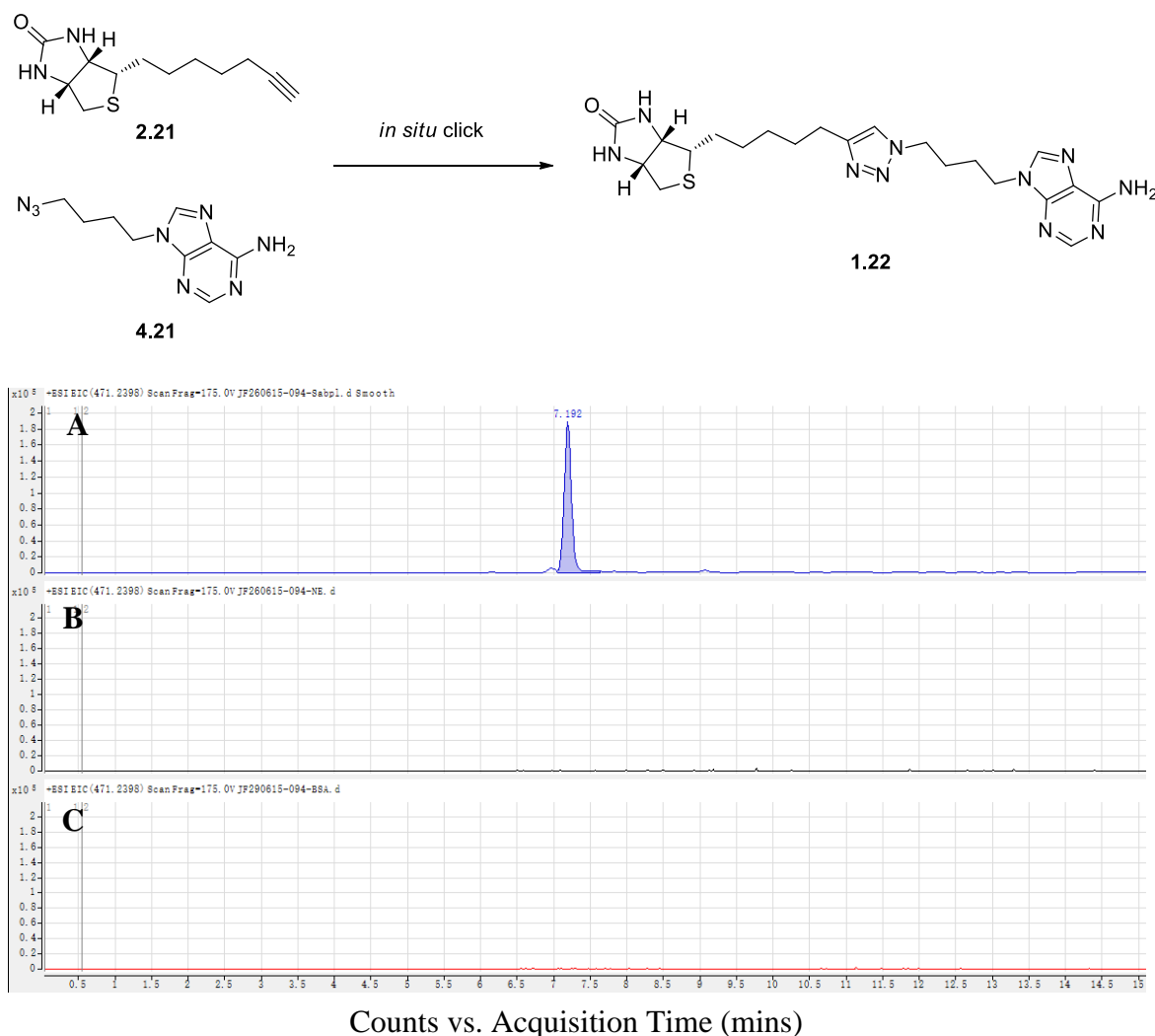
Figure 2: LC/HRMS traces of *in situ* reaction of biotin acetylene **2.21** and azide **4.21** to give triazole **1.22** with selective ion monitoring for triazole **1.22** (M+H$^+$ = 471.2398). (A) Product from *in situ* assembly in the presence of *Sa*BPL; (B) *In situ* reaction in the absence of enzyme; (C) *In situ* reaction with BSA.

The crude products from the reaction of biotin acetylene **2.21** and azide **4.21** were analysed by LC/HRMS using a reverse phase column indicated. Formation of triazole **1.22** was evident in the reaction using wild type *Sa*BPL only as evident by a peak at 7.2 min with the corresponding M+H$^+$ = 471.2392 Da (Figure 2A). Importantly, triazole **1.22** was not observed in the absence of BPL (Figure 2B), or using BSA (Figure 2C). Thus chemical ligation is specifically catalysed by *Sa*BPL and not by any exogenous copper or other

_____

catalytic species that might be present. Thus *Sa*BPL (and mutant *Sa*BPL-R122G) are both capable of catalysing the 1,3-cycloadditon reaction between acetylene **2.21** and azide **4.21** to give triazole product **1.22**.[11] The detection of **1.22** in the reaction mixture using native *Sa*BPL demonstrates that LC/HRMS is able to detect *in situ* triazole product even with low turnover rate of the wild type enzyme. Analysis by LC/HRMS provides significant advantage in that it allows directly use native *Sa*BPL (actual drug target) in future experiments rather than relying on the use of the mutant enzyme.

Regioselectivity determination

As discussed previously, HPLC analysis does not allow ready resolution of the regioselectivity (1,4- vs 1,5-) of *in situ* generated triazole product. Here complete structural determination relies is best carried out by complete NMR analysis. In the earlier study, the *in situ* product of *Sa*BPL action was presumed to be the 1,4-triazole **1.22** ($K_i = 0.7\,\mu M$ against *Sa*BPL), given that its 1,5-triazole isomer (**6.01** in Scheme 1) was known to be inactive towards *Sa*BPL ($K_i > 33\,\mu M$).[11,12] In order to confirm this, pure 1,4- **1.22** and 1,5-**6.01** were synthesised and used as reference samples in LC/HRMS analysis. These analogues were separately prepared by respective CuAAC and RuAAC reaction of adenine azide **4.21** and biotin acetylene **2.21** according to the literature procedure[12] (see Scheme 1).
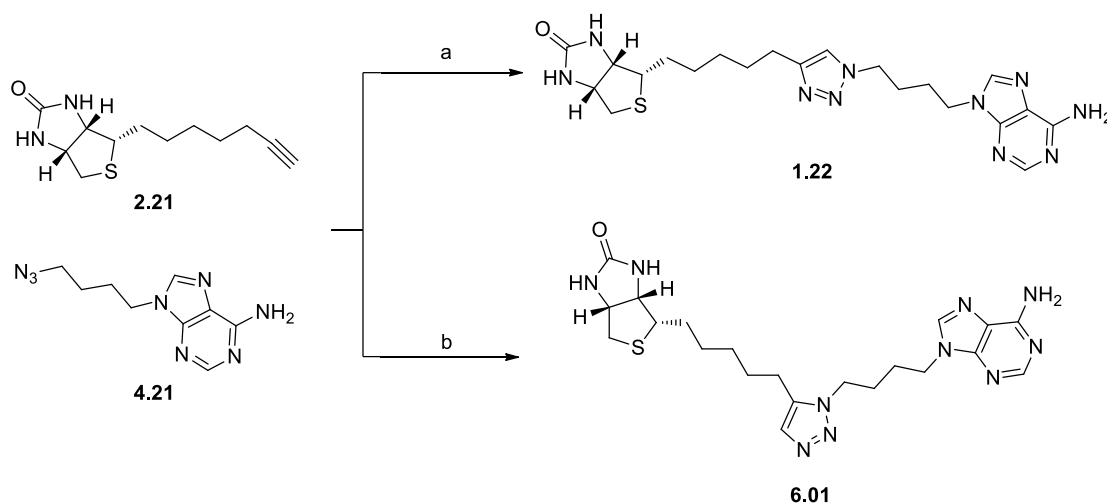
Scheme 1: a) Cu nanopowder, 2:1 AcCN/H$_2$O, 12 h, sonication, 35 ℃; b) Cp*Ru(PPh$_3$)$_2$Cl, 1:1 DMF/THF, 12 h, 35℃.

LC/HRMS analysis of the authentic samples of **1.22** and **6.01** revealed a striking difference in retention times, with the 1,4-triazole isomer (**1.22**) detected at 7.2 min and the 1,5-triazole

_____

isomer (**6.01**) detected at 8.2 min, as shown in Figures 3B and 3C, respectively. This compared with a retention time of 7.2 min for the in situ experiment shown in Figure 2A. Thus 1,4-triazole **1.22** is produced in the *in situ* experiment, where this is known to be the active isomer.[11]

Counts vs. Acquisition Time (mins)
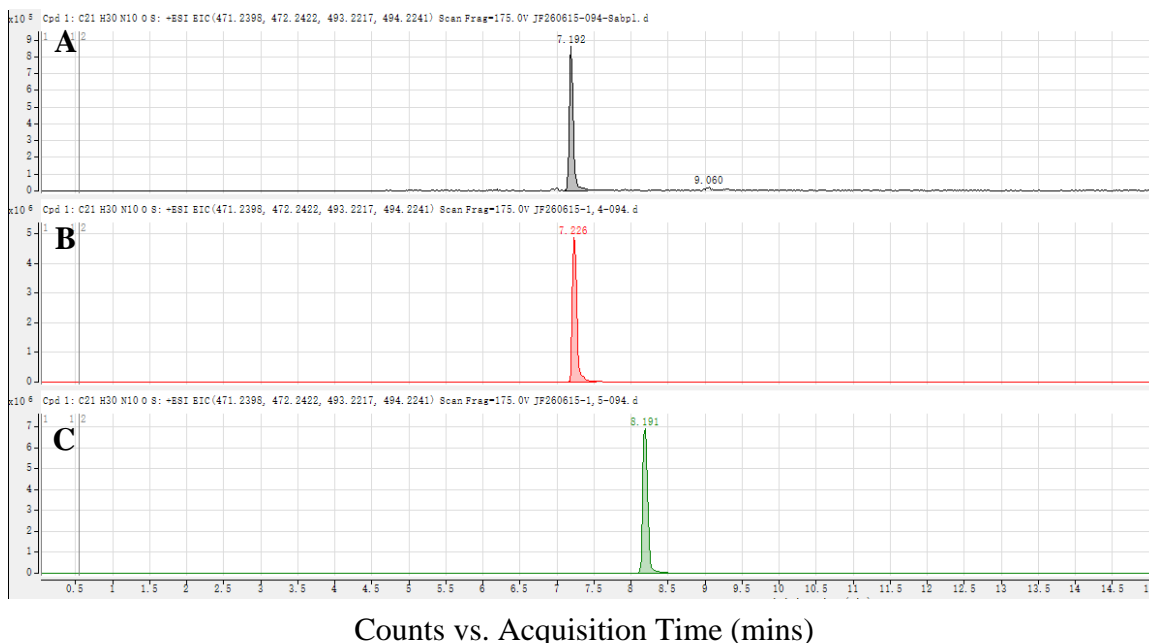
Figure 3: LC/HRMS traces of reference compounds and *in situ* click produced triazole **1.22** at selective ion monitoring (M+H$^+$ = 471.2398 Da). (A) Product from *in situ* assembly in the presence of *Sa*BPL; (B) 1,4-Triazole prepared by CuAAC; (C) 1,5-Triazole prepared by RuAAC.

Standard curve of 1,4-triazole 1.22

A calibration curve using various concentrations of **1.22** was established to determine: 1) accuracy and limits of sensitivity of the LC/HRMS system; 2) yield of *in situ* generated triazole product. Solutions of 1,4-triazole **1.22** in PBS buffer (concentration ranging from 0 to 20 µM) were prepared and each sample analysed by LC/HRMS. Triazole **1.22**, with a corresponding M+H$^+$ = 471.2398 Da, was detected for each individual sample at 7.2 min. The area under the peak (i.e. ion counts) at each concentration was calculated and is listed in supplementary data (chapter 7, Table 1). A calibration curve of 1,4-triazole **1.22** was then plotted with concentrations on the x-axis against area under the peak on the y-axis as shown in Figure 4.
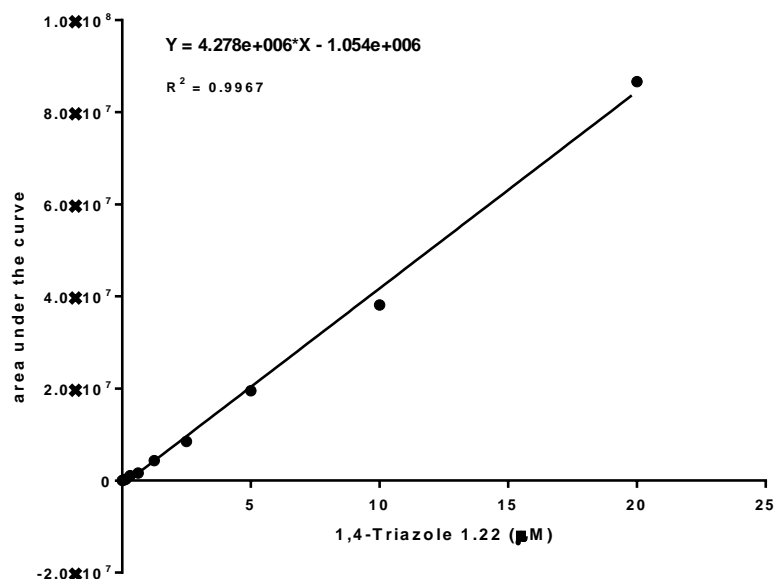
Figure 4: Calibration curve for LC/HRMS showing linear correlation between triazole **1.22** concentration and measured peak area.

As shown above in Figure 4, linear correlation between the area under the peak and the compound concentrations was observed. The line of best-fit was plotted and the corresponding equation was calculated. Results indicated that LC/HRMS is capable of accurately measuring concentrations of **1.22** from 0 to 20 µM. The equation of the line was used to estimate the yield of *in situ* generated **1.22** by *Sa*BPL (2 µM) to be approximately 0.6 µM. The detailed calculations are shown in chapter 7, Table 1.

The success of this proof of concept experiment suggests that the use of LC/HRMS may greatly improve detection sensitivity. This improved sensitivity, together with high resolution mass spectrometry, allowed detection of the low level of **1.22** generated using native *Sa*BPL. Moreover, the ability to distinguish triazole regioisomers (1,4 and 1,5-) makes LC/MS a more efficient and reliable approach for analysis of the *in situ* click chemistry reported here and elsewhere.

6.2.2 Experiment 2: *in situ* screening using a panel of BPLs from different species.

Encouraged by the successful *in situ* click experiments using wild type *Sa*BPL, we turned our attention to expanding the panel of native BPL enzymes for use in in situ experiments,

including *Mycobacterium tuberculosis* (*Mtb*BPL), *Acinetobacter calcoaceticus* (*Ac*BPL), *Klebsiella pneumoniae* (*Kp*BPL), and *Candida albicans* (*Ca*BPL).

The reaction of biotin acetylene **2.21** (500 µM) and adenine azide **4.21** (500 µM) was thus repeated with 2 µM of either *Mtb*BPL, *Ac*BPL, *Kp*BPL, or *Ca*BPL in place of wild type *Sa*BPL as described in section 6.2.1. Analysis of each reaction mixture by LC/HRMS as before revealed formation of desired 1,4-triazole **1.22** by *Mtb*BPL and *Kp*BPL with the expected retention time of 7.2 min for the 1,4-isomer (Figure 5B and 5C). *Ac*BPL, *Ca*BPL, BSA and the control experiment lacking enzyme did not form triazole **1.22**.
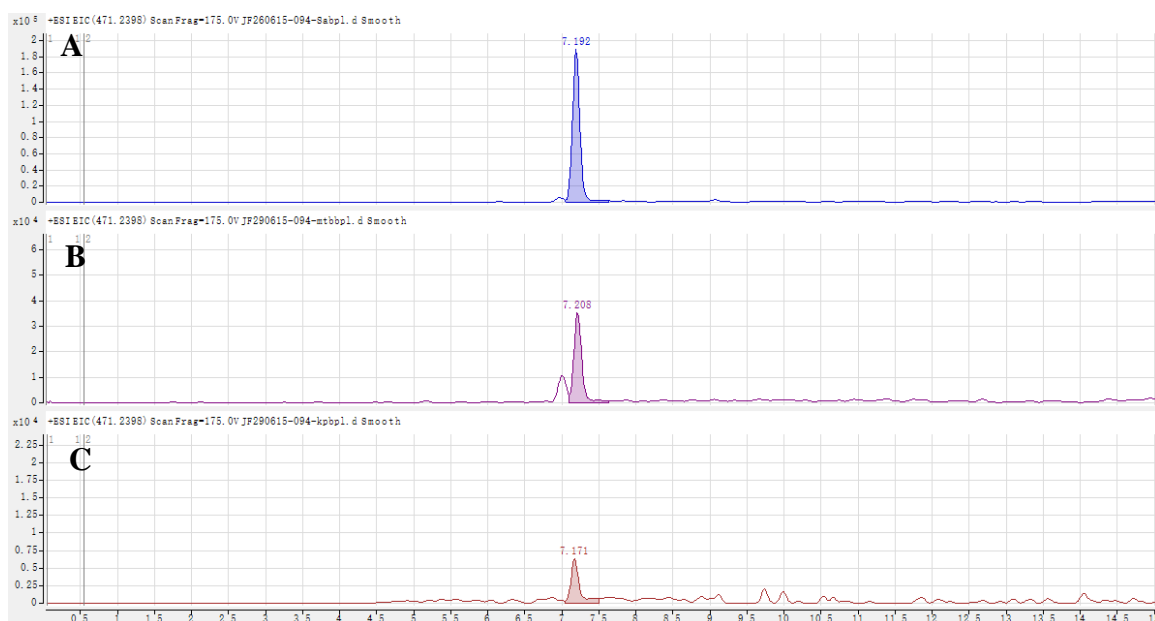
Figure 5: Panel of BPLs. LC/HRMS traces of *in situ* click produced triazole **1.22** at selective ion monitoring (m/z = 471.2398). Product from *in situ* assembly in the presence of (A) *Sa*BPL; (B) *Mtb*BPL; (C) *Kp*BPL.

The yield of triazole generated by *Mtb*BPL and *Kp*BPL were calculated based on the calibration curve developed earlier as shown in Figure 3. The experiment using *Mtb*BPL generated 0.4 µM of **1.22**, whereas *Kp*BPL produced approximately 0.3 µM of **1.22**. These results suggest overwhelming bias towards the formation of a larger amount of triazole **1.22** by *Mtb*BPL compared to *Kp*BPL. This is consistent with the observation that **1.22** was found to be more potent against *Mtb*BPL (K_i = 0.64 µM) compared to *Kp*BPL ($K_i \approx$ 1.0 µM). Interestingly **1.22** displayed a K_i of 0.66 µM against *Sa*BPL and this was observed to be formed in a yield of 0.6 µM in the corresponding in situ experiment. Significantly, **1.22** was found inactive against *Ac*BPL and *Ca*BPL at the highest assay concentrations (K_i > 33 µM). These results are consistent with the observation that *Ac*BPL and *Ca*BPL failed to produce

1.22 in the *in situ* click experiments, validating triazole **1.22** as an *in situ* hit and demonstrating that the formation of **1.22** requires enzyme activity.

6.2.3 Experiment 3: library screening of biotin acetylene 2.21 and azides 3.01k, 3.01t, and 6.02-6.08 via *in situ* click chemistry.

The methodology was then expanded to *in situ* click experiments involving separate library reactions of biotin acetylene **2.21** with azides **3.03k**, **3.03t**, and also **6.02-6.08**. As discussed in chapter 3, the 1,4-triazoles **3.01k** and **3.01t** (See Table 1 below) produced from azides **3.03k** and **3.03t** were shown to be potent *Sa*BPL inhibitors with K_i values of 0.28 µM and 1.00 µM, respectively. These simple benzylic substituted triazoles were thus good candidates for extended *in situ* experiments. The azide building blocks **6.02-6.07** (shown in Figure 6) were provided by Prof Matthew Copper from University of Queensland. These analogues are fluorescent and were initially designed to accommodate in the ATP pocket.
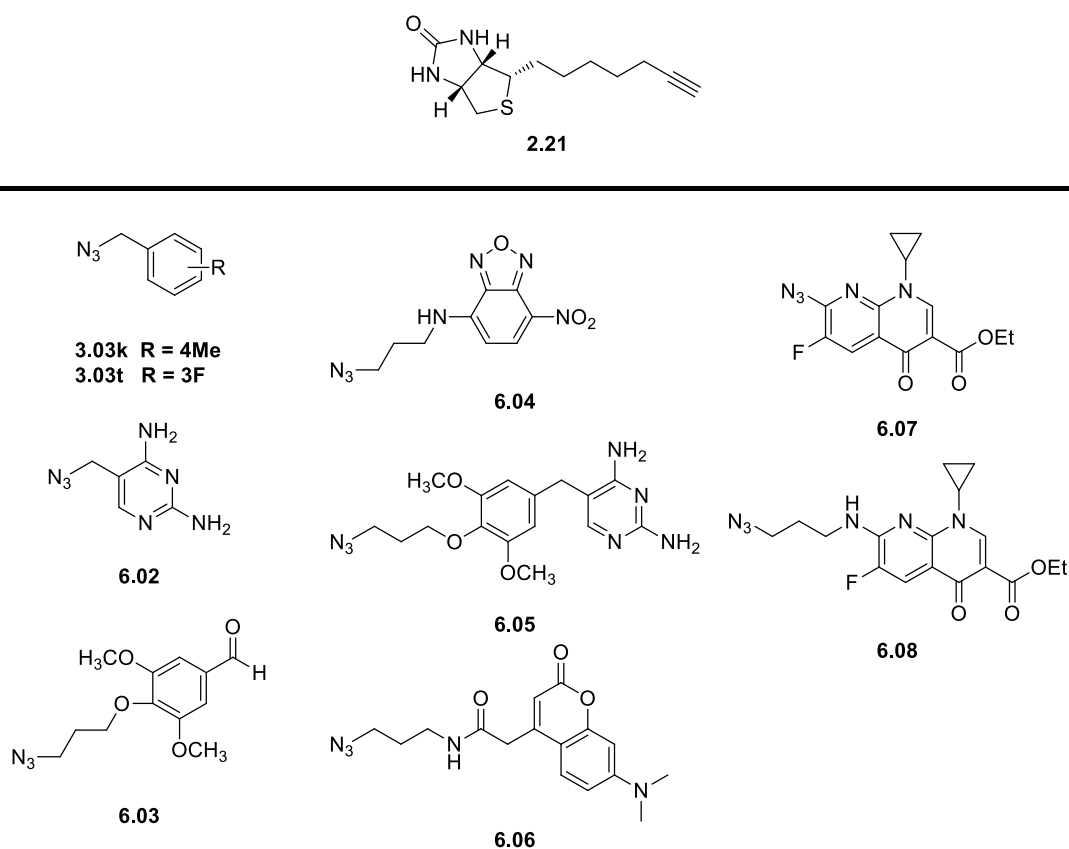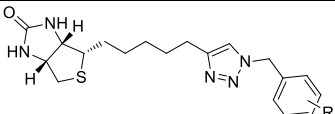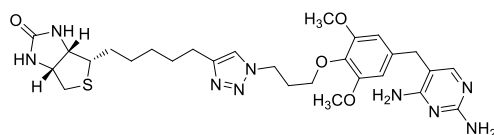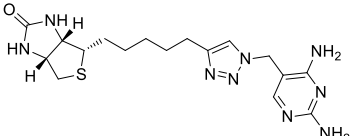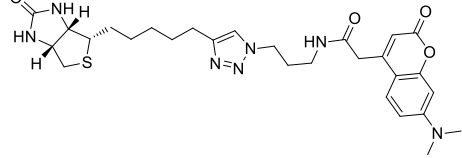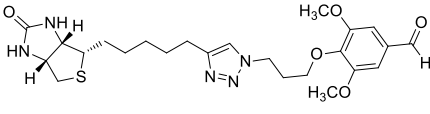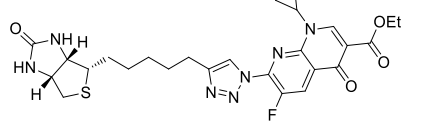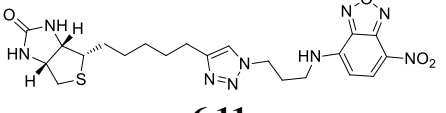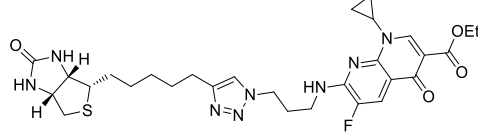
Figure 6: Biotin acetylene **2.21** and a library of nine azides **3.03k**, **3.03t**, and **6.02-6.08** for *in situ* click chemistry screening.

_____

Experiments were conducted in parallel using a 96-well microtiter plate. Each well contained phosphate buffered saline (pH 7.4) with a binary mixture of biotin acetylene **2.21** (500 µM) and one azide building block, either **3.03k**, **3.03t** or **6.02-6.08** (500 µM). These were then treated with a given BPL, either *Sa*BPL, *Mtb*BPL, *Ac*BPL, *Kp*BPL, or *Ca*BPL (2 µM). Control experiments were also run for all nine acetylene-azide mixtures in the absence of BPL, and with added BSA in place of BPL. Each reaction mixture was then analysed by LC/HRMS in positive mode with selective ion monitoring according to the molecular weight of each individual triazole product (see Table 1). The potential *in situ* generated triazole products from biotin acetylene **2.21** and azide library of **3.03k**, **3.03t** and **6.02-6.08** are listed below in Table 1 with the results shown therein.

Table 1. Proposed *in situ* generated 1,2,3-triazoles

Potential *in situ* products	Hits[a]	Potential *in situ* products	Hits[a]
3.01k R = 4Me **3.01t** R = 3F	None	**6.12**	None
6.09	None	**6.13**	None
6.10	None	**6.14**	None
6.11	*Sa*BPL	**6.15**	None

[a] obtained through LC/HRMS.

Somewhat surprisingly, 1,4-triazoles **3.01k** and **3.01t** which are both good inhibitors of *Sa*BPL (K_i = 0.28 µM and 1.0 µM respectively) were not observed in any of the *in situ* reactions by LC/HRMS (Table 1). It thus seems likely that the smaller benzyl groups of 1,4-triazole **3.01k** and **3.01t** does not bind to the ATP binding pocket of *Sa*BPL and as such an *in situ* BPL promoted reaction is not possible. As discussed above, *in situ* click chemistry relies on simultaneous binding of two ligands (acetylenes and azides) to adjacent sites on the

protein. Both ligands must be positioned close enough to allow the 'click' reaction to proceed. A C4 linker length between the triazole ring and ATP pocket binding moiety has been previously determined to optimum as in triazoles **1.22** which has K_i values of 0.64 µM against *Sa*BPL.[12] Triazoles **3.01k** and **3.01t** with a shorter C1 linker would likely result in a unique binding mode that the benzylic groups bind on the edge of the ATP binding pocket or elsewhere. Therefore, the *in situ* click reaction would not occur when benzyl azides **3.03k** and **3.03t** could not fit in the appropriate ATP binding pocket.

For the azide library of **6.02-6.08**, LC/HRMS traces revealed that only 1,4-triazole **6.11** was formed (retention time = 9.2 min as in Figure 7B) in the *in situ* experiment between acetylene **2.21** and azide **6.04** using *Sa*BPL as the template. Whilst LC/HRMS analysis of *in situ* experiments between acetylene **2.21** and the azides **6.02**, **6.03**, and **6.05-6.08** showed that no triazole analogues (**6.09**, **6.10**, and **6.12-6.15** as in Table 1) were formed.

The 1,4-regioisomer of *in situ* produced **6.11** was confirmed on LC/HRMS-based comparison with an authentic and independently prepared sample of 1,4-triazole **6.11**. This gave the same retention time of 9.2 min (Figure 7A). The synthesis of the authentic sample of **6.11** is presented below in Scheme 3 as is its assay against *Sa*BPL, *Mtb*BPL, *Ac*BPL, *Kp*BPL, and *Ca*BPL. Interestingly, no trace of 1,4-triazole **6.11** (or its 1,5-triazole regioisomer) was detected with BPLs from *Mtb*BPL, *Ac*BPL, *Kp*BPL and *Ca*BPL . This observation highlights selectivity of binding to *Sa*BPL and *in situ* synthesis of the 1,4-isomer. Finally, as expected, control experiments in the absence of BPLs and with BSA, did not give triazole **6.11** (Figure 7C).
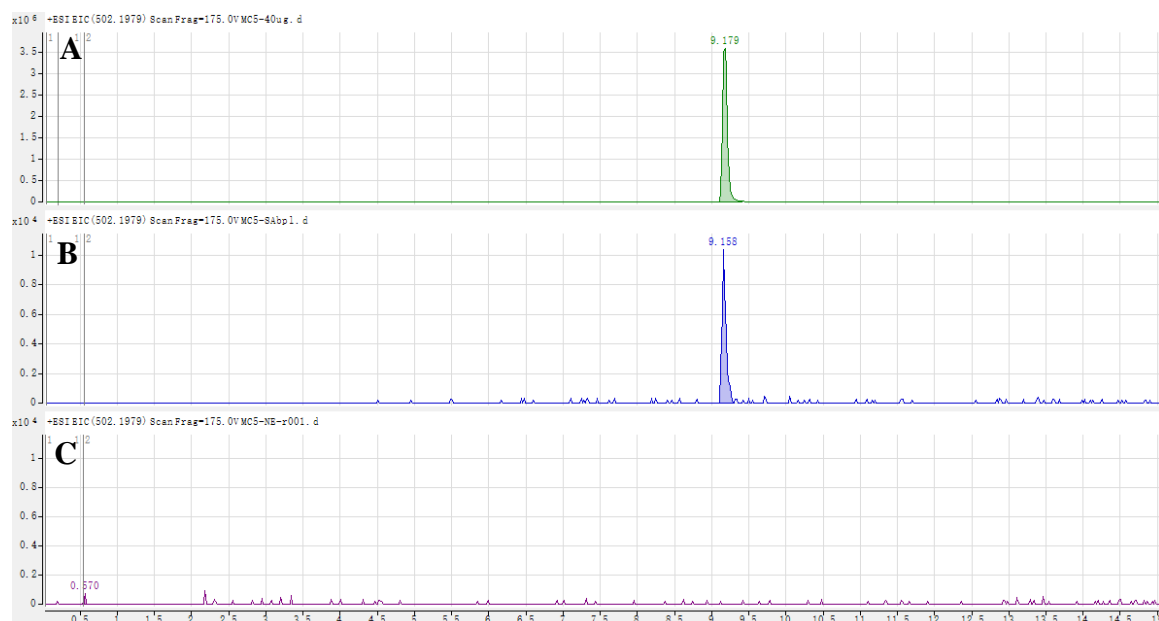
Figure 7: LC/HRMS traces of reference compounds and in situ click produced triazole **6.11** at selective ion monitoring (M+H⁺ = 502.1979 Da). (A) 1,4-Triazole prepared by CuAAC. (B) Product from *in situ* assembly in the presence of *Sa*BPL. (C) Controls (no enzyme).

Preparation of 1,4-triazole 6.11 via CuAAC

An authentic sample of 1,4-triazole **6.11** was synthesised by Dr. Beatriz Blanco-Rodriguez of the Abell research group as depicted below in Scheme 2.
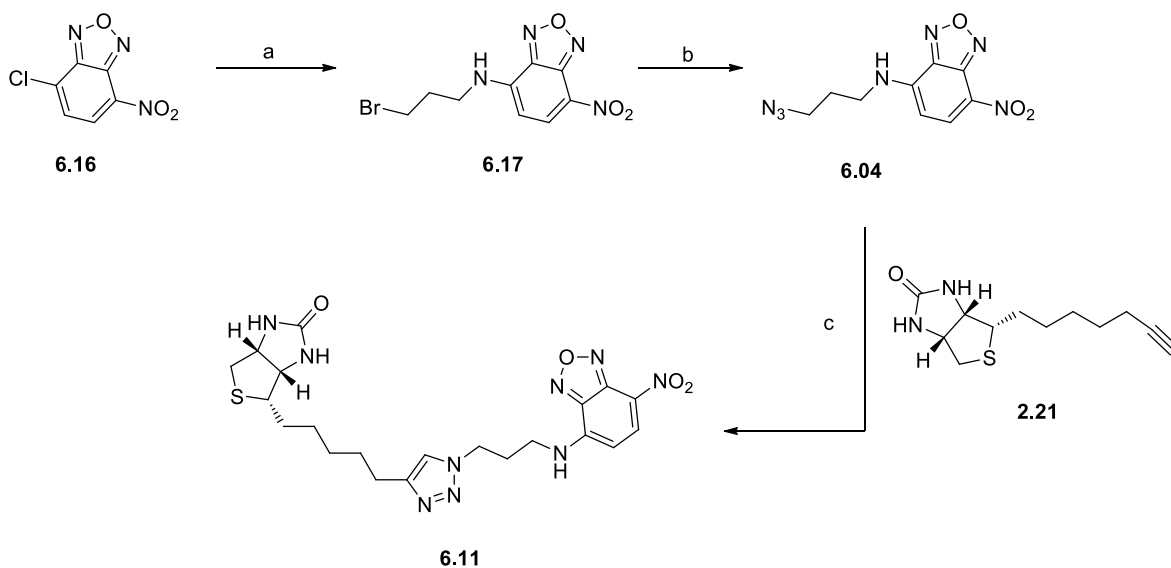
Scheme 2: a) MeOH, Br(CH₂)₃NH₂ HBr; b) DMF, NaN₃; c) Cu nano powder, 2:1 acetonitrile/water, sonication, 35ºC.

Commercially available 4-chloro-7-nitrobenzofurazan **6.16** was firstly reacted with 3-bromopropylamine hydrobromide in ice-cold MeOH to give nitrobenzofurazan bromide **6.17** in 32% yield after purification by flash chromatography. The bromide was then converted to the corresponding azide **6.04** by reacting sodium azide in DMF to give **6.04** in 73% yield without the need for chromatography. 1,4-Triazole **6.11** was synthesised via CuAAC by reacting biotin acetylene **2.21** and nitrobenzofurazan azide **6.04** in 2:1 acetonitrile and water mixture using copper nano powder as the catalyst. The crude reaction mixture was finally purified by flash chromatography to give **6.11** in 38% yield as yellow powder.

Biological assay of 1,4-triazole 6.11

The authentic sample of 1,4-triazole **6.11** was assayed against *Sa*BPL, *Mtb*BPL, *Ac*BPL, *Kp*BPL, and *Ca*BPL by collaborators at Biological Sciences, University of Adelaide, using an *in vitro* biotinylation assay described by Chapman-Smith and co-workers[16]. 1,4-Triazole **6.11** was found to be only active towards *Sa*BPL with $K_i = 1.4\ \mu M$ and inactive against other BPL enzymes (i.e. *Mtb*BPL, *Ac*BPL, *Kp*BPL, and *Ca*BPL). The results highlights the above mentioned species-specific binding that the 1,4-triazole product **6.11** was only produced *in situ* using *Sa*BPL as the template and the formation of triazole products required enzyme activity.

Standard curve of 1,4-triazole 6.11

A calibration curve of **6.11** was generated using the approach described in section 6.2.2. Solutions of triazole **6.11** in PBS buffer at concentrations ranging from 0 to 20 μM were prepared and each sample was analysed using LC/HRMS. Triazole **6.11** with the corresponding $M+H^+ = 502.1979$ Da was detected for each individual sample at 9.2 min. The area under the peak for each concentration was calculated as listed in chapter 7, Table 2. The line of best-fit was plotted with the area under the peak on the y-axis and the corresponding concentration on the x-axis as shown in Figure 8. The equation of the line was calculated and used to estimate the yield of **6.11** produced by *Sa*BPL to be 0.6 μM.
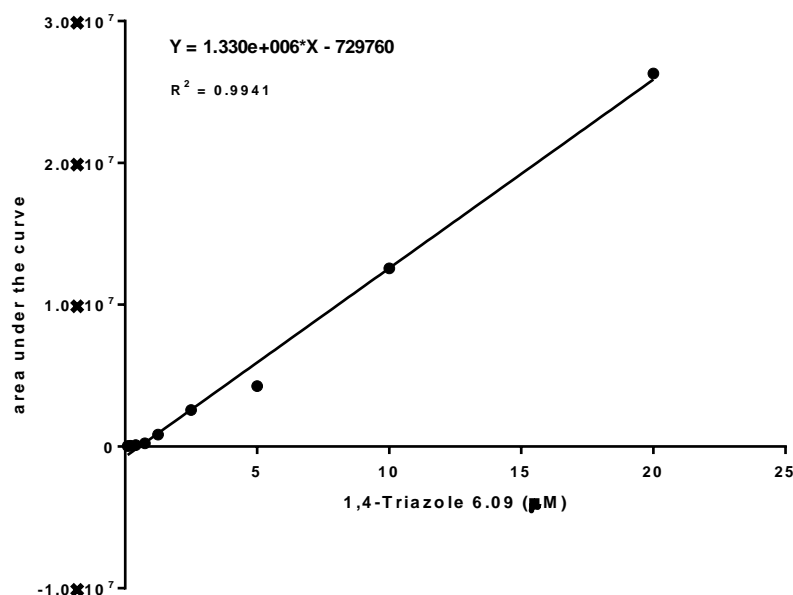
Figure 8: A calibration curve by LC/HRMS showing linear correlation between the concentration of triazole **6.11** and corresponding peak area. Each point corresponds to the average of three independent measurements.

6.2.4 Experiment 4: *in situ* synthesis of 1,4,5-trisubstituted triazole

The *in situ* click chemistry experiments highlight that the BPL enzymes (i.e. *Sa*BPL, *Mtb*BPL, *Ac*BPL, *Kp*BPL, and *Ca*BPL) are able to bind biotin acetylene **2.21** and azides (**4.21** and **6.04**) and then synthesise the corresponding 1,4-disubstituted triazoles **1.22** and **6.11**. This occurs in the absence of copper catalyst as is used in conventional CuAAC.

Recent applications of *in situ* click chemistry are limited to the assembly of terminal acetylenes (such as biotin acetylene **2.21**) and organic azides.[15] The possibility that *in situ* click chemistry can assemble a non-terminal acetylene and an azide, to produce 1,4,5-trisubstituted triazole, has not been explored. The mechanism of CuAAC (as shown in Figure 9) indicates that cycloaddition requires coordination of Cu(I) to a terminal acetylene (**6.18**) to form a copper acetylide **6.19** as a key intermediate.[17] Subsequent ligation of the azide **6.20** to the copper acetylide and formation of an unusual six-membered Cu(III) metallacycle **6.22**, lowers the energy barrier for this process. This metallacycle is then rearranged and constrained to give the five-membered triazolyl-copper species **6.23**, which is followed by protonolysis to give a 1,4-disubstituted triazole **6.24** with closure of the catalytic cycle.[17] This mechanism suggests that a non-terminal acetylene, such as 1-methylacetylenes **6.25**

and **6.26** in Figure 9B, would not react with Cu, such that subsequent cycloaddition would not proceed to give fully-decorated triazole analogues **6.27** and **6.28**. Indeed reaction of 1-methylacetylene (**6.25** and **6.26**) with azide **4.21** does not to proceed in the presence of copper catalyst as discussed below.
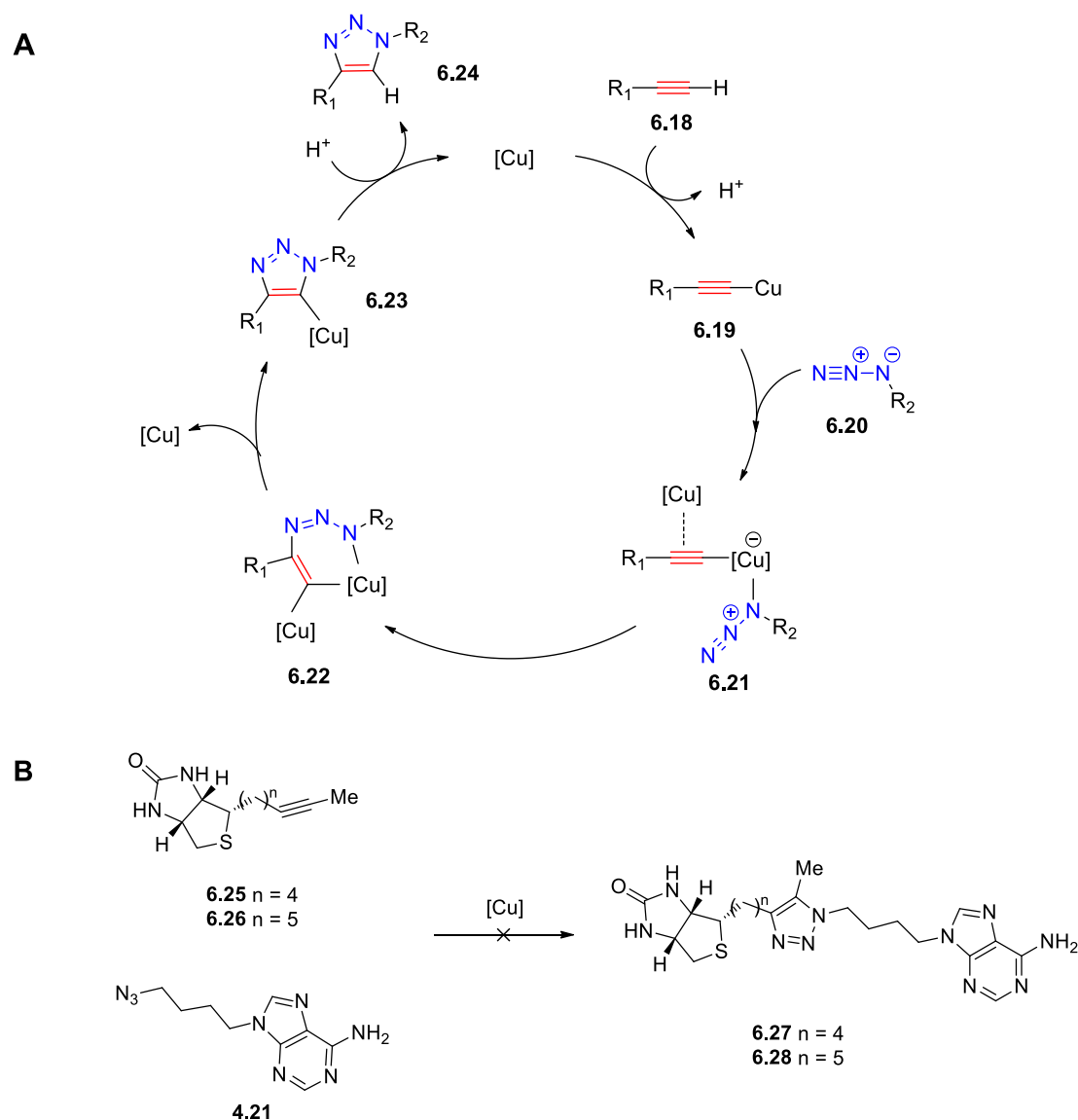
Figure 9: (A) Mechanism of the copper-catalysed azide-alkyne cycloaddition (CuAAC)[17]; (B) CuAAC reactions between methylated acetylenes (**6.25** and **6.26**) and azide **4.21** failed to give 1,4,5-trisubstituted triazoles (**6.27** and **6.28**).

Recent efforts on the synthesis of 1,4,5-trisubstituted triazoles have focused on three strategies: (i) interception of 5-cuprated-1,2,3-triazole (i.e. **6.23** in Scheme 3) with reactive electrophiles (such as aryl halides),[18] (ii) the conversion of functionalized acetylenes **6.29** to

5-halogenated triazole **6.30** and subsequent palladium-catalysed cross coupling to give fully-decorated 1,2,3-triazole **6.31**,[19,20] and (iii) direct functionalizations of the C-H bond of 1,2,3-triazole **6.24** using palladium-catalysed direct arylations would give **6.31** (Scheme 3).[21,22] However, all three approaches share some related limitations. Firstly, a source of Cu is required as catalyst for the formation of 5-cuprated-1,2,3-triazole **6.23** or 5-halogenated-1,2,3-triazole **6.30** (Scheme 3). Therefore, 1,2,3-trisubstituted triazole cannot be directly accessed from non-terminal acetylenes and azides. Secondly, substituents on the C5 of triazole ring are limited to aromatic groups (such as phenyl and benzyl). Direct substitution with a methyl group as in **6.27** and **6.28** (see Figure 9B) has not been explored.
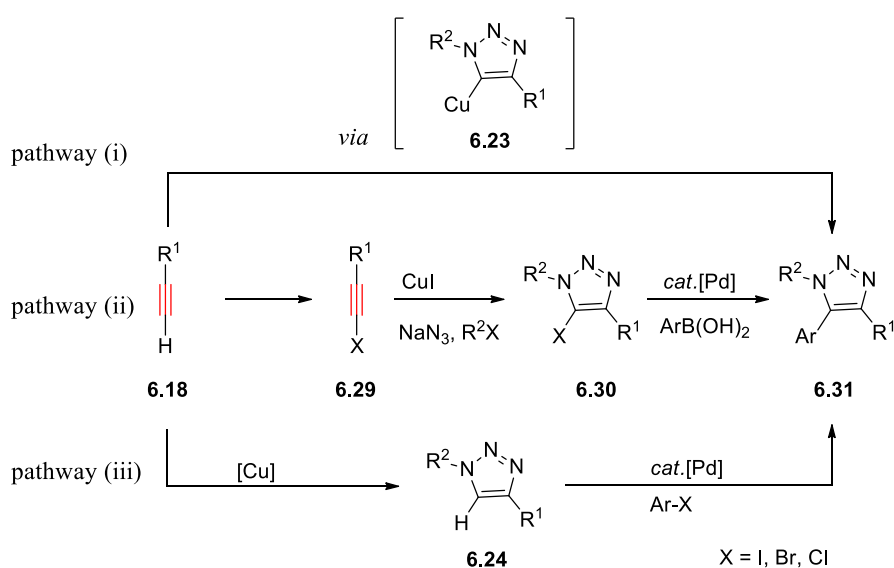
Scheme 3: Schematic summary of three approaches for catalytic syntheses of 1,4,5-trisubstituted 1,2,3-triazoles. (i) Interception of 5-cuprated 1,2,3-triazoles; (ii) Stoichiometrically functionalized acetylenes; (iii) catalytic C-H bond functionalizations.

Moreover, chapter 4 has discussed the regioselective synthesis of 1,4,5-trisubstituted 1,2,3-triazoles from functionalized acetylenes and organic azides (i.e. 1-iodoacetylene **4.02** reacted with azide **4.21** to give 5-iodo triazole **4.09** as shown below in Scheme 3). The proposed mechanistic pathway for such a synthesis is similar to that proposed for the CuAAC (Figure 9A), where CuI is involved to form the 5-cuprated 1,2,3-triazole **6.30** as the first key intermediate.[19,23] However, further functionalization of the 5-iodo substituent of **4.09** with palladium-catalysed cross-coupling and nucleophilic substitution reactions is problematic (see chapter 4 for detail discussion).
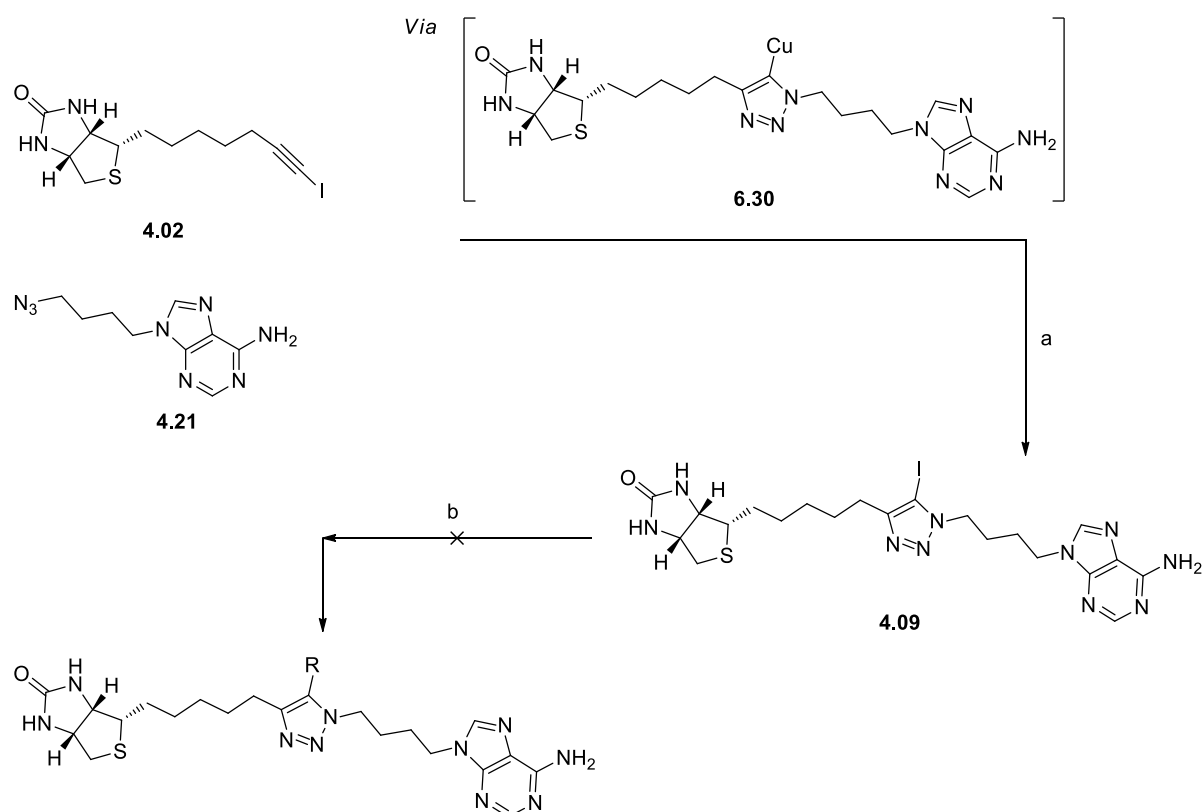
Scheme 4: a) THF, CuI, TEA, Rt; b) *cat.* [Pd], TEA, RB(OH)$_2$, THF, 60 $^\circ$C;

It is known that *in situ* click chemistry using *Sa*BPL can bypass the mechanism of CuAAC and produce 1,4-triazole without the need for an external catalyst. Thus, enzyme catalysed synthesis provides an unmet opportunity for the formation of 1,4,5-trisubstituted triazoles from non-terminal acetylenes. The experiments discussed in this section were designed to investigate enzyme promoted synthesis of 5-methylated 1,2,3-triazoles **6.27** and **6.28** from the adenine azide **4.21** and methylated biotin acetylenes **6.25** and **6.26** (Scheme 5).
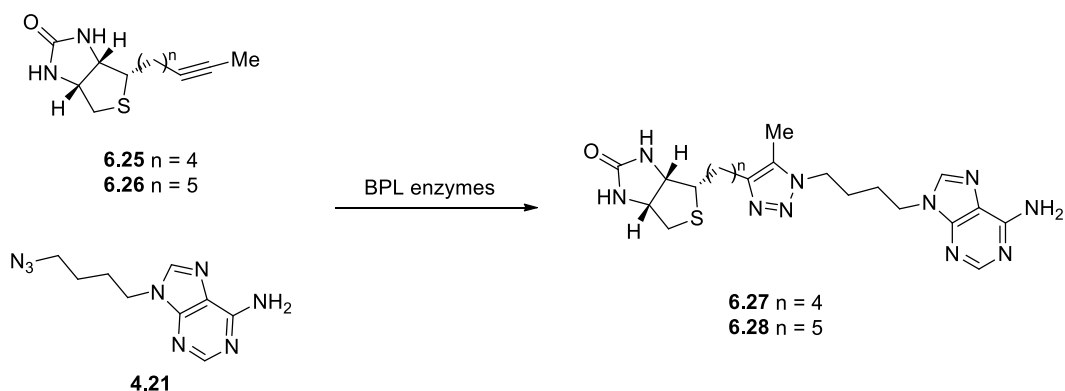
Scheme 5: *In situ* click reaction of acetylenes **6.25** and **6.26** with azide **4.21** using BPL enzymes (*Sa*BPL and *Sa*BPL-R122G).

Two acetylene-azide mixtures (**6.25-4.21** and **6.26-4.21**) were prepared using the general procedure described in section 6.2.1. An *in situ* click experiment was then performed for each mixture using either *Sa*BPL or *Sa*BPL-R122G. Three control experiments were run in parallel by treating each mixture with either BSA (2 µM), Cu$_2$SO$_4$ (5 µM), or water instead of BPL. All reaction mixtures were incubated at 37°C for 48 h prior to LC/HRMS analysis. The LC/HRMS traces of *in situ* reactions between biotin acetylene **6.25** and azide **2.26** are shown below (Figure 10).

Figure 10: LC/HRMS traces of reference compounds and *in situ* click produced triazole **6.27** at selective ion monitoring (M+H$^+$ = 471.2398 Da). (A) Product from *in situ* assembly in the presence of *Sa*BPL. (B) Product from *in situ* assembly in the presence of *Sa*BPL-R122G. (C) Control using BSA. (D) Controls (no enzyme). (E) Control using Cu$_2$SO$_4$ (5 µM).

A trace of triazole **6.27** was detected above background at 8.8 min by LC/HRMS for *in situ* click experiments using *Sa*BPL and *Sa*BPL-R122G (Figure 10A and 10B). It is known that triazole-based inhibitors require biotin and adenine moieties at positions 1 and 4 of the triazole ring to maintain appropriate geometry for active site binding.[11,12] Moreover, the *in situ* experiments discussed in section 6.2.1 and 6.2.3 demonstrate that only 1,4-disubstituted 1,2,3-triazoles (e.g. 5-proton-1,2,3-triazole) are formed using a BPL as catalyst. This suggests that triazole product formed on reaction of biotin acetylene **6.25** and azide **2.26** under *in situ* conditions, is likely the 5-methyl-1,2,3-triazole **6.27**, rather than the alternative 4-methyl-1,2,3-triazole isomer. As expected, control experiments in the absence of BPL and using BSA failed to give desired triazoles (Figure 10C and 10D). Importantly, the control experiment using Cu_2SO_4 as the catalyst also failed to give triazole **6.27** (Figure 10E). This result is consistent with the mechanism of CuAAC, as discussed above, where the non-terminal acetylene, such as **6.27**, does not participate in the copper catalysed cycloaddition. This is a very interesting preliminary observation and future investigations may include the synthesis of sufficient quantities of pure 5-methyl-1,2,3-triazole **6.27** and its subsequent characterization and biological assay.

6.3 Conclusion

In summary, this chapter describes the use of LC/HRMS as a sensitive and efficient approach for detecting the products of *in situ* click chemistry. Our previously reported *in situ* experiment between biotin acetylene **2.21** and adenine azide **4.21**[11] was repeated with LC/HRMS analysis of the resulting reaction mixtures. This allowed detection of *in situ* generated 1,4-triazole **1.22** using wild type *Sa*BPL rather than simply by using the more reactive leaky mutant enzyme (*Sa*BPL-R122G). Additionally, use of LC/HRMS distinguished between 1,4- and 1,5-regioisomer of triazoles allowing rapid identification of desired *in situ* products.

The *in situ* click chemistry was then applied to synthesise and screening of triazole analogues using a range of BPLs as catalysts, namely *Sa*BPL, *Mtb*BPL, *Ac*BPL, *Kp*BPL, and *Ca*BPL. The experiments were performed using biotin acetylene **2.21** and a library of azides **3.03k**, **3.03t**, and **6.02-6.08**. Of these, biotin acetylene **2.21** and azide **6.04** reacted to give 1,4-triazole **6.11** in the presence of *Sa*BPL. Triazole **6.11** was then independently synthesised and assayed against all five BPLs to reveal that it was only active against *Sa*BPL with $K_i =$ 0.5 µM. This further supports the use of an *in situ* click approach for screening libraries of potential triazole analogues from fragments of azides and acetylenes. Importantly, preliminary success in the production of 5-methyl-1,2,3-triazole **6.27** using *Sa*BPL and its mutant *Sa*BPL-R122G highlight that *in situ* click chemistry was capable of catalysing unusual cycloaddition reactions from non-terminal acetylenes, whilst such reactions were mechanistically difficult to proceed with traditional CuAAC. Future investigations are required to synthesise the authentic sample of 5-methyl-1,2,3-triazole **6.27** and assay its inhibitory activity.

6.4   References for Chapter Six

(1)   Erlanson, D. A. *Current Opinion in Biotechnology* **2006**, *17*, 643-52.

(2)   Daniel A. Erlanson , R. S. M., and Tom O'Brien *Journal of Medicinal Chemistry* **2004**, *47*, 3463-3482.

(3)   Moses, H.; Dorsey, E. R.; Matheson, D. H.; Thier, S. O. *Jama* **2005**, *294*, 1333-1342.

(4)   Erlanson, D. A.; Hansen, S. K. *Current Opinion in Biotechnology* **2004**, *8*, 399-406.

(5)   Ciulli, A.; Abell, C. *Current Opinion in Biotechnology* **2007**, *18*, 489-496.

(6)   Inglese, J.; Benkovic, S. J. *Tetrahedron* **1991**, *47*, 2351-2364.

(7)   Boger, D. L.; Haynes, N.-E.; Kitos, P. A.; Warren, M. S.; Ramcharan, J.; Marolewski, A. E.; Benkovic, S. J. *Bioorganic & Medicinal Chemistry* **1997**, *5*, 1817-1830.

(8)   Nguyen, R.; Huc, I. *Angewandte Chemie International Edition* **2001**, *40*, 1774-1776.

(9)   Kolb, H. C.; Finn, M. G.; Sharpless, K. B. *Angewandte Chemie International Edition* **2001**, *40*, 2004-2021.

(10)   Huisgen, R.; Szeimies, G.; Moebius, L. *Chemische Berichte* **1967**, *100*, 2494-2507.

(11)   Tieu, W.; da Costa, T. P. S.; Yap, M. Y.; Keeling, K. L.; Wilce, M. C.; Wallace, J. C.; Booker, G. W.; Polyak, S. W.; Abell, A. D. *Chemical Science* **2013**, *4*, 3533-3537.

(12)   Soares da Costa, T. P.; Tieu, W.; Yap, M. Y.; Pendini, N. R.; Polyak, S. W.; Sejer Pedersen, D.; Morona, R.; Turnidge, J. D.; Wallace, J. C.; Wilce, M. C.; Booker, G. W.; Abell, A. D. *Journal of Biological Chemistry* **2012**, *287*, 17823-32.

(13)   Krasiński, A.; Radić, Z.; Manetsch, R.; Raushel, J.; Taylor, P.; Sharpless, K. B.; Kolb, H. C. *Journal of the American Chemical Society* **2005**, *127*, 6686-6692.

(14)   Manetsch, R.; Krasinski, A.; Radic, Z.; Raushel, J.; Taylor, P.; Sharpless, K. B.; Kolb, H. C. *Journal of the American Chemical Society* **2004**, *126*, 12809-12818.

(15)   Sharpless, K. B.; Manetsch, R. *Expert Opinion on Drug Discovery* **2006**, *1*, 525-538.

(16)   Chapman-Smith, A.; Cronan, J. E. *Trends in Biochemical Sciences* **1999**, *24*, 359-363.

_____

(17)   Himo, F.; Lovell, T.; Hilgraf, R.; Rostovtsev, V. V.; Noodleman, L.; Sharpless, K. B.; Fokin, V. V. *Journal of the American Chemical Society* **2005**, *127*, 210-216.

(18)   Deng, J.; Wu, Y.-M.; Chen, Q.-Y. *Synthesis* **2005**, 2730-2738.

(19)   Hein, J. E.; Tripp, J. C.; Krasnova, L. B.; Sharpless, K. B.; Fokin, V. V. *Angewandte Chemie International Edition* **2009**, *48*, 8018-21.

(20)   Worrell, B. T.; Hein, J. E.; Fokin, V. V. *Angewandte Chemie International Edition* **2012**, *51*, 11791-4.

(21)   Do, H.-Q.; Daugulis, O. *Journal of the American Chemical Society* **2007**, *129*, 12404-12405.

(22)   Chuprakov, S.; Chernyak, N.; Dudnik, A. S.; Gevorgyan, V. *Organic Letters* **2007**, *9*, 2333-2336.

(23)   Buckley, B. R.; Dann, S. E.; Heaney, H. *Chemistry–A European Journal* **2010**, *16*, 6278-6284.

7.1   General methods

All reagents were obtained from commercial sources and are of reagent grade or as specified. Solvents were also obtained from commercial sources, except for anhydrous THF, anhydrous DCM and anhydrous DMF which were dried over solvent purifier (PS-Micro, Innovative Technology, USA). Reactions were monitored by TLC using precoated plates (silica gel 60 F254, 250 μm, Merck, Darmstadt, Germany), spots were visualised under ultraviolet light at 254 nm and with either sulfuric acid-vanillin spray, potassium permanganate dip or Hanessian's stain. Column chromatography was performed with silica gel (40-63 μm 60 Å, Davisil, Grace, Germany). HPLC was performed on HP Series 1100 with Phenomenex Gemini C18 5 μM (250 x 4.60 mm) for Analytical HPLC and Phenomenex Luna C18 10 μM (50 x 10.00 mm) for Semi-preparative HPLC. Microwave reactions were performed on a CEM Discovery SP with external IR temperature monitoring. Reactions were stirred for 5 min in a sealed container at ambient temperature, followed by 5 min stirring with increased microwave power until the prescribed temperature was reached. Both power and pressure were kept variable. ^{1}H and ^{13}C NMR spectra were recorded on a Varian Inova 500 MHz or a Varian Inova 600 MHz. Chemical shifts are given in ppm (δ) relative to the residue signals, which in the case of DMSO-d_6 were 2.55 ppm for ^{1}H and 39.55 ppm for ^{13}C, CDCl$_3$ were 7.26 ppm for 1H and 77.23 ppm for 13C and D$_2$O was 4.79 for 1H. Structural assignment was confirmed with COSY, ROESY, HMQC and HMBC. Nomenclature describing proton assignment for biotin and triazole containing compounds are shown in Figure 1. Mixtures of isomers are designated A and B in NMR spectra without individual assignment. Partial integrals are also reported for each isomer. High-resolution mass spectra (HRMS) were recorded on an Agilent 6230 time of flight (TOF) liquid chromatography mass spectra (LC/MS) (Δ < 5 ppm).
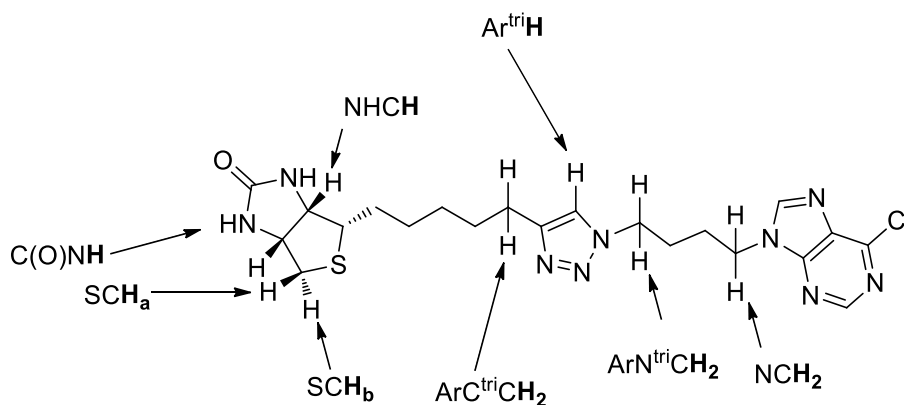
Figure 1: Nomenclature describing proton assignment for biotin and triazole containing compounds as depicted in representative example **2.36.**

7.2   Docking studies

The docking experiments were performed by using the software AutoDockTools 1.5.6 and the binding affinities were predicted. All molecules were drawn using ChemBio3D Ultra 12.0 with energy minimized before loading to the AutoDockTools. The protein for docking was taken form RCSB protein data bank: *Staphylococcus aureus* 3V7S. The original bound ligand was removed and all water molecules were also removed from the original Protein Data Bank file. Grid map in AutoDock was generated from the coordinates of 3V7S ligand, expanded by 5 Å in all directions and equally spaced at 0.375 Å. Docking was performed using the Lamarkian genetic algorithm. Each docking experiment was performed 10 times, yielding 10 docked conformations. Parameters for the docking are as follows: population size of 150; random starting position and conformation; simulations were performed with a maximum of 250,000 energy evaluations and a maximum of 27,000 generations. Final docked conformations were ranked by binding energy and the most similar conformation was selected to compare and overlay with the original bound ligand.

7.3   General procedures

General procedure A1: CuAAC Method 1

To a solution of the azide (1.0 equiv) and alkyne (1.0 equiv) in acetonitrile (1 ml per 100 mg of alkyne) and de-ionised water (0.5 ml per 100 mg of alkyne) was added copper nano powder (0.2 equiv), and the mixture was sonicated for 15 min followed by stirring at ambient temperature for 4 h. The reaction mixture was concentrated *in vacuo* and the residue was purified by column chromatography on silica gel. See individual experiments for details.

General procedure A2: CuAAC Method 2

To a suspension of azide (1.0 equiv) and alkyne (1.0 equiv) in DMSO and water (1:1, 1 ml per 100 mg of alkyne) were added a solution of $Cu_2SO_4.5H_2O$ (0.15 equiv) and sodium ascorbate (0.3 equiv) in water (1 ml per 100 mg of sodium ascorbate) and stirred at ambient temperature for 4 h. The reaction mixture was concentrated *in vacuo* and the resulting residue was purified by column chromatography on silica gel. See individual experiments for details.

General procedure B1: Alkylation of aryl amines and aryl alcohol

To a solution of the alcohol or amine (1.0 equiv) in dry DMF (1 ml per 100 mg of alcohol/amine) was added potassium carbonate (1.5 equiv) and stirred at 50 ºC for 30 min, followed by addition of the alkyl dihalide (1.5 equiv) and stirred at 50 ºC for 12 h under nitrogen atmosphere. The reaction mixture was diluted with DCM and washed with 0.5 M aqueous HCl, aqueous saturated Na_2SO_4, water and brine, dried over $NaSO_4$, filtered, concentrated *in vacuo* and the residue was purified by column chromatography on silica gel. See individual experiments for details.

General procedure B2: Preparation of alkyl azide

To a solution of the bromide (1.0 equiv) in dry DMF (1 ml per 100 mg of bromide) was added sodium azide (1.2 equiv) and the mixture was stirred for 12 h under nitrogen atmosphere. The reaction mixture was diluted with DCM and washed with water and brine, dried over $NaSO_4$, filtered, concentrated *in vacuo* and the residue was purified by column chromatography on silica gel. See individual experiments for details.

General procedure C1: Preparation of benzyl azide Method 1

A solution of the corresponding benzyl alcohol (1 equiv.), triphenylphosphine (1.2 equiv.)

and sodium azide (1.2 equiv) in 1:4 CCl4/DMF (1 mL/50mg) was stirred at 60ºC for overnight. The reaction mixture was diluted with ethyl acetate and washed with water and brine. The organic layer was gently concentrated. The residue was dissolved in diethyl ether and filtered to remove the P(O)Ph3. The filtrate was concentrated *in vacuo* and the residue was used in the next step without further purification.

General procedure C2: Preparation of benzyl azide Method 2

A solution of the corresponding halide (1 equiv.) and sodium azide (1.2 equiv.) in DMF (1 mL/50mg) was stirred under nitrogen at ambient temperature overnight. The reaction mixture was diluted with ethyl acetate and washed with water and brine. The organic layer was dried over sodium sulfate, filtered and concentrated *in vacuo.* The residue was used in the next step without further purification.

General Procedure D: Synthesis of 5-Iodo-1,2,3-triazoles

To a solution of 1-iodoalkyne (1.0 euiqv) and azide (1.0 equiv) in dry DMF (1 ml per 10 mg of 1-iodoalkyne) was added CuI (0.05 equiv) and TEA (2.0 equiv) and the mixture was stirred at ambient temperature for 12 h. The volatiles were removed under reduced pressure and the resulting residue was purified by column chromatography on silica gel. See individual experiments for details.

General Procedure E: Halogen exchange of 5-Iodo-1,2,3-triazole

To a 5 ml round-bottomed microwave vial was added a solution of 5-iodo-1,2,3-triazole (1.0 equiv) in acetonitrile (1 ml per 100 mg of triazole) and de-ionised water (1 ml per 100 mg of triazole) and potassium halide (5.0 equiv). The vial was placed into the microwave reactor set at a pressure of 250 psi and heated at 180 ºC for 10 min. After the vial was cooled to room temperature, the mixture was concentrated *in vacuo* and the residue was purified by column chromatography on silica gel. See individual experiments for details.

General Procedure F: Preparation of sulfonamide

To a suspension of sulfonyl amine (1.0 equiv) in dry DMF (0.5 ml per 100 mg of sulfonyl amine) was added CsCO3 (1.2 equiv) and biotin succinimide **5.07** (1.1 equiv). The reaction mixture was stirred at ambient temperature for 12 h. The solvent was then removed under reduced pressure and the residue was purified by flash chromatography on silica. See individual experiments for details.

General Procedure G: Removal of Boc group

To a solution of boc-protected sulfamoylcarbamate (1.0 equiv) in DCM (1 ml per 100 mg of sulfamoylcarbamate) at 0 °C was added trifluoroacetic acid (9.0 equiv) and allowed to stir at room temperature for 2 h. Trifluoroacetic acid (9.0 equiv) was then added and the reaction was stirred at room temperature for 12 h. The solvent removal under reduced pressure gave crude product which was used without purification or purified by flash chromatography on silica. See individual experiments for details.

General Procedure H: Preparation of boc-protected sulfamoylcarbamate

To a solution of amine (1.0 equiv) in DCM (1 ml per 100 mg of amine) was added TEA (2.0 equiv), followed by addition of sulfamoylating agent **5.21** (1.0 equiv). The reaction mixture was stirred at room temperature for 12 h. The solvent removal under reduced pressure gave the crude material which was purified by flash chromatography on silica. See individual experiments for details.

General procedure I: LC/MS analysis of *in situ* reactions

Aliquots of each reaction (50 µL) were diluted with a stock solution of 0.1% TFA in acetonitrile (50 µL). Samples of the diluted reaction mixtures (10 µL) was separately injected into the LC/MS system, and the analytes were fractionated using the Poroshell 120 EC-C18 reverse phase column (dimensions 2.1 mm x 50 mm), using eluents A (0.1% TFA in water) and B (0.08% TFA in acetonitrile) at a flow rate of 0.3 mL/min. The gradient increased from 2% acetonitrile to 98% acetonitrile over 20 min and this was followed by 100% acetonitrile wash for 5 min. The mass spectroscopy detector was tuned to the positive mode with selective ion monitoring of the target molecule. The presence of the *in situ* product was identified by the retention time and molecular weights (Δ <5 ppm).

7.4 Experimental work as described in Chapter 2

5-methyl-3-((*E*)-4-(4-(5-((3a*S*,4*S*,6a*R*)-2-oxohexahydro-1*H*-thieno[3,4-*d*]imidazol-4-yl)pentyl)-1*H*-1,2,3-triazol-1-yl)but-2-en-1-yl)benzo[*d*]oxazol-2(3*H*)-one 2.05
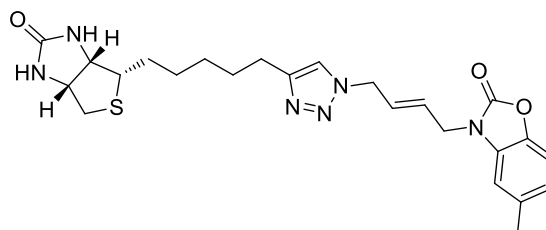
Biotin acetylene **2.21** (30 mg, 0.13 mmol) was reacted with azide **2.13** (32 mg, 0.13 mmol) and Cu nanopowder (2 mg, 0.026 mmol) using General Procedure **A1**. The crude material was purified by flash chromatography on silica gel eluting with 3% MeOH in DCM to give a crystalline white solid (47 mg, 75%).

¹H NMR (300 MHz; CDCl$_3$): δ 7.29 (1H, s, Ar^{tri}**H**), 7.09 (1H, d, *J* = 7.8 Hz, Ar**H**), 6.92 (1H, d, *J* = 8.4 Hz, Ar**H**), 6.74 (1H, s, Ar**H**), 5.91 (1H, m, C**H**), 5.81 (1H, m, C**H**), 5.62 (1H, bs, N**H**), 5.22 (1H, bs, N**H**), 4.96 (2H, d, *J* = 5.7 Hz, NC**H₂**), 4.49-4.53 (1H, m, NHC**H**), 4.54 (2H, d, *J* = 5.4 Hz, ArN^{tri}C**H₂**), 4.29-4.33 (1H, m, NHC**H**), 3.15-3.16 (1H, m, SC**H**), 2.89 (1H, dd, *J* = 5.1, 12.6 Hz, SC**Hₐ**), 2.67-2.75 (3H, m, SC**H_b**, ArC^{tri}C**H₂**), 2.38 (3H, s, ArC**H₃**), 1.33-1.76 (8H, m, 4 x C**H₂**);

¹³C NMR (125 MHz; CDCl$_3$): δ 164.0, 155.8, 147.8, 140.6, 134.3, 131.1, 123.2, 122.7, 109.7, 109.6, 61.8, 60.0, 55.5, 49.9, 49.7, 49.6, 40.4, 28.5, 28.4, 28.3, 28.2, 24.9, 24.8, 21.5;

HRMS calcd. for (M + H$^+$) C$_{24}$H$_{31}$N$_6$O$_3$S: requires 483.2178, found 483.2175

HPLC R$_t$ = 15.4 min

3-((2*R/S*,3*R/S*)-2,3-dihydroxy-4-(4-(5-((3a*S*,4*S*,6a*R*)-2-oxohexahydro-1*H*-thieno[3,4-*d*]imidazol-4-yl)pentyl)-1*H*-1,2,3-triazol-1-yl)butyl)-5-methylbenzo[*d*]oxazol-2(3*H*)-one 2.06a and 2.06b
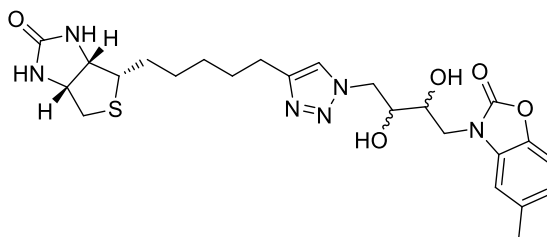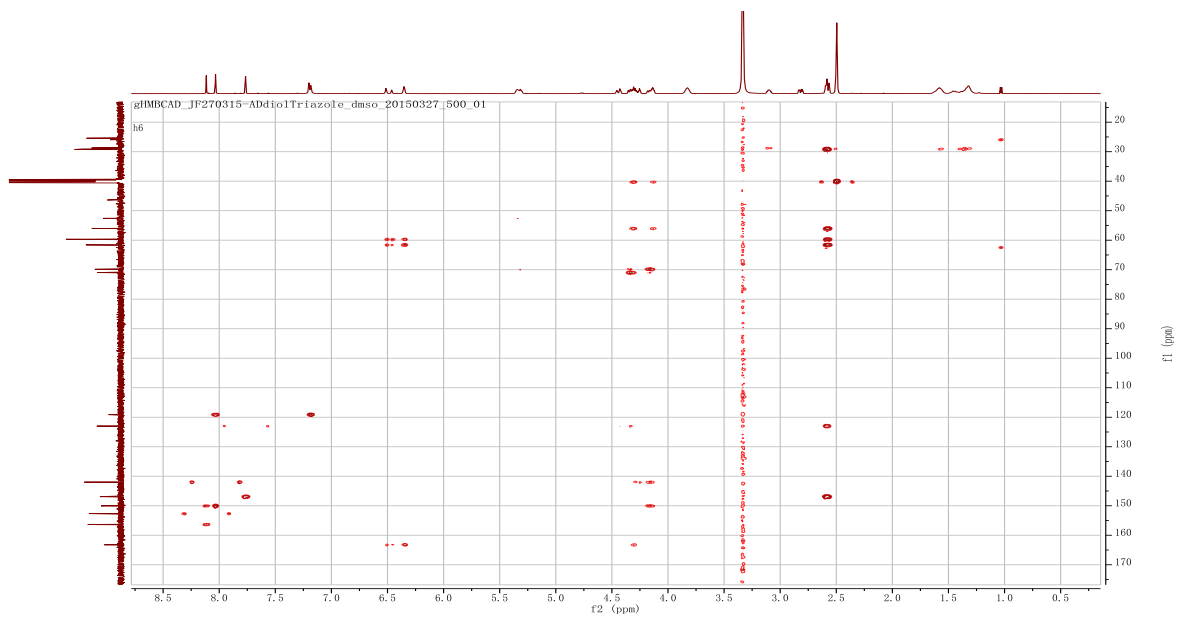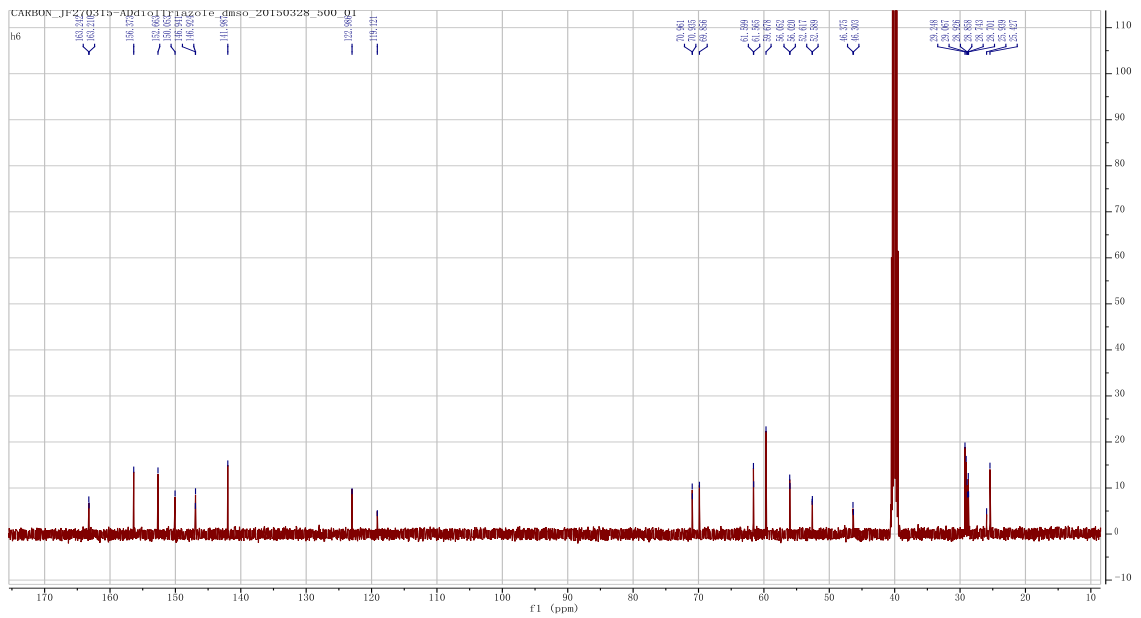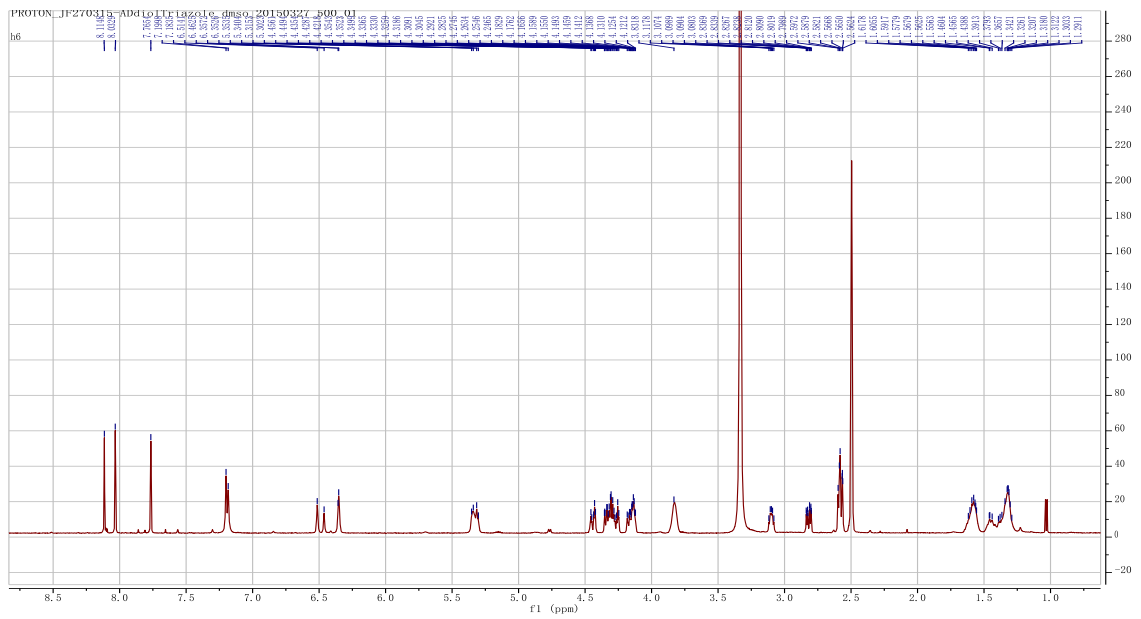

Biotin acetylene **2.21** (30 mg, 0.13 mmol) was reacted with azide **2.14** (36 mg, 0.13 mmol) and Cu nanopowder (2 mg, 0.026 mmol) using General Procedure **A1**. The crude material was purified by flash chromatography on silica gel eluting with 5% MeOH in DCM to give a crystalline white solid (22 mg, 33%).

¹H NMR (500 MHz, CDCl₃): δ 7.76 (1H, s, Ar^tri**H**), 7.17 (1H, d, *J* = 8.1 Hz, Ar**H**), 7.08 (1H, s, Ar**H**), 6.70 (1H, d, *J* = 8.2 Hz, Ar**H**), 6.70 (1H, bs, N**H**), 6.33 (1H, bs, N**H**), 5.27-5.28 (1H, m, O**H**), 5.22 (1H, d, *J* = 6.9 Hz, O**H**), 4.46 (1H, dd, *J* = 3.6, 13.9 Hz, NC**H₂ₐ**), 4.27-4.34 (2H, m, NHC**H**, NC**H₂ᵦ**), 4.10-4.13 (1H, m, NHC**H**), 3.80-3.90 (4H, m, 2 x OHC**H**, ArN^tri**CH₂**), 3.07-3.11 (1H, m, SC**H**), 2.80 (1H, dd, *J* = 5.0, 12.8 Hz, SC**Hₐ**), 2.55-2.60 (3H, m, SC**Hᵦ**, ArC^tri**CH₂**), 2.33 (3H, s, ArC**H₃**), 1.43-1.62 (4H, m, 2 x C**H₂**), 1.30-1.38 (4H, m, 2 x C**H₂**);

¹³C NMR (125 MHz, CDCl₃)**:** δ 163.9, 155.8, 147.8, 140.5, 134.2, 131.2, 123.1, 122.6, 109.6, 109.5, 70.2 (isomer a/b), 68.8, 62.0, 60.0, 55.6, 52.8 (isomer a/b), 44.8, 40.2, 28.8, 28.7 (isomer a/b), 58.6, 28.3, 25.0 (isomer a/b), 21.3.

HRMS calcd. for (M + H⁺) C₂₄H₃₃N₆O₅S: requires 517.2233, found 517.2223.

HPLC R_t = 14.2 min
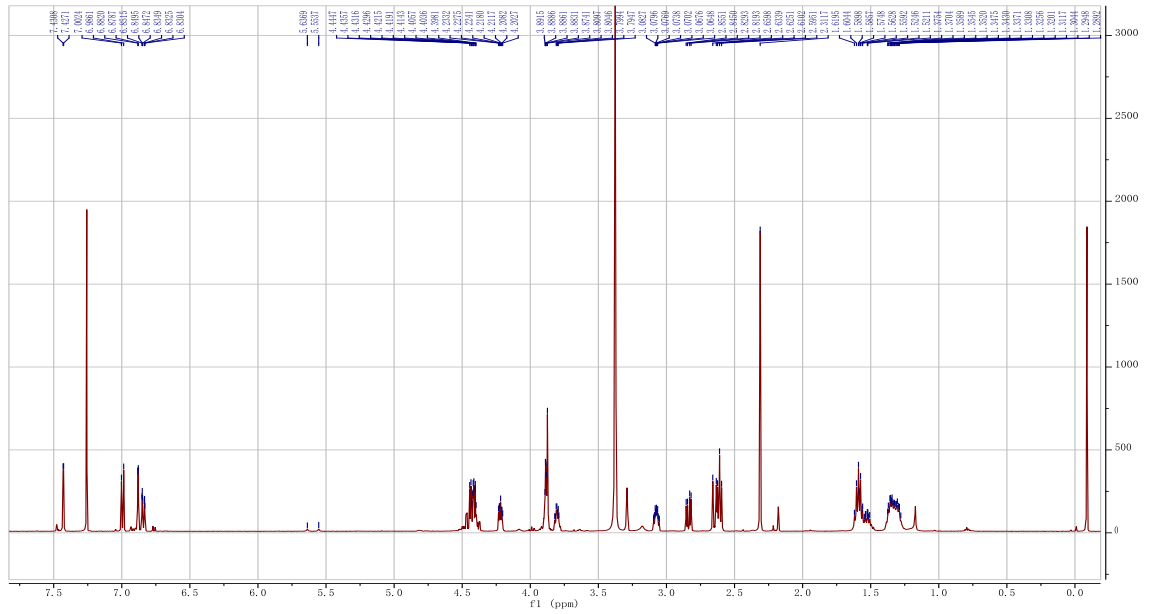
3-((((4S/R,5S/R)-2,2-dimethyl-5-((4-(5-((3aS,4S,6aR)-2-oxohexahydro-1H-thieno[3,4-d]imidazol-4-yl)pentyl)-1H-1,2,3-triazol-1-yl)methyl)-1,3-dioxolan-4-yl)methyl)-5-methylbenzo[d]oxazol-2(3H)-one 2.07a and 2.07b
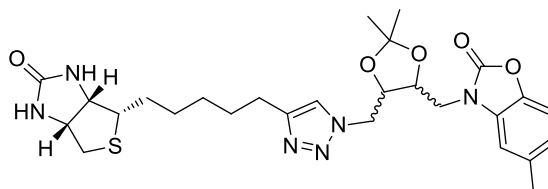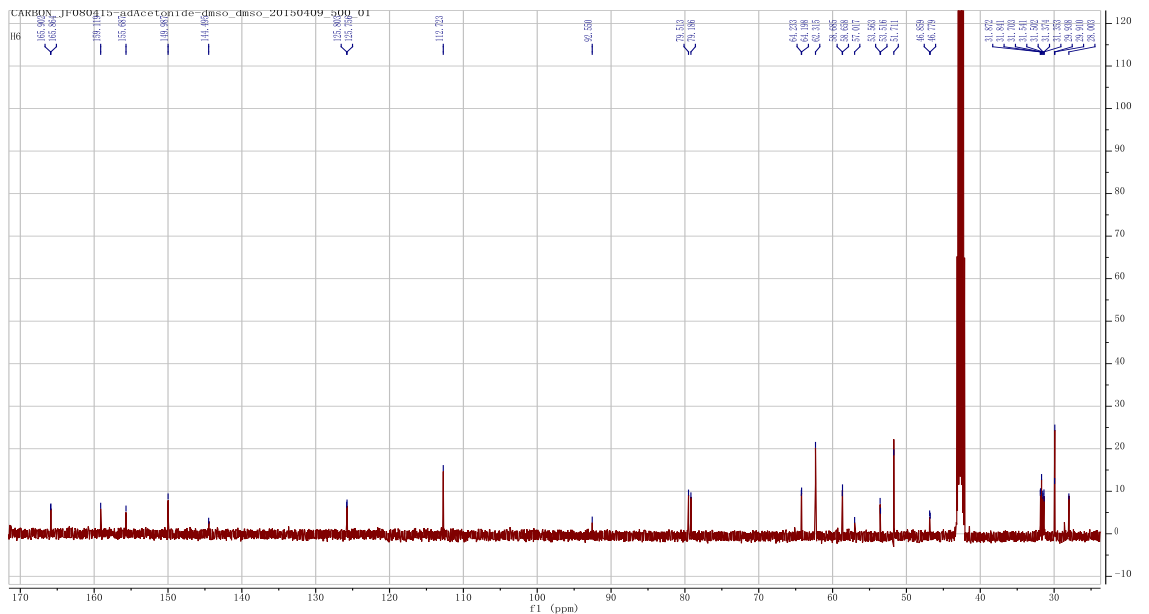

Biotin acetylene **2.21** (30 mg, 0.13 mmol) was reacted with azide **2.15** (41 mg, 0.09 mmol) and Cu nanopowder (2 mg, 0.026 mmol) using General Procedure **A1**. The crude material was purified by flash chromatography on silica gel eluting with 3% MeOH in DCM to give a crystalline white solid (31 mg, 43%).

^{1}H NMR (500 MHz; CDCl$_3$): δ 7.46 (1H, s, Ar^{tri}**H**), 7.06 (1H, d, J = 8.1 Hz, Ar**H**), 6.94 (1H, s, Ar**H**), 6.90 (1H, d, J = 8.2 Hz, Ar**H**), 5.54 (1H, bs, N**H**), 5.16 (1H, bs, N**H**), 4.71 (1H, dd, J = 4.4, 14.7 Hz, NC**H$_{2a}$**), 4.58 (1H, dd, J = 4.1, 14.7, NC**H$_{2b}$**), 4.49-4.52 (1H, m, OC**H**), 4.29-4.32 (1H, m, OC**H**), 4.14-4.17 (1H, m, NHC**H**), 4.00-4.04 (2H, m, NHC**H**, ArN^{tri}C**H$_{2a}$**), 3.92 (1H, dd, J = 4.9, 15.9 Hz, ArN^{tri}C**H$_{2b}$**), 3.13-3.17 (1H, m, SC**H**), 2.92 (1H, dd, J = 5.0, 12.8 Hz, SC**H$_a$**), 2.70-2.70 (3H, m, SC**H$_b$**, ArC^{tri}C**H$_2$**), 2.39 (3H, s, ArC**H$_3$**), 1.62-1.70 (4H, m, 2 x C**H$_2$**), 1.39-1.47 (4H, m, 2 x C**H$_2$**), 1.22 (3H, s, CC**H$_3$**), 1.19 (3H, s, CC**H$_3$**);

^{13}C NMR (125 MHz; CDCl$_3$): δ 163.4, 155.5, 148.3, 140.6, 133.9, 131.5, 123.1, 122.6, 110.4, 110.1, 109.4, 76.1 (isomer a/b), 75.8, 62.0, 60.1, 55.7 (isomer a/b), 50.8, 50.1, 42.8, 40.5, 29.0, 28.7, 28.5, 26.7 (isomer a/b), 25.5 (isomer a/b), 21.5.

HRMS calcd. for (M + H$^+$) C$_{21}$H$_{29}$ClN$_9$OS: requires 490.1904, found 490.1904

HPLC R$_t$ = 13.3 min
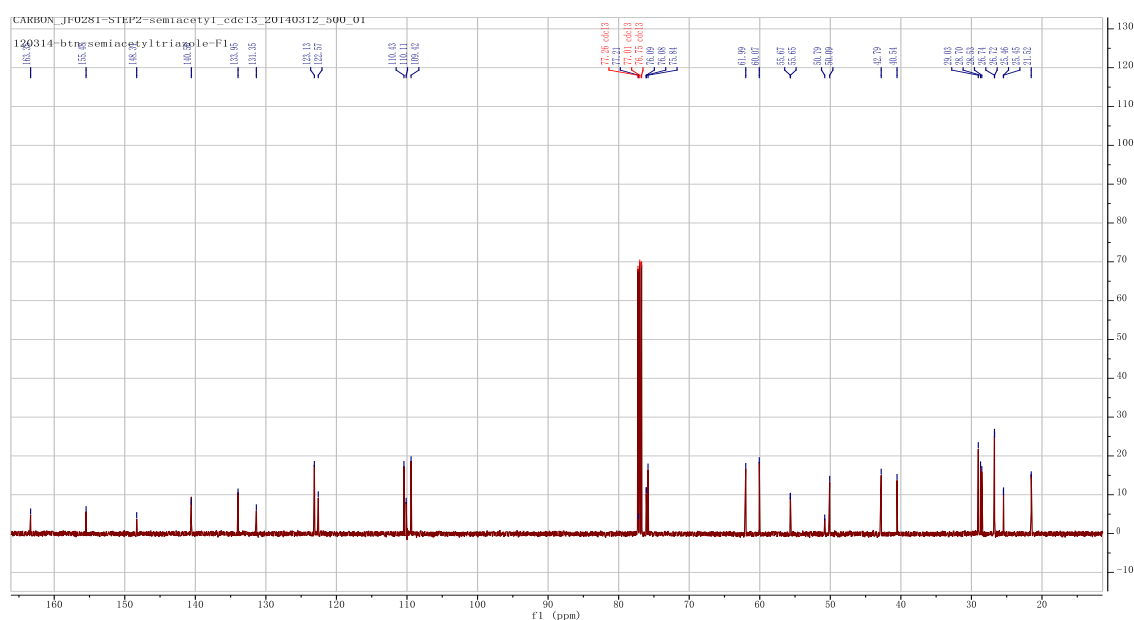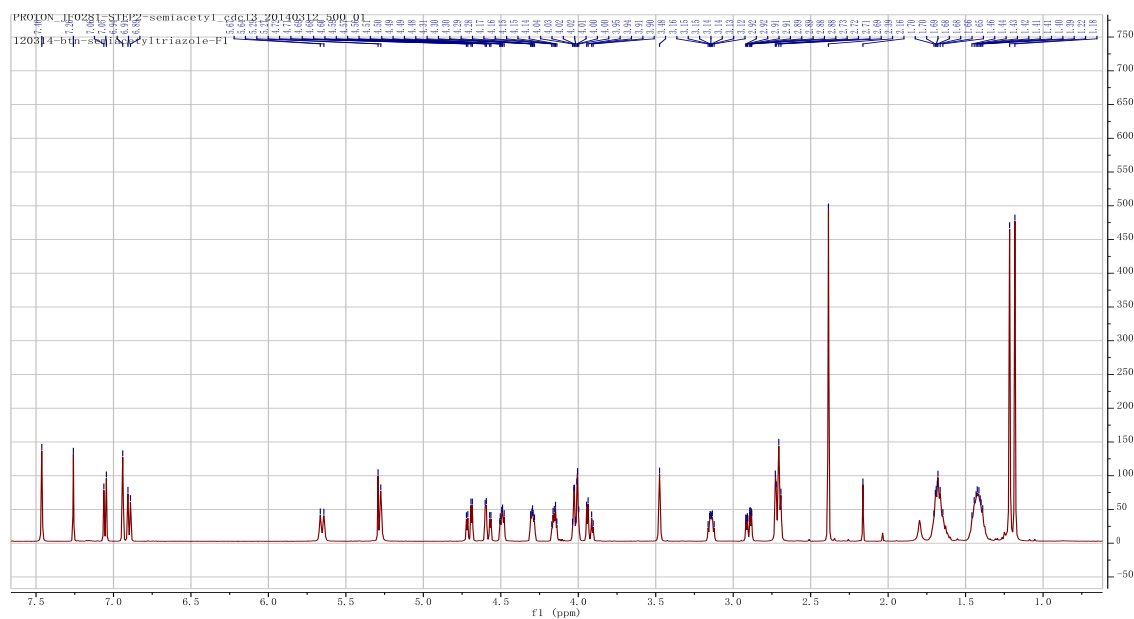
5-methyl-3-((2-(4-(5-((3a*S*,4*S*,6a*R*)-2-oxohexahydro-1*H*-thieno[3,4-*d*]imidazol-4-yl)pentyl)-1*H*-1,2,3-triazol-1-yl)ethoxy)methyl)benzo[*d*]oxazol-2(3*H*)-one 2.08
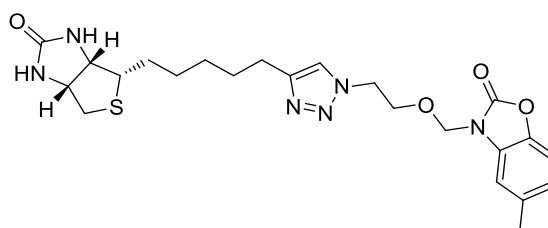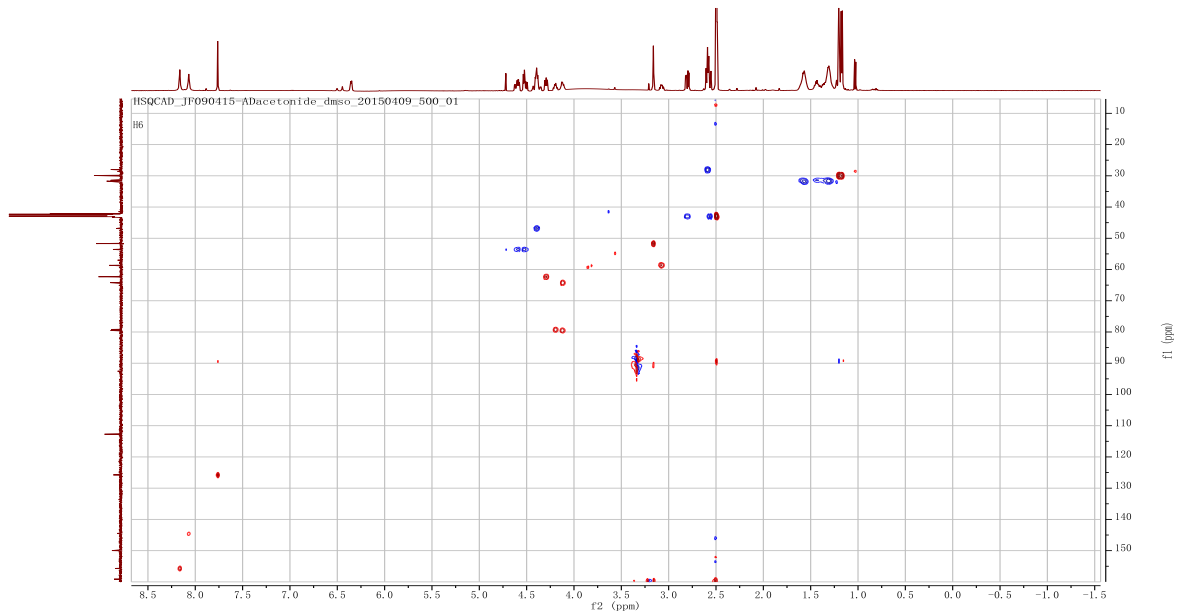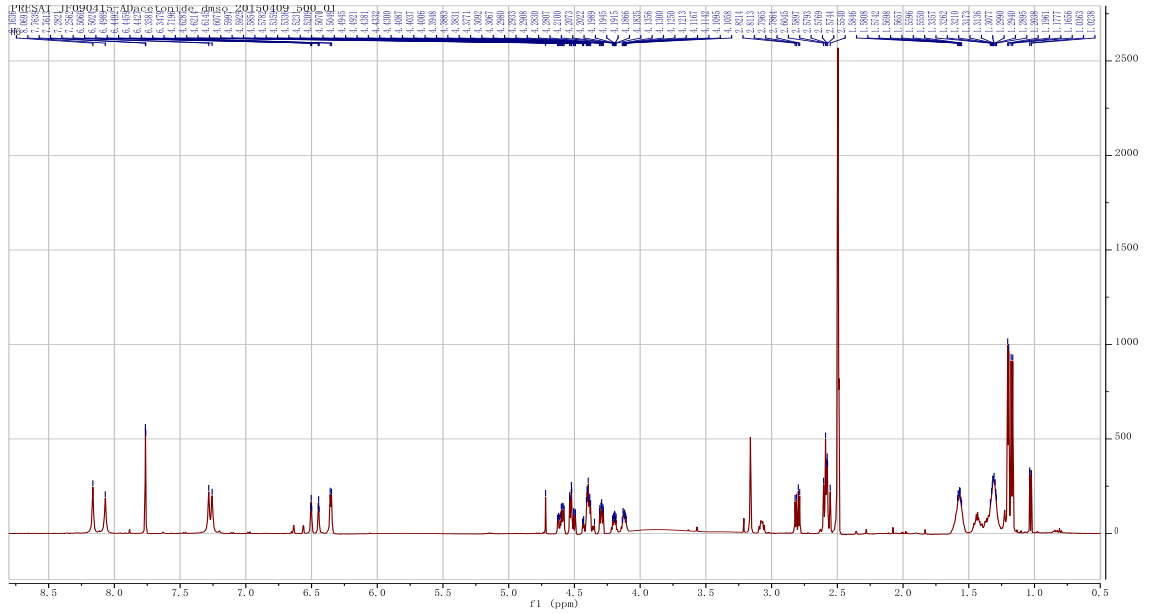

Biotin acetylene **2.21** (24 mg, 0.10 mmol) was reacted with azide **2.16** (25 mg, 0.10 mmol) and Cu nanopowder (2 mg, 0.026 mmol) using General Procedure **A1**. The crude material

was purified by flash chromatography on silica gel eluting with 3% MeOH in DCM to give a crystalline white solid (37 mg, 77%).

^{1}H NMR (500 MHz, CDCl$_3$): δ 7.32 (1H, s, Ar^{tri}**H**), 7.09 (1H, d, *J* = 8.2 Hz, Ar**H**), 6.94-6.96 (1H, m, Ar**H**), 6.86 (1H, s, Ar**H**), 5.41 (1H, bs, N**H**), 5.24 (2H, s, NC**H$_2$**), 5.07 (1H, bs, N**H**), 4.50 (3H, m, OC**H$_2$**, NHC**H**), 4.29-4.32 (1H, m, NHC**H**), 3.97 (2H, t, *J* = 5.1 Hz, ArN^{tri}C**H$_2$**), 3.14-3.17 (1H, m, SC**H**), 2.90-2.93 (1H, dd, *J* = 4.8, 12.6 Hz, SC**H$_a$**), 2.73 (1H, d, *J* = 12.8, SC**H$_b$**), 2.64 (2H, t, *J* = 7.6 Hz, ArC^{tri}C**H$_2$**), 2.39 (3H, s, ArC**H$_3$**), 1.61-1.71 (4H, m, 2 x C**H$_2$**), 1.36-1.47 (4H, m, 2 x C**H$_2$**);

^{13}C NMR (125 MHz, CDCl$_3$): δ 163.1, 154.7, 148.2, 140.5, 134.3, 129.7, 123.8, 121.3, 109.9, 109.5, 72.4, 67.6, 62.0, 60.1, 55.6, 49.6, 40.5, 29.1, 29.0, 28.7, 28.6, 25.4;

HRMS calcd. for (M + Na$^+$) C$_{23}$H$_{30}$N$_6$NaO$_4$S: requires 509.1947, found 509.1938.

HPLC R$_t$ = 12.5 min

(3a*S*,4*S*,6a*R*)-4-(5-(1-((*E*)-4-(6-amino-9*H*-purin-9-yl)but-2-en-1-yl)-1*H*-1,2,3-triazol-4-yl)pentyl)tetrahydro-1*H*-thieno[3,4-*d*]imidazol-2(3*H*)-one 2.09
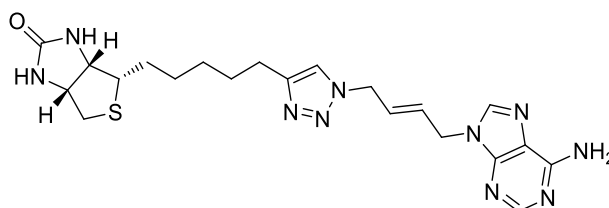
Biotin acetylene **2.21** (30 mg, 0.13 mmol) was reacted with azide **2.17** (30 mg, 0.13 mmol) and Cu nanopowder (2 mg, 0.026 mmol) using General Procedure **A1**. The crude material was purified by flash chromatography on silica gel eluting with 5% MeOH in DCM to give a crystalline white solid (33 mg, 53%).

^{1}H NMR (500 MHz; CDCl$_3$): δ 8.12 (1H, s, Ar**H**), 8.10 (1H, s, Ar**H**), 7.76 (1H, s, Ar^{tri}**H**), 7.26 (2H, bs, N**H$_2$**), 6.56 (1H, bs, N**H**), 6.37 (1H, bs, N**H**), 5.84-5.90 (1H, m, C**H**), 5.72-5.78 (1H, m, C**H**), 4.93-4.94 (2H, m, NC**H$_2$**), 4.78-4.80 (2H, m, ArN^{tri}C**H$_2$**), 4.29-4.32 (1H, m, NHC**H**), 4.12-4.15 (1H, m, NHC**H**), 3.07-3.11 (1H, m, SC**H**), 2.81 (1H, dd, *J* = 5.1, 12.4 Hz, SC**H$_b$**), 2.56-2.59 (3H, m, SC**H$_a$**, ArC^{tri}C**H$_2$**), 1.40-1.63 (4H, m, 2 x C**H$_2$**), 1.22-1.38 (4H, m, 2 x C**H$_2$**);

^{13}C NMR (125 MHz; DMSO-d6): 165.9, 159.1, 155.6, 152.4, 150.1, 143.7, 132.4, 130.7, 124.8, 64.3, 62.3, 58.7, 53.3, 46.9, 31.9, 31.7, 31.6, 31.4, 28.1;

HRMS calcd. for (M + H$^+$) $C_{21}H_{29}N_{10}OS$: requires 469.2247, found 469.2246

HPLC R_t = 12.3 min

(3aS,4S,6aR)-4-(5-(1-(4-(6-amino-9H-purin-9-yl)-(2R/S,3R/S)-dihydroxybutyl)-1H-1,2,3-triazol-4-yl)pentyl)tetrahydro-1H-thieno[3,4-d]imidazol-2(3H)-one 2.10a and 2.10b
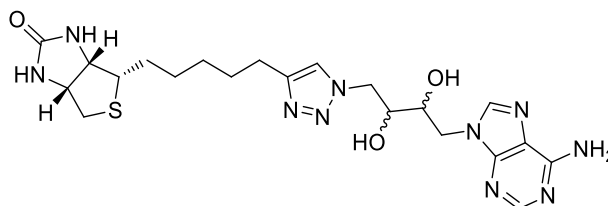
Biotin acetylene **2.21** (30 mg, 0.13 mmol) was reacted with azide **2.18** (34 mg, 0.13 mmol) and Cu nanopowder (2 mg, 0.026 mmol) using General Procedure **A1**. The crude material was purified by flash chromatography on silica gel eluting with 10% MeOH in DCM to give a crystalline white solid (21 mg, 32%).

¹H NMR (500 MHz; CDCl₃): δ 8.11 (1H, s, Ar**H**), 8.03 (1H, s, Ar**H**), 7.77 (1H, s, Ar$^{\text{tri}}$**H**), 7.19 (2H, bs, **NH₂**), 6.51 (1H, bs, **NH**), 6.35 (1H, bs, **NH**), 5.30-5.35 (2H, m, 2 x **OH**), 4.42-4.46 (1H, m, ArN$^{\text{tri}}$**CH₂ₐ**), 4.25-4.35 (3H, m, ArN$^{\text{tri}}$**CH₂ᵦ**, NC**Hₐ**,NHC**H**), 4.12-4.18 (2H, m, NC**Hᵦ**, NHC**H**), 3.83 (2H, bs, 2 x OC**H**), 3.08-3.12 (1H, m, SC**H**), 2.82 (1H, dd, J = 5.1, 12.4 Hz, SC**Hᵦ**), 2.56-2.60 (3H, m, SC**Hₐ**, ArC$^{\text{tri}}$**CH₂**), 1.44-1.62 (4H, m, 2 x **CH₂**), 1.29-1.34 (4H, m, 2 x **CH₂**);

¹³C NMR (125 MHz; CDCl₃): 163.2, 156.4, 152.7, 150.1, 146.9 (isomer a/b), 142.0, 130.0, 119.1, 71.0 (isomer a/b), 69.9, 61.6 (isomer a/b), 59.7, 56.1 (isomer a/b), 52.6 (isomer a/b), 46.4 (isomer a/b), 29.2, 29.1, 28.9 (isomer a/b), 28.7 (isomer a/b), 25.4;

HRMS calcd. for (M + H$^+$) $C_{21}H_{31}N_{10}O_3S$: requires 503.2301, found 503.2289

HPLC R_t = 11.8 min

(3a*S*,4*S*,6a*R*)-4-(5-(1-(((4*S/R*,5*S/R*)-5-((6-amino-9*H*-purin-9-yl)methyl)-2,2-dimethyl-1,3-dioxolan-4-yl)methyl)-1*H*-1,2,3-triazol-4-yl)pentyl)tetrahydro-1*H*-thieno[3,4-*d*]imidazol-2(3*H*)-one 2.11a and 2.11b
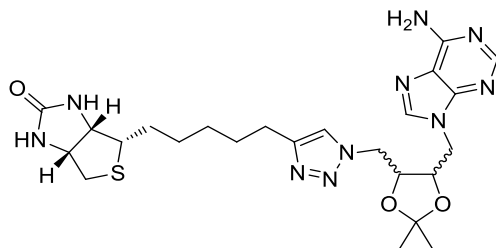
Biotin acetylene **2.21** (30 mg, 0.13 mmol) was reacted with azide **2.18** (40 mg, 0.13 mmol) and Cu nanopowder (2 mg, 0.026 mmol) using General Procedure **A1**. The crude material was purified by flash chromatography on silica gel eluting with 5% MeOH in DCM to give a crystalline white solid (31 mg, 44%).

¹H NMR (500 MHz; DMSO-*d6*): δ 8.16 (1H, s, Ar**H**, isomer a/b), 8.07 (1H, s, Ar**H**, isomer a/b), 7.76 (0.5H, s, Ar^{tri}**H**, isomer a), 7.76 (0.5H, s, Ar^{tri}**H**, isomer b), 7.28 (1H, bs, N**H₂**, isomer a), 7.26 (1H, bs, N**H₂**, isomer b), 6.50 (0.5H, bs, N**H**, isomer a), 6.44 (0.5H, bs, N**H,** isomer b), 6.36 (0.5H, bs, N**H**, isomer a), 6.35 (0.5H, bs, N**H**, isomer b), 4.10-4.63 (8H, m, NC**H₂**, ArN^{tri}C**H₂**, 2 x OC**H**, 2 x NHC**H**, isomer a/b), 3.06-3.09 (1H, m, SC**H**, isomer a/b), 2.80 (1H, dd, *J* = 5.1, 12.4 Hz, SC**H$_a$,** isomer a/b), 2.55-2.60 (3H, m, SC**H$_b$**, ArC^{tri}C**H₂**, isomer a/b), 1.42-1.60 (4H, m, 2 x C**H₂**, isomer a/b), 1.28-1.36 (4H, m, 2 x C**H₂**, isomer a/b), 1.20 (1.5H, s, CC**H₃**, isomer a), 1.20 (1.5H, s, CC**H₃**, isomer b), 1.18 (1.5H, s, CC**H₃**, isomer a), 1.17 (15H, s, CC**H₃**, isomer b).

¹³C NMR (125 MHz; DMSO-*d6*): δ 165.9, 159.1, 155.7, 145.0, 144.5, 125.8 (isomer a/b), 112.7, 92.6, 79.5, 79.2, 64.23/64.20 (isomer a/b), 62.3, 58.7 (isomer a/b), 57.0, 53.6 (isomer a/b), 51.7, 46.9 (isomer a/b), 31.8 (isomer a/b), 31.7, 31.5 (isomer a/b), 31.4 (isomer a/b), 29.9 (isomer a/b), 28.0;

HRMS calcd. for (M + H⁺) C₂₄H₃₅N₁₀O₃S: requires 543.2614, found 543.2619

HPLC R$_t$ = 18.0 min

(3a*S*,4*S*,6a*R*)-4-(5-(1-(2-((6-amino-9*H*-purin-9-yl)methoxy)ethyl)-1*H*-1,2,3-triazol-4-yl)pentyl)tetrahydro-1*H*-thieno[3,4-*d*]imidazol-2(3*H*)-one 2.12
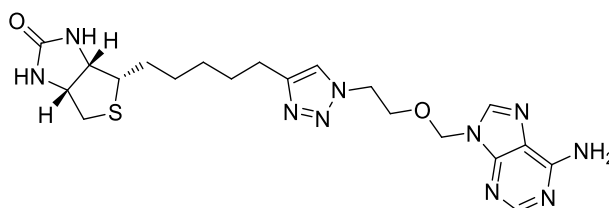
Biotin acetylene **2.21** ((30 mg, 0.13 mmol)) was reacted with azide **2.20** (31 mg, 0.13 mmol) and Cu nanopowder (2 mg, 0.026 mmol) using General Procedure **A1**. The crude material was purified by flash chromatography on silica gel eluting with 5% MeOH in DCM to give a crystalline white solid (46 mg, 75%).

^{1}H NMR (500 MHz; DMSO-*d6*): δ 8.19 (1H, s, Ar**H**), 8.15 (1H, s, Ar**H**), 7.68 (1H, s, Ar^{tri}**H**), 7.30 (2H, bs, N**H$_2$**), 6.50 (1H, bs, N**H**), 6.35 (1H, bs, N**H**), 5.52 (2H, s, NC**H$_2$**), 4.43 (2H, t, *J* = 5.2 Hz, ArN^{tri}C**H$_2$**), 4.28-4.30 (1H, m, NHC**H**), 4.11-4.14 (1H, m, NHC**H**), 3.88 (2H, t, *J* = 5.2 Hz, C**H$_2$**O), 3.07-3.11 (1H, m, SC**H**), 2.80 (1H, dd, *J* = 5.2, 12.4 Hz, SC**H$_a$**), 2.51-2.57 (3H, m, SC**H$_b$**, ArC^{tri}C**H$_2$**), 1.24-1.62 (8H, m, 4 x C**H$_2$**),;
^{13}C NMR (125 MHz; DMSO-*d6*): δ 163.2, 156.5, 153.4, 150.1, 147.2, 141.5, 122.3, 118.9, 72.3, 67.8, 61.6, 59.7, 56.0, 55.4, 49.3, 29.1, 29.1, 28.9, 28.7, 25.4;
HRMS calcd. for (M + H$^+$) C$_{20}$H$_{29}$N$_{10}$O$_2$S: requires 473.2196, found 473.2149
HPLC R$_t$ = 11.5 min

(*E*)-3-(4-azidobut-2-en-1-yl)-5-methylbenzo[*d*]oxazol-2(3*H*)-one 2.13
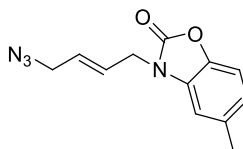
Bromide **2.28** (200 mg, 0.71 mmol) was reacted NaN$_3$ (69 mg, 1.06 mmol) according to general procedure **B2** and purified by flash chromatography on silica eluting with 30% EtOAc in hexane to yield a yellowish oil (152 mg, 88%).

^{1}H NMR (500 MHz; CDCl$_3$): δ 7.05 (1H, s, Ar**H**), 6.97 (1H, d, *J* = 8.0 Hz, Ar**H**), 6.83 (1H, d, *J* = 8.0 Hz, Ar**H**), 5.75-5.87 (2H, m, 2 x C**H**), 4.46 (2H, d, *J* = 5.4 Hz, NC**H$_2$**), 3.80 (2H, d, *J* = 5.8 Hz, N$_3$C**H$_2$**), 2.39 (3H, s, ArC**H$_3$**);

---

¹³C NMR (125 MHz; CDCl₃): δ 154.4, 142.8, 132.9, 128.3, 127.5, 127.3, 124.2, 110.8, 108.2, 51.8, 43.2, 21.4;

HRMS calcd. for (2M + H⁺) C₂₄H₂₅N₈O₄, requires 489.1999, found 489.1949

(2*S/R*,3*S/R*)-3-(4-azido-2,3-dihydroxybutyl)-5-methylbenzo[*d*]oxazol-2(3*H*)-one   2.14a and 2.14b
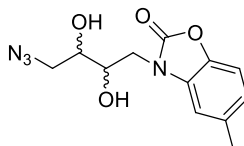
Method 1 (entry 1)[1,2]

To a stirred solution of AD-mix α (1.76 G, 2.26 mmol) in a mixture of tBuOH and H₂O (1:1) was added methanesulfonamide (143 mg, 1.51 mmol) and NaHCO₃ (257 mg, 2.99 mmol). The reaction mixture was stirred at ambient temperature for 15 min, and cooled to 0 ºC. A solution of the azide **2.13** (267 mg, 1.09 mmol) in *t*BuOH and H₂O (1:1) was then added and the reaction mixture was warmed up to the room temperature and stirred for overnight. The reaction mixture was diluted with EtOAc and washed with aqueous saturated Na₂SO₄, water and brine, dried over NaSO₄, filtered, concentrated *in vacuo* and purified by column chromatography on silica gel using 30% EtOAc in hexane resulted in no trace of the title compound and the starting material azide **2.13** was recovered (200 mg, 75%).

Method 2 (entry 2)[1,2]

The procedure outline in method 1 above was repeated using AD-mix β in place of AD-mix α. This gave the recovered starting material azide **2.13** (180 mg, 90%) only.

Method 3 (entry 3)[3]

To a solution of azide **2.13** (100 mg, 0.41 mmol) in a mixture of acetone and water (10:1, 10 mL) was added *N*-methyl morpholine *N*-oxide (72 mg, 0.61 mmol) and OsO₄ (5 mg, 0.02 mmol). The mixture was stirred at ambient temperature for 18 h. The reaction mixture was then poured into a pad of sodium metasulfite and washed with MeOH, filtered by vacuum. The filtrates were combined and concentrated *in vacuo* and the crude material was purified

by column chromatography on silica gel using 5% MeOH in DCM to give the desired azide **2.14** as an off white solid (53 mg, 46%).

^{1}H NMR (500 MHz; CDCl$_3$): δ 7.06 (1H, s, Ar**H**), 7.01 (2H, m, J = 8.6 Hz, Ar**H**), 6.97 (1H, d, J = 8.0 Hz, Ar**H**), 3.94-3.99 (3H, m, C**H**OH, NC**H₂**), 3.73-3.76 (1H, m, C**H**OH), 3.56 (1H, dd, J = 7.0, 12.6 Hz, N$_3$C**H₂ₐ**), 3.47 (1H, dd, J = 4.8, 12.6 Hz, N$_3$C**H₂ᵦ**), 2.92 (1H, d, J = 6.1 Hz, O**H**), 2.65 (1H, d, J = 6.8 Hz, O**H**), 2.40 (3H, s, ArC**H₃**);

^{13}C NMR (125 MHz; CDCl$_3$): δ 142.8, 124.6, 110.9, 108.3, 69.8, 69.6, 53.6, 44.9, 21.4;

HRMS calcd. for (M + H$^+$) C$_{12}$H$_{15}$N$_4$O$_4$, requires 279.1093, found 279.1092

3-((((4S/R,5S/R)-5-(azidomethyl)-2,2-dimethyl-1,3-dioxolan-4-yl)methyl)-5-methylbenzo[d]oxazol-2(3H)-one 2.15a and 2.15b
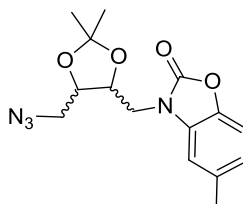
To a solution of azide **2.14** (23 mg, 0.08 mmol) in a mixture of 2, 2-dimethoxypropane and acetone (1:1 1 mL) was added p-toluenesulfonic acid monohydrate (1 mg, 0.005 mmol) and stirred at ambient temperature for 12 h. The resulting residue was purified by silica gel chromatography eluting with 10% EtOAc in hexane to give the title compound as an off white solid (15 mg, 58%).

^{1}H NMR (500 MHz; CDCl$_3$): δ7.06 (1H, d, J = 8.1 Hz, Ar**H**), 6.94 (1H, s, Ar**H**), 6.90 (1H, d, J = 8.2 Hz, Ar**H**), 4.71 (1H, dd, J = 4.4, 14.7 Hz, NC**H₂ₐ**), 4.58 (1H, dd, J = 4.1, 14.7, NC**H₂ᵦ**), 3.90 -4.04 (2H, m**,** N$_3$C**H₂**), 2.39 (3H, s, ArC**H₃**), 1.22 (3H, s, CC**H₃**), 1.19 (3H, s, CC**H₃**);

^{13}C NMR (125 MHz; CDCl$_3$): δ 148.3, 123.1, 120.4, 110.4, 109.4, 82.1, 80.3, 50.8, 42.8, 25.5, 21.3.

HRMS calcd. for (M + H$^+$) C$_{15}$H$_{19}$N$_4$O$_4$, requires 319.1406, found 319.1403.

### 3-((2-azidoethoxy)methyl)-5-methylbenzo[*d*]oxazol-2(3*H*)-one 2.16
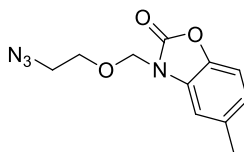
To a solution of glycol alcohol **2.33** (80 mg, 0.36 mmol) in dry DMF (1mL) was added CCl$_4$ (83 mg, 0.54 mmol) was added TEA (54 mg, 0.54 mmol) and NaN$_3$ (35 mg, 0.54 mmol). the reaction mixture was stirred at 80 °C for 1.5 h, and then the residues were cooled to room temperature, diluted with EtOAc, and washed with water and brine. The organic layers were collected and dried over Na$_2$SO$_4$, concentrated *in vacuo* and purified by column chromatography eluting with 30% EtOAc in hexane to give the title compound as colorless oil (60 mg, 67%).

^{1}H NMR (500 MHz; CDCl$_3$): δ 7.02 (1H, d, *J* = 8.2 Hz, Ar**H**), 6.99 (1H, s, Ar**H**), 6.96 (1H, d, *J* = 8.2 Hz, Ar**H**), 5.32 (2H, s, NC**H$_2$**), 3.85 (2H, t, *J* = 5.8 Hz, N$_3$C**H$_2$**), 3.62 (2H, t, *J* = 5.8 Hz, OC**H$_2$**), 2.90 (3H, s, ArC**H$_3$**);

^{13}C NMR (125 MHz; CDCl$_3$): δ 154.8, 140.8, 132.9, 129.3, 123.2, 109.8, 109.2, 72.6, 70.5, 50.5, 21.5;

HRMS calcd. for (M + H$^+$) C$_{11}$H$_{13}$N$_4$O$_3$, requires 249.0988, found 249.0985

(*E*)-9-(4-azidobut-2-en-1-yl)-9*H*-purin-6-amine 2.17
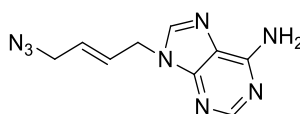
Bromide **2.30** (100 mg, 0.37 mmol) was reacted with NaN$_3$ (36 mg, 0.56 mmol) according to general procedure **B2** and purified by flash chromatography on silica eluting with 10% MeOH in DCM to yield a white solid (66 mg, 77%)

^{1}H NMR (500 MHz; CDCl$_3$): δ 8.12 (1H, s, Ar**H**), 8.09 (1H, s,Ar**H**), 7.19 (2H, bs, N**H$_2$**), 6.00 (1H, dt, *J* = 5.9, 15.2 Hz, **CH**), 5.62 (1H, dt, *J* = 6.3, 15.2 Hz, **CH**), 4.80 (2H, d, *J* = 5.8 Hz, NC**H$_2$**), 3.85 (2H, d, *J* = 6.2 Hz, N$_3$C**H2**);

^{13}C NMR (125 MHz; CDCl$_3$): δ 156.4, 153.0, 149.8, 140.9, 130.0, 127.3, 119.1, 51.4, 44.2;

HRMS calcd. for (M + H$^+$) C$_9$H$_{11}$N$_8$, requires 231.1107, found 231.1112

HPLC R$_t$ = 11.9 min

(2*S/R*, 3*S/R*)-1-(6-amino-9*H*-purin-9-yl)-4-azidobutane-2,3-diol 2.18a and 2.18b
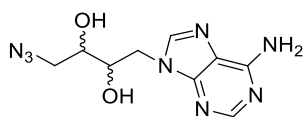
To a solution of azide **2.17** (100 mg, 0.43 mmol) in a mixture of acetone and water (10:1, 10 mL) was added *N*-methyl morpholine *N*-oxide (76 mg, 0.65 mmol) and OsO_4 (5 mg, 0.02 mmol). The mixture was stirred at ambient temperature for 18 h. The reaction mixture was then poured into a pad of sodium metasulfite and washed with MeOH, filtered by vacuum. The filtrates were combined and concentrated *in vacuo* and the crude material was purified by column chromatography on silica gel using 15% MeOH in DCM to give the desired azide as an off white solid (34 mg, 43%).

¹H NMR (500 MHz; CDCl₃): δ 8.11 (1H, s, Ar**H**), 8.01 (1H, s,Ar**H**), 7.15 (2H, bs, N**H₂**), 5.37 (1H, d, *J* = 6.2 Hz, O**H**), 5.14 (1H, d, *J* = 6.5 Hz, O**H**), 4.24 (1H, dd, *J* = 3.9, 13.9 Hz, NC**H₂a**), 4.06-4.10 (1H, m, NC**H₂b**), 3.19-3.84 (1H, m, OC**H**), 3.56-3.59 (1H, m, OC**H**), 3.34-3.38 (1H, m, N₃C**H₂a**), 3.27-3.30 (1H, m, N₃C**H₂b**);

¹³C NMR (125 MHz; CDCl₃): δ 156.4, 152.7, 150.0, 142.0, 119.1, 71.2, 70.4, 53.2, 46.3;

HRMS calcd. for (M + H⁺) $C_9H_{13}N_8O_2$, requires 265.1161, found 265.1164

HPLC R_t = 10.2 min

9-(((4*S/R*,5*S/R*)-5-(azidomethyl)-2,2-dimethyl-1,3-dioxolan-4-yl)methyl)-9*H*-purin-6-amine 2.19a and 2.19b
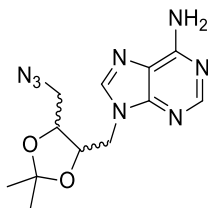
To a solution of azide **2.18** (30 mg, 0.11 mmol) in a mixture of 2, 2-dimethoxypropane and acetone (1:1 3 mL) was added *p*-toluenesulfonic acid monohydrate (1 mg, 0.005 mmol) and stirred at ambient temperature for 12 h. The resulting residue was purified by silica gel chromatography eluting with 10% MeOH in DCM to give the title compound as an off white solid (10 mg, 29%).

---

¹H NMR (500 MHz; CDCl₃): δ 8.37 (1H, s, Ar**H**), 7.95 (1H, s,Ar**H**), 5.62 (2H, bs, N**H₂**), 4.44 (2H, t, *J* = 3.6 Hz, NC**H₂**), 4.28 (1H, dt, *J* = 3.8, 7.9 Hz, OC**H**), 3.71 (1H, dt, *J* = 4.2, 8.3 Hz, OC**H**), 3.62 (1H, dd, *J* = 3.9, 13.3 Hz, N₃C**H₂ₐ**), 3.39 (1H, dd, *J* = 4.5, 13.3 Hz, N₃C**H₂ᵦ**), 1.45 (3H, s, CC**H₃**), 1.26 (3H, s, CC**H₃**);

¹³C NMR (125 MHz; CDCl₃): δ 158.0, 155.9, 144.4, 112.9, 79.0, 78.8, 53.5, 45.9, 29.5, 29.5, 2.7;

HRMS calcd. for (M + H⁺) C₁₂H₁₇N₈O₂, requires 305.1474, found 305.1477

HPLC R$_t$ = 13.0 min

9-((2-azidoethoxy)methyl)-9*H*-purin-6-amine 2.20
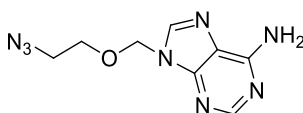
To a solution of glycol alcohol **2.35** (100 mg, 0.48 mmol) in dry DMF (1mL) was added CCl₄ (110 mg, 0.72 mmol) was added TEA (72 mg, 0.72 mmol) and NaN₃ (47 mg, 0.72). the reaction mixture was stirred at 80 °C for 1.5 h, and then the residues were cooled to room temperature, diluted with EtOAc, and washed with water and brine. The organic layers were collected and dried over Na₂SO₄, concentrated *in vacuo* and purified by column chromatography eluting with with 10% MeOH in DCM to give the title compound as colorless oil (15 mg, 13%).

¹H NMR (500 MHz; DMSO-*d6*): δ 8.27 (1H, s, Ar**H**), 8.16 (1H, s,Ar**H**), 7.27 (2H, bs, N**H₂**), 5.58 (2H, s, NC**H₂**), 3.76-3.78 (1H, m, OC**H₂ₐ**), 3.67-3.69 (2H, m, N₃C**H₂**), 3.36-3.38 (1H, m, OC**H₂ᵦ**);

¹³C NMR (125 MHz; DMSO-*d6*): δ 156.5, 153.4, 150.2, 141.6, 118.9, 72.4, 69.6, 50.2;

HRMS calcd. for (M + H⁺) C₈H₁₁N₈O, requires 235.1056, found 235.1045

(3a*S*,4*S*,6a*R*)-4-hept-6-ynyl-1,3,3a,4,6,6a-hexahydrothieno[3,4-*d*]imidazol-2-one 2.21
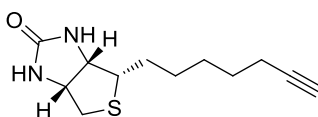
To a suspension of 90% lithium acetylide EDA complex (0.959 g, 9.39 mmol) in dry DMSO (2.5 mL) cooled at 15 °C was added dropwise a solution of biotin bromide **2.25** (1.10 g, 3.75

mmol) in dry DMSO (2.5 mL) and stirred at ambient temperature for 3 h. The reaction mixture was poured into ice-water and extracted with DCM. The organic layer was collected and washed with water and brine, dried over Na_2SO_4, filtered, concentrated *in vacuo* and purified by silica gel chromatography eluting with 4% MeOH in DCM to give a white solid (0.679 g, 71%). ^{1}H NMR was consistent with literature.[4]

^{1}H NMR (500 MHz, CDCl$_3$): δ 5.30 (1H, bs, C(O)N**H**), 5.19 (1H, s, C(O)N**H**), 4.50-4.54 (1H, NHC**H**), 4.31 (1H, ddd, *J* = 1.5, 4.6, 7.8 Hz, NHC**H**), 3.13-3.20 (1H, m, SC**H**), 2.93 (1H, dd, *J* = 5.1, 12.8 Hz, SC**H$_a$**), 2.74 (1H, d, *J* = 12.8 Hz, SC**H$_b$**), 2.19 (2H, td, *J* =6.8, 2.6 Hz, **CH$_2$**C≡CH), 1.94 (0.6H, t, *J* = 2.6 Hz, CH$_2$C≡C**H**), 1.64-1.71 (2H, m, **CH$_2$**), 1.39-1.56 (6H, m, 3 x **CH$_2$**);

^{13}C NMR (125 Mhz, CDCl$_3$): δ 163.3, 84.7, 68.6, 62.2, 60.3, 55.7, 40.8, 28.8, 29.8, 28.4, 18.5.

Methyl 5-[(3aS,4S,6aR)-2-oxo-1,3,3a,4,6,6a-hexahydrothieno[3,4-d]imidazol-4-yl] pentanoate 2.22
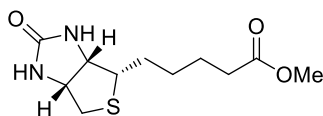
To a suspension of biotin **1.01** (4.00 g, 16.4 mmol) in MeOH (200 mL) was added drop-wise thionyl chloride (3.5 mL, 49.2 mmol) and the mixture stirred for 90 min with a calcium chloride drying tube. The reaction mixture was concentrated *in vacuo*, diluted with DCM, concentrated *in vacuo* and purified by silica gel chromatography eluting with 10% MeOH in DCM to give a white solid (4.23 g, 100%). >95% purity as judge by NMR. ^{1}H NMR was consistent with literature.[4]

^{1}H NMR (500 MHz, CDCl$_3$): δ 6.01 (1H, bs, C(O)N**H**), 5.59 (1H, bs, C(O)N**H**), 4.47-4.52 (1H, m, NHC**H**), 4.30 (1H, ddd, *J* = 1.5, 4.5, 7.8 Hz, NHC**H**), 3.65 (3H, s, COOC**H$_3$**), 3.11-3.18 (1H, m, SC**H**), 2.90 (1H, dd, *J* = 5.1, 12.6 Hz, SC**H$_a$**), 2.73 (1H, d, *J* = 12.6 Hz, SC**H$_b$**), 2.33 (2H, t, *J* = 7.8 Hz, **CH$_2$**COO), 1.61-1.74 (4H, m, 2 x **CH$_2$**), 1.40-1.48 (2H, m, C**H$_2$**);

^{13}C NMR (125 MHz, CDCl$_3$): δ 174.3, 163.8, 62.1, 60.3, 55.6, 51.8, 40.8, 33.9, 28.5, 28.4, 25.0.

**(3aS,4S,6aR)-4-(5-hydroxypentyl)-1,3,3a,4,6,6a-hexahydrothieno[3,4-d]imidazol-2-one 2.23**
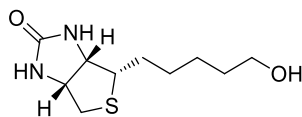
To a suspension of biotin methyl ester **2.22** (3.00 g, 11.63 mmol) in freshly distilled THF (225 mL) was added portion-wise lithium aluminium hydride (661 mg, 17.40 mmol) and the mixture stirred overnight under a nitrogen atmosphere. The reaction mixture was quenched with MeOH and water. To the mixture was added saturated sodium sulfate, stirred for 20 min and concentrated *in vacuo*. The residue was dissolved in 1:4 MeOH and DCM, stirred for 30 min, filtered, washed with 1:4 MeOH and DCM. The filtrate was concentrated *in vacuo* to give a white solid (2.25 g, 84%). >95% purity as judge by NMR. ^{1}H NMR was consistent with literature.[4]

^{1}H NMR (500 MHz, DMSO-*d6*): δ 6.44 (1H, bs, C(O)N**H**), 6.36 (1H, bs, C(O)N**H**), 4.28-4.37 (2H, m, C**H**₂OH, NHC**H**), 4.10-4.15 (1H, NHC**H**), 3.38 (2H, t, J = 6.0 Hz, C**H₂**OH), 3.07-3.13 (1H, m, SC**H**), 2.81 (1H, dd, J = 5.1, 12.6 Hz, SC**H**ₐ), 2.57 (1H, d, J = 12.6 Hz, SC**H**ᵦ), 1.25-1.67 (8H, m, C**H₂**);
^{13}C NMR (125 MHz, CDCl₃): δ 166.2, 63.4, 62.8, 61.6, 57.2, 41.0, 33.4, 33.4, 30.2, 29.8, 26.9.

5-[(3aS,4S,6aR)-2-oxo-1,3,3a,4,6,6a-hexahydrothieno[3,4-d]imidazol-4-yl]pentyl 4-methylbenzenesulfonate 2.24
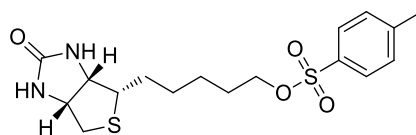
To a suspension of biotinol **2.23** (2.5 g, 10.80 mmol) in dry pyridine (25 mL) was added dropwise a solution of tosyl chloride (3.10 g, 16.30 mmol) in dry pyridine (45 mL), and the solution was stirred with an ice bath for 1 h and left for 5 h in a 4 °C fridge. The reaction mixture was diluted with DCM and washed with 0.5 M aqueous HCl, aqueous saturated sodium bicarbonate, water and brine. The organic layer was dried over Na₂SO₄, filtered and concentrated *in vacuo* to give a white solid (2.79 g, 67%). >95% purity as judge by ^{1}H NMR. ^{1}H NMR was consistent with literature.[4]

_____

¹H NMR (500 MHz, CDCl₃): δ 7.78 (2H, d, *J* = 8.7 Hz, Ar**H**), 7.35 (2H, d, *J* =8.7 Hz, Ar**H**), 6.09 (1H, bs, C(O)N**H**), 5.47 (1H, bs, C(O)N**H**),4.47-4.51 (1H, m, NHC**H**), 4.26-4.30 (1H, m, NHC**H**), 4.01 (2H, t, *J* = 6.3 Hz, OC**H₂**), 3.07-3.14 (1H, m, SC**H**), 2.89 (1H, dd, *J* = 5.1, 12.6 Hz, SC**Hₐ**), 2.73 (1H, d, *J* = 12.6 Hz, SC**Hᵦ**), 2.45 (3H, s, ArC**H₃**), 1.60-1.69 (4H, m, 2 x C**H₂**), 1.33-1.39 (4H, m, 2 x C**H₂**);

¹³C NMR (125 MHz, CDCl₃): 164.0, 145.0, 133.2, 130.1, 128.1, 70.84, 62.1, 60.3, 55.8, 40.8, 28.8, 28.6, 28.5, 25.6, 21.9.

(3aS,4S,6aR)-4-(5-bromopentyl)-1,3,3a,4,6,6a-hexahydrothieno[3,4-d]imidazol-2-one 2.25
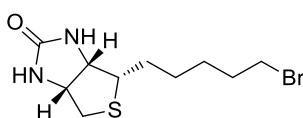
To a suspension of biotin tosylate **3.18** (2.0 g, 5.21 mmol) in methyl ethyl ketone (20 mL) was added lithium bromide (0.90 g, 10.40 mmol) and stirred at 80 °C for 3 h. The reaction mixture was cool, diluted with DCM and washed with water and brine. The organic layer was dried over Na₂SO₄, filtered and concentrated *in vacuo* and purified by silica gel chromatography eluting with 5% MeOH in DCM to give a white solid (1.16 g, 76%). ¹H NMR was consistent with literature.[4]

¹H NMR (500 MHz, CDCl₃): δ 5.51 (1H, bs, C(O)N**H**), 5.21 (1H, bs, C(O)N**H**), 4.49-4.54 (1H, m, NHC**H**), 4.31 (1H, ddd, *J* = 1.5, 4.6, 7.8 Hz, NHC**H**), 3.41 (2H, t, *J* = 6.7 Hz, C**H₂**Br), 3.13-3.20 (1H, m, SC**H**), 2.93 (1H, dd, *J* = 5.1, 12.8 Hz, SC**Hₐ**), 2.74 (1H, d, *J* = 12.8 Hz, SC**Hᵦ**), 1.83-1.92 (2H, m, C**H₂**), 1.65-1.72 (2H, m, C**H₂**), 1.43-1.53 (4H, m, 2 x C**H₂**);

¹³C NMR (125 MHz, CDCl₃), 163.5, 62.3, 60.3, 55.7, 40.8, 34.0, 32.7, 28.8, 28.5, 28.3;

5-methyl-3*H*-1,3-benzoxazol-2-one 2.27[4]
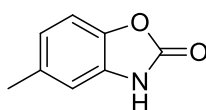
To a solution of 2-amino-cresol (5.10 g, 41.40 mmol) in 50 ml of DCM was added 1,1-carbonyldiimidazole (7.39 g, 45.60 mmol) and the solution was stirred at ambient

temperature under nitrogen atmosphere for 45 min. The reaction mixture was poured into water (100 ml) and extracted with DCM (2 x 100 ml). The organic layers were pooled, washed with saturated aqueous sodium bicarbonate (1 x 150 ml), water (1 x 150ml) and brine (1 x 150 ml), dried over Na_2SO_4, filtered and concentrated *in vacuo* to give a white solid (5.93 g, 96%). >95% purity as judged by ^{1}H NMR. ^{1}H NMR was consistent with literature. [4]

^{1}H NMR (500 MHz, CDCl$_3$): δ 10.07 (1H, bs, N**H**), 7.06 (1H, d, *J* = 8.1 Hz, Ar**H**), 6.90 (1H, s, Ar**H**), 6.87 (1H, d, *J* = 8.1 Hz, Ar**H**), 2.36 (3H, s, ArC**H₃**);

^{13}C NMR (125 MHz, CDCl$_3$): δ 157.0, 142.0, 134.3, 129.6, 123.2, 111.0, 109.7, 21.6.

(*E*)-3-(4-bromobut-2-en-1-yl)-5-methylbenzo[*d*]oxazol-2(3*H*)-one 2.28
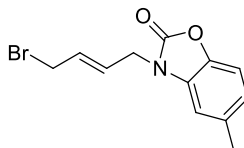
5-Methylbenzoxazolone **2.27** (149 mg, 1.01 mmol) and 1,4-dibromobutene (321 mg, 1.50 mmol) was reacted according to general procedure **B1** and was purified by flash chromatography on silica eluting with 20% EtOAc in hexane to yield bromide as a yellowish oil (184 mg, 65%).

^{1}H NMR (500 MHz; CDCl$_3$): δ 7.09 (1H, d, *J* = 8.1 Hz, Ar**H**), 6.92 (1H, d, *J* = 8.2 Hz, Ar**H**), 6.79 (1H, s, Ar**H**), 5.96-6.02 (1H, m, CH**CH**), 5.82-5.88 (1H, m, **CH**CH), 4.46 (2H, d, *J* = 5.9 Hz, NC**H₂**), 3.95 (2H, d, *J* = 7.4 Hz, BrC**H2**), 2.40 (3H, s, ArC**H₃**);

^{13}C NMR (125 MHz; CDCl$_3$): δ 154.6, 140.7, 134.1, 130.7, 130.7, 127.5, 123.1, 109.8, 109.5, 42.3, 31.0, 21.6;

HRMS calcd. for (M + H⁺) $C_{12}H_{13}BrNO_2$, requires 282.0130, found 282.0138

_____

(*E*)-9-(4-bromobut-2-en-1-yl)-9*H*-purin-6-amine 2.30
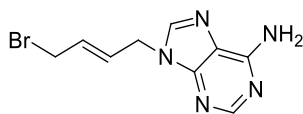
Entry 1

Adenine **2.29** (100 mg, 0.74 mmol) was reacted according to general procedure **B1** and purified by flash chromatography on silica eluting with 10% MeOH in DCM to yield a white solid (20 mg, 10%).

Entry 2

A solution of adenine **2.29** (100 mg, 0.74 mmol) in dry DMF (5 ml) was cooled to -78 °C under nitrogen atmosphere, followed by addition of sodium hydrate (26 mg, 1.11 mmol) and 1,4-dibromobutene (236 mg, 1.11 mmol). The reaction mixture was slowly warmed to the room temperature over 4 h, and stirred at room temperature for 3 h. The reaction mixture was then diluted with DCM and washed with 0.5 M aqueous HCl, aqueous saturated Na_2SO_4, water and brine, dried over $NaSO_4$, filtered, concentrated *in vacuo*. The crude material was purified by flash chromatography on silica gel eluting with 10% MeOH in DCM to yield a white solid (10 mg, 5%)

Entry 3

To a solution of adenine **2.29** (100 mg, 0.74 mmol) in dry DMF (5 ml) was added Cs_2CO_3 (361 mg, 1.11 mmol) and stirred at ambient temperature for 30 min, followed by addition of 1,4-dibromobutene (236 mg, 1.11 mmol) and stirred at ambient temperature for 4 h under nitrogen atmosphere. The reaction mixture was then diluted with DCM and washed with 0.5 M aqueous HCl, aqueous saturated Na_2SO_4, water and brine, dried over $NaSO_4$, filtered, concentrated *in vacuo*. The crude material was purified by flash chromatography on silica gel eluting with 10% MeOH in DCM to yield a white solid (109 mg, 55%).

¹H NMR (500 MHz; $CDCl_3$): δ 8.12 (1H, s, Ar**H**), 8.09 (1H, s,Ar**H**), 7.19 (2H, bs, **H₂**), 6.00 (1H, dt, *J* = 5.9, 15.2 Hz, CHC**H**), 5.62 (1H, dt, *J* = 6.3, 15.2 Hz, CHC**H**), 4.80 (2H, d, *J* = 5.8 Hz, NC**H₂**), 3.85 (2H, d, *J* = 6.2 Hz, N₃C**H2**);
¹³C NMR (125 MHz; $CDCl_3$): δ 156.1, 152.4, 149.8, 141.8, 129.0, 128.3, 119.1, 50.4, 33.3;
HRMS calcd. for (M + H⁺) $C_9H_{11}BrN_5$, requires 268.0198, found 268.0201.

2-(bromomethoxy)ethyl acetate 2.31
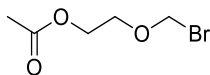
To a solution of acetyl bromide (1.10 g, 9.01 mmol) was added 1,3-dioxolane (0.67 g, 9.01 mmol) dropwise and stirred at 60 ºC for 3 h. The excess starting material were removed *in vacuo* to give a colorless oil which was used without further purification. >90% purity as judge by NMR.

2-((5-methyl-2-oxobenzo[d]oxazol-3(2*H*)-yl)methoxy)ethyl acetate 2.32
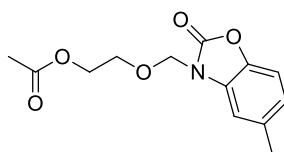
To a solution of 5-methylbenzoxazolone **2.27** (200 mg, 1.34 mmol) in dry DMF (3mL) was added potassium carbonate (277mg, 2.01 mmol) and stirred at 50 ºC for 30 min, followed by addition of the 2-(bromomethoxy)ethyl acetate **2.31** (305 mg, 2.00 mmol) and stirred at 50 ºC for 12 h under nitrogen atmosphere. The reaction mixture was diluted with DCM and washed with aqueous saturated Na_2SO_4, water and brine, dried over $NaSO_4$, filtered, concentrated *in vacuo* and the residue was purified by flash chromatography on silica eluting with 2% MeOH in DCM to yield acetate as a yellowish oil (294 mg, 83%).

^{1}H NMR (500 MHz; CDCl$_3$): δ 7.09 (1H, d, *J* = 8.1 Hz, Ar**H**), 6.94-6.97 (2H, m, 2 x Ar**H**), 5.30 (2H, s, NC**H$_2$**), 4.19 (2H, t, *J* = 4.7 Hz, COOC**H$_2$**), 3.79 (2H, t, *J* = 4.6 Hz, COOC**H$_2$**), 2.39 (3H, s, ArC**H$_3$**), 1.97 (3H, s, C**H$_3$**);

^{13}C NMR (125 MHz; CDCl$_3$): δ 140.6, 134.2, 123.6, 109.9, 109.7, 72.6, 67.1, 62.9, 21.4, 20.7;

HRMS calcd. for (M + H$^+$) $C_{13}H_{16}NO_5$, requires 266.1028, found 266.1026

3-((2-hydroxyethoxy)methyl)-5-methylbenzo[d]oxazol-2(3*H*)-one 2.33
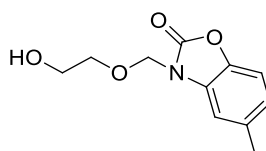
A solution of acetate **2.32** (134 mg, 0.51 mmol) in THF (5 ml) was cooled in an ice bath. To the solution was reacted dropwise 1.0 M aqueous LiOH (1 ml, 1.02 mmol). MeOH was then added to the reaction until all reagents were dissolved and allowed to stir at ambient temperature for 1 h. The reaction mixture was diluted with DCM and washed with water and brine. The organic layers were combined, dried over Na_2SO_4, filtered, concentrated *in vacuo*. The residue was purified by silica gel chromatography eluting with 3% MeOH in DCM to give the alcohol as a colourless oil (36 mg, 32%).

^{1}H NMR (500 MHz; $CDCl_3$): δ 7.08 (1H, d, *J* = 8.2 Hz, Ar**H**), 6.93-6.96 (2H, m, 2 x Ar**H**), 5.31 (2H, s, NC**H$_2$**), 3.68-3.74 (4H, m, OC**H$_2$**, HOC**H$_2$**), 2.89 (3H, s, ArC**H$_3$**);

^{13}C NMR (125 MHz; $CDCl_3$): δ140.6, 134.2, 129.9, 123.6, 109.8, 109.7, 109.7, 72.6, 70.5, 61.5, 21.5;

HRMS calcd. for (M + H$^+$) $C_{11}H_{14}NO_4$, requires 224.0923, found 224.0920

2-((6-amino-9*H*-purin-9-yl)methoxy)ethyl acetate 2.34
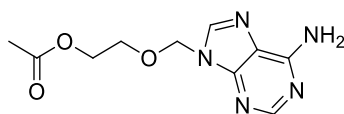
To a solution of Adenine **2.29** (500 mg, 3.70 mmol) in dry DMF (5mL) was added potassium carbonate (766 mg, 5.55 mmol) and stirred at 50 ^{o}C for 30 min, followed by addition of the 2-(bromomethoxy)ethyl acetate **2.31** (848 mg, 5.56 mmol) and stirred at 50 ^{o}C for 12 h under nitrogen atmosphere. The reaction mixture was diluted with DCM and washed with aqueous saturated Na_2SO_4, water and brine, dried over $NaSO_4$, filtered, concentrated *in vacuo* and the residue was purified by flash chromatography on silica eluting with 5% MeOH in DCM to yield acetate as a yellowish oil (770 mg, 83%).

^{1}H NMR (500 MHz; DMSO-*d6*): δ 8.26 (1H, s, Ar**H**), 8.15 (1H, s,Ar**H**), 7.27 (2H, bs, N**H$_2$**), 5.55 (2H, s, NC**H$_2$**), 4.04-4.06-3.51 (2H, m, OC**H$_2$**), 3.68-3.70 (2H, m, COOC**H$_2$**), 2.07 (1H, s, C**H$_3$**);

^{13}C NMR (125 MHz; DMSO-*d6*): δ 206.9, 170.6, 156.5, 153.4, 150.2, 141.6, 72.4, 67.3, 63.2, 31.1,

HRMS calcd. for (M + H$^+$) $C_{10}H_{14}N_5O_3$, requires 252.1097, found 252.1095

_____

9-((2-bromoethoxy)methyl)-9*H*-purin-6-amine 2.35
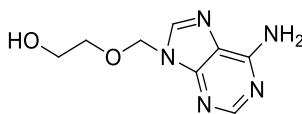
A solution of acetate **2.34** (200 mg, 0.80 mmol) in THF (8 ml) was cooled in an ice bath. To the solution was reacted dropwise 1.0 M aqueous LiOH (1 ml, 1.02 mmol). MeOH was then added to the reaction until all reagents were dissolved and allowed to stir at ambient temperature for 1 h. The reaction mixture was diluted with DCM and washed with water and brine. The organic layers were combined, dried over Na_2SO_4, filtered, and concentrated *in vacuo*. The residue was purified by silica gel chromatography eluting with 3% MeOH in DCM to give the alcohol as a colourless oil (80 mg, 48%).

¹H NMR (500 MHz; DMSO-*d6*): δ 8.25 (1H, s, Ar**H**), 8.16 (1H, s,Ar**H**), 7.26 (2H, bs, N**H₂**), 5.54 (2H, s, NC**H₂**), 3.48-3.51 (2H, m, OC**H₂**), 3.44-3.45 (2H, m, BrC**H₂**);

¹³C NMR (125 MHz; DMSO-*d6*): δ 156.5, 153.3, 150.2, 141.6, 118.9, 72.7, 71.2, 60.3;

HRMS calcd. for (M + H⁺) $C_8H_{12}N_5O_2$, requires 210.0991, found 210.0989

(3a*S*,4*S*,6a*R*)-4-(5-(1-(4-(6-chloro-9*H*-purin-9-yl)butyl)-1*H*-1,2,3-triazol-4-yl)pentyl)tetrahydro-1*H*-thieno[3,4-*d*]imidazol-2(3*H*)-one 2.36
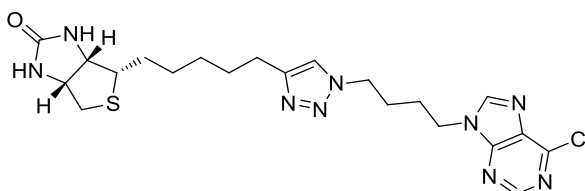
Biotin acetylene **2.21** (21 mg, 0.09 mmol) was reacted with azide **2.44** (23 mg, 0.09 mmol) and Cu nanopowder (2 mg, 0.026 mmol) using General Procedure **A1**. The crude material was purified by flash chromatography on silica gel eluting with 5% MeOH in DCM to give a crystalline white solid (36 mg, 83%).

¹H NMR (500 MHz; CDCl₃): δ 8.75 (1H, s, Ar**H**), 8.11 (1H, s, Ar**H**), 7.23 (1H, s, Ar^tri**H**), 5.04 (1H, bs, C(O)N**H**), 4.71 (1H, bs, C(O)N**H**), 4.50-4.53 (1H, m, NHC**H**), 4.31-4.40 (5H, m, NC**H₂**, ArN^triC**H₂**, NHC**H**), 3.14-3.18 (1H, m, SC**H**), 2.93 (1H, dd, *J* = 5.1, 12.8 Hz, SC**H_b**), 2.68-2.74 (3H, m, SC**H_a**, ArC^triC**H₂**), 1.94-1.97 (4H, m, 2 x C**H₂**), 1.62-1.70 (4H, m, 2 x C**H₂**), 1.36-1.47 (4H, m, 2 x C**H₂**);

---

¹³C NMR (125 MHz; CDCl₃): 163.6, 151.9, 151.8, 151.1, 148.4, 145.2, 131.6, 120.8, 62.0, 60.1, 55.8, 49.1, 43.6, 40.5, 29.0, 28.9, 28.7, 28.6, 27.3, 26.9, 25.4

HRMS calcd. for (M + H⁺) $C_{21}H_{29}ClN_9OS$: requires 490.1904, found 490.1904

HPLC R_t = 13.3 min

(3a*S*,4*S*,6a*R*)-4-(5-(1-(4-(6-methoxy-9*H*-purin-9-yl)butyl)-1*H*-1,2,3-triazol-4-yl)pentyl)tetrahydro-1*H*-thieno[3,4-*d*]imidazol-2(3*H*)-one 2.37
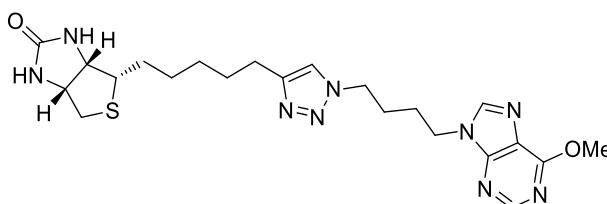
Biotin acetylene **2.21** (30 mg, 0.13 mmol) was reacted with azide **2.45** (32 mg, 0.13 mmol) and Cu nanopowder (2 mg, 0.026 mmol) using General Procedure **A1**. The crude material was purified by flash chromatography on silica eluting with 5% MeOH in DCM to give a crystalline white solid (55 mg, 88%).

¹H NMR (500 MHz; CDCl₃): δ 8.52 (1H, s, Ar**H**), 7.90 (1H, s, Ar**H**), 7.23 (1H, s, Ar^tri**H**), (1H, bs, C(O)N**H**), 5.28 (1H, bs, C(O)N**H**), 4.40 (1H, dd, *J* = 5.0, 7.8 Hz, NHC**H**), 4.26-4.37 (5H, m, NC**H₂**, ArN^triC**H₂**, NHC**H**), 4.18 (3H, s, OC**H₃**), 3.12-3.16 (1H, m, SC**H**), 2.90 (1H, dd, *J* = 5.0, 12.8 Hz, SC**Hb**), 2.66-2.73 (3H, m, SC**Ha**, ArC^triC**H₂**), 1.90-1.93 (4H, m, 2 x C**H₂**), 1.62-1.68 (4H, m, 2 x C**H₂**), 1.36-1.45 (4H, m, 2 x C**H₂**);

¹³C NMR (125 MHz; CDCl₃): 163.3, 161.1, 152.1, 152.0, 148.3, 142.0, 121.5, 120.7, 62.0, 60.1, 55.7, 54.2, 49.2, 43.2, 40.5, 29.0, 28.9, 28.7, 28.6, 27.3, 27.1, 25.4;

HRMS calcd. for (M + H⁺) C22H32N9O2S: requires 486.2400, found 486.2432

HPLC R_t = 12.3 min

(3a*S*,4*S*,6a*R*)-4-(5-(1-(4-(2,6-diamino-9*H*-purin-9-yl)butyl)-1*H*-1,2,3-triazol-4-yl)pentyl)tetrahydro-1*H*-thieno[3,4-*d*]imidazol-2(3*H*)-one 2.38
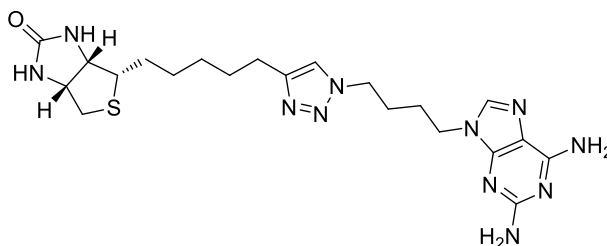
Biotin acetylene **2.21** (30 mg, 0.13 mmol) was reacted with azide **2.46** (33 mg, 0.13 mmol) and Cu nanopowder (2 mg, 0.026 mmol) using General Procedure **A1**. The crude material was purified by flash chromatography on silica eluting with 10% MeOH in DCM to give a crystalline white solid (27 mg, 43%).

^{1}H NMR (500 MHz DMSO-*d6*): δ 7.81 (1H, s, Ar**H**), 7.68 (1H, s, Ar^{tri}**H**), 6.65 (2H, bs, N**H$_2$**), 6.55 (1H, bs, C(O)N**H**), 6.36 (1H, bs, C(O)N**H**), 5.75 (2H, bs, N**H$_2$**), 4.29-4.34 (3H, m, ArN^{tri}**CH$_2$**, NHC**H**), 4.12-4.15 (1H, m, NHC**H**), 3.96 (2H, t, , *J* = 6.8 Hz, NC**H$_2$**), 3.08-3.10 (1H, m, SC**H**), 2.81 (1H, dd, *J* = 5.1, 12.5 Hz, SCH**b**), 2.56-2.59 (3H, m, SCH**a**, ArC^{tri}**CH$_2$**), 1.27-1.75 (12H, m, 6 x C**H$_2$**);

^{13}C NMR (125 MHz; DMSO-*d6*): 163.2, 160.7, 156.5, 152.2, 147.2, 137.8, 122.2, 61.6, 59.6, 56.1, 49.0, 42.0, 40.5, 29.2, 29.0, 28.9, 28.7, 27.4, 27.0, 25.4;

HRMS calcd. for (M + H$^+$) C$_{21}$H$_{32}$N$_{11}$OS: requires 486.2512, found 486.2514

HPLC R$_t$ = 11.9 min.

(3a*S*,4*S*,6a*R*)-4-(5-(1-(4-(3*H*-imidazo[4,5-b]pyridin-3-yl)butyl)-1*H*-1,2,3-triazol-4-yl)pentyl)tetrahydro-1*H*-thieno[3,4-*d*]imidazol-2(3*H*)-one 2.39
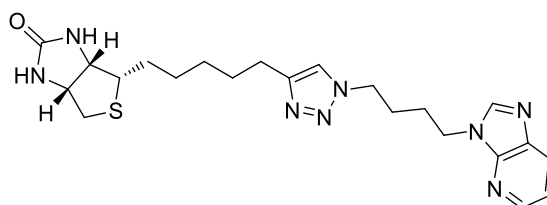
Biotin acetylene **2.21** (30 mg, 0.13 mmol) was reacted with azide **2.47** (28 mg, 0.13 mmol) and Cu nanopowder (2 mg, 0.026 mmol) using General Procedure **A1**. The crude material was purified by flash chromatography on silica eluting with 5% MeOH in DCM to give a crystalline white solid (37 mg, 63%).

_____

^{1}**H NMR** (500 MHz; CDCl$_3$): δ 8.39 (1H, dd, J = 1.3, 4.8 Hz, Ar**H**), 8.08 (1H, d, J = 8.0 Hz, Ar**H**), 8.03 (1H, s, Ar**H**), 7.25 (1H, dd, J = 4.9, 8.1 Hz, Ar**H**), 7.22 (1H, s, Ar^{tri}**H**), 5.70 (1H, bs, C(O)N**H**), 5.21 (1H, bs, C(O)N**H**), 4.48-4.51 (1H, m, NHC**H**), 4.28-4.37 (5H, m, ArN^{tri}C**H$_2$**, NHC**H**, NC**H$_2$**), 3.12-3.16 (1H, m, SC**H**), 2.90 (1H, dd, J = 5.0, 12.8 Hz, SC**H$_b$**), 2.66-2.73 (3H, m, SC**H$_a$**, ArC^{tri}C**H$_2$**), 1.92-1.97 (4H, m, 2 x C**H$_2$**), 1.62-1.69 (4H, m, 2 x C**H$_2$**), 1.34-1.45 (4H, m, 2 x C**H$_2$**);

^{13}**C NMR** (125 MHz; CDCl$_3$): 163.3, 148.3, 144.3, 143.8, 135.4, 128.1, 120.7, 118.4, 62.0, 60.1, 55.7, 49.3, 42.9, 40.5, 29.0, 29.0, 28.7, 28.6, 27.4, 27.1, 25.4;

HRMS calcd. for (M + H+) C$_{22}$H$_{31}$N$_8$OS: requires 455.2342, found 455.2346

HPLC R$_t$ = 12.2 min.

(3aS,4S,6aR)-4-(5-(1-(4-(4-amino-7H-pyrrolo[2,3-d]pyrimidin-7-yl)butyl)-1H-1,2,3-triazol-4-yl)pentyl)tetrahydro-1H-thieno[3,4-d]imidazol-2(3H)-one 2.40
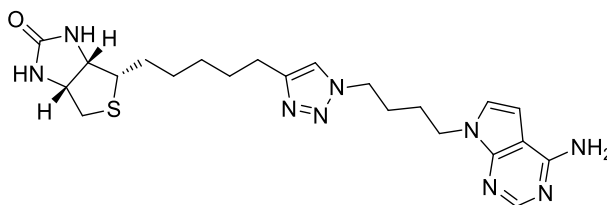
Biotin acetylene **2.21** (30 mg, 0.13 mmol) was reacted with azide **2.48** (30 mg, 0.13 mmol) and Cu nanopowder (2 mg, 0.026 mmol) using General Procedure **A1**. The crude material was purified by flash chromatography on silica eluting with 5% MeOH in DCM to give a crystalline white solid (44 mg, 73%).
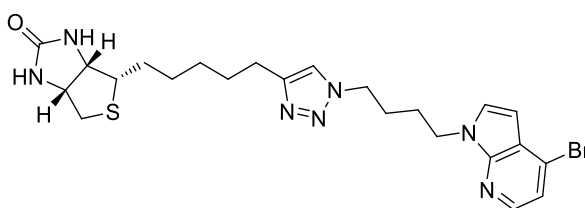
^{1}**H NMR** (500 MHz; CDCl$_3$): δ 8.12 (1H, s, Ar**H**), 8.11 (1H, s, Ar**H**), 7.29 (1H, s, Ar^{tri}**H**), 6.87 (1H, d, J = 3.5 Hz, Ar**H**), 6.41 (1H, d, J = 3.5 Hz, Ar**H**), 6.11 (1H, bs, C(O)N**H**), 5.68 (1H, bs, C(O)N**H**), 4.43-4.46 (1H, m, NHC**H**), 4.24-4.30 (3H, m, ArN^{tri}C**H$_2$**, NHC**H**), 4.09-4.13 (2H, m, NC**H$_2$**), 3.08-3.12 (1H, m, SC**H**), 2.86 (1H, dd, J = 5.0, 12.8 Hz, SC**H$_b$**), 2.60-2.68 (3H, m, SC**H$_a$**, ArC^{tri}C**H$_2$**), 1.74-1.83 (4H, m, 2 x C**H$_2$**), 1.53-1.64 (4H, m, 2 x C**H$_2$**), 1.28-1.41 (4H, m, 2 x C**H$_2$**);

^{13}**C NMR** (125 MHz; CDCl$_3$): 164.0, 157.1, 150.9, 149.4, 147.9, 124.4, 121.0, 103.0, 98.5, 62.1, 60.0, 55.8, 49.8, 43.7, 40.3, 28.8, 28.8, 28.7, 28.4, 27.2, 27.1, 25.1;

HRMS calcd. for (M + H+) C$_{22}$H$_{32}$N$_9$OS: requires 470.2451, found 470.1931

HPLC R$_t$ = 12.2 min.

_____

(3aS,4S,6aR)-4-(5-(1-(4-(4-amino-1H-pyrazolo[3,4-d]pyrimidin-1-yl)butyl)-1H-1,2,3-triazol-4-yl)pentyl)tetrahydro-1H-thieno[3,4-d]imidazol-2(3H)-one 2.41
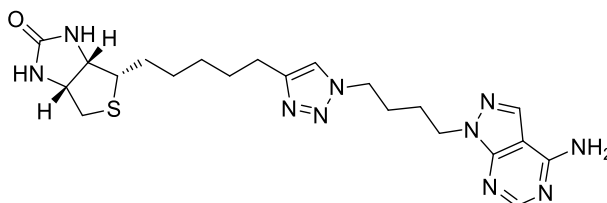

Biotin acetylene **2.21** (30 mg, 0.13 mmol) was reacted with azide **2.49** (32 mg, 0.14 mmol) and Cu nanopowder (2 mg, 0.026 mmol) using General Procedure **A1**. The crude material was purified by flash chromatography on silica eluting with 5% MeOH in DCM to give a crystalline white solid (35 mg, 58%).

^{1}H NMR (500 MHz; DMSO-d_6): δ 8.15 (1H, s, Ar**H**), 8.06 (1H, s, Ar**H**), 7.78 (1H, s, Ar^{tri}**H**), 6.45 (1H, bs, C(O)N**H**), 6.35 (1H, bs, C(O)N**H**), 4.27-4.31 (5H, m, ArN^{tri}C**H$_2$**, NHC**H**, NC**H$_2$**), 4.11-4.14 (1H, m, NHC**H**), 3.07-3.10 (1H, m, SC**H**), 2.81 (1H, dd, J = 5.1, 12.4 Hz, SC**H$_b$**), 2.55-2.58 (3H, m, SC**H$_a$**, ArC^{tri}C**H$_2$**), 1.70-1.74 (4H, m, 2 x C**H$_2$**), 1.29-1.59 (8H, m, 4 x C**H$_2$**);

^{13}C NMR (125 MHz; DMSO-d_6): 163.2, 158.5, 156.2, 153.4, 147.2, 132.3, 122.1, 100.3, 61.5, 596, 56.0, 49.0, 45.9, 29.2, 29.0, 28.8, 28.7, 27.4, 26.6, 25.4;

HRMS calcd. for (M + H$^+$) C$_{21}$H$_{31}$N$_{10}$OS: requires 471.2403, found 471.2406

HPLC R_t = 12.1 min.

(3aS,4S,6aR)-4-(5-(1-(4-(1H-pyrrolo[2,3-b]pyridin-1-yl)butyl)-1H-1,2,3-triazol-4-yl)pentyl)tetrahydro-1H-thieno[3,4-d]imidazol-2(3H)-one 2.42
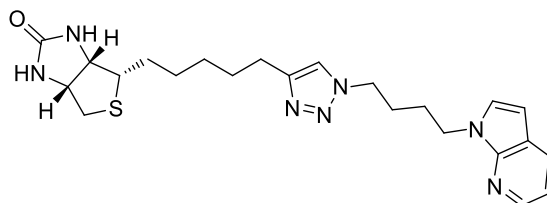
Biotin acetylene **2.21** (30 mg, 0.13 mmol) was reacted with azide **2.50** (30 mg, 0.14 mmol) and Cu nanopowder (2 mg, 0.026 mmol) using General Procedure **A1**. The crude material was purified by flash chromatography on silica eluting with 5% MeOH in DCM to give a crystalline white solid (45 mg, 77%).

¹H NMR (500 MHz; CDCl₃): δ 8.30 (1H, dd, *J* = 1.5, 4.7 Hz, Ar**H**),), 7.91 (1H, dd, *J* = 1.6, 7.8 Hz Ar**H**), 7.17 (1H, d, *J* = 3.3 Hz, Ar**H**), 7.17 (1H, s, Ar^tri**H**), 7.06 (1H, dd, *J* = 4.7, 7.8 Hz, Ar**H**), 6.46 (1H, d, *J* = 3.5 Hz, Ar**H**), 5.22 (1H, bs, C(O)N**H**), 4.94 (1H, bs, C(O)N**H**), 4.48-4.51 (1H, m, NHC**H**), 4.29-4.34 (5H, m, ArN^tri**CH₂**, NHC**H**, NC**H₂**), 3.12-3.16 (1H, m, SC**H**), 2.90 (1H, dd, *J* = 5.0, 12.8 Hz, SC**H**b), 2.66-2.73 (3H, m, SC**H**a, ArC^tri**CH₂**), 1.87-1.91 (4H, m, 2 x C**H₂**), 1.62-1.69 (4H, m, 2 x C**H₂**), 1.36-1.46 (4H, m, 2 x C**H₂**);

¹³C NMR (125 MHz; CDCl₃): 163.0, 148.1, 142.8, 128.9, 127.7, 120.6, 120.5, 115.7, 99.8, 61.9, 60.0, 55.5, 49.4, 43.6, 40.5, 30.9, 29.0, 29.0, 28.7, 28.5, 27.5, 27.4, 25.5;

HRMS calcd. for (M + H⁺) C₂₃H₃₂N₇OS: requires 454.2398, found 454.2365

HPLC R$_t$ = 12.8 min

(3a*S*,4*S*,6a*R*)-4-(5-(1-(4-(4-bromo-1*H*-pyrrolo[2,3-b]pyridin-1-yl)butyl)-1*H*-1,2,3-triazol-4-yl)pentyl)tetrahydro-1*H*-thieno[3,4-*d*]imidazol-2(3*H*)-one 2.43

Biotin acetylene **2.21** (30 mg, 0.13 mmol) was reacted with azide **2.51** (41 mg, 0.14 mmol) and Cu nanopowder (2 mg, 0.026 mmol) using General Procedure **A1**. The crude material was purified by flash chromatography on silica eluting with 5% MeOH in DCM to give a crystalline white solid (52 mg, 75%).

¹H NMR (500 MHz; CDCl₃): δ 8.10 (1H, d, *J* = 5.1 Hz, Ar**H**),), 7.26 (1H, d, *J* = 5.2 Hz Ar**H**), 7.29 (1H, s, Ar^tri**H**), 6.87 (1H, d, *J* = 3.5 Hz, Ar**H**), 6.50 (1H, d, *J* = 3.5 Hz, Ar**H**), 5.75 (1H, bs, C(O)N**H**), 5.34 (1H, bs, C(O)N**H**), 4.47-4.50 (1H, m, NHC**H**), 4.27-4.34 (5H, m, ArN^tri**CH₂**, NHC**H**, NC**H₂**), 3.12-3.15 (1H, m, SC**H**), 2.89 (1H, dd, *J* = 5.0, 12.8 Hz, SC**H**b), 2.66-2.72 (3H, m, SC**H**a, ArC^tri**CH₂**), 1.84-1.90 (4H, m, 2 x C**H₂**), 1.63-1.70 (4H, m, 2 x C**H₂**), 1.36-1.46 (4H, m, 2 x C**H₂**);

¹³C NMR (125 MHz; CDCl₃): 163.4, 148.2, 147.3, 142.9, 128.4, 125.2, 120.6, 119.0, 100.0, 62.0, 60.1, 55.7, 49.4, 44.1, 40.5, 30.9, 29.1, 29.0, 28.7, 28.5, 27.4, 27.3, 25.5;

HRMS calcd. for (M + H⁺) C₂₃H₃₁BrN₇OS: requires 532.1494, found 532.1492

HPLC R$_t$ = 15.7 min.

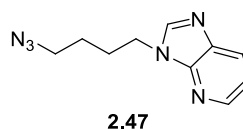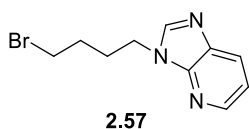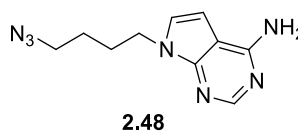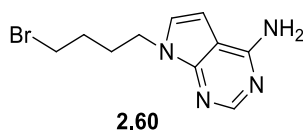### 9-(4-azidobutyl)-6-chloro-9*H*-purine 2.44
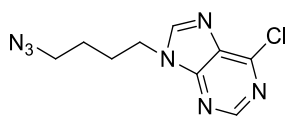
Bromide **2.54** (200 mg, 0.79 mmol) was reacted with NaN_3 (77 mg, 1.18 mmol) according to general procedure **B2** and purified by flash chromatography on silica eluting with 10% MeOH in DCM to yield a white solid (144 mg, 83%)

^{1}H NMR (500 MHz; CDCl$_3$): δ 8.76 (1H, s, Ar**H**), 8.15 (1H, s, Ar**H**), 4.36 (2H, t, *J* = 7.2 Hz, NC**H₂**), 4.38 (2H, t, *J* = 6.7 Hz, N$_3$C**H2**), 2.07-2.04 (2H, m, C**H₂**), 1.67-1.62 (2H, m, C**H₂**);

^{13}C NMR (125 MHz; CDCl$_3$): 152.0, 151.1, 144.9, 133.8, 50.7, 43.9, 27.3, 26.0;

HRMS calcd. for (M + H$^+$) $C_9H_{11}ClN_7$: requires 252.0764, found 252.0760

9-(4-azidobutyl)-6-methoxy-9*H*-purine 2.45
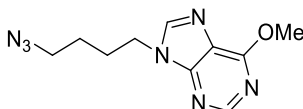
Azide **2.44** (100 mg, 0.40 mmol) was treated with a solution of sodium methoxide (44 mg, 0.81 mmol) in MeOH (2 ml). The reaction mixture was stirred at ambient temperature for 3 h, and the residues was concentrated *in vacuo* and purified by flash chromatography on silica eluting with 5% MeOH in DCM to afford a white solid (71 mg, 72%).

^{1}H NMR (500 MHz; DMSO-*d₆*): δ 8.54(1H, s, Ar**H**), 7.91 (1H, s, Ar**H**), 4.28 (2H, t, *J* = 7.2 Hz, NC**H₂**), 4.19 (3H, s, OC**H₃**), 3.34 (2H, t, *J* = 6.7 Hz, N$_3$C**H2**), 2.03-2.00 (2H, m, C**H₂**), 1.63-1.60 (2H, m, C**H₂**);

^{13}C NMR (125 MHz; DMSO-*d₆*):161.1, 152.1, 141.8, 121.6, 54.2, 50.7, 43.5, 27.4, 26.0;

HRMS calcd. for (M + H$^+$) $C_{10}H_{14}N_7O$: requires 248.1260, found 248.1236

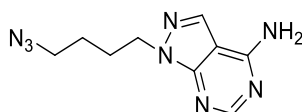### 9-(4-azidobutyl)-9*H*-purine-2,6-diamine 2.46
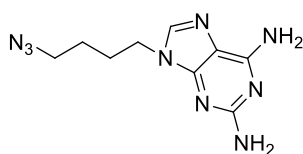
Bromide **2.55** (170 mg, 0.60 mmol) was reacted with NaN_3 (59 mg, 0.90 mmol) according to general procedure **B2** and purified by flash chromatography on silica eluting with 10% MeOH in DCM to yield a white solid (93 mg, 62%)

^{1}H NMR (500 MHz; DMSO-d_6): δ 6.96 (1H, s, Ar**H**), 3.29 (2H, t, J = 7.1 Hz, NC**H$_2$**), 2.53 (2H, t, J = 6.8 Hz, N$_3$C**H$_2$**), 1.07-1.12 (2H, m, C**H$_2$**), 0.74-0.80 (2H, m, C**H$_2$**);

^{13}C NMR (125 MHz; DMSO-d_6): 137.5, 49.7, 41.6, 26.0, 24.8;

HRMS calcd. for (M + H$^+$) $C_9H_{14}N_9$: requires 248.1372, found 248.1365

3-(4-bromobutyl)-3*H*-imidazo[4,5-*b*]pyridine   **2.57**   and   3-(4-azidobutyl)-3*H*-imidazo[4,5-*b*]pyridine 2.47

3*H*-imidazo[4,5-b]pyridine **2.56** (120 mg, 1.01 mmol) and 1,4-dibromobutane (324 mg, 1.50 mmol) was reacted according to general procedure **B1**. The crude material was used for the next step without purification.
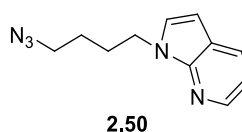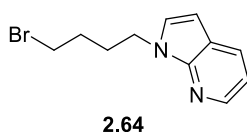
Bromide **2.57** (48 mg, 0.19 mmol) was reacted with NaN_3 (18 mg, 0.29 mmol) according to general procedure **B2** and purified by flash chromatography on silica eluting with 5% MeOH in DCM to yield a white solid (36 mg, 88%)

^{1}H NMR (500 MHz; CDCl$_3$): δ 8.39 (1H, dd, J = 4.8, 1.3 Hz , Ar**H**), 8.06-8.07 (2H, m, 2 x Ar**H**), 7.22-7.26 (1H, m, Ar**H**), 4.33 (2H, t, J = 7.1 Hz, NC**H$_2$**), 3.33 (2H, t, J = 6.8 Hz, N$_3$C**H$_2$**), 2.00-2.06 (2H, m, C**H$_2$**), 1.59-1.65 (2H, m, C**H$_2$**);

^{13}C NMR (125 MHz; CDCl$_3$): 144.3, 142.8, 132.1, 128.5, 128.0, 118.3, 50.8, 43.2, 27.4, 26.2;

HRMS calcd. for (M + H$^+$) $C_{10}H_{13}N_6$: requires 217.1202, found 217.1253

7-(4-bromobutyl)-7*H*-pyrrolo[2,3-*d*]pyrimidin-4-amine 2.60 and 7-(4-azidobutyl)-7*H*-pyrrolo[2,3-*d*]pyrimidin-4-amine 2.48

7*H*-pyrrolo[2,3-d]pyrimidin-4-amine **2.58** (135 mg, 1.01 mmol) and 1,4-dibromobutane (324 mg, 1.50 mmol) was reacted according to general procedure **B1** and the crude material was used for the next step without purification.

Bromide **2.60** (65 mg, 0.24 mmol) was reacted with NaN_3 (23 mg, 0.36 mmol) according to general procedure **B2** and purified by flash chromatography on silica eluting with 10% MeOH in DCM to yield a white solid (52 mg, 93%)

^{1}H NMR (500 MHz; DMSO-d_6): δ 8.02 (1H, s, Ar**H**), 7.14 (1H, d, J = 3.5 Hz , Ar**H**), 6.90 (2H, s, N**H$_2$**), 6.550 (1H, d, J = 3.5 Hz , Ar**H**), 4.11 (2H, t, J = 7.0 Hz, NC**H$_2$**), 3.32 (2H, t, J = 7.0 Hz, N$_3$C**H2**), 1.79-1.76 (2H, m, C**H$_2$**), 1.44-1.41 (2H, m, C**H$_2$**);
^{13}C NMR (125 MHz; DMSO-d_6): 157.9, 152.0, 150.0, 124.4, 102.7, 98.9, 50.7, 43.5, 27.6,
HRMS calcd. for (M + H$^+$) $C_{10}H_{14}N_7$: requires 232.1311, found 232.1219

1-(4-azidobutyl)-1*H*-pyrazolo[3,4-*d*]pyrimidin-4-amine 2.49

Bromide **2.61** (100 mg, 0.37 mmol) was reacted with NaN_3 (36 mg, 0.56 mmol) according to general procedure **B2** and purified by flash chromatography on silica eluting with 10% MeOH in DCM to yield a white solid (40 mg, 47%)

^{1}H NMR (500 MHz; DMSO-d_6): δ 8.13 (1H, s, Ar**H**), 7.92 (1H, s, Ar**H**), 4.28 (2H, t, J = 6.9 Hz, NC**H$_2$**), 3.19 (2H, t, J = 6.8 Hz, N$_3$C**H$_2$**), 1.90-1.84 (2H, m, C**H$_2$**), 1.49-1.42 (2H, m, C**H$_2$**);
^{13}C NMR (125 MHz; DMSO-d_6): 162.0, 159.3, 156.7, 135.8, 104.5, 54.7, 50.3, 30.6, 29.8;
HRMS calcd. for (M + H$^+$) $C_9H_{13}N_8$: requires 233.1263, found 233.1260

1-(4-bromobutyl)-1*H*-pyrrolo[2,3-*b*]pyridine 2.64 and 1-(4-azidobutyl)-1*H*-pyrrolo[2,3-*b*]pyridine 2.50

2.64   **2.50**

1*H*-pyrrolo[2,3-b]pyridine **2.62** (118 mg, 1.01 mmol) and 1,4-dibromobutane (324 mg, 1.50 mmol) was reacted according to general procedure B**1** and was purified by flash chromatography on silica eluting with 5% MeOH in DCM to yield bromide as an off white solid (95 mg, 44 %)
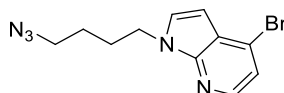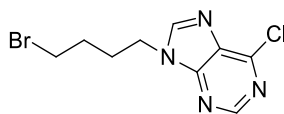
Bromide **2.64** (160 mg, 0.63 mmol) was reacted with NaN$_3$ (61 mg, 0.95 mmol) according to general procedure B**2** and purified by flash chromatography on silica eluting with 10% MeOH in DCM to yield a white solid (122 mg, 90%)

¹H NMR (500 MHz; CDCl$_3$): δ 8.32 (1H, dd, *J* = 4.7, 1.6 Hz , Ar**H**), 7.90 (1H, dd, *J* = 7.8, 1.6 Hz , Ar**H**), 7.21 (1H, d, *J* = 3.5 Hz , Ar**H**), 7.05 (1H, dd, *J* = 7.8, 4.7 Hz , Ar**H**), 6.46 (1H, d, *J* = 3.5 Hz , Ar**H**), 4.33 (2H, t, *J* = 7.0 Hz, NC**H₂**), 3.29 (2H, t, *J* = 6.8 Hz, N$_3$C**H₂**), 2.00-1.94 (2H, m, **CH₂**), 1.63-1.57 (2H, m, **CH₂**);

¹³C NMR (125 MHz; CDCl$_3$): δ 147.5, 142.8, 128.8, 127.7, 120.5, 115.7, 99.6, 51.0, 43.9, 27.7, 26.2;

HRMS calcd. for (M + H⁺) C$_{11}$H$_{14}$N$_5$: requires 216.2490, found 216.2496

1-(4-azidobutyl)-4-bromo-1*H*-pyrrolo[2,3-*b*]pyridine 2.51

Bromide **2.65** (212 mg, 0.64 mmol) was reacted according with NaN$_3$ (62 mg, 0.96 mmol) to general procedure **B2** and purified by flash chromatography on silica eluting with 10% MeOH in DCM to yield azide as brown oil (123 mg, 65%)

¹H NMR (500 MHz; CDCl$_3$): δ 8.11 (1H, d, *J* = 5.1 Hz, Ar**H**), 7.25 (2H, m, 2 x Ar**H**), 6.51 (1H, d, *J* = 3.6 Hz, Ar**H**), 4.31 (2H, t, *J* = 7.0 Hz, NC**H₂**), 3.29 (2H, t, *J* = 6.8 Hz, N$_3$C**H₂**), 1.97-1.94 (2H, m, **CH₂**), 1.59-1.56 (2H, m, **CH₂**);

¹³C NMR (125 MHz; CDCl$_3$): δ150.0, 145.6, 130.9, 127.9, 124.7, 121.60, 102.6, 53.6, 47.0, 30.3, 28.8.

HRMS calcd. for (M + H⁺) C$_{11}$H$_{13}$BrN$_5$: requires 294.0354, found 294.0366
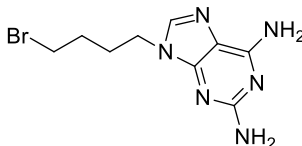
_____

9-(4-bromobutyl)-6-chloro-9*H*-purine 2.54

6-chloro-9*H*-purine **2.52** (154 mg, 1.01 mmol) and 1,4-dibromobutane (324 mg, 1.50 mmol) was reacted according to general procedure **B1** and was purified by flash chromatography on silica eluting with 10% MeOH in DCM to yield bromide as an off white solid (211 mg, 73%)

^{1}H NMR (500 MHz; CDCl$_3$): δ 8.76 (1H, s, Ar**H**), 8.16 (1H, s, Ar**H**), 4.37 (2H, t, *J* = 7.2 Hz, NC**H$_2$**), 3.45 (2H, t, *J* = 6.5 Hz, BrC**H$_2$**), 2.16-2.12 (2H, m, C**H$_2$**), 1.94-1.90 (2H, m, C**H$_2$**);

^{13}C NMR (125 MHz; CDCl$_3$): 152.0, 151.8, 151.1, 131.6, 43.6, 32.2, 29.4, 28.5;

HRMS calcd. for (M + H$^+$) C$_9$H$_{11}$BrClN$_7$: requires 288.9857, found 288.9896

9-(4-bromobutyl)-9*H*-purine-2,6-diamine 2.55

9*H*-purine-2,6-diamine **2.53** (150 mg, 1.01 mmol) and 1,4-dibromobutane (324 mg, 1.50 mmol) was reacted according to general procedure **B1** and was purified by flash chromatography on silica eluting with 10% MeOH in DCM to yield bromide as an off white solid (178 mg, 72%)

^{1}H NMR (500 MHz; DMSO-*d$_6$*): δ 7.69 (1H, s, Ar**H**), 6.60 (2H, s, N**H$_2$**), 5.73 (2H, s, N**H$_2$**), 3.96 (2H, t, *J* = 6.8 Hz, NC**H$_2$**), 3.54 (2H, t, *J* = 6.8 Hz, BrC**H$_2$**), 1.86-1.81 (2H, m, C**H$_2$**), 1.76-1.71 (2H, m, C**H$_2$**);

^{13}C NMR (125 MHz; DMSO-*d$_6$*): 160.7, 156.5, 137.8, 113.6, 41.8, 34.8, 29.8, 28.5;

HRMS calcd. for (M + H$^+$) C$_9$H$_{14}$BrN$_6$: requires 285.0463, found 285.0445

_____

1-(4-bromobutyl)-1*H*-pyrazolo[3,4-*d*]pyrimidin-4-amine 2.61
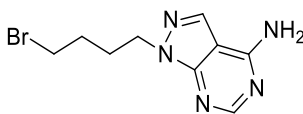
1*H*-pyrazolo[3,4-d]pyrimidin-4-amine **2.59** (135 mg, 1.01 mmol) and 1,4-dibromobutane (324 mg, 1.50 mmol) was reacted according to general procedure **B1** and was purified by flash chromatography on silica eluting with 10% MeOH in DCM to yield bromide as an off white solid (116 mg, 50%)

^{1}H NMR (500 MHz; DMSO-d_6): δ 8.15 (1H, s, Ar**H**), 8.06 (1H, s, Ar**H**), 4.28 (2H, t, J = 6.8 Hz, NC**H2**), 3.52 (2H, t, J = 6.8 Hz, BrC**H2**), 1.93-1.87 (2H, m, C**H2**), 1.74-1.68 (2H, m, C**H2**);

^{13}C NMR (125 MHz; DMSO-d_6): 158.5, 156.3, 153.4, 132.3, 100.3, 45.6, 34.8, 29.9, 28.2

HRMS calcd. for (M + H$^+$) $C_9H_{13}BrN_5$: requires 270.0354, found 270.0335

1-(4-bromobutyl)-4-bromo-1*H*-pyrrolo[2,3-*b*]pyridine 2.65
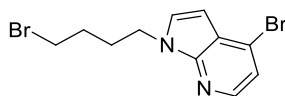
4-bromo-1*H*-pyrrolo[2,3-b]pyridine **2.62** (197 mg, 1.01 mmol) and 1,4-dibromobutane (324 mg, 1.50 mmol) was reacted according to general procedure **B1** and was purified by flash chromatography on silica eluting with 10% MeOH in DCM to yield bromide as an off white solid (98 mg, 33%)

^{1}H NMR (500 MHz; CDCl$_3$): δ 8.10 (1H, d, J = 5.1 Hz, Ar**H**), 7.26 (2H, m, 2 x Ar**H**), 6.51 (1H, d, J = 3.6 Hz, Ar**H**), 4.32 (2H, t, J = 7.0 Hz, NC**H2**), 3.41 (2H, t, J = 6.6 Hz, BrC**H2**), 2.05-2.02 (2H, m, C**H2**), 1.86-1.83 (2H, m, C**H2**);

^{13}C NMR (125 MHz; CDCl$_3$): 147.3, 142.9, 128.2, 125.1, 122.0, 118.9, 99.9, 44.0, 32.9, 29.7, 28.9;

HRMS calcd. for (M + H$^+$) $C_{11}H_{13}Br_2N_2$: requires 330.9445, found 330.9495

7.5 Experimental work as described in Chapter 3

2-(azidomethyl)phenol 3.03a and (3a*S*,4*S*,6a*R*)-4-(5-(1-(2-hydroxybenzyl)-1*H*-1,2,3-triazol-4-yl)pentyl)tetrahydro-1*H*-thieno[3,4-d]imidazol-2(3*H*)-one 3.01a

3.03a   **3.01a**
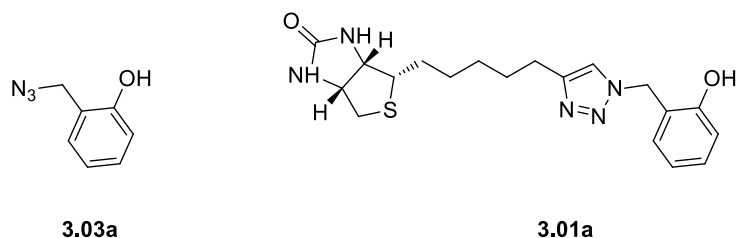
Benzyl alcohol **3.02a** (125 mg, 1.00 mmol) was reacted with P(O)Ph₃ (333 mg, 1.20 mmol), NaN₃ (78 mg, 1.20 mmol) in 1 :4 CCl₄/DMF (10 mL) according to general procedure **C1**. Crude **3.03a** was used in the next step without further purification.

Biotin acetylene **2.21** (50 mg, 0.21 mmol) was reacted with crude azide **3.03a** (37 mg) and Cu nanopowder (4 mg, 0.05 mmol) using General Procedure **A2**. The crude material was purified by flash chromatography on silica gel eluting with 5% MeOH in DCM to give **3.01a** as a crystalline white solid (69 mg, 85%).

^{1}H NMR (500 MHz; DMSO-d_6): δ 9.84 (1H, bs, **OH**), 7.71 (1H, s, Ar^{tri}**H**), 7.13 (1H, m, Ar**H**), 6.98-6.66 (1H, m, Ar**H**), 6.84 (1H, d, *J* = 8.0 Hz, Ar**H**), 6.75 (1H, td, *J* = 7.4, 1.2 Hz, Ar**H**), 6.40 (1H, bs, N**H**), 6.33 (1H, bs, N**H**), 5.40 (2H, s, ArN^{tri}**CH₂**), 4.30-4.26 (1H, m, NHC**H**), 4.11-4.08 (1H, m, NHC**H**), 3.09-3.05 (1H, m, SC**H**), 2.79 (1H, dd, *J* = 12.4, 5.1 Hz, SC**H$_a$**), 2.57-2.52 (3H, m, SC**H$_b$**, ArC^{tri}**CH₂**), 1.61-1.27 (8H, m, 4 x **CH₂**);
^{13}C NMR (125 MHz; DMSO-d_6): 163.1, 155.5, 130.1, 130.0, 122.6, 22.3, 119.5, 61.5, 59.6, 56.0, 48.6, 29.3, 29.1, 28.8, 28.7, 25.4;
HRMS calcd. for (M + H⁺) C₁₉H₂₆N₅O₂S: requires 388.1807, found 388.1790.
HPLC R_t = 14.10 min

3-(azidomethyl)phenol 3.03b and (3a*S*,4*S*,6a*R*)-4-(5-(1-(3-hydroxybenzyl)-1*H*-1,2,3-triazol-4-yl)pentyl)tetrahydro-1*H*-thieno[3,4-d]imidazol-2(3*H*)-one 3.01b

3.03b   **3.01b**
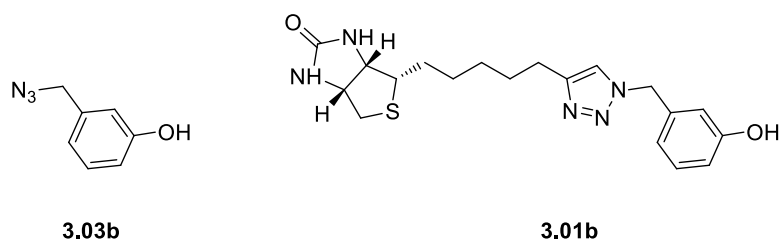
Benzyl alcohol **3.02b** (125 mg, 1.00 mmol) was reacted with P(O)Ph$_3$ (333 mg, 1.20 mmol), NaN$_3$ (78 mg, 1.20 mmol) in 1 :4 CCl$_4$/DMF (10 mL) according to general procedure **C1**. Crude **3.03b** was used in the next step without further purification.

Biotin acetylene **2.21** (30 mg, 0.13 mmol) was reacted with crude azide **3.03b** (24 mg) and Cu nanopowder (2 mg, 0.03 mmol) using General Procedure **A2**. The crude material was purified by flash chromatography on silica gel eluting with 5% MeOH in DCM to give **3.01b** as a crystalline white solid (38 mg, 77%).

^{1}H NMR (500 MHz; DMSO-d_6): δ 9.48 (1H, bs, O**H**), 7.83 (1H, s, Ar^{tri}**H**), 7.13 (1H, t, J = 7.9 Hz, Ar**H**), 6.68-6.66 (2H, m, 2 x Ar**H**), 6.61-6.60 (1H, m, Ar**H**), 6.40 (1H, bs, N**H**), 6.32 (1H, bs, N**H**), 5.41 (2H, s, ArN^{tri}C**H$_2$**), 4.27 (1H, dd, J = 7.5, 4.9 Hz, NHC**H**), 4.11-4.08 (1H, m, NHC**H**), 3.09-3.05 (1H, m, SC**H**), 2.79 (1H, dd, J = 12.4, 5.1 Hz, SC**H$_a$**), 2.59-2.54 (3H, m, SC**H$_b$**, ArC^{tri}C**H$_2$**), 1.59-1.29 (8H, m, 4 x C**H$_2$**);

^{13}C NMR (125 MHz; DMSO-d_6): 167.9, 162.8, 152.4, 142.8, 134.9, 134.9, 127.1, 123.4, 120.1, 119.6, 65.2, 64.4, 60.7, 57.8, 34.0, 33.8, 33.5, 33.4, 30.2;

HRMS calcd. for (M + H$^+$) C$_{19}$H$_{26}$N$_5$O$_2$S: requires 388.1807, found 388.1787.

HPLC R$_t$ = 13.97 min

4-(azidomethyl)phenol 3.03c and (3aS,4S,6aR)-4-(5-(1-(4-hydroxybenzyl)-1H-1,2,3-triazol-4-yl)pentyl)tetrahydro-1H-thieno[3,4-d]imidazol-2(3H)-one 3.01c
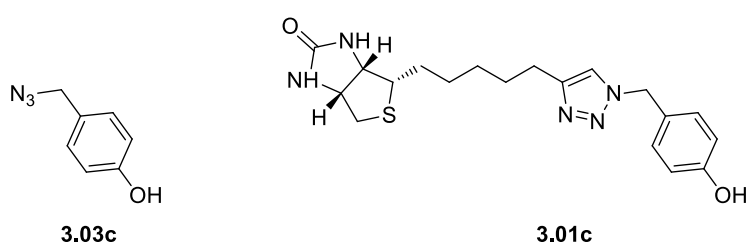
Benzyl alcohol **3.02c** (125 mg, 1.00 mmol) was reacted with P(O)Ph$_3$ (333 mg, 1.20 mmol), NaN$_3$ (78 mg, 1.20 mmol) in 1 :4 CCl$_4$/DMF (10 mL) according to general procedure **C1**. Crude **3.03c** was used in the next step without further purification.

Biotin acetylene **2.21** (30 mg, 0.13 mmol) was reacted with crude azide **3.03c** (24 mg) and Cu nanopowder (2 mg, 0.03 mmol) using General Procedure **A2**. The crude material was purified by flash chromatography on silica gel eluting with 5% MeOH in DCM to give **3.01c** as a crystalline white solid (52 mg, 84%).

¹H NMR (500 MHz; DMSO-d_6): δ 9.48 (1H, bs, O**H**), 7.78 (1H, s, Ar^{tri}**H**), 7.12 (2H, d, J = 8.3 Hz, 2 x Ar**H**), 6.72-6.70 (2H, m, 2 x Ar**H**), 6.40 (1H, bs, N**H**), 6.33 (1H, bs, N**H**), 5.35 (2H, s, ArN^{tri}C**H₂**), 4.29-4.26 (1H, m, NHC**H**), 4.11-4.08 (1H, m, NHC**H**), 3.08-3.04 (1H, m, SC**H**), 2.79 (1H, dd, J = 12.4, 5.2 Hz, SC**H$_a$**), 2.56-2.53 (3H, m, SC**H$_b$**, ArC^{tri}C**H₂**), 1.60-1.28 (8H, m, 4 x C**H₂**);

¹³C NMR (125 MHz; DMSO-d_6): 163.1, 157.7, 147.5, 129.9, 126.9, 121.9, 115.8, 61.5, 59.6, 56.0, 52.8, 29.2, 29.1, 28.8, 28.7, 25.4;

HRMS calcd. for (M + Na⁺) $C_{19}H_{25}N_5NaO_2S$: requires 410.1627, found 410.1606.

HPLC R_t = 13.66 min

1-(azidomethyl)-2-methoxybenzene 3.03d and (3a*S*,4*S*,6a*R*)-4-(5-(1-(2-methoxybenzyl)-1*H*-1,2,3-triazol-4-yl)pentyl)tetrahydro-1*H*-thieno[3,4-*d*]imidazol-2(3*H*)-one 3.01d

3.03d   **3.01d**
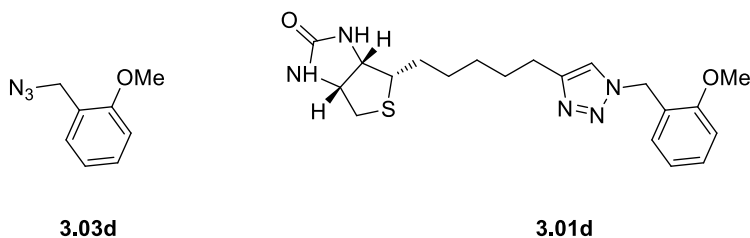
Benzyl alcohol **3.02d** (140 mg, 1.00 mmol) was reacted with P(O)Ph₃ (333 mg, 1.20 mmol), NaN₃ (78 mg, 1.20 mmol) in 1 :4 CCl₄/DMF (11 mL) according to general procedure **C1**. Crude **3.03d** was used in the next step without further purification.

Biotin acetylene **2.21** (30 mg, 0.13 mmol) was reacted with crude azide **3.03d** (25 mg) and Cu nanopowder (2 mg, 0.03 mmol) using General Procedure **A2**. The crude material was purified by flash chromatography on silica gel eluting with 5% MeOH in DCM to give **3.01d** as a crystalline white solid (45 mg, 90%).

¹H NMR (500 MHz; CDCl₃): δ 7.30 (1H, dd, J = 7.6, 8.4 Hz, Ar**H**), 7.21 (1H, s, Ar^{tri}**H**), 6.89 (1H, dd, J = 8.4, 2.6 Hz, Ar**H**), 6.85 (1H, d, J = 7.5 Hz, Ar**H**), 6.79 (1H, t, J = 2.1 Hz, Ar**H**), 5.47 (2H, s, ArN^{tri}C**H₂**), 4.80 (1H, bs, N**H**), 4.63 (1H, bs, N**H**), 4.52-4.50 (1H, m, NHC**H**), 4.33-4.30 (1H, m, NHC**H**), 3.80 (3H, s, OC**H₃**), 3.18-3.14 (1H, m, SC**H**), 2.93 (1H, dd, J = 12.8, 5.1 Hz, SC**H$_a$**), 2.74-2.68 (3H, m, SC**H$_b$**, ArC^{tri}C**H₂**), 1.71-1.63 (4H, m, 2 x C**H₂**), 1.47-1.38 (4H, m, 2 x C**H₂**);

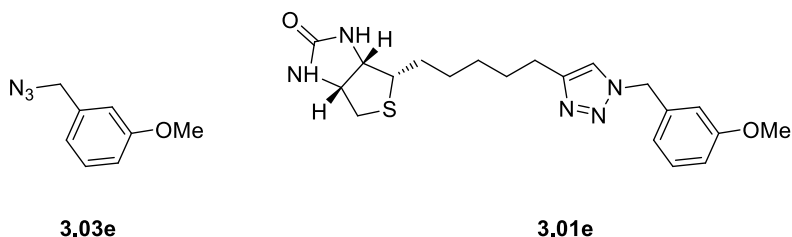**¹³C NMR** (125 MHz; CDCl₃): 160.1, 136.4, 130.1, 120.6, 120.2, 114.1, 113.6, 61.9, 60.0, 55.4, 55.3, 54.0, 40.5, 29.0, 29.0, 28.7, 28.6, 25.5;

HRMS calcd. for (M + H⁺) C₂₀H₂₈N₅O₂S: requires 402.1964, found 402.1945.

HPLC R$_t$ = 15.11 min

1-(azidomethyl)-3-methoxybenzene 3.03e and (3a*S*,4*S*,6a*R*)-4-(5-(1-(3-methoxybenzyl)-1*H*-1,2,3-triazol-4-yl)pentyl)tetrahydro-1*H*-thieno[3,4-*d*]imidazol-2(3*H*)-one 3.01e

Benzyl alcohol **3.02e** (140 mg, 1.00 mmol) was reacted with P(O)Ph₃ (333 mg, 1.20 mmol), NaN₃ (78 mg, 1.20 mmol) in 1 :4 CCl₄/DMF (11 mL) according to general procedure **C1**. Crude **3.03e** was used in the next step without further purification.

Biotin acetylene **2.21** (30 mg, 0.13 mmol) was reacted with crude azide **3.03e** (25 mg) and Cu nanopowder (2 mg, 0.03 mmol) using General Procedure **A2**. The crude material was purified by flash chromatography on silica gel eluting with 5% MeOH in DCM to give **3.01e** as a crystalline white solid (38 mg, 73%).

¹H NMR (500 MHz; CDCl₃): δ 7.29-7.26 (1H, m, Ar**H**), 7.20 (1H, s, Ar^tri**H**), 6.87 (1H, dd, *J* = 8.2, 2.6 Hz, Ar**H**), 6.84 (1H, d, *J* = 7.2 Hz, Ar**H**), 6.77 (1H, s, Ar**H**), 5.45 (3H, bs, N**H**, ArN^tri**CH₂**), 5.09 (1H, bs, N**H**), 4.50-4.47 (1H, m, NHC**H**), 4.30-4.27 (1H, m, NHC**H**), 3.78 (3H, s, OC**H₃**), 3.15-3.11 (1H, m, SC**H**), 2.89 (1H, dd, *J* = 12.8, 5.0 Hz, SC**H**$_a$), 2.72-2.67 (3H, m, SC**H**$_b$, ArC^tri**CH₂**), 1.70-1.62 (4H, m, 2 x C**H₂**), 1.45-1.36 (4H, m, 2 x C**H₂**);

¹³C NMR (125 MHz; CDCl₃): 163.2, 160.0, 148.6, 130.1, 120.6, 120.1, 114.1, 113.6, 62.0, 60.1, 55.6, 55.3, 53.9, 41.0, 40.5, 39.0, 28.7, 28.5, 25.5;

HRMS calcd. for (M + H⁺) C₂₀H₂₈N₅O₂S: requires 402.1964, found 402.1944.

HPLC R$_t$ = 15.12 min

1-(azidomethyl)-4-methoxybenzene 3.03f and (3a*S*,4*S*,6a*R*)-4-(5-(1-(4-methoxybenzyl)-1*H*-1,2,3-triazol-4-yl)pentyl)tetrahydro-1*H*-thieno[3,4-*d*]imidazol-2(3*H*)-one 3.01f

3.03f   **3.01f**
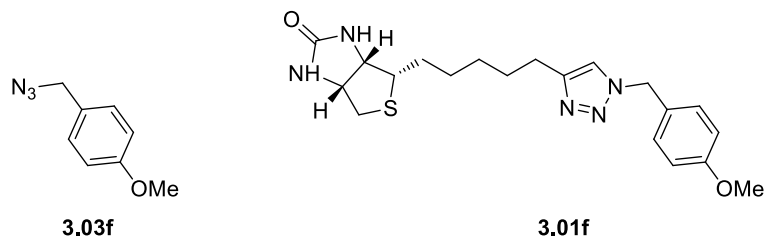
Benzyl alcohol **3.02f** (140 mg, 1.0 mmol) was reacted with P(O)Ph$_3$ (333 mg, 1.20 mmol), NaN$_3$ (78 mg, 1.20 mmol) in 1 :4 CCl$_4$/DMF (11 mL) according to general procedure **C1**. Crude **3.03f** was used in the next step without further purification.

Biotin acetylene **2.21** (30 mg, 0.13 mmol) was reacted with crude azide **3.03f** (25 mg) and Cu nanopowder (2 mg, 0.03 mmol) using General Procedure **A2**. The crude material was purified by flash chromatography on silica gel eluting with 5% MeOH in DCM to give **3.01f** as a crystalline white solid (40 mg, 75%).

^{1}H NMR (500 MHz; CDCl$_3$): δ 7.2 (2H, d, *J* = 8.4 Hz, 2 x Ar**H**), 7.15 (1H, s, Ar^{tri}**H**), 6.69 (2H, d, *J* = 8.7 Hz, 2 x Ar**H**), 5.50 (1H, bs, N**H**), 5.41 (2H, s, ArN^{tri}**CH$_2$**), 5.13 (1H, bs, N**H**), 4.50-4.47 (1H, m, NHC**H**), 4.30-4.27 (1H, m, NHC**H**), 3.80 (3H, s, OC**H$_3$**), 3.15-3.11 (1H, m, SC**H**), 2.89 (1H, dd, *J* = 12.8, 5.0 Hz, SC**H$_a$**), 2.72-2.64 (3H, m, SC**H$_b$**, ArC^{tri}**CH$_2$**), 1.70-1.62 (4H, m, m, 2 x C**H$_2$**), 1.44-1.37 (4H, m, m, 2 x C**H$_2$**);
^{13}C NMR (125 MHz; CDCl$_3$): 163.2, 159.8, 148.5, 129.5, 126.9, 120.3, 114.4, 61.9, 60.1, 55.6, 55.3, 53.5, 40.5, 29.1, 29.0, 28.7, 28.5, 25.6;
HRMS calcd. for (M + H$^+$) C$_{20}$H$_{28}$N$_5$O$_2$S: requires 402.1964, found 402.1943.
HPLC R$_t$ = 15.00 min

2-(azidomethyl)aniline 3.03g and (3a*S*,4*S*,6a*R*)-4-(5-(1-(2-aminobenzyl)-1*H*-1,2,3-triazol-4-yl)pentyl)tetrahydro-1*H*-thieno[3,4-*d*]imidazol-2(3*H*)-one 3.01g

3.03g   **3.01g**
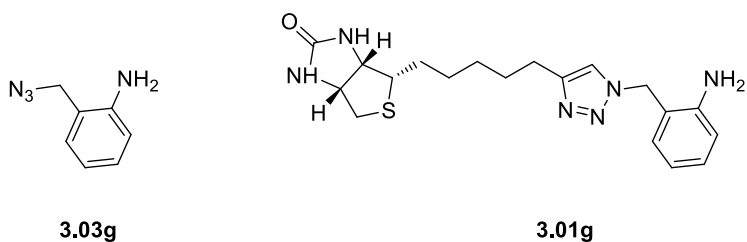
Benzyl alcohol **3.02g** (125 mg, 1.00 mmol) was reacted with P(O)Ph$_3$ (333 mg, 1.20 mmol), NaN$_3$ (78 mg, 1.20 mmol) in 1 :4 CCl$_4$/DMF (10 mL) according to general procedure **C1**. Crude **3.03g** was used in the next step without further purification.
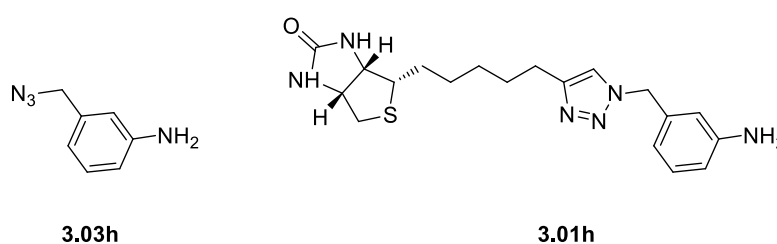
Biotin acetylene **2.21** (50 mg, 0.21 mmol) was reacted with crude azide **3.03g** (37 mg) and Cu nanopowder (4 mg, 0.05 mmol) using General Procedure **A2**. The crude material was purified by flash chromatography on silica gel eluting with 5% MeOH in DCM to give **3.01g** as a crystalline white solid (19 mg, 24%).

¹H NMR (500 MHz; DMSO-d_6): δ 7.76 (1H, s, Ar^{tri}**H**), 7.00 (1H, t, J = 7.6 Hz, Ar**H**), 6.88 (1H, d, J = 7.6 Hz, Ar**H**), 6.65 (1H, d, J = 7.9 Hz, Ar**H**), 6.88 (1H, t, J = 7.6 Hz, Ar**H**), 6.40 (1H, bs, N**H**), 6.33 (1H, bs, N**H**), 5.36 (2H, s, ArN^{tri}**CH$_2$**), 5.18 (2H, bs, N**H$_2$**), 4.29-4.26 (1H, m, NHC**H**), 4.10-4.08 (1H, m, NHC**H**), 3.08-3.05 (1H, m, SC**H**), 2.79 (1H, dd, J = 12.3, 5.1 Hz, SC**H$_a$**), 2.57-2.54 (3H, m, SC**H$_b$**, ArC^{tri}**CH$_2$**), 1.60-1.22 (8H, m, 4 x **CH$_2$**);

¹³C NMR (125 MHz; DMSO-d_6): 163.1, 147.4, 146.9, 130.0, 129.5, 122.3, 119.6, 116.7, 115.8, 61.5, 59.6, 56.0, 50.0, 29.2, 29.1, 28.8, 28.7, 25.4;

HRMS calcd. for (M + H$^+$) C$_{19}$H$_{27}$N$_6$OS: requires 387.1967, found 387.1940.

HPLC R$_t$ = 13.33 min

3-(azidomethyl)aniline 3.03h and (3aS,4S,6aR)-4-(5-(1-(3-aminobenzyl)-1H-1,2,3-triazol-4-yl)pentyl)tetrahydro-1H-thieno[3,4-d]imidazol-2(3H)-one 3.01h

3.03h   **3.01h**

Benzyl alcohol **3.02h** (125 mg, 1.0 mmol) was reacted with P(O)Ph$_3$ (333 mg, 1.20 mmol), NaN$_3$ (78 mg, 1.20 mmol) in 1 :4 CCl$_4$/DMF (10 mL) according to general procedure **C1**. Crude **3.03h** was used in the next step without further purification.

Biotin acetylene **2.21** (50 mg, 0.21 mmol) was reacted with crude azide **3.03h** (37 mg) and Cu nanopowder (4 mg, 0.05 mmol) using General Procedure **A2**. The crude material was purified by flash chromatography on silica gel eluting with 5% MeOH in DCM to give **3.01h** as a crystalline white solid (26 mg, 33%).

¹H NMR (500 MHz; CDCl₃): δ 7.19 (1H, s, Ar^{tri}**H**), 7.14 (1H, t, *J* = 7.8 Hz, Ar**H**), 6.66-6.64 (2H, m, 2 x Ar**H**), 6.52-6.51 (1H, m, Ar**H**), 5.39 (2H, s, ArN^{tri}**CH₂**), 4.82 (1H, bs, N**H**), 4.61 (1H, bs, N**H**), 4.52-4.49 (1H, m, NHC**H**), 4.31-4.28 (1H, m, NHC**H**), 3.16-3.12 (1H, m, SC**H**), 2.92 (1H, dd, *J* = 12.8, 5.0 Hz, SC**H_a**), 2.73-2.67 (3H, m, SC**H_b**, ArC^{tri}**CH₂**), 1.68-1.61 (4H, m, 2 x **CH₂**), 1.45-1.35 (4H, m, 2 x **CH₂**);

¹³C NMR (125 MHz; CDCl₃): 162.6, 148.4, 147.1, 136.1, 130.0, 120.6, 117.9, 115.2, 114.2, 61.9, 60.0, 55.4, 54.0, 40.5, 29.0, 28.9, 28.7, 28.6, 25.5;

HRMS calcd. for (M + H⁺) $C_{19}H_{27}N_6OS$: requires 387.1967, found 387.1967.

HPLC R_t = 12.12 min

4-(azidomethyl)aniline 3.03i and (3a*S*,4*S*,6a*R*)-4-(5-(1-(4-aminobenzyl)-1*H*-1,2,3-triazol-4-yl)pentyl)tetrahydro-1*H*-thieno[3,4-*d*]imidazol-2(3*H*)-one 3.01i

3.03i   **3.01i**
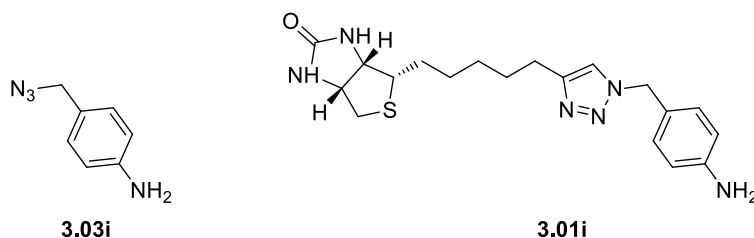
Benzyl alcohol **3.02i** (125 mg, 1.00 mmol) was reacted with P(O)Ph₃ (333 mg, 1.20 mmol), NaN₃ (78 mg, 1.20 mmol) in 1 :4 CCl₄/DMF (10 mL) according to general procedure **C1**. Crude **3.03i** was used in the next step without further purification.

Biotin acetylene **2.21** (50 mg, 0.21 mmol) was reacted with crude azide **3.03i** (46 mg) and Cu nanopowder (4 mg, 0.05 mmol) using General Procedure **A2**. The crude material was purified by flash chromatography on silica gel eluting with 5% MeOH in DCM to give **3.01i** as a crystalline white solid (28 mg, 35%).

¹H NMR (500 MHz; DMSO-*d₆*): δ 7.72 (1H, s, Ar^{tri}**H**), 6.98 (2H, d, *J* = 8.2 Hz, 2 x Ar**H**), 6.49 (2H, d, *J* = 8.2 Hz, 2 x Ar**H**), 6.40 (1H, bs, N**H**), 6.32 (1H, bs, N**H**), 5.26 (2H, s, ArN^{tri}**CH₂**), 5.12 (2H, bs, N**H₂**), 4.29-4.26 (1H, m, NHC**H**), 4.11-4.08 (1H, m, NHC**H**), 3.08-3.04 (1H, m, SC**H**), 2.79 (1H, dd, *J* = 12.5, 5.1 Hz, SC**H_a**), 2.56-2.52 (3H, m, SC**H_b**, ArC^{tri}**CH₂**), 1.54-1.29 (8H, m, 4 x **CH₂**);

¹³C NMR (125 MHz; DMSO-*d₆*): 163.1, 149.1, 147.5, 129.6, 123.2, 121.7, 114.1, 61.5, 59.6, 56.0, 53.2, 29.2, 29.1, 28.8, 28.7, 25.4;

HRMS calcd. for (M + H) $C_{19}H_{27}N_6OS$: requires 387.1967, found 387.1942.

HPLC R_t = 12.30 min

1-(azidomethyl)-3-methylbenzene 3.03j and (3a*S*,4*S*,6a*R*)-4-(5-(1-(3-methylbenzyl)-1*H*-1,2,3-triazol-4-yl)pentyl)tetrahydro-1*H*-thieno[3,4-*d*]imidazol-2(3*H*)-one 3.01j

3.03j   3.01j
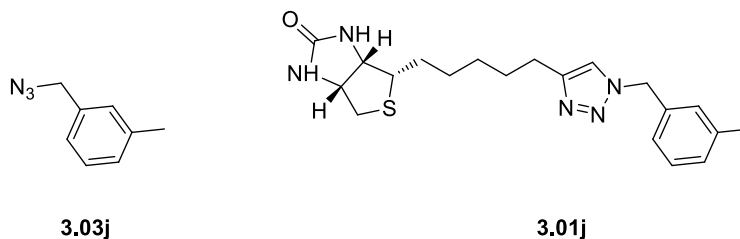
Benzyl bromide **3.04j** (185 mg, 1.00 mmol) was reacted with NaN$_3$ (78 mg, 1.20 mmol) in DMF (6 mL) according to general procedure **C2**. Crude **3.03j** was used in the next step without further purification.

Biotin acetylene **2.21** (30 mg, 0.13 mmol) was reacted with crude azide **3.03j** (22 mg) and Cu nanopowder (2 mg, 0.03 mmol) using General Procedure **A2**. The crude material was purified by flash chromatography on silica gel eluting with 3% MeOH in DCM to give **3.01j** as a crystalline white solid (37 mg, 74%).

^{1}H NMR (500 MHz; CDCl$_3$): δ 7.27-7.21 (2H, m, Ar**H**, Ar^{tri}**H**), 7.15 (1H, d, *J* = 7.6 Hz, Ar**H**), 7.07-7.04 (2H, m, 2 x Ar**H**), 5.44 (2H, s, ArN^{tri}**CH$_2$**), 5.33 (1H, bs, **NH**), 5.00 (1H, bs, **NH**), 4.49 (1H, dd, *J* = 7.7, 4.9 Hz, NHC**H**), 4.30-4.28 (1H, m, NHC**H**), 3.16-3.12 (1H, m, SC**H**), 2.90 (1H, dd, *J* = 12.8, 5.0 Hz, SC**H$_a$**), 2.72-2.66 (3H, m, C**H$_3$**), 2.34 (3H, s, SC**H$_b$**, ArC^{tri}**CH$_2$**), 1.69-1.64 (4H, m, 2 x C**H$_2$**), 1.44-1.38 (4H, m, 2 x C**H$_2$**);
^{13}C NMR (125 MHz; CDCl$_3$): 163.1, 138.9, 134.8, 129.4, 128.9, 128.7, 125.1, 61.9, 60.1, 64.0, 40.5, 29.0, 28.9, 28.7, 28.5, 25.6, 21.3;
HRMS calcd. for (M + H$^+$) C$_{20}$H$_{28}$N$_5$OS: requires 386.2015, found 386.2007.
HPLC R$_t$ = 14.19 min

1-(azidomethyl)-4-methylbenzene 3.03k and (3a*S*,4*S*,6a*R*)-4-(5-(1-(4-methylbenzyl)-1*H*-1,2,3-triazol-4-yl)pentyl)tetrahydro-1*H*-thieno[3,4-*d*]imidazol-2(3*H*)-one 3.01k

3.03k   3.01k
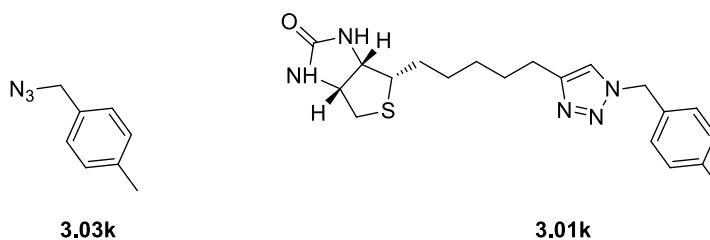
Benzyl bromide **3.04k** (200 mg, 1.10 mmol) was reacted with NaN_3 (78 mg, 1.20 mmol) in DMF (6 mL) according to general procedure **C2**. Crude **3.03k** was used in the next step without further purification.

Biotin acetylene **2.21** (30 mg, 0.13 mmol) was reacted with azide **3.03k** (19 mg) and Cu nanopowder (2 mg, 0.03 mmol) using General Procedure **A2**. The crude material was purified by flash chromatography on silica gel eluting with 3% MeOH in DCM to give **3.01k** as a crystalline white solid (34 mg, 68%).

^{1}H NMR (500 MHz; CDCl$_3$): δ 7.18-7.14 (5H, m, 4 x Ar**H**, Ar^{tri}**H**), 5.65 (1H, bs, N**H**), 5.44 (2H, s, ArN^{tri}C**H$_2$**), 5.26 (1H, bs, N**H**), 4.80-4.47 (1H, m, NHC**H**), 4.30-4.27 (1H, m, NHC**H**), 3.14-3.12 (1H, m, SC**H**), 2.89 (1H, dd, J = 12.8, 5.0 Hz, SC**H$_a$**), 2.72-2.65 (3H, s, , SC**H$_b$**, ArC^{tri}C**H$_2$**), 2.37 (3H, s, C**H$_3$**), 1.70-1.62 (4H, m, 2 x C**H$_2$**), 1.45-1.36 (4H, m, 2 x C**H$_2$**);

^{13}C NMR (125 MHz; CDCl$_3$): 163.4, 148.6, 138.5, 131.9, 129.7, 128.0, 120.5, 62.0, 60.1, 55.7, 53.8, 40.5, 29.1, 29.0, 28.7, 28.5, 25.6, 21.2;

HRMS calcd. for (M + H$^+$) C$_{20}$H$_{28}$N$_5$OS: requires 386.2015, found 386.2009.

HPLC R$_t$ = 12.37 min

1-(azidomethyl)-3-(trifluoromethyl)benzene 3.03l and (3a*S*,4*S*,6a*R*)-4-(5-(1-(3-(trifluoromethyl)benzyl)-1*H*-1,2,3-triazol-4-yl)pentyl)tetrahydro-1*H*-thieno[3,4-*d*]imidazol-2(3*H*)-one 3.01l

3.03l   3.01l
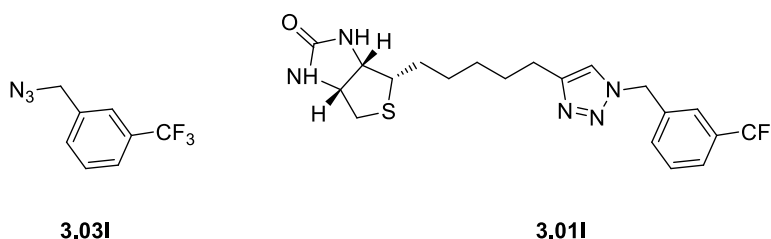
Benzyl bromide **3.04l** (240 mg, 1.00 mmol) was reacted with NaN_3 (78 mg, 1.20 mmol) in DMF (6 mL) according to general procedure **C2**. Crude **3.03l** was used in the next step without further purification.

Biotin acetylene **2.21** (30 mg, 0.13 mmol) was reacted with crude azide **3.03l** (32 mg) and Cu nanopowder (2 mg, 0.03 mmol) using General Procedure **A2**. The crude material was

purified by flash chromatography on silica gel eluting with 5% MeOH in DCM to give **3.01l** as a crystalline white solid (53 mg, 85%).

^{1}H NMR (500 MHz; CDCl$_3$): δ 7.61-7.59 (1H, m, Ar**H**), 7.51-7.48 (2H, m, 2 x Ar**H**), 7.42-7.41 (1H, m, Ar**H**), 7.24 (1H, s, Ar^{tri}**H**), 5.59 (1H, bs, N**H**), 5.55 (2H, s, ArN^{tri}**CH$_2$**), 5.21 (1H, bs, N**H**), 4.47-4.50 (1H, m, NHC**H**), 4.30-4.27 (1H, m, NHC**H**), 3.15-3.11 (1H, m, SC**H**), 2.89 (1H, dd, *J* = 12.8, 5.0 Hz, SC**H$_a$**), 2.72-2.68 (3H, m, SC**H$_b$**, ArC^{tri}**CH$_2$**), 1.72-1.61 (4H, m, 2 x **CH$_2$**), 1.45-1.36 (4H, m, 2 x **CH$_2$**);

^{13}C NMR (125 MHz; CDCl$_3$): 163.3, 149.0, 136.0, 131.2, 129.7, 125.5 (q, *J* = 3.7 Hz), 124.5 (q, *J* = 3.7 Hz), 120.7, 62.0, 60.1, 55.6, 53.3, 40.5, 29.0, 28.9, 28.7, 28.5, 25.5;

^{19}F NMR (125 MHz; CDCl$_3$): δ -62.7;

HRMS calcd. for (M + K$^+$) C$_{20}$H$_{24}$F$_3$N$_5$KOS: requires 478.1291, found 478.1268.

HPLC R$_t$ = 16.13 min

1-(azidomethyl)-4-(trifluoromethyl)benzene 3.03m and (3a*S*,4*S*,6a*R*)-4-(5-(1-(4-(trifluoromethyl)benzyl)-1*H*-1,2,3-triazol-4-yl)pentyl)tetrahydro-1*H*-thieno[3,4-*d*]imidazol-2(3*H*)-one 3.01m
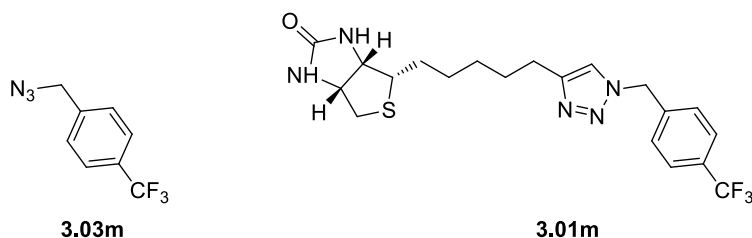
Benzyl bromide **3.04m** (240 mg, 1.00 mmol) was reacted with NaN$_3$ (78 mg, 1.20 mmol) in DMF (6 mL) according to general procedure **C2**. Crude **3.03m** was used in the next step without further purification.

Biotin acetylene **2.21** (30 mg, 0.13 mmol) was reacted with crude azide **3.03m** (32 mg, 0.16 mmol) and Cu nanopowder (2 mg, 0.03 mmol) using General Procedure **A2**. The crude material was purified by flash chromatography on silica gel eluting with 5% MeOH in DCM to give **3.01m** as a crystalline white solid (41 mg, 73%).

^{1}H NMR (500 MHz; CDCl$_3$): δ 7.63 (2H, d, *J* = 8.1 Hz, 2 x Ar**H**), 7.35 (2H, d, *J* = 8.2 Hz, 2 x Ar**H**), 7.23 (1H, s, Ar^{tri}**H**), 5.56 (2H, s, ArN^{tri}**CH$_2$**), 4.97 (1H, bs, N**H**), 4.74 (1H, bs, N**H**), 4.52-4.49 (1H, m, NHC**H**), 4.31-4.28 (1H, m, NHC**H**), 3.17-3.13 (1H, m, SC**H**), 2.91

_____

(1H, dd, J = 12.8, 5.1 Hz, SC**H**$_a$), 2.73-2.69 (3H, m, SC**H**$_b$, ArC^{tri}**CH$_2$**), 1.70-1.62 (4H, m, 2 x **CH$_2$**), 1.47-1.38 (4H, m, 2 x **CH$_2$**);
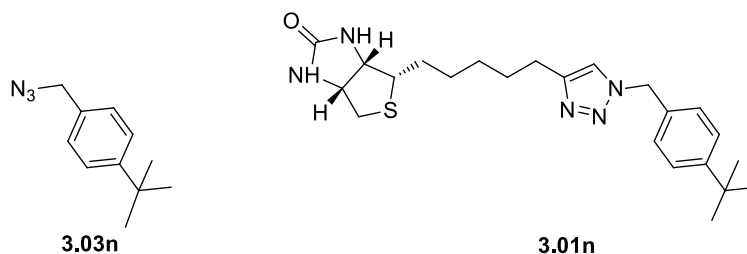
^{13}C NMR (125 MHz; CDCl$_3$): 162.9, 161.5, 130.8, 130.7, 130.5 (d), 124.8 (d), 115.7, 61.9, 60.1, 55.5, 47.5, 40.5, 29.0, 28.7, 28.5, 25.5 ;

^{19}F NMR (125 MHz; CDCl$_3$): δ -62.8;

HRMS calcd. for (M + Na$^+$) C$_{20}$H$_{24}$F$_3$N$_5$NaOS: requires 462.1551, found 462.1570.

HPLC R$_t$ = 15.14 min

1-(azidomethyl)-4-(*tert*-butyl)benzene 3.03n and (3a*S*,4*S*,6a*R*)-4-(5-(1-(4-(tert-butyl)benzyl)-1*H*-1,2,3-triazol-4-yl)pentyl)tetrahydro-1*H*-thieno[3,4-*d*]imidazol-2(3*H*)-one 3.01n

Benzyl alcohol **3.02n** (165 mg, 1.00 mmol) was reacted with P(O)Ph$_3$ (333 mg, 1.20 mmol), NaN$_3$ (78 mg, 1.20 mmol) in 1 :4 CCl$_4$/DMF (12 mL) according to general procedure **C1**. Crude **3.03n** was used in the next step without further purification.

Biotin acetylene **2.21** (10 mg, 0.04 mmol) was reacted with crude azide **3.03n** (10 mg) and Cu nanopowder (2 mg, 0.03 mmol) using General Procedure **A2**. The crude material was purified by flash chromatography on silica gel eluting with 5% MeOH in DCM to give **3.01n** as a crystalline white solid (6 mg, 35%).

^{1}H NMR (500 MHz; CDCl$_3$): δ 7.39 (2H, d, J = 7.9 Hz, 2 x Ar**H**), 7.27 (1H, s, Ar^{tri}**H**), 7.19 (2H, d, J = 8.0 Hz, 2 x Ar**H**), 5.46 (2H, s, ArN^{tri}**CH$_2$**), 4.85 (1H, bs, **NH**), 5.00 (1H, bs, **NH**), 4.52-4.49 (1H, m, NHC**H**), 4.32-4.30 (1H, m, NHC**H**), 3.15 (1H, s, SC**H**), 2.91 (1H, dd, J = 13.1, 4.8 Hz, SC**H$_a$**), 2.73-2.67 (3H, m, SC**H$_b$**, ArC^{tri}**CH$_2$**), 1.71-1.63 (4H, m, 2 x **CH$_2$**), 1.47-1.41 (4H, m, 2 x **CH$_2$**), 1.31 (9H, m, 3 x **CH$_3$**);
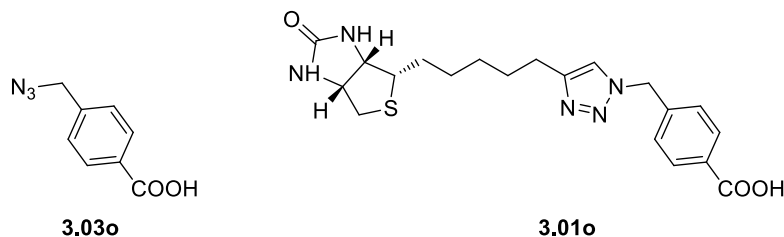
^{13}C NMR (125 MHz; CDCl$_3$): 151.7, 131.8, 127.8, 126.0, 62.0, 60.1, 55.7, 23.9,41.0, 40.6, 34.6, 31.3, 29.1, 28.9,28.7, 28.5, 25.6;

HRMS calcd. for (M + H$^+$) C$_{20}$H$_{28}$N$_5$O$_2$S: requires 428.2484, found 428.2451

HPLC R$_t$ = 17.34 min

4-(azidomethyl)benzoic acid 3.03o and 4-((4-(5-((3a*S*,4*S*,6a*R*)-2-oxohexahydro-1*H*-thieno[3,4-d]imidazol-4-yl)pentyl)-1*H*-1,2,3-triazol-1-yl)methyl)benzoic acid 3.01o

3.03o   **3.01o**

Benzyl bromide **3.04o** (215 mg, 1.00 mmol) was reacted with NaN$_3$ (78 mg, 1.20 mmol) in DMF (5 mL) according to general procedure **C2**. Crude **3.03o** was used in the next step without further purification.

Biotin acetylene **2.21** (50 mg, 0.21 mmol) was reacted with crude azide **3.03o** (44 mg) and Cu nanopowder (2 mg, 0.03 mmol) using General Procedure **A2**. The crude material was purified by flash chromatography on silica gel eluting with 5% MeOH in DCM to give **3.01o** as a crystalline white solid (26 mg, 25%).

^{1}H NMR (500 MHz; DMSO-d_6): δ 7.86 (1H, s, Ar^{tri}**H**), 7.83 (2H, d, *J* = 7.9 Hz, 2 x Ar**H**), 7.19 (2H, d, *J* = 7.8 Hz, 2 x Ar**H**), 6.41 (1H, bs, N**H**), 6.33 (1H, bs, N**H**), 5.52 (2H, s, ArN^{tri}**CH$_2$**), 4.30-4.18 (1H, m, NHC**H**), 4.11-4.10 (1H, m, NHC**H**), 3.08-3.07 (1H, m, SC**H**), 2.80 (1H, dd, *J* = 12.5, 5.1 Hz, SC**H$_a$**), 2.60-2.55 (3H, m, SC**H$_b$**, ArC^{tri}**CH$_2$**), 1.61-1.55 (4H, m, 2 x C**H$_2$**), 1.28-1.25 (4H, m, 2 x C**H$_2$**);

^{13}C NMR (125 MHz; DMSO-d_6): 165.8, 159.7, 150.3, 132.5, 129.9, 125.1, 64.2, 63.8, 63.3, 58.6, 55.7, 31.9, 31.7, 31.7, 31.5, 31.3, 28.7, 28.6, 28.1, 25.4;

HRMS calcd. for (M + K$^+$) C$_{20}$H$_{26}$KN$_5$O$_3$S: requires 454.1315, found 454.1303

HPLC R$_t$ = 13.82 min

1-(azidomethyl)-2-bromobenzene 3.03p and (3a*S*,4*S*,6a*R*)-4-(5-(1-(2-bromobenzyl)-1*H*-1,2,3-triazol-4-yl)pentyl)tetrahydro-1*H*-thieno[3,4-*d*]imidazol-2(3*H*)-one 3.01p

3.03p   **3.01p**
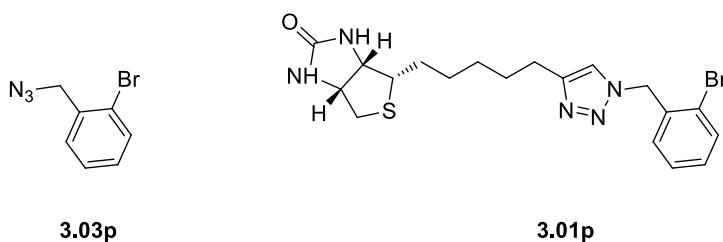
Benzyl chloride **3.04p** (205 mg, 1.00 mmol) was reacted with NaN$_3$ (78 mg, 1.20 mmol) in DMF (5 mL) according to general procedure **C2**. Crude **3.03p** was used in the next step without further purification.

Biotin acetylene **2.21** (30 mg, 0.13 mmol) was reacted with crude azide **3.03p** (34 mg) and Cu nanopowder (2 mg, 0.03 mmol) using General Procedure **A2**. The crude material was purified by flash chromatography on silica gel eluting with 5% MeOH in DCM to give **3.01p** as a crystalline white solid (55 mg, 77%).

¹H NMR (500 MHz; CDCl$_3$): δ 7.61 (1H, d, J = 8.0 Hz, Ar**H**), 7.32-7.28 (2H, m, Ar**H**, Ar^{tri}**H**), 7.23-7.20 (1H, m, Ar**H**), 7.11 (1H, dd, J = 7.5,1.7 Hz, Ar**H**), 5.62 (2H, s, ArN^{tri}C**H₂**), 5.23 (1H, bs, N**H**), 4.94 (1H, bs, N**H**), 4.51-4.49 (1H, m, NHC**H**), 4.31-4.28 (1H, m, NHC**H**), 3.16-3.12 (1H, m, SC**H**), 2.90 (1H, dd, J = 12.8, 5.0 Hz, SC**Hₐ**), 2.73-2.69 (3H, m, SC**H_b**, ArC^{tri}C**H₂**), 1.69-1.64 (4H, m, 2 x C**H₂**), 1.46-1.37 (4H, m, 2 x C**H₂**);

¹³C NMR (125 MHz; CDCl$_3$): 163.2, 148.5, 134.4, 133.1, 130.2, 130.1, 123.3, 121.0, 62.0, 60.1, 55.6, 53.6, 40.5, 29.0, 29.0, 28.7, 28.5, 25.5;

HRMS calcd. for (M + H$^+$) C$_{19}$H$_{25}$BrN$_5$OS: requires 450.0963, found 450.0931.

HPLC R$_t$ = 15.78 min

1-(azidomethyl)-3-iodobenzene 3.03q and (3a*S*,4*S*,6a*R*)-4-(5-(1-(3-iodobenzyl)-1*H*-1,2,3-triazol-4-yl)pentyl)tetrahydro-1*H*-thieno[3,4-*d*]imidazol-2(3*H*)-one 3.01q

3.03q   3.01q
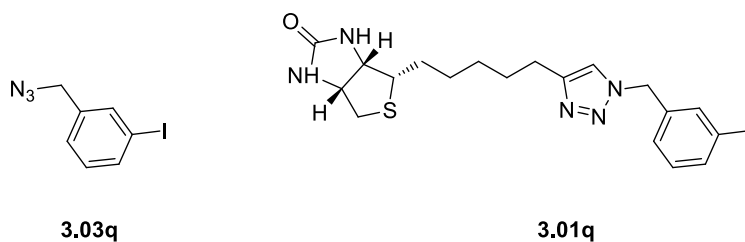
Benzyl chloride **3.04q** (250 mg, 1.00 mmol) was reacted with NaN$_3$ (78 mg, 1.20 mmol) in DMF (6 mL) according to general procedure **C2**. Crude **3.03q** was used in the next step without further purification.

Biotin acetylene **2.21** (30 mg, 0.13 mmol) was reacted with crude azide **3.03q** (41 mg) and Cu nanopowder (2 mg, 0.026 mmol) using General Procedure **A2**. The crude material was purified by flash chromatography on silica gel eluting with 5% MeOH in DCM to give **3.01q** as a crystalline white solid (51 mg, 64%).

---

¹H NMR (500 MHz; CDCl₃): δ 7.68 (1H, d, J = 7.9 Hz, Ar**H**), 7.61 (1H, s, Ar**H**), 7.22-7.20 (2H, m, Ar**H**, Ar^tri**H**), 7.11 (1H, t, J = 7.8 Hz, Ar**H**), 5.45 (2H, s, ArN^tri**CH₂**), 5.00 (1H, bs, N**H**), 4.77 (1H, bs, N**H**), 4.52-4.50 (1H, m, NH**CH**), 4.32-429 (1H, m, NH**CH**), 3.17-3.14 (1H, m, S**CH**), 2.91 (1H, dd, J = 12.8, 5.0 Hz, S**CH_a**), 2.73-2.69 (3H, m, S**CH_b**, ArC^tri**CH₂**), 1.71-1.62 (4H, m, 2 x **CH₂**), 1.47-1.37 (4H, m, 2 x **CH₂**);

¹³C NMR (125 MHz; CDCl₃): 162.8, 148.8, 137.7, 137.2, 136.7, 130.7, 127.1, 120.6, 94.7, 61.9, 60.1, 55.5, 53.1, 40.5, 29.0, 29.0, 28.7, 28.6, 25.5;

HRMS calcd. for (M + H⁺) $C_{19}H_{25}IN_5OS$: requires 498.0824, found 498.0830.

HPLC R_t = 16.22 min

1-(azidomethyl)-4-iodobenzene   3.03r   and   (3aS,4S,6aR)-4-(5-(1-(4-iodobenzyl)-1H-1,2,3-triazol-4-yl)pentyl)tetrahydro-1H-thieno[3,4-d]imidazol-2(3H)-one 3.01r
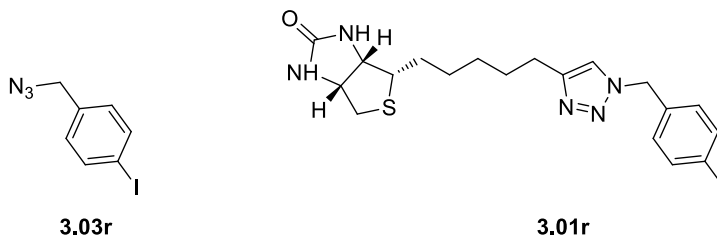
Benzyl chloride **3.04r** (250 mg, 1.00 mmol) was reacted with NaN₃ (78 mg, 1.20 mmol) in DMF (6 mL) according to general procedure **C2**. Crude **3.03r** was used in the next step without further purification.

Biotin acetylene **2.21** (30 mg, 0.13 mmol) was reacted with azide **3.03r** (32 mg) and Cu nanopowder (2 mg, 0.03 mmol) using General Procedure **A2**. The crude material was purified by flash chromatography on silica gel eluting with 5% MeOH in DCM to give **3.01r** as a crystalline white solid (56 mg, 71%).

¹H NMR (500 MHz; CDCl₃): δ 7.70 (2H, d, J = 8.0 Hz, 2 x Ar**H**), 7.19 (1H, s, Ar^tri**H**), 7.00 (2H, d, J = 8.0 Hz, 2 x Ar**H**), 5.43 (2H, s, ArN^tri**CH₂**), 5.19 (1H, bs, N**H**), 4.93 (1H, bs, N**H**), 4.50 (1H, dd, J = 7.7, 5.2 Hz, NH**CH**), 4.28-4.31 (1H, m, NH**CH**), 3.16-3.12 (1H, m, S**CH**), 2.90 (1H, dd, J = 12.8, 5.0 Hz, J = 12.8, 5.0 Hz, S**CH_a**), 2.73-2.67 (3H, m, S**CH_b**, ArC^tri**CH₂**), 1.67-1.59 (4H, m, 2 x **CH₂**), 1.46-1.36 (4H, m, 2 x **CH₂**);

¹³C NMR (125 MHz; CDCl₃): 163.0, 148.8, 138.2, 134.6, 129.8, 120.5, 94.4, 61.9, 60.1, 55.5, 53.4, 40.5, 29.0, 29.0, 28.7, 28.5, 25.5;

HRMS calcd. for (M + Na⁺) $C_{19}H_{24}IN_5NaOS$: requires 520.0644, found 520.0648.

HPLC R_t = 16.29 min

_____

1-(azidomethyl)-2-fluorobenzene 3.03s and (3a*S*,4*S*,6a*R*)-4-(5-(1-(2-fluorobenzyl)-1*H*-1,2,3-triazol-4-yl)pentyl)tetrahydro-1*H*-thieno[3,4-*d*]imidazol-2(3*H*)-one 3.01s

3.03s   3.01s
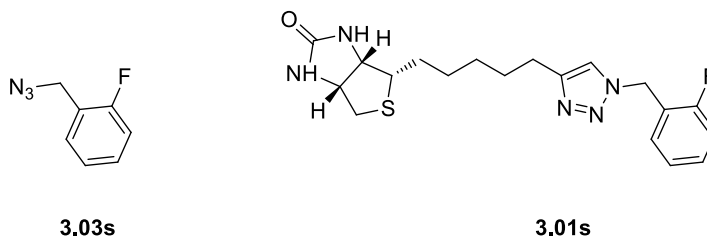
Benzyl chloride **3.04s** (145 mg, 1.00 mmol) was reacted with NaN$_3$ (78 mg, 1.20 mmol) in DMF (4 mL) according to general procedure **C2**. Crude **3.03s** was used in the next step without further purification.

Biotin acetylene **2.21** (30 mg, 0.13 mmol) was reacted with crude azide **3.03s** (24 mg) and Cu nanopowder (2 mg, 0.03 mmol) using General Procedure **A2**. The crude material was purified by flash chromatography on silica gel eluting with 5% MeOH in DCM to give **3.01s** as a crystalline white solid (22 mg, 35%).

^{1}H NMR (500 MHz; CDCl$_3$): δ 7.37-7.32 (1H, m, Ar**H**), 7.28 (1H, s, Ar^{tri}**H**), 7.25-7.23 (1H, m, Ar**H**), 7.16-7.09 (2H, m, 2 x Ar**H**), 5.55 (2H, s, ArN^{tri}**CH$_2$**), 5.37 (1H, bs, N**H**), 5.04 (1H, bs, N**H**), 4.50-4.47 (1H, m, NHC**H**), 4.30-4.27 (1H, m, NHC**H**), 3.15-3.12 (1H, m, SC**H**), 2.90 (1H, dd, *J* = 12.8, 5.1 Hz, SC**H$_a$**), 2.72 (1H, d, *J* = 12.2 Hz, m, SC**H$_b$**), 2.69 (2H, t, *J* = 7.7 Hz, ArC^{tri}**CH$_2$**), 1.66-1.20 (4H, m, 2 x **CH$_2$**), 1.47-1.37 (4H, m, 2 x **CH$_2$**);

^{13}C NMR (125 MHz; CDCl$_3$): 163.1, 148.6, 130.7, 130.5, 124.8, 122.3, 120.7, 115.8, 61.9, 60.1, 55.6, 47.5, 40.5, 29.0, 29.0, 28.7, 28.5, 25.5,

HRMS calcd. for (M + H$^+$) C$_{19}$H$_{25}$FN$_5$OS: requires 390.1764, found 390.1731.

HPLC R$_t$ = 16.23 min

1-(azidomethyl)-3-fluorobenzene 3.03t and (3a*S*,4*S*,6a*R*)-4-(5-(1-(3-fluorobenzyl)-1*H*-1,2,3-triazol-4-yl)pentyl)tetrahydro-1*H*-thieno[3,4-*d*]imidazol-2(3*H*)-one 3.01t

3.03t   3.01t
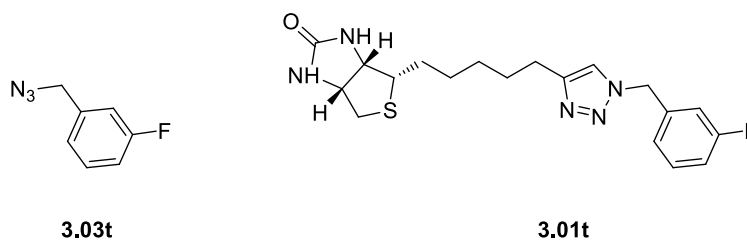
Benzyl chloride **3.04t** (145 mg, 1.00 mmol) was reacted with NaN$_3$ (78 mg, 1.20 mmol) in DMF (4 mL) according to general procedure **C2**. Crude **3.03t** was used in the next step without further purification.

Biotin acetylene **2.21** (30 mg, 0.13 mmol) was reacted with azide **3.03t** (24 mg) and Cu nanopowder (2 mg, 0.03 mmol) using General Procedure **A2**. The crude material was purified by flash chromatography on silica gel eluting with 5% MeOH in DCM to give **3.01t** as a crystalline white solid (43 mg, 69%).

^{1}H NMR (500 MHz; CDCl$_3$): δ 7.35-7.32 (1H, m, Ar**H**), 7.23 (1H, s, Ar$^{\text{tri}}$**H**), 7.06-7.02 (2H, m, 2 x Ar**H**), 6.95-6.92 (1H, m, Ar**H**), 5.49 (1H, bs, N**H**), 5.31 (2H, s, ArN$^{\text{tri}}$C**H$_2$**), 4.99 (1H, bs, N**H**), 4.51-4.49 (1H, m, NHC**H**), 4.31-4.28 (1H, m, NHC**H**), 3.16-3.12 (1H, m, SC**H**), 2.90 (1H, dd, J = 12.8, 5.0 Hz, SC**H$_a$**), 2.73-2.68 (3H, m, SC**H$_b$**, ArC$^{\text{tri}}$C**H$_2$**), 1.70-1.37 (8H, m, 4 x C**H$_2$**);

^{13}C NMR (125 MHz; CDCl$_3$): 164.0, 163.1, 148.8, 137.3, 130.7, 123.4, 120.7, 115.7, 115.5, 115.0, 114.8, 61.9, 60.0, 55.5, 53.3, 40.5, 29.0, 29.0, 28.7, 28.5, 25.5;

^{19}F NMR (125 MHz; CDCl$_3$): δ -111.7;

HRMS calcd. for (M + H$^+$) C$_{19}$H$_{25}$FN$_5$OS: requires 390.1764, found 390.1749.

HPLC R$_t$ = 15.49 min

1-(azidomethyl)-4-fluorobenzene 3.03u and (3a*S*,4*S*,6a*R*)-4-(5-(1-(4-fluorobenzyl)-1*H*-1,2,3-triazol-4-yl)pentyl)tetrahydro-1*H*-thieno[3,4-*d*]imidazol-2(3*H*)-one 3.01u
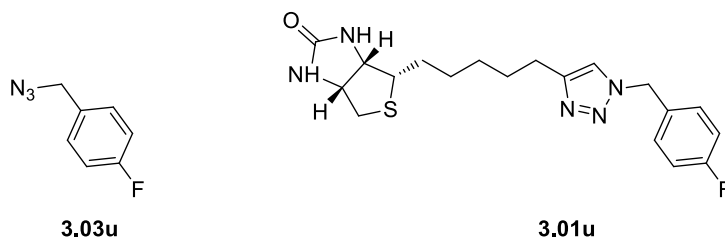
Benzyl bromide **3.04u** (190 mg, 1.00 mmol) was reacted with NaN$_3$ (78 mg, 1.20 mmol) in DMF (5 mL) according to general procedure **C2**. Crude **3.03u** was used in the next step without further purification.

Biotin acetylene **2.21** (30 mg, 0.13 mmol) was reacted with azide **3.03u** (24 mg) and Cu nanopowder (2 mg, 0.03 mmol) using General Procedure **A2**. The crude material was

purified by flash chromatography on silica gel eluting with 5% MeOH in DCM to give **3.01u** as a crystalline white solid (47 mg, 76%).

^{1}H NMR (500 MHz; CDCl$_3$): δ 7.25-7.23 (2H, m, 2 x Ar**H**), 7.20 (1H, s, Ar^{tri}**H**), 7.07-7.03 (2H, m, 2 x Ar**H**), 5.54 (1H, bs, N**H**), 5.45 (2H, s, ArN^{tri}**CH$_2$**), 5.16 (1H, bs, N**H**), 4.49 (1H, dd, J = 7.8, 5.0 Hz, NHC**H**), 4.30-4.27 (1H, m, NHC**H**), 3.15-3.11 (1H, m, SC**H**), 2.89 (1H, dd, J = 12.8, 5.0 Hz, SC**H$_a$**), 2.72-2.66 (3H, m, SC**H$_b$**, ArC^{tri}**CH$_2$**), 1.66-1.36 (8H, m, 4 x C**H$_2$**);

^{13}C NMR (125 MHz; CDCl$_3$): 162.5, 148.6, 129.9, 120.4, 116.1, 62.2, 60.3, 55.9, 53.5, 53.5, 40.8, 29.3, 29.2, 28.9, 28.7, 25.8;

HRMS calcd. for (M + H$^+$) C$_{19}$H$_{25}$FN$_5$OS: requires 390.1764, found 390.1759.

HPLC R$_t$ = 15.13 min

1-(azidomethyl)-2-chlorobenzene 3.03v and (3aS,4S,6aR)-4-(5-(1-(2-chlorobenzyl)-1H-1,2,3-triazol-4-yl)pentyl)tetrahydro-1H-thieno[3,4-d]imidazol-2(3H)-one 3.01v

3.03v   **3.01v**
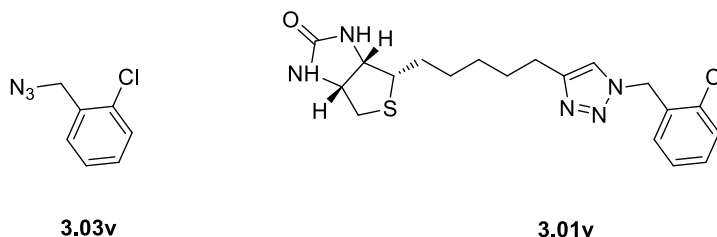
Benzyl bromide **3.04v** (205 mg, 1.00 mmol) was reacted with NaN$_3$ (78 mg, 1.20 mmol) in DMF (5 mL) according to general procedure **C2**. Crude **3.03v** was used in the next step without further purification.

Biotin acetylene **2.21** (30 mg, 0.13 mmol) was reacted with azide **3.03v** (27 mg) and Cu nanopowder (2 mg, 0.03 mmol) using General Procedure **A2**. The crude material was purified by flash chromatography on silica gel eluting with 5% MeOH in DCM to give **3.01v** as a crystalline white solid (40 mg, 61%).

^{1}H NMR (500 MHz; DMSO-d_6): δ 7.86 (1H, s, Ar**H**), 7.49 (1H, dd, J = 7.8, 1.8 Hz, Ar**H**), 7.38-7.33 (2H, m, Ar**H**, Ar^{tri}**H**), 7.13 (1H, dd, J = 7.8, 2.0 Hz, Ar**H**), 6.41 (1H, bs, N**H**), 6.33 (1H, bs, N**H**), 5.62 (2H, s, ArN^{tri}**CH$_2$**), 4.29-4.27 (1H, m, NHC**H**), 4.12-4.09 (1H, m, NHC**H**), 3.08-3.06 (1H, m, SC**H**), 2.79 (1H, dd, J = 12.5, 5.1 Hz, SC**H$_a$**), 2.60-2.54 (3H, m, SC**H$_b$**, ArC^{tri}**CH$_2$**), 1.59-1.28 (8H, m, 4 x C**H$_2$**);

¹³C NMR (125 MHz; DMSO-d_6): 163.2, 134.0, 132.9, 130.7, 130.5, 130.0, 128.1, 61.5, 59.6, 56.0, 50.8, 29.2, 29.0, 28.8, 28.7, 25.4;

HRMS calcd. for (M + H) $C_{19}H_{25}ClN_5OS$: requires 406.1468, found 406.1448.

HPLC R_t = 15.62 min

1-(azidomethyl)-3-chlorobenzene 3.03w and (3a*S*,4*S*,6a*R*)-4-(5-(1-(3-chlorobenzyl)-1*H*-1,2,3-triazol-4-yl)pentyl)tetrahydro-1*H*-thieno[3,4-*d*]imidazol-2(3*H*)-one 3.01w

3.03w   **3.01w**
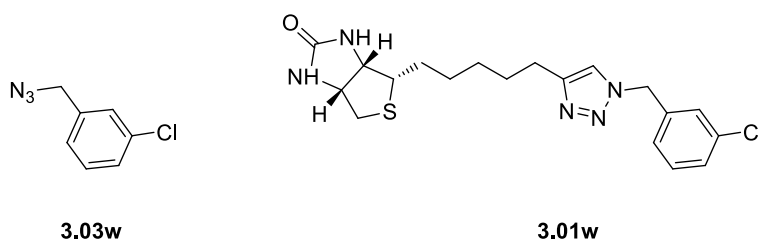
Benzyl bromide **3.04w** (205 mg, 1.00 mmol) was reacted with NaN_3 (78 mg, 1.20 mmol) in DMF (5 mL) according to general procedure **C2**. Crude **3.03w** was used in the next step without further purification.
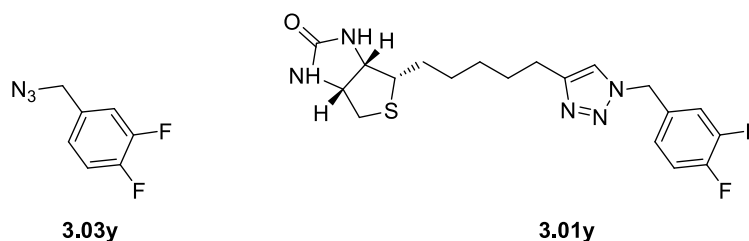
Biotin acetylene **2.21** (30 mg, 0.13 mmol) was reacted with azide **3.03w** (27 mg) and Cu nanopowder (2 mg, 0.03 mmol) using General Procedure **A2**. The crude material was purified by flash chromatography on silica gel eluting with 5% MeOH in DCM to give **3.01w** as a crystalline white solid (55 mg, 85%).

¹H NMR (500 MHz; DMSO-d_6): δ 7.91 (1H, s, Ar**H**), 7.39-7.33 (3H, m, 2 x Ar**H**, Ar^{tri}**H**), 7.22-7.20 (1H, m, Ar**H**), 6.40 (1H, bs, N**H**), 6.33 (1H, bs, N**H**), 5.54 (2H, s, ArN^{tri}C**H₂**), 4.29-4.27 (1H, m, NHC**H**), 4.10 (1H, dd, *J* = 7.8, 4.3 Hz, NHC**H**), 3.08-3.06 (1H, m, SC**H**), 2.79 (1H, dd, *J* = 12.4, 5.4 Hz, SC**Hₐ**), 2.60-2.54 (3H, m, SC**Hᵦ**, ArC^{tri}C**H₂**), 1.58-1.29 (8H, m, 4 x C**H₂**);

¹³C NMR (125 MHz; DMSO-d_6): 163.1, 147.8, 139.2, 133.7, 131.1, 128.4, 128.1, 126.9, 122.5, 61.5, 61.4, 59.6, 56.0, 52.3, 29.2, 29.0, 28.8, 28.7, 25.4;

HRMS calcd. for (M + H⁺) $C_{19}H_{25}ClN_5OS$: requires 406.1468, found 406.1450.

HPLC R_t = 15.75 min

_____

1-(azidomethyl)-4-chlorobenzene 3.03x and (3a*S*,4*S*,6a*R*)-4-(5-(1-(4-chlorobenzyl)-1*H*-1,2,3-triazol-4-yl)pentyl)tetrahydro-1*H*-thieno[3,4-*d*]imidazol-2(3*H*)-one 3.01x

3.03x   **3.01x**
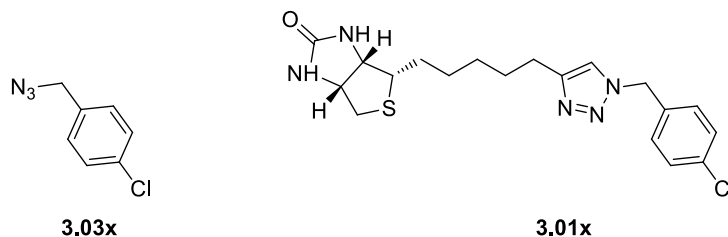
Benzyl bromide **3.04x** (205 mg, 1.00 mmol) was reacted with NaN$_3$ (78 mg, 1.20 mmol) in DMF (5 mL) according to general procedure **C2**. Crude **3.03x** was used in the next step without further purification.

Biotin acetylene **2.21** (30 mg, 0.13 mmol) was reacted with azide **3.03x** (27 mg) and Cu nanopowder (2 mg, 0.03 mmol) using General Procedure **A2**. The crude material was purified by flash chromatography on silica gel eluting with 5% MeOH in DCM to give **3.01x** as a crystalline white solid (50 mg, 77%).

^{1}H NMR (500 MHz; CDCl$_3$): δ 7.35-7.33 (2H, m, 2 x Ar**H**), 7.26 (1H, s, Ar^{tri}**H**), 7.21-7.18 (2H, m, 2 x Ar**H**), 5.46 (2H, s, ArN^{tri}**CH$_2$**), 5.30 (1H, bs, N**H**), 4.97 (1H, bs, N**H**), 4.51-4.48 (1H, m, NHC**H**), 4.31-4.28 (1H, m, NHC**H**), 3.16-3.12 (1H, m, SC**H**), 2.90 (1H, dd, *J* = 12.8, 5.0 Hz, SC**H$_a$**), 2.73-2.67 (3H, m, SC**H$_b$**, ArC^{tri}**CH$_2$**), 1.70-1.36 (8H, m, 4 x C**H$_2$**);
^{13}C NMR (125 MHz; CDCl$_3$): 163.0, 148.8, 134.6, 133.4, 129.3, 129.2, 120.5, 61.9, 60.0, 55.5, 53.2, 40.5, 29.0, 28.9, 28.7, 28.5, 25.5;
HRMS calcd. for (M + H$^+$) C$_{19}$H$_{25}$ClN$_5$OS: requires 406.1468, found 406.1451.
HPLC R$_t$ = 15.78 min

4-(azidomethyl)-1,2-difluorobenzene 3.03y and (3a*S*,4*S*,6a*R*)-4-(5-(1-(3,4-difluorobenzyl)-1*H*-1,2,3-triazol-4-yl)pentyl)tetrahydro-1*H*-thieno[3,4-*d*]imidazol-2(3*H*)-one 3.01y

3.03y   **3.01y**

Benzyl bromide **3.04y** (205 mg, 1.00 mmol) was reacted with NaN$_3$ (78 mg, 1.20 mmol) in DMF (5 mL) according to general procedure **C2**. Crude **3.03y** was used in the next step without further purification.

Biotin acetylene **2.21** (30 mg, 0.13 mmol) was reacted with azide **3.03y** (27 mg, 0.16 mmol) and Cu nanopowder (2 mg, 0.03 mmol) using General Procedure A2. The crude material was purified by flash chromatography on silica gel eluting with 5% MeOH in DCM to give **3.01y** as a crystalline white solid (49 mg, 75%).

^{1}H NMR (500 MHz; CDCl$_3$): δ 7.24 (1H, s, Ar^{tri}**H**), 7.18 (1H, dt, J = 9.9, 8.2 Hz, Ar**H**), 7.08 (1H, ddd, J = 10.2, 7.3, 2.2 Hz, Ar**H**), 7.03-7.00 (1H, m , Ar**H**), 5.46 (2H, s, ArN^{tri}**CH$_2$**), 5.2 (1H, bs, N**H**), 4.91 (1H, bs, N**H**), 4.53-4.50 (1H, m, NHC**H**), 4.32-4.30 (1H, m, NHC**H**), 3.18-3.14 (1H, m, SC**H**), 2.92 (1H, dd, J = 12.8, 5.1 Hz, SC**H$_a$**), 2.74-2.69 (3H, m, SC**H$_b$**, ArC^{tri}**CH$_2$**), 1.72-1.65 (4H, m, 2 x **CH$_2$**), 1.48-1.39 (4H, m, 2 x **CH$_2$**);

^{13}C NMR (125 MHz; CDCl$_3$): 163.0, 148.9, 124.0 (q, J = 4.1 Hz)), 120.5, 118.0, 117.9, 117.1, 117.0, 62.0, 60.0, 55.5, 52.9, 40.5, 29.0, 28.9, 28.7, 28.6, 25.5;

^{19}F NMR (125 MHz; CDCl$_3$): δ -136.0, -137.3;

HRMS calcd. for (M + H$^+$) C$_{19}$H$_{24}$F$_2$N$_5$OS: requires 408.1670, found 408.1685.

HPLC R$_t$ = 15.49 min

7.6   Experimental work as described in Chapter 4

(3a*S*,4*S*,6a*R*)-4-(7-iodohept-6-yn-1-yl)tetrahydro-1*H*-thieno[3,4-*d*]imidazol-2(3*H*)-one 4.02
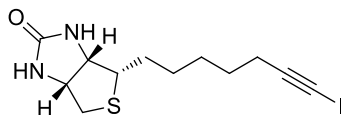
Method 1 (See chapter 4, table 1 entry 1)[5]

To a solution of biotin acetylene **2.21** (100 mg, 0.42 mmol) in dry TFH (5 ml) was added CuI (5 mg, 0.08 mmol) and *N*-iodomorpholine (143 mg, 0.42 mmol). The reaction mixture was stirred at ambient temperature for 3 h, after which a fine white precipitate had formed. The suspension was filtered through a pad of natural alumina, which was further washed with 10% MeOH in DCM (3 x 20 ml). The combined organics were concentrated *in vacuo* and purified by flash chromatography on silica eluting with 10% MeOH in DCM to give a yellow solid. ¹H NMR indicated a 3:1 mixture of starting biotin acetylene **2.21** and 1-iodoacetylene **4.02**.

Method 2 (See chapter 4, table 1 entry 2)

Following the condition described in method 1. However the reaction time was increased to 12 h. ¹H NMR indicated a 1:3 mixture of starting biotin acetylene **2.21** and 1-iodoacetylene **4.02**.

Method 3 (See chapter 4, table 1 entry 3)

Following the condition described in method 1. However the reaction was undertaken in a mixture solvent of THF and DMF (1:1, 5 ml). ¹H NMR indicated a 1:5 mixture of starting biotin acetylene **2.21** and 1-iodoacetylene **4.02**.

Method 4 (See chapter 4, table 1 entry 4)

Following the condition described in method 1. However the reaction was undertaken in dry DMF (5 ml). ¹H NMR of purified compound confirmed the presence of the target compound **4.02** as a yellow solid (145 mg, 95%) > 98% by ¹H NMR.

¹H NMR (500 MHz, DMSO-*d₆*): δ 6.42 (1H, bs, C(O)N**H**), 6.34 (1H, s, C(O)N**H**), 4.29-4.31 (1H, m, NHC**H**), 4.11-4.14 (1H, m, NHC**H**), 3.08-3.10 (1H, m, SC**H**), 2.80-2.83 (1H,m,

SC**H**a), 2.53-2.59 (3H, m, SC**H**b, C**H₂**C≡C-I), 1.43-1.65 (4H, m, 2 x C**H₂**), 1.27-1.39 (4H, m, 2 x C**H₂**);

¹³C NMR (125 MHz, DMSO-d_6): δ 165.8, 122.2, 79.8, 64.2, 62.3, 58.6, 52.8, 31.5, 31.3, 31.4, 30.9

HPLC R_t = 16.9 min

3-(4-(5-iodo-4-(5-((3a*S*,4*S*,6a*R*)-2-oxohexahydro-1*H*-thieno[3,4-*d*]imidazol-4-yl)pentyl)-1*H*-1,2,3-triazol-1-yl)butyl)-5-methylbenzo[*d*]oxazol-2(3*H*)-one 4.06
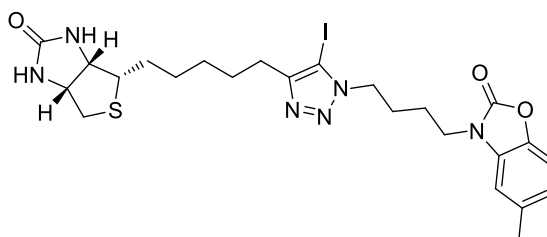
The iodo-acetylene **4.02** (20 mg, 0.06 mmol) and azide **4.20** (14 mg, 0.06 mmol) was reacted according to general procedure **D** and was purified by flash chromatography on silica eluting with 5% MeOH in DCM to give a yellowish solid (12 mg, 36%).

¹H NMR (500 MHz; CDCl₃): δ 7.08 (1H, d, *J* = 8.1 Hz, Ar**H**), 6.90-6.92 (1H, m, Ar**H**), 6.78 (1H, m, Ar**H**), 5.08 (1H, bs, N**H**), 4.86 (1H, bs, N**H**), 4.50-4.53 (1H, m, NHC**H**), 4.42 (2H, t, *J* = 6.9 Hz, ArNᵗʳⁱC**H₂**), 4.30-4.33 (1H, m, NHC**H**), 3.84 (2H, t, *J* = 6.9 Hz, NC**H₂**), 3.14-3.19 (1H, m, SC**H**), 2.93 (1H, dd, *J* = 5.0, 12.8 Hz, SC**H**a), 2.74 (1H, d, *J* = 12.8 Hz, SC**H**b), 2.64 (2H, d, *J* = 7.5 Hz, ArCᵗʳⁱC**H₂**), 2.40 (3H, s, ArC**H₃**), 1.97-2.02 (2H, m, C**H₂**), 1.79-1.84 (2H, m, C**H₂**), 1.64-1.72 (4H, m, 2 x C**H₂**), 1.38-1.49 (4H, m, 2 x C**H₂**);

¹³C NMR (125 MHz; CDCl₃): δ 162.8, 154.9, 151.8, 140.7, 134.0, 130.8, 122.9, 109.7, 108.8, 61.9, 60.1, 55.5, 49.7, 41.3, 40.6, 28.9, 28.6, 28.6, 28.4, 26.6, 25.8, 24.5, 21.5,

HRMS calcd. for (M + H) C₂₄H₃₂IN₆O₃S, requires 611.1301, found 611.1298

HPLC R_t = 17.0 min

3-(4-(5-fluoro-4-(5-((3a*S*,4*S*,6a*R*)-2-oxohexahydro-1*H*-thieno[3,4-*d*]imidazol-4-yl)pentyl)-1*H*-1,2,3-triazol-1-yl)butyl)-5-methylbenzo[*d*]oxazol-2(3*H*)-one 4.07
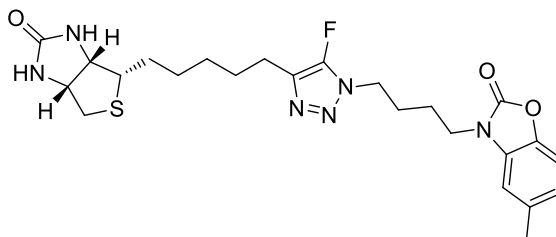
The 5-iodo-triazole **4.06** (15 mg, 0.03 mmol) was reacted with potassium fluoride (7 mg, 0.12 mmol) according to general procedure **E** and was purified by flash chromatography on silica eluting with 5% MeOH in DCM to yield 5-fluoro-triazole as an off white solid (11 mg, 89%).

^{1}H NMR (500 MHz; CDCl$_3$): δ 7.08 (1H, d, *J* = 8.1 Hz, Ar**H**), 6.90-6.92 (1H, m, Ar**H**), 6.76-6.77 (1H, m, Ar**H**), 5.06 (1H, bs, **NH**), 4.82 (1H, bs, **NH**), 4.49-4.52 (1H, m, NHC**H**), 4.30-4.33 (1H, m, NHC**H**), 4.27 (2H, t, *J* = 6.9 Hz, ArN^{tri}C**H$_2$**), 3.85 (2H, t, *J* = 6.9 Hz, NC**H$_2$**), 3.14-3.17 (1H, m, SC**H**), 2.92 (1H, dd, *J* = 5.0, 12.8 Hz, SC**H$_a$**), 2.73 (1H, d, *J* = 12.8 Hz, SC**H$_b$**), 2.62 (2H, d, *J* = 7.5 Hz, ArC^{tri}C**H$_2$**), 2.40 (3H, s, ArC**H$_3$**), 1.96-2.02 (2H, m, C**H$_2$**), 1.79-1.85 (2H, m, C**H$_2$**), 1.63-1.70 (4H, m, 2 x C**H$_2$**), 1.37-1.48 (4H, m, 2 x C**H$_2$**);
^{13}C NMR (125 MHz; CDCl$_3$): δ 162.8, 154.9, 140.7, 134.0, 130.7, 122.9, 110.0, 109.7, 108.7, 61.9, 60.0, 55.5, 46.1, 41.2, 40.5, 28.9, 28.6, 28.6, 28.0, 26.2, 24.7, 23.4, 21.5,
HRMS calcd. for (M + H$^+$) C$_{24}$H$_{32}$FN$_6$O$_3$S, requires 503.2241, found 503.2220
HPLC R$_t$ = 16.7 min

3-(4-(5-chloro-4-(5-((3a*S*,4*S*,6a*R*)-2-oxohexahydro-1*H*-thieno[3,4-*d*]imidazol-4-yl)pentyl)-1*H*-1,2,3-triazol-1-yl)butyl)-5-methylbenzo[*d*]oxazol-2(3*H*)-one 4.08
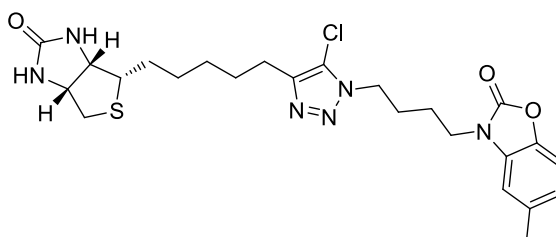
The 5-iodo-triazole **4.06** (15 mg, 0.03 mmol) was reacted with potassium cloride (9 mg, 0.12 mmol) according to general procedure **E** and was purified by flash chromatography on silica eluting with 5% MeOH in DCM to yield 5-fluoro-triazole as an off white solid (10 mg, 80%).

¹H NMR (500 MHz; CDCl₃): δ 7.03 (1H, m, Ar**H**), 6.97-6.99 (1H, m, Ar**H**), 6.83 (1H, d, *J* = 8.1 Hz, Ar**H**), 5.39 (1H, bs, N**H**), 5.08 (1H, bs, N**H**), 4.49-4.51 (1H, m, NHC**H**), 4.35 (2H, t, *J* = 6.9 Hz, ArN^tri**CH₂**), 4.29-4.32 (1H, m, NHC**H**), 3.84 (2H, t, *J* = 6.9 Hz, NC**H₂**), 3.13-3.17 (1H, m, SC**H**), 2.91 (1H, dd, *J* = 5.0, 12.8 Hz, SC**H**ₐ), 2.72 (1H, d, *J* = 12.8 Hz, SC**H**ᵦ), 2.62 (2H, t, *J* = 7.5 Hz, ArC^tri**CH₂**), 2.38 (3H, s, ArC**H₃**), 1.95-2.01 (2H, m, C**H₂**), 1.77-1.83 (2H, m, C**H₂**), 1.63-1.73 (4H, m, 2 x C**H₂**), 1.36-1.47 (4H, m, 2 x C**H₂**);

¹³C NMR (125 MHz; CDCl₃): δ 163.1, 154.8, 143.6, 142.8, 132.7, 128.4, 124.3, 122.2, 110.8, 107.8, 62.0, 60.1, 55.6, 47.3, 41.3, 40.5, 28.9, 28.6, 28.5, 28.0, 26.2, 24.6, 24.3, 21.4;

HRMS calcd. for (M + H⁺) C₂₄H₃₂ClN₆O₃S, requires 519.1945, found 519.1909

HPLC R_t = 17.1 min

(3a*S*,4*S*,6a*R*)-4-(5-(1-(4-(6-amino-9*H*-purin-9-yl)butyl)-5-iodo-1*H*-1,2,3-triazol-4-yl)pentyl)tetrahydro-1*H*-thieno[3,4-*d*]imidazol-2(3*H*)-one 4.09
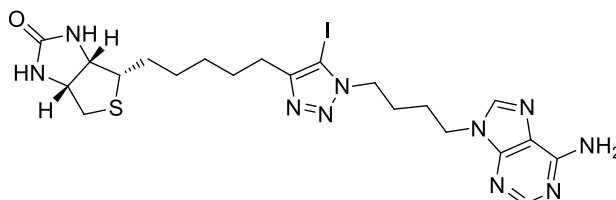
The iodo-acetylene **4.02** (50 mg, 0.14 mmol) and azide **4.21** (32 mg, 0.14 mmol) was reacted according to general procedure **D** and was purified by flash chromatography on silica eluting with 5% MeOH in DCM to give a white solid (55 mg, 66%).

¹H NMR (500 MHz; CDCl₃): δ 8.11 (2H, s, 2 x Ar**H**), 7.19 (2H, bs, ArN**H₂**), 6.50 (1H, bs, N**H**), 6.35 (1H, bs, N**H**), 4.26-4.36 (3H, m, ArN^tri**CH₂**, NHC**H**), 4.11-4.17 (3H, m, NC**H₂**, NHC**H**), 3.07-3.10 (1H, m, SC**H**), 2.51 (1H, dd, *J* = 5.1, 12.4 Hz, SC**H**ₐ), 2.50-2.58 (3H, m, SC**H**ᵦ, ArC^tri**CH₂**), 1.54-1.79 (6H, m, 3 x C**H₂**), 1.23-1.46 (6H, m, 3 x C**H₂**);

¹³C NMR (125 MHz; CDCl₃): δ 165.9, 159.1, 155.5, 153.7, 143.9, 85.1, 64.2, 62.3, 58.7, 52.4, 45.4, 31.6, 31.5, 31.5, 31.4, 29.7, 29.5, 28.5;

HRMS calcd. for (M + H⁺) C₂₄H₃₂IN₆O₃S, requires 611.1301, found 611.1298

HPLC R_t = 13.1 min

Attempted synthesis of (3a*S*,4*S*,6a*R*)-4-(5-(1-(4-(6-amino-9*H*-purin-9-yl)butyl)-5-fluoro-1*H*-1,2,3-triazol-4-yl)pentyl)tetrahydro-1*H*-thieno[3,4-*d*]imidazol-2(3*H*)-one 4.10
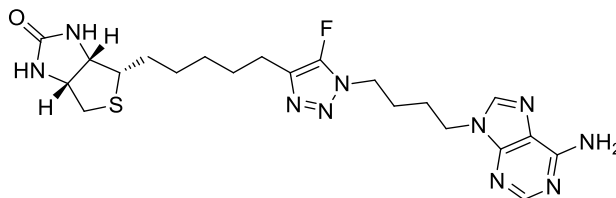
Method 1 (See chapter 4, table 3 entry 1)

The 5-iodo-triazole **4.09** (15 mg, 0.02 mmol) was reacted with potassium fluoride (7 mg, 0.12 mmol) according to general procedure **E** for 10 min. The crude material was purified by flash chromatography on silica eluting with 5% MeOH in DCM to give a white solid (9 mg, 61%). ^{1}H NMR was consistent with the 5-iodo-triazole **4.09** only.

Method 2 (See chapter 4, table 3 entry 2)

Following the condition described in method 1, however the reaction time was increased to 30 min. ^{1}H NMR indicated a complex mixture containing some starting material **4.09**.

Method 3 (See chapter 4, table 3 entry 3)

Following the condition described in method 1, but used THF instead of MeCN/H$_2$O (1:1). The residue was purified by flash chromatography on silica eluting with 5% MeOH in DCM to give a white solid (5 mg, 41%). ^{1}H NMR was consistent with the literature data of the 5-H-triazole.[6]

Method 3 (See chapter 4, table 3 entry 4)

Following the condition described in method 1, but used DMF instead of MeCN/H$_2$O (1:1). ^{1}H NMR indicated a complex mixture which could not be assigned.

Attempted synthesis of (3a*S*,4*S*,6a*R*)-4-(5-(1-(4-(6-amino-9*H*-purin-9-yl)butyl)-5-chloro-1*H*-1,2,3-triazol-4-yl)pentyl)tetrahydro-1*H*-thieno[3,4-*d*]imidazol-2(3*H*)-one 4.11
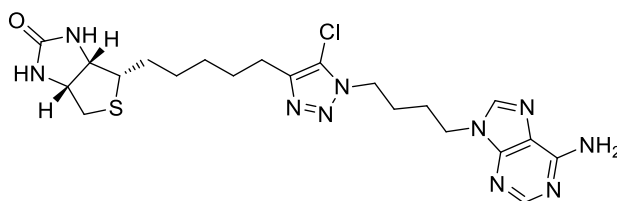
Method 1 (See chapter 4, table 3 entry 5)

The 5-iodo-triazole **4.09** (15 mg, 0.03 mmol) was reacted with potassium chloride (11 mg, 0.15 mmol) according to general procedure **E** for 10 min. The crude material was purified by flash chromatography on silica eluting with 5% MeOH in DCM to give a white solid (12 mg, 77%). ^{1}H NMR was consistent with the 5-iodo-triazole **4.09** only.

Method 2 (See chapter 4, table 3 entry 6)

Following the condition described in method 1, however the reaction time was increased to 30 min. ^{1}H NMR indicated a complex mixture containing some starting material **4.09**.

Method 3 (See chapter 4, table 3 entry 7)

Following the condition described in method 1, but used THF instead of MeCN/H_2O (1:1). The residue was purified by flash chromatography on silica eluting with 5% MeOH in DCM to give a white solid (6 mg, 56%). ^{1}H NMR was consistent with the literature data of the 5-H-triazole.[6]

Method 3 (See chapter 4, table 3 entry 8)

Following the condition described in method 1, but used DMF instead of MeCN/H_2O (1:1). ^{1}H NMR of crude material confirmed the presence of a complex mixture only.

(3a*S*,4*S*,6a*R*)-4-(5-(5-iodo-1-(4-methylbenzyl)-1*H*-1,2,3-triazol-4-yl)pentyl)tetrahydro-1*H*-thieno[3,4-*d*]imidazol-2(3*H*)-one 4.12
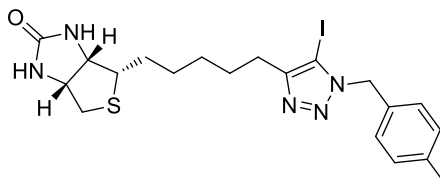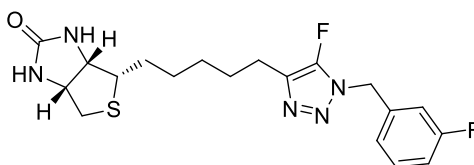

The iodo-acetylene **4.02** (30 mg, 0.08 mmol) and azide **3.03k** (12 mg, 0.08 mmol) was reacted according to general procedure **D** and was purified by flash chromatography on silica eluting with 5% MeOH in DCM to give a white solid (20 mg, 48%).

¹H NMR (500 MHz; CDCl₃): δ 7.14-7.18 (4H, m, 4 x Ar**H**), 5.53 (2H, s, ArN^{tri}C**H₂**), 4.90 (1H, bs, N**H**), 4.72 (aH, bs, N**H**) 4.51-4.53 (1H, m, NHC**H**), 4.30-4.33 (1H, m, NHC**H**), 3.15-3.19 (1H, m, SC**H**), 2.93 (1H, dd, *J* = 5.0, 12.8 Hz SC**H**ₐ), 2.73 (1H, d, *J* = 12.8 Hz, SC**H**_b), 2.65 (2H, t, *J* = 7.6 Hz, ArC^{tri}C**H₂**), 2.34 (3H, s, C**H₃**), 1.65-1.75 (4H, m, 2 x C**H₂**), 1.39-1.52 (4H, m, 2 x C**H₂**);

¹³C NMR (125 MHz; CDCl₃): δ 138.2, 131.4, 129.5, 127.8, 61.9, 60.0, 55.4, 54.0, 40.6, 28.9, 28.6, 28.5, 28.4, 25.9, 21.2.

HRMS calcd. for (M + H⁺) C₂₀H₂₇IN₅OS, requires 512.0981, found 512.0987

HPLC R$_t$ = 16.2 min

(3a*S*,4*S*,6a*R*)-4-(5-(5-fluoro-1-(4-methylbenzyl)-1*H*-1,2,3-triazol-4-yl)pentyl)tetrahydro-1*H*-thieno[3,4-*d*]imidazol-2(3*H*)-one 4.13
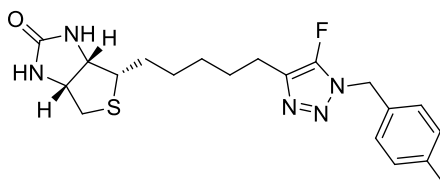
The 5-iodo-triazole **4.12** (20 mg, 0.04 mmol) was reacted with potassium fluoride (11 mg, 0.20 mmol) according to general procedure **E** and was purified by flash chromatography on silica eluting with 3% MeOH in DCM to yield 5-fluoro-triazole as an off white solid (11 mg, 89%).

¹H NMR (500 MHz; CDCl₃): δ 7.17-7.23 (4H, m, 4 x Ar**H**), 5.35 (2H, s, ArN^{tri}C**H₂**), 4.61 (1H, bs, C(O)N**H**), 4.51-4.53 (2H, m, C(O)N**H**, NHC**H**), 4.30-4.33 (1H, m, NHC**H**), 3.14-

3.18 (1H, m, SC**H**), 2.94 (1H, dd, J = 5.0, 12.8 Hz SC**H**$_a$), 2.73 (1H, d, J = 12.8 Hz, SC**H**$_b$), 2.62 (2H, t, J = 7.6 Hz, ArC^{tri}**CH**$_2$), 2.35 (3H, s, **CH**$_3$), 1.63-1.72 (4H, m, 2 x **CH**$_2$), 1.38-1.50 (4H, m, 2 x **CH**$_2$);

^{13}C NMR (125 MHz; CDCl$_3$): δ 143.0, 141.3, 132.3, 130.6, 64.5, 62.7, 58.0, 53.5, 43.2, 31.6, 31.3, 31.2, 30.7, 26.1, 23.8.

HRMS calcd. for (M + H$^+$) C$_{20}$H$_{27}$FN$_5$OS, requires 404.1920, found 404.1953

HPLC R$_t$ = 16.6 min

(3aS,4S,6aR)-4-(5-(1-(3-fluorobenzyl)-5-iodo-1H-1,2,3-triazol-4-yl)pentyl)tetrahydro-1H-thieno[3,4-d]imidazol-2(3H)-one 4.14
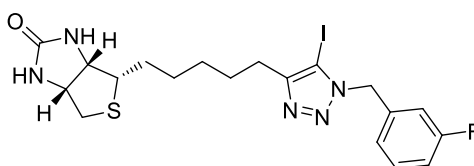
The iodo-acetylene **4.02** (30 mg, 0.08 mmol) and azide **3.03t** (12 mg, 0.08 mmol) was reacted according to general procedure **D** and was purified by flash chromatography on silica eluting with 5% MeOH in DCM to give a white solid (20 mg, 48%).

^{1}H NMR (500 MHz; CDCl$_3$): δ 7.31-7.35 (1H, m, Ar**H**), 7.01-7.06 (2H, m, 2 x Ar**H**), 6.92-6.95 (1H, m, Ar**H**), 5.57 (2H, s, ArN^{tri}**CH**$_2$), 4.91 (1H, bs, N**H**), 4.74 (1H, bs, N**H**) 4.51-4.54 (1H, m, NHC**H**), 4.31-4.33 (1H, m, NHC**H**), 3.15-3.19 (1H, m, SC**H**), 2.93 (1H, dd, J = 5.0, 12.8 Hz SC**H**$_a$), 2.65-2.75 (3H, m, SC**H**$_b$, ArC^{tri}**CH**$_2$), 1.65-1.76 (4H, m, 2 x **CH**$_2$), 1.40-1.50 (4H, m, 2 x **CH**$_2$);

^{13}C NMR (125 MHz; CDCl$_3$): δ 169.1, 162.7, 152.4, 150.5, 130.5, 123.3, 115.5, 114.8, 109.9, 61.9, 60.1, 55.4, 53.5, 40.5, 28.9, 28.6, 28.5, 28.4, 25.9.

HRMS calcd. for (M + H$^+$) C$_{19}$H$_{24}$FIN$_5$OS, requires 516.0730, found 516.0725.

(3aS,4S,6aR)-4-(5-(5-fluoro-1-(3-fluorobenzyl)-1H-1,2,3-triazol-4-yl)pentyl)tetrahydro-1H-thieno[3,4-d]imidazol-2(3H)-one 4.15

The 5-iodo-triazole **4.14** (20 mg, 0.04 mmol) was reacted with potassium fluoride (11 mg, 0.20 mmol) according to general procedure **E** and was purified by flash chromatography on silica eluting with 3% MeOH in DCM to yield 5-fluoro-triazole as an off white solid (11 mg, 89%).

^{1}H NMR (500 MHz; CDCl$_3$): δ 7.25-7.31 (1H, m, Ar**H**), 6.98-7.01 (2H, m, 2 x Ar**H**), 6.89-6.91 (1H, m, Ar**H**), 5.55 (2H, s, ArN^{tri}**CH$_2$**), 4.88 (1H, bs, N**H**), 4.72 (1H, bs, N**H**) 4.45-4.49 (1H, m, NHC**H**), 4.30-4.32 (1H, m, NHC**H**), 3.11-3.15 (1H, m, SC**H**), 2.91 (1H, dd, J = 5.0, 12.8 Hz SC**H$_a$**), 2.60-2.70 (3H, m, SC**H$_b$**, ArC^{tri}**CH$_2$**), 1.62-1.73 (4H, m, 2 x C**H$_2$**), 1.41-1.52 (4H, m, 2 x C**H$_2$**);

^{13}C NMR (125 MHz; CDCl$_3$): δ 165.7, 162.8, 132.3, 123.3, 115.5, 114.8, 109.9, 63.2, 62.1, 55.6, 53.7, 45.5, 28.9, 28.6, 28.5, 28.4, 25.3.

HRMS calcd. for (M + H$^+$) C$_{19}$H$_{24}$F$_2$N$_5$OS, requires 407.1591, found 407.1596

Attempted synthesis of 3-(4-(5-methoxy-4-(5-((3a*S*,4*S*,6aR)-2-oxohexahydro-1*H*-thieno[3,4-*d*]imidazol-4-yl)pentyl)-1*H*-1,2,3-triazol-1-yl)butyl)-5-methylbenzo[*d*]oxazol-2(3*H*)-one 4.16
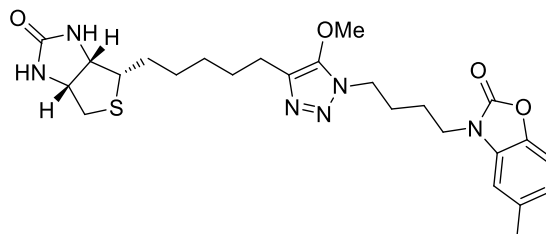
Method 1 (See chapter 4, table 4 entry 1)

To a solution of 5-fluoro-triazole **4.07** (20 mg, 0.04 mmol) in dry THF (3 ml) was added NaH (2 mg, 0.06 mmol) and sodium methoxide (5 mg, 0.09 mmol). The reaction was hearted to reflux for 3 h and monitored by TLC. ^{1}H NMR of crude material confirmed the presence of the starting material **4.07** only.

Method 2 (See chapter 4, table 4 entry 2)

To a solution of 5-fluoro-triazole **4.07** (20 mg, 0.04 mmol) in dry THF (3 ml) was added NaH (5 mg, 0.12 mmol) and sodium methoxide (5 mg, 0.09 mmol). The reaction was hearted to reflux for 3 h and monitored by TLC. ^{1}H NMR of crude material confirmed the presence of the starting material **4.07** only.

Method 3 (See chapter 4, table 4 entry 3)

To a solution of 5-fluoro-triazole **4.07** (20 mg, 0.04 mmol) in dry THF (3 ml) was added K_2CO_3 (8 mg, 0.06 mmol) and sodium methoxide (5 mg, 0.09 mmol). The reaction was hearted to reflux for 3 h and monitored by TLC. ^{1}H NMR of crude material confirmed the presence of the starting material **4.07** only.

Method 4 (See chapter 4, table 4 entry 4)

To a solution of 5-fluoro-triazole **4.07** (20 mg, 0.04 mmol) in dry THF (3 ml) was added Cs_2CO_3 (20 mg, 0.06 mmol) and sodium methoxide (5 mg, 0.09 mmol). The reaction was hearted to reflux for 3 h and monitored by TLC. ^{1}H NMR of crude material confirmed the presence of the starting material **4.07** only.

Method 5 (See chapter 4, table 4 entry 5)

Following the conditions described in method 1. However the reaction was undertaken in drug DMF (3 ml) at 80 ^{o}C for 3 h. ^{1}H NMR of crude material confirmed the presence of the starting material **4.07** only.

Method 6 (See chapter 4, table 4 entry 6)

Following the conditions described in method 1. However the reaction was undertaken in drug DMF (3 ml) at 130 ^{o}C for 12 h. The reaction mixture was cooled, diluted with DCM (25 ml), washed with water (1 x 25 ml) and brine (1 x 25 ml), dried over Na2SO4, filtered and concentrated *in vacuo*. The residue was purified by silica gel chromatography eluting with 5% MeOH in DCM to give a white solid (11 mg, 55%). ^{1}H NMR indicated the presence of the 5-proton-triazole **1.23** and consistent with the literature data.[6]

Method 7 (See chapter 4, table 4 entry 7)

To a solution of 5-fluoro-triazole **4.07** (20 mg, 0.04 mmol) in dry DMF (3 ml) was added NaH (2 mg, 0.06 mmol) and sodium methoxide (5 mg, 0.09 mmol). The reaction mixture was transferred to a 5 ml round-bottomed microwave vial and placed into the microwave reactor with pressure set to **250** psi and temperature to 180 ^{o}C for 10 min. After the vial was cooled to room temperature. ^{1}H NMR of crude material confirmed the presence of a complex mixture only.

Attempted synthesis of 3-(4-(5-hydroxy-4-(5-((3aS,4S,6aR)-2-oxohexahydro-1H-thieno[3,4-d]imidazol-4-yl)pentyl)-1H-1,2,3-triazol-1-yl)butyl)-5 methylbenzo[d]oxazol-2(3H)-one 4.17
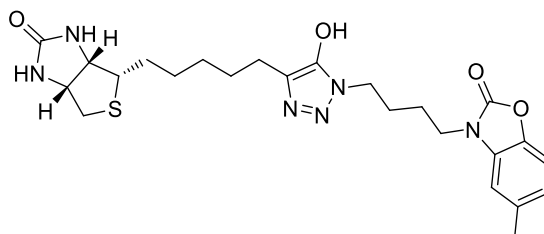
Method 1 (See chapter 4, table 4 entry 8)

To a solution of 5-fluoro-triazole **4.07** (20 mg, 0.04 mmol) in dry THF (3 ml) was added NaH (2 mg, 0.06 mmol) and NaOH (5 mg, 0.09 mmol). The reaction was hearted to reflux for 3 h and monitored by TLC. ^{1}H NMR of crude material confirmed the presence of a complex mixture only.

5-methyl-3-(4-(4-(5-((3aS,4S,6aR)-2-oxohexahydro-1H-thieno[3,4-d]imidazol-4-yl)pentyl)-5-phenyl-1H-1,2,3-triazol-1-yl)butyl)benzo[d]oxazol-2(3H)-one 4.18
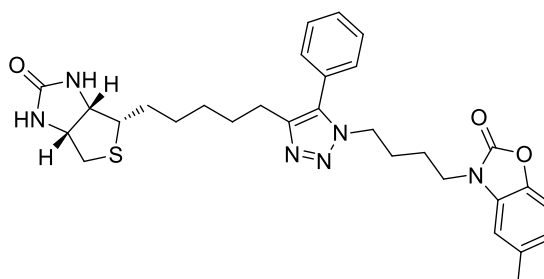
Method 1 (See chapter 4, table 5 entry 1)

To a solution of 5-iodo-triazole **4.06** (75 mg, 0.13 mmol) in dry DMF (5 ml) was added K$_2$CO$_3$ (52 mg, 0.38 mmol), followed by adding phenylboronic acid (15 mg, 0.13 mmol) and PdCl$_2$(PPh$_3$)$_3$ (8 mg, 5 mol %). The reaction mixture was stirred at room temperature for 12 h, after which the solvent was removed *in vacuo.* TLC eluting with 5% MeOH in DCM indicated the trace amount of the target triazole **4.18** and the presence of starting material **4.06**.

Method 2 (See chapter 4, table 5 entry 2)

Following the condition described in method 1. However the reaction was undertake at 150 °C for 3 h. The residue was concentrated *in vacuo* and purified by flash chromatography on silica eluting with 5% MeOH in DCM to a white solide (38 mg, 63%). ^{1}H NMR of the purified compound was consistent with the literature data of 5-H-triaozle **1.23** with > 99% purity.[6]

Method 3 (See chapter 4, table 5 entry 3)

The procedure outlined in method 1 was repeated using THF (5 ml) instead of DMF. The reaction was stirred at 70 °C for 12 h, after which the residue was concentrated *in vacuo* and purified by flash chromatography on silica eluting with 5% MeOH in DCM to give the title compound as a yellowish solid (30 mg, 41%).

^{1}H NMR (500 MHz; CDCl$_3$): δ 7.44-7.47 (3H, m, 3 x Ar^{Bn}**H**), 7.17-7.19 (2H, m, 2 x Ar^{Bn}**H**), 7.00-7.01 (1H, m, Ar**H**), 6.94-6.96 (1H, m, Ar**H**), 6.77 (1H, d, J = 7.9 Hz, Ar**H**), 5.86 (1H, bs, C(O)N**H**), 5.52 (1H, bs, C(O)N**H**), 4.45-4.49 (1H, m, NHC**H**), 4.24-4.27 (3H, m, NHC**H,** ArN^{tri}C**H$_2$**), 3.70 (2H, t, J = 6.9 Hz, NC**H$_2$**), 3.06-3.10 (1H, m, SC**H**), 2.84-2.88 (1H, m, SC**H$_a$**), 2.70 (1H, dd, J = 5.1, 12.8 Hz, SC**H$_b$**), 2.56 (2H, dt, J = 1.5, 7.3 Hz, ArC^{tri}C**H$_2$**), 2.37 (3H, s, ArC**H$_3$**), 1.73-1.79 (2H, m, C**H$_2$**), 1.56-1.69 (6H, m, 3x C**H$_2$**), 1.28-1.38 (4H, m, 2 x C**H$_2$**);

^{13}C NMR (125 MHz; CDCl$_3$): δ 166.2, 157.3, 148.3, 145.4, 136.8, 135.3, 132.1, 132.0, 131.9, 131.1, 130.1, 126.9, 113.4, 110.5, 64.7, 62.8, 58.5, 50.1, 44.0, 43.2, 31.8, 31.7, 31.3, 31.1, 29.4, 27.5, 27.2, 24.1.

HRMS calcd. for (M + H$^+$) C$_{30}$H$_{37}$N$_6$O$_3$S, requires 561.2648, found 561.2640

HPLC R$_t$ = 17.4 min

Attempted synthesis of 3-(4-(5-isobutyl-4-(5-((3aS,4S,6aR)-2-oxohexahydro-1H-thieno[3,4-d]imidazol-4-yl)pentyl)-1H-1,2,3-triazol-1-yl)butyl)-5-methylbenzo[d]oxazol-2(3H)-one 4.19
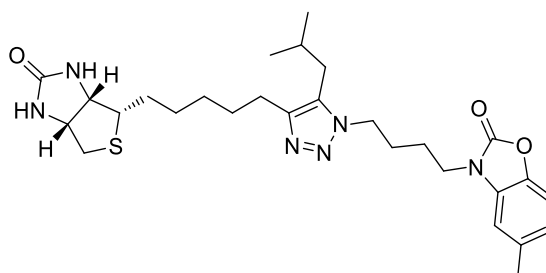
**Method 1 (See chapter 4, table 6 entry 1)**

To a solution of 5-iodo-triazole **4.06** (75 mg, 0.13 mmol) in dry THF (5 ml) was added K_2CO_3 (52 mg, 0.38 mmol), followed by adding isobutylboronic acid (15 mg, 0.13 mmol) and $PdCl_2(PPh_3)_3$ (8 mg, 5 mol %). The reaction was stirred at 70 ºC for 12 h, after which the residue was concentrated *in vacuo* and purified by flash chromatography on silica eluting with 5% MeOH in DCM. ^{1}H NMR of the purified compound was consistent with the literature data of 5-H-triaozle **1.11** with > 99% purity.[6]

Method 2 (See chapter 4, table 6 entry 1)

Following the condition described in method 1. However $Pd(OAc)_2$ (8 mg, 5 mol %) was used instead of $PdCl_2(PPh_3)_3$ (8 mg, 5 mol %). TLC of the crude material indicated a 3:5 mixture of starting material **4.06** and 5-proton-triazole **1.11** only.

Method 2 (See chapter 4, table 6 entry 1)

Following the condition described in method 2. Additional PPh_3 (102 mg, 0.39 mmol) was added to the reaction. TLC of the crude material indicated a 1:7 mixture of starting material **4.06** and 5-proton-triazole **1.11** only.

***N*-iodomorpholine-hydrogen iodide[7]**
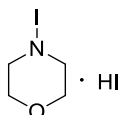
To a solution of iodine (10 g, 0.04 mol) in MeOH (150 ml) was added dropwise morphline (3.43 ml, 0.04 mol), after which a fine orange precipitate was formed. The suspension was stirred for 45 min then solid was isolated by filtration. The solid was dried under vacuum to give *N*-iodomorpholine-hydrogen iodide as an orange crystalline powder (12.9 g, 95%). The compound was used without further purification or characterization.

3-(4-azidobutyl)-5-methylbenzo[*d*]oxazol-2(3*H*)-one 4.20
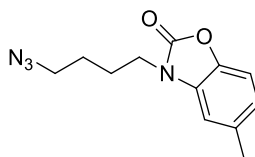
2-Benzoxazolone bromide **4.22** (256 mg, 0.90 mmol) was reacted according to general procedure **B2** and purified by silica gel chromatography eluting with15% ethyl acetate in petroleum ether to yield a colourless oil (205 mg, 91%).^{1}H NMR was consistent with literature.[4]

Compound 4.20[4]

^{1}H NMR (500 MHz; CDCl$_3$): δ 7.08 (1H, d, *J* = 8.1 Hz, Ar**H**), 6.91 (1H, d, *J* = 8.1 Hz, Ar**H**), 6.79 (1H, s, Ar**H**), 3.83 (2H, t, *J* = 6.9 Hz, NC**H$_2$**), 3.36 (2H, t, *J* = 6.9 Hz, C**H$_2$**N$_3$), 2.40 (3H, s, ArC**H$_3$**), 1.83-1.93 (2H, m, C**H$_2$**), 1.63-1.72 (2H, m, C**H$_2$**);

^{13}C NMR (125 MHz; CDCl$_3$): δ 155.0, 140.9, 134.0, 131.1, 123.0, 109.8, 108.9, 51.0, 41.7, 26.2, 25.2, 21.7;

9-(4-azidobutyl)-9*H*-purin-6-amine 4.21
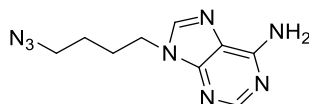
Adenine bromide **4.23** (150 mg, 0.56 mmol) was treated according to general procedure **B1** and purified by silica gel chromatography eluting with 8% MeOH in DCM to give a white solid (121 mg, 92%). ^{1}H NMR was consistent with literature.[8]

Compound 4.21[8]

^{1}H NMR (500 MHz, DMSO-*d$_6$*): δ 8.30 (1H, s, Ar**H**) 7.84 (1H, s, Ar**H**), 7.21 (2H, bs, ArN**H$_2$**), 4.25 (2H, t, *J* = 7.2 Hz, ArC**H$_2$**), 3.36 (2H, t, *J* = 6.6 Hz, C**H$_2$**N$_3$), 1.95-2.04 (2H, m, C**H$_2$**), 1.58-1.68 (2H, m, C**H$_2$**);

^{13}C NMR(125 MHz; DMSO-*d$_6$*): δ 155.9, 152.4, 149.9, 140.8, 118.6, 50.1, 42.4, 26.7, 25.5.

3-(4-bromobutyl)-5-methylbenzo[*d*]oxazol-2(3*H*)-one 4.22
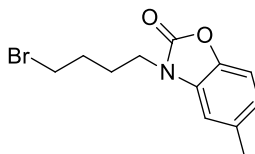
2-benzoxazolone **2.27** (366 mg, 2.46 mmol) and 1,2-dibromoethane (788 mg, 3.68 mmol) was reacted according to general procedure **B1** and was purified by flash chromatography on silica eluting with 20% ethyl acetate in petroleum ether to yield an off white solid (647 mg, 93%). ^{1}H NMR was consistent with literature.[4]

Compound 4.22[4]

[1]**H NMR** (500 MHz; CDCl$_3$): δ 7.07 (1H, d, *J* = 8.1 Hz, Ar**H**), 6.90 (1H, d, *J* = 8.1 Hz, Ar**H**), 6.78 (1H, s, Ar**H**), 3.84 (2H, t, *J* = 6.6 Hz, NC**H$_2$**), 3.43 (2H, t, *J* = 6.6 Hz, C**H$_2$**Br), 2.39 (3H, s, ArC**H$_3$**), 1.92-1.97 (4H, m, C**H$_2$**);

[13]**C NMR** (125 MHz; CDCl$_3$): δ 155.0, 140.9, 134.1, 131.0, 123.0, 109.8, 108.9, 41.4, 32.9, 29.6, 26.5, 21.7

9-(4-bromobutyl)-9*H*-purin-6-amine 4.23
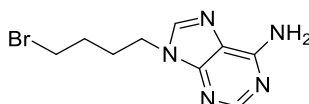
Adenine **2.29** (250 mg, 1.85 mmol) was alkylated following general procedure **B1**, using 1,4-dibromobutane (789 mg, 3.70 mmol) and purified by silica gel chromatography eluting with 6% MeOH in DCM to give a white solid (427 mg, 86%)

Compound 4.23[8]

[1]**H NMR** (500 MHz; DMSO-*d$_6$*): δ 8.15 (1H, s, Ar**H**), 8.14 (1H, s, Ar**H**), 7.21 (2H, bs, ArN**H$_2$**), 4.18 (2H, t, *J* = 6.6 Hz, ArC**H$_2$**), 3.55 (2H, t, *J* = 6.3 Hz, C**H$_2$**Br), 1.88-1.97 (2H, m, C**H$_2$**), 1.70-1.79 (2H, m, C**H$_2$**);

[13]**C NMR** (125 MHz; DMSO-*d$_6$*): δ 155.9, 152.4, 149.6, 140.8, 118.7, 42.0, 34.3, 29.3, 28.1.

7.7   Experimental work as described in Chapter 5

N-(*N*-(4-methylbenzyl)sulfamoyl)-5-((3a*S*,4*S*,6a*R*)-2-oxohexahydro-1*H*-thieno[3,4-*d*]imidazol-4-yl)pentanamide 5.03
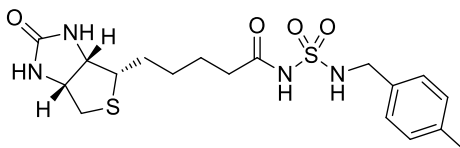
A suspension of the sulfonamide **5.08** (200 mg, 1.00 mmol), CsCO$_3$ (232 mg, 1.20 mmol) and biotin succinimide **5.07** (375 mg, 1.10 mmol) in DMF (3 mL) was reacted according to general procedure **F**. The solvent were removed under reduced pressure and the crude was purified by flash chromatography on silica gel eluting with 10% MeOH in DCM to give the title compound as a crystalline solid (225 mg, 53%).

^{1}H NMR (500 MHz, DMSO-*d6*): δ 8.06 (1H, s, SN**H**), 7.15 (2H, d, *J* = 8.0 Hz, 2 x Ar**H**), 7.09 (2H, d, *J* = 8.0 Hz, 2 x Ar**H**), 6.38 (1H, bs, N**H**), 6.33 (1H, bs, N**H**), 4.27-4.30 (1H, m, NHC**H**), 4.09-4.12 (1H, m, NHC**H**), 4.02 (2H, d, *J* = 6.1 Hz, NHC**H₂**), 3.04-3.08 (1H, m, SC**H**), 2.80 (1H, dd, *J* = 5.0, 12.4 Hz, SC**H**ₐ), 2.47-2.49 (1H, m, SC**H**ᵦ), 2.25 (3H, s, C**H₃**), 2.03 (2H, t, *J* = 7.4 Hz, COC**H₂**), 1.19-1.62 (6H, m, 3 x C**H₂**),
^{13}C NMR (125 MHz, DMSO-*d6*): δ 176.5, 167.9, 141.4, 139.7, 133.9, 132.9, 66.3, 64.4, 60.5, 51.2, 39.9, 35.9, 33.2, 30.4, 29.3, 25.9.
HRMS calcd. for (M + H$^+$) C$_{18}$H$_{27}$N$_4$O$_4$S$_2$: requires 427.1474, found 427.1480.
HPLC R$_t$ = 14.8 min

N-(*N*-(3-fluorobenzyl)sulfamoyl)-5-((3a*S*,4*S*,6a*R*)-2-oxohexahydro-1*H*-thieno[3,4-*d*]imidazol-4-yl)pentanamide 5.04
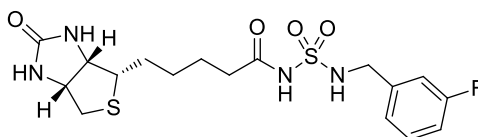
A suspension of the sulfonamide **5.09** (205 mg, 1.00 mmol), CsCO$_3$ (232 mg, 1.20 mmol) and biotin succinimide **5.07** (375 mg, 1.10 mmol) in DMF (3 mL) was reacted according to general procedure **F**. The solvent was removed under reduced pressure and the crude was

purified by flash chromatography on silica gel eluting with 10% MeOH in DCM to give the title compound as a crystalline solid (270 mg, 63%).

¹H NMR (500 MHz, DMSO-*d6*): δ 11.27 (1H, bs, SN**H**), 8.17 (1H, t, *J* = 6.1 Hz, SN**H**), 7.30-7.33 (2H, m, 2 x Ar**H**), 7.10-7.14 (2H, m, 2 x Ar**H**), 6.38 (1H, bs, N**H**), 6.34 (1H, bs, N**H**), 4.27-4.30 (1H, m, NHC**H**), 4.10-4.12 (1H, m, NHC**H**), 4.06 (2H, d, *J* = 6.2 Hz, NHC**H₂**), 3.05-3.09 (1H, m, SC**H**), 2.81 (1H, dd, *J* = 5.1, 12.4 Hz, SC**Hₐ**), 2.56 (1H, d, *J* = 12.5 Hz, SC**Hᵦ**), 2.06 (2H, t, *J* = 7.4 Hz, COC**H₂**), 1.22-1.62 (6H, m, 3 x C**H₂**),

¹³C NMR (125 MHz, DMSO-*d6*): δ 171.8, 163.1, 162.8, 134.3, 134.3, 130.1, 130.1, 115.4, 115.3, 61.5, 59.6, 55.8, 45.9, 35.3, 28.4, 24.6.

HRMS calcd. for (M + H⁺) $C_{17}H_{24}FN_4O_4S_2$: requires 431.1223, found 431.1225.

HPLC R_t = 14.8 min

N-(*N*-(4-(6-amino-9*H*-purin-9-yl)butyl)sulfamoyl)-5-((3a*S*,4*S*,6a*R*)-2-oxohexahydro-1*H*-thieno[3,4-*d*]imidazol-4-yl)pentanamide 5.05
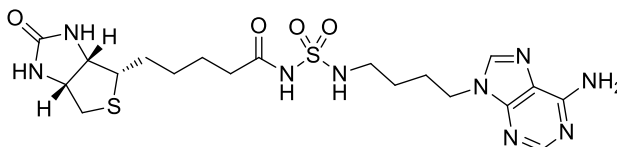
A suspension of the sulfonamide **5.10** (258 mg, 1.00 mmol), CsCO₃ (232 mg, 1.20 mmol) and biotin succinimide **5.07** (375 mg, 1.10 mmol) in DMF (3 mL) was reacted according to general procedure **F**. The solvent were removed under reduced pressure and the crude was purified by flash chromatography on silica gel eluting with 10% MeOH in DCM to give the title compound as a crystalline solid (178 mg, 35%).

¹H NMR (500 MHz, DMSO-*d6*): δ 11.26 (1H, s, SN**H**), 8.13 (1H, s, Ar**H**), 8.11 (1H,s, Ar**H**), 7.59 (1H, t, *J* = 5.7 Hz, SN**H**), 7.20 (2H, s, N**H₂**), 6.50 (1H, s, C(O)N**H**), 6.38 (1H, s, C(O)N**H**), 4.30 (1H, dd, *J* = 5.2, 7.6 Hz, NHC**H**), 4.20–4.07 (3H, m, NC**H₂**, NHC**H**), 3.12–3.04 (1H, m, SC**H**), 2.88 (2H, m, NHC**H₂**), 2.80 (1H, dd, *J* = 5.1, 12.4 Hz, SC**Hₐ**), 2.57 (1H, d, *J* = 12.4 Hz, SC**Hᵦ**), 2.18 (2H, t, *J* = 7.4 Hz, C(O)C**H₂**), 1.91–1.73 (2H, m, C**H₂**), 1.67–1.55 (1H, m, C**H₂ₐ**), 1.55–1.36 (5H, m, 2 x C**H₂**, C**H₂ᵦ**), 1.35–1.21 (2H, m, C**H₂**).

¹³C NMR (125 MHz, DMSO-*d6*): 171.5, 162.8, 155.9, 152.4, 149.5, 140.8, 118.7, 61.1, 59.2, 55.4, 48.6, 42.4, 42.2, 35.0, 28.0, 26.8, 25.8, 24.3.

HRMS calcd. for (M + H⁺) $C_{19}H_{30}N_9O_4S_2$: requires 512.1862, found 512.1834.

2,5-Dioxopyrrolidin-1-yl   5-((3a*S*,4*S*,6a*R*)-2-oxohexahydro-1*H*-thieno[3,4-*d*]imidazol-4-yl)pentanoate 5.07
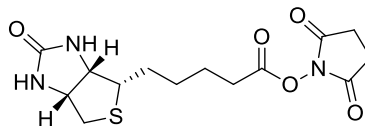

To a solution of *d*-Biotin **1.01** (500 mg, 2.06 mmol) in dry DMF (5 mL) was added *N*-hydroxysuccinimide (283 mg, 2.46 mmol) and EDC hydrochloric salt (470 mg, 2.46 mmol). The reaction mixture was stirred under nitrogen atmosphere at room temperature overnight. The mixture was partitioned between ethyl acetate and water and the aqueous phase was extracted with ethyl acetate (3 x 20 mL). The organics combined were dried NaSO$_4$, filtered, concentrated *in vacuo*. The solid obtained was triturated from diethyl ether to afford the title compound as a colourless solid (400 mg, 57%).

¹H NMR (500 MHz, DMSO-*d6*) δ 6.41 (1H, s, N**H**), 6.35 (1H, s, N**H**), 4.51–4.20 (1H, m, SC**H**), 4.20–4.07 (1H, m, CH**H**), 3.11 (1H, dd, *J* = 12.3, 6.5 Hz, SC**H**$_a$), 2.87–2.78 (5H, m, 2 x C**H**$_2$, SC**H**$_b$), 2.67 (2H, t, *J* = 7.4 Hz, C**H**$_2$), 2.58 (1H, d, *J* = 12.2 Hz, C**H**H), 1.65 (3H, dt, *J* = 15.2, 7.7 Hz, C**H**$_2$, CH**H**), 1.55–1.46 (1H, m, C**H**H) and 1.43 (2H, dd, *J* = 12.4, 6.4 Hz, C**H**$_2$).

¹³C NMR (125 MHz, DMSO-d6): δ 170.2, 168.9, 162.6, 61.0, 59.2, 55.2, 40.0, 30.0, 27.8, 27.6, 25.4, 24.3.

N-(4-methylbenzyl)-sulfamide 5.08
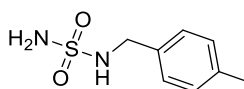
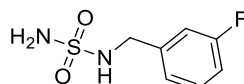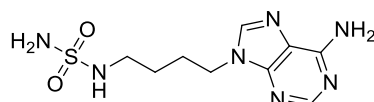
Tert-butyl N-(4-(6-amino-9H-purin-9-yl)butyl)sulfamoylcarbamate **5.16** (450 mg, 1.5 mmol) was treated with trifluoroacetic acid (2.1 mL, 27 mmol) according to general procedure **G**. The crude material was purified by flash chromatography on silica gel eluting with 5% MeOH in DCM to give a crystalline white solid (189 mg, 63%).

¹H NMR (500 MHz, DMSO-*d6*): δ 7.21 (2H, d, *J* = 7.7 Hz, 2 x Ar**H**), 7.11 (2H, d, *J* = 7.7 Hz, 2 x Ar**H**), 6.94 (1H, t, *J* = 6.5 Hz, N**H**), 6.57 (2H, bs, N**H₂**), 4.01 (2H, d, *J* = 6.5 Hz, C**H₂**), 2.26 (3H, s, C**H₃**)

¹³C NMR (125 MHz, DMSO-*d6*): δ 136.4, 136.0, 129.1, 128.1, 46.3, 21.1

N-(3-fluorobenzyl)-sulfamide 5.09

Tert-butyl N-(4-(6-amino-9H-purin-9-yl)butyl)sulfamoylcarbamate **5.17** (455 mg, 1.5 mmol) was treated with trifluoroacetic acid (2.1 mL, 27 mmol) according to general procedure **G**. The crude material was purified by flash chromatography on silica gel eluting with 5% MeOH in DCM to give a crystalline white solid (230 mg, 75%).

¹H NMR (500 MHz, DMSO-*d6*): δ 7.36-7.39 (2H, m, 2 x Ar**H**), 7.12-7.15 (2H, m, 2 x Ar**H**), 6.63 (2H, bs, N**H₂**), 4.05 (2H, s, C**H₂**).

¹³C NMR (125 MHz, DMSO-*d6*): δ 165.3, 138.0 (d), 132.7 (d), 118.9 (d), 48.4.

N-(4-(6-amino-9*H*-purin-9-yl)butyl)-sulfamide 5.10

Tert-butyl N-(4-(6-amino-9H-purin-9-yl)butyl)sulfamoylcarbamate **5.21** (664 mg, 1.72 mmol) was treated with trifluoroacetic acid (2.4 mL, 31.4 mmol) according to general procedure **G**. The solvent was removed under reduced pressure to give the title compound as a crystalline solid (641 mg) and was used without further purification.

HRMS calcd. for (M + Na⁺) C₉H₁₅N₇NaO₂S: requires 308.0906, found 308.0883.
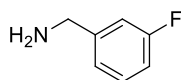
p-Tolylmethanamine 5.12
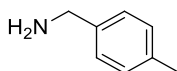
To a solution of azide **3.03k** (150 mg, 1.02 mmol) in dry MeOH (15 mL) was added PPh$_3$ (404 mg, 1.53 mmol). The reaction was heated to reflux at 80 °C for 1 h. After all the starting material had disappeared (monitored by TLC), the reaction mixture was cooled to room temperature. The solvent was removed under reduced pressure and the resulting residue was used without further purification. ^{1}H NMR of the crude sample is consistent with literature data.[9]

^{1}**H NMR** (500 MHz, CDCl$_3$): δ 7.36-7.39 (4H, m, 4 x Ar**H**), 7.12-7.15 (2H,m, 2 x Ar**H**), 3.84 (2H, s, C**H$_2$**), 2.34 (2H, s, C**H$_3$**), 2.15 (2H, bs, N**H$_2$**).

^{13}**C NMR** (125 MHz, CDCl$_3$): δ 139.5, 136.4, 129.3, 127.1, 45.6, 21.0

(3-Fluorophenyl)methanamine 5.13

To a solution of azide **3.03t** (151 mg, 1.00 mmol) in dry MeOH (15 mL) was added PPh$_3$ (393 mg, 1.50 mmol). The reaction was heated to reflux at 80 °C for 1 h. After all the starting material had disappeared (monitored by TLC), the reaction mixture was cooled to room temperature. The solvent was removed under reduced pressure and the resulting residue was used without further purification. ^{1}H NMR of the crude sample is consistent with literature data.[9]

^{1}**H NMR** (500 MHz, CDCl$_3$): δ 7.23-7.39 (3H, m, 3 x Ar**H**), 7.15 (1H, s, Ar**H**), 3.80 (2H, s, C**H$_2$**), 2.85 (2H, bs, N**H$_2$**).

^{13}**C NMR** (125 MHz, D CDCl$_3$): δ 144.0, 130.2, 126.1, 122.7, 45.3

N-(1-(*N*-(tert-butoxycarbonyl)sulfamoyl)pyridin-4(1*H*)-ylidene)-*N*-methylmethanaminium 5.15
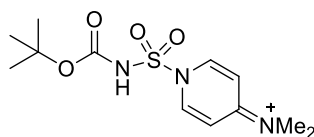
To a solution of *tert*-butyl alcohol (1.7 mL,18.63 mmol) in dry methylene chloride (15 ml) at 0 °C was added dropwise chlorosulfonyl isocyanate (CSI) **5.14** (1.6 mL, 18.63 mmol),

_____

followed by addition of DMAP (4.55 g, 37.25 mmol). The reaction mixture was stirred at room temperature for 1 h, and then washed with water (3 x 15 mL). The organic layers were combined and dried over NaSO$_4$, filtered, concentrated *in vacuo*. The crude compound was then crystallized from acetonitrile to afford the title compound as a colorless powder (4.50 g, 80%). ^{1}H NMR is consistent with literature data.[10]
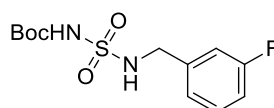
Tert-butyl *N*-(4-methylbenzyl)sulfamoylcarbamate 5.16
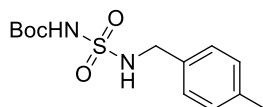
Amine **5.12** (605 mg, 5.0 mmol) was reacted with TEA (1.40 mL, 10.00 mmol) and **5.15** (1.5 G, 5.00 mmol) according to general procedure **H**. The crude material was purified by flash chromatography on silica gel eluting with 5% MeOH in DCM to give a crystalline white solid (645 mg, 43%).

^{1}H NMR (500 MHz, DMSO-*d6*): δ 7.24 (2H, d, *J* = 7.7 Hz, 2 x Ar**H**), 7.15 (2H, d, *J* = 7.7 Hz, 2 x Ar**H**), 7.04 (1H, t, *J* = 6.5 Hz, N**H**), 4.05 (2H, d, *J* = 6.5 Hz, C**H₂**), 2.30 (3H, s, C**H₃**), 1.38 (9H, s, *t***Bu**).
^{13}C NMR (125 MHz, DMSO-*d6*): δ 152.3, 139.0,138.7, 131.8, 130.7, 79.2, 49.0, 27.9, 23.8

**Tert-butyl *N*-(3-fluorobenzyl)sulfamoylcarbamate 5.17**

Amine **5.13** (625 mg, 5.0 mmol) was reacted with TEA (1.40 mL, 10.00 mmol) and **5.15** (1.5 G, 5.00 mmol) according to general procedure **H**. The crude material was purified by flash chromatography on silica gel eluting with 5% MeOH in DCM to give a crystalline white solid (684 mg, 45%).

^{1}H NMR (500 MHz, CDCl$_3$): δ 7.30-7.32 (1H, m, Ar**H**), 7.02-7.05 (3H,m, 3 x Ar**H**), 4.22 (2H, s, C**H₂**), 1.45 (9H, s, *t***Bu**)
^{13}C NMR (125 MHz, CDCl$_3$): δ 150.0, 129.9, 129.8, 115.8, 115.7, 84.0, 47.2, 27.9.

2-(4-(6-amino-9*H*-purin-9-yl)butyl)isoindoline-1,3-dione 5.19
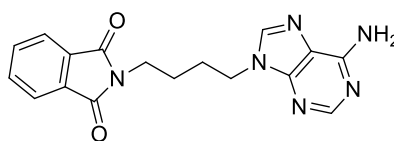
Method 1

To a suspension of adenine bromide **4.23** (500 mg, 1.86 mmol) in DMF (5 mL) was added K$_2$CO$_3$ (385 mg, 2.79 mmol) and potassium phthalamide (575 mg, 2.05 mmol) and allowed to stir at room temperature for 12 h. The reaction mixture was diluted with EtOAc and washed with water, aqueous saturated Na$_2$SO$_4$, water and brine, dried over NaSO$_4$, filtered, concentrated *in vacuo*. The solid obtained was triturated from diethyl ether to afford the title compound as a pale yellow solid (300 mg, 48%). ^{1}H NMR was consistent with Method 2.

Method 2

To a suspension of adenine **2.29** (1.1 g, 4.09 mmol) in DMF (10 mL) was added K$_2$CO$_3$ (847 mg, 6.14 mmol) and *N*-(4-bromobutyl)phthalamide **5.18** (1.26 g, 4.50 mmol) and the mixture was stirred at 70 °C overnight. The mixture was allowed to cool down to room temperature and diluted with EtOAc and washed with water, aqueous saturated Na$_2$SO$_4$, water and brine, dried over NaSO$_4$, filtered, concentrated *in vacuo*. The solid obtained was triturated from diethyl ether to afford the title compound as a pale yellow solid (920 mg, 67%).

^{1}H NMR (500 MHz, DMSO-*d6*): δ 8.12 (1H, s, Ar**H**), 8.07 (1H, s, Ar**H**), 7.84 (4H, m, Ar**H**), 7.16 (2H, s, N**H$_2$**), 4.17 (2H, t, *J* = 6.7 Hz, C**H$_2$**), 3.61 (2H, t, *J* = 6.7 Hz, C**H$_2$**), 1.83 (2H, dd, *J* = 14.7, 6.9 Hz, C**H$_2$**), 1.56 (2H, dt, *J* = 13.8, 6.9 Hz, C**H$_2$**).
^{13}C NMR (125 MHz, DMSO-*d6*): δ 167.9, 155.9, 152.3, 149.5, 140.8, 134.3, 131.6, 123.0, 118.7, 42.4, 36.8, 26.7, 25.1.
HRMS calcd. for (M + H$^+$) C$_{17}$H$_{16}$N$_6$O$_2$: requires 336.1322, found 336.1335

**9-(4-aminobutyl)-9*H*-purin-6-amine 5.20**
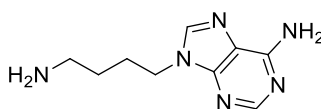
To a suspension of 2-(4-(6-amino-9H-purin-9-yl)butyl)isoindoline-1,3-dione **5.19** (2.5 G, 7.43 mmol) in ethanol (125 mL) was added hydrazine hydrate (3.5 mL, 114.45 mmol) and the mixture was stirred at reflux overnight. The mixture was allowed to cooled down to room temperature and concentrated under reduced pressure. A solid was formed which was filtrated and washed with DCM. Trituration from MeOH afforded the title compound (1G, 67%) as a colourless solid.

¹H NMR (500 MHz, DMSO-*d6*): δ 8.12 (1H, s, Ar**H**), 8.11 (1H, s, Ar**H**), 7.14 (2H, s, N**H₂**), 4.11 (2H, t, *J* = 7.1 Hz, C**H₂**), 3.06 (2H, bs, N**H₂**), 2.51 (2H, t, *J* = 6.9 Hz, C**H₂**), 1.79 (2H, dd, *J* = 14.9, 7.3 Hz, C**H₂**) and 1.28 (2H, dd, *J* = 14.9, 7.3 Hz, C**H₂**).

¹³C NMR (125 MHz, DMSO-*d6*): δ 155.9, 152.3, 149.5, 140.8, 118.7, 42.8, 41.0, 30.0, 26.9.

HRMS calcd. for (M + H⁺) $C_9H_{15}N_6$: requires 207.1358, found 207.1513.

*T*ert-butyl *N*-(4-(6-amino-9*H*-purin-9-yl)butyl)sulfamoylcarbamate 5.21
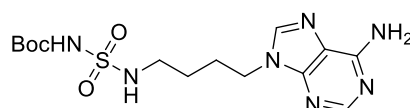

Amine **5.20** (1.6 G, 7.75 mmol) was reacted with TEA (2.1 mL, 15.5 mmol) and **5.15** (2.6 G, 7.75 mmol) according to general procedure **H**. The crude material was purified by flash chromatography on silica gel eluting with 5% MeOH in DCM to give a crystalline white solid (664 mg, 23%).

¹H NMR (500 MHz, DMSO-*d6*): δ 10.77 (1H, s, N**H**), 8.12 (1H, s, Ar**H**), 8.11 (1H, s, Ar**H**), 7.55 (1H, bs, N**H**), 7.16 (2H, s, N**H₂**), 4.12 (2H, t, *J* = 7.0 Hz, C**H₂**), 2.90 (2H, dd, *J* = 13.0, 6.7 Hz, C**H₂**), 1.82 (2H, m, C**H₂**), 1.41 (2H, m, C**H₂**) and 1.38 (9H, s, *t***Bu**) ppm.

¹³C NMR (125 MHz, DMSO-*d6*): δ 155.9, 152.3, 150.6, 149.5, 140.7, 118.7, 81.0, 42.4, 42.2, 27.7, 26.7, 25.8.

HRMS calcd. for (M + H⁺) $C_{14}H_{24}N_7O_4S$: requires 386.1610, found 386.1689.
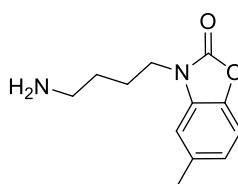
_____

2-(4-(5-methyl-2-oxobenzo[*d*]oxazol-3(2*H*)-yl)butyl)isoindoline-1,3-dione 5.22
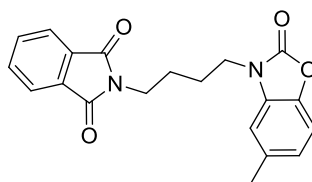
To a suspension of 2-benzoxazolone **2.27** (150 mg, 1.0 mmol) in DMF (3 mL) was added K$_2$CO$_3$ (207 mg, 1.5 mmol) and *N*-(4-bromobutyl)phthalamide **5.18** (309 mg, 1.1 mmol) and the mixture was stirred at 70 °C overnight. The mixture was allowed to cool down to room temperature and diluted with EtOAc and washed with water, aqueous saturated Na$_2$SO$_4$, water and brine, dried over NaSO$_4$, filtered, concentrated *in vacuo*. The solid obtained was triturated from diethyl ether to afford the title compound as a pale yellow solid (185 mg, 53%).

¹H NMR (500 MHz, CDCl$_3$): δ 7.84 (4H, m, Ar**H**), 7.16 (2H, s, N**H₂**), 7.10 (1H, d, *J* = 8.1 Hz, Ar**H**), 6.91 (1H, d, *J* = 8.1 Hz, Ar**H**), 6.79 (1H, s, Ar**H**), 3.97 (2H, t, *J* = 6.7 Hz, C**H₂**), 3.61 (2H, t, *J* = 6.7 Hz, C**H₂**), 1.83-1.93 (2H, m, C**H₂**), 1.56-1.63 (2H, m, C**H₂**).
¹³C NMR (125 MHz, CDCl$_3$): δ 167.9, 155.3, 140.9, 134.0, 131.1, 123.0, 118.7, 51.0, 41.7, 26.2, 25.2, 21.7.

Attempt synthesis of 3-(4-aminobutyl)-5-methylbenzo[*d*]oxazol-2(3*H*)-one 5.23

Method 1:

To a solution of azide **4.20** (250 mg, 1.02 mmol) in dry MeOH (15 mL) was added PPh$_3$ PPh$_3$ (404 mg, 1.53 mmol). The reaction was heated to reflux at 80 °C for 1 h. After all the starting material had disappeared (monitored by TLC), the reaction mixture was cooled to room temperature and concentrated under reduced pressure. The resulted residue was analysed by ¹H NMR and TLC (eluting with 3% Method in DCM) to give a complex mixture with no desired product observed.

Method 2:

_____

To a suspension of 2-(4-(5-methyl-2-oxobenzo[*d*]oxazol-3(2*H*)-yl)butyl)isoindoline-1,3-dione **5.22** (100 mg, 0.28 mmol) in ethanol (5 mL) was added hydrazine hydrate (0.13 mL, 4.2 mmol, 15 eq) and the mixture was stirred at reflux overnight. The mixture was allowed to cooled down to room temperature and concentrated under reduced pressure. The resulted residue was analysed by ^{1}H NMR and TLC (eluting with 3% Method in DCM) to give a complex mixture with no desired product observed.

7.8 Experimental work as described in Chapter 6

7.8.1 In situ experiments

2.21

6.25 n = 4
6.26 n = 5

4.21

3.03k R = 4Me
3.03t R = 3F

6.04

6.07

6.02

6.05

6.08

6.03

6.06
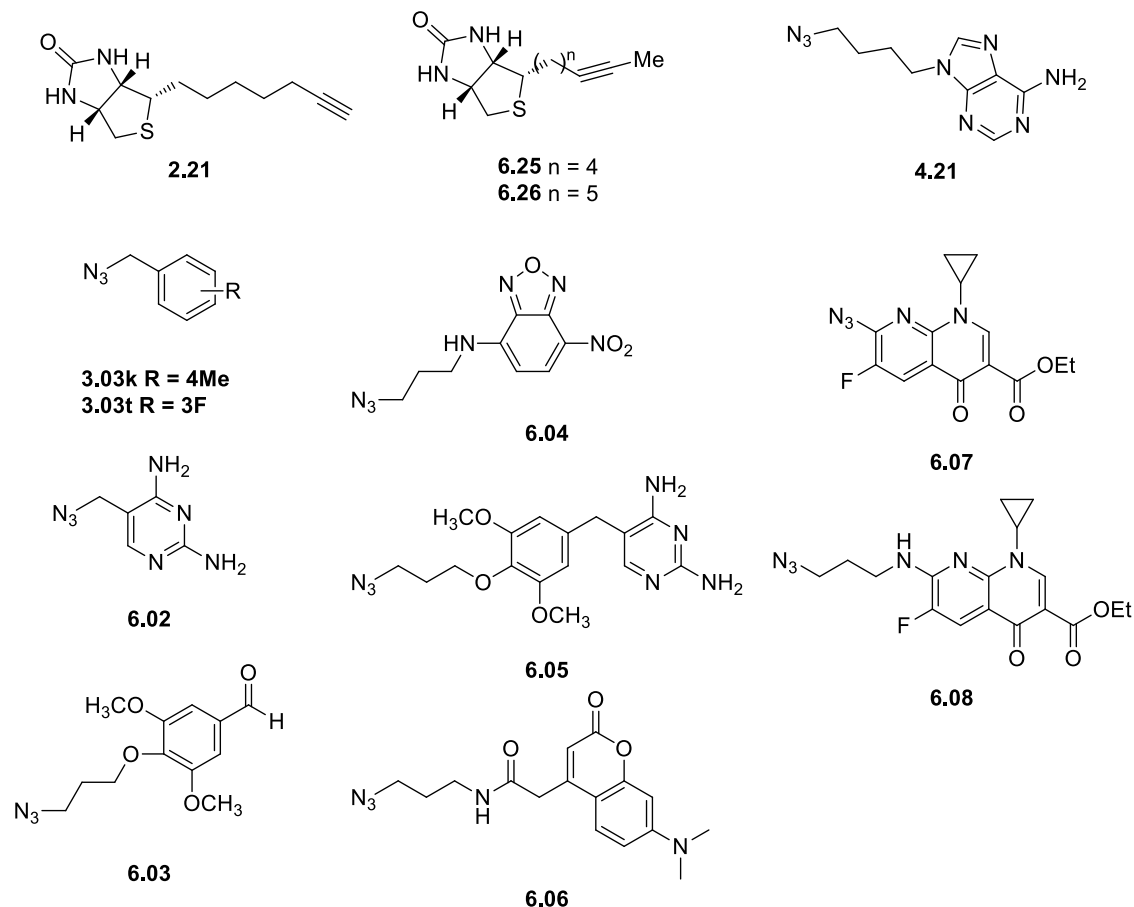
Figure 1: An overview of building blocks used in the *in situ* click reactions described in this section.

In situ click experiment 1

The stock solutions of biotin acetylene **2.21** and azide **4.21** were separately prepared by dissolving each in a mixture of 10 % DMSO in Milli-Q water to give a concentration of 25mM. The *in situ* click reaction mixture was then prepared by adding both solutions to PBS buffer* to give final concentration of 500 µM for each component (final DMSO concentration 4% (v/v)). *Sa*BPL was then added to the mixture to give a final concentration of 2 µM. Control samples were prepared in parallel using: 1) PBS only, 2) bovine serum albumin (BSA) with final concentration of 2 µM in place of *Sa*BPL. All 3 reaction mixtures were incubated at 37°C for 48 h and then analyzed by LC/MS according to general procedure **I** with selective ion monitoring of the target triazole **1.22** (M+H⁺ = 471.2398 Da) as depicted in Figure 2. The regioselectivity of cycloaddition products was identified by comparison of

_____

retention times with the authentic samples of 1,4-triazole **1.22** and 1,5-triazole **6.01**, which were prepared as described in section 7.8.3 through CuAAC and RuAAC respectively. To quantitate the yield of triazole formed, the area under the peak on the LC/MS trace was calculated and compared against a standard curve established using known amounts of the synthesized triazole product as depicted in Figure 4 (see section 7.8.2).

*PBS buffer use throughout contains 137 mM NaCl, 2.7 mM KCl, 8 mM Na_2HPO_4, 1.46 mM KH_2PO_4, pH 7.4

In situ click experiment 2

In situ click reactions were performed using biotin acetylene **2.21** and azide **4.21** as described above in experiment 1 except using either *Mtb*BPL, *Kp*BPL, *Ac*BPL, or *Ca*BPL in place of *Sa*BPL. Control samples were also prepared in parallel using: PBS only, BSA (final concentration 2 µM), in place of BPL enzymes and all 6 sample mixtures were incubated at 37°C for 48 h. Each reaction was analyzed by LC/MS according to general procedure **I** with selective ion monitoring of the target triazole **1.13** ($M+H^+$ = 471.2398 Da) as depicted in Figure 3. The regioselectivity of cycloaddition products was identified as before. The yield of *in situ* generated triazole was calculated according to the standard curve (Figure 4) was described before.

In situ click experiment 3

The *in situ* click library screening was performed using biotin acetylene **2.21** and two classes of azides (**3.03k**, **3.03t**) and (**6.02-6.08**). Each binary reaction mixture was prepared as described in experiment 1 by mixing acetylene **2.21** (final concentration 500 µM) and one of the azides **3.03k**, **3.03t**or **6.02-6.08** (Final concentration 500 µM each). Samples of each individual reaction mixture was then treated in parallel with 1) *Sa*BPL, 2) *Mtb*BPL, 3) *Kp*BPL, 4) *Ac*BPL, 5) *Ca*BPL, 6) BSA, or 7) no enzyme to give total 49 samples. All 49 reactions were incubated at 37°C for 48 h and then analyzed by LC/MS according to general procedure **I**. The cycloaddition product (1,4-triazole **6.11**) from reaction of biotin acetylene **2.21** and azide **6.04** was identified (see Figure 5) by comparison of retention times with the authentic samples of 1,4-triazole **6.11** which was prepared as described in section 7.8.3 through CuAAC. To calculate the yield of triazole product **6.11**, the area under the peak on the LC/MS trace was calculated and compared against a standard curve established using known amounts of the synthesized **6.11** as depicted in Figure 6 (see section 7.8.2).

In situ click experiment 4

Reactions were performed between the 1-methyl acetylenes (**6.25** or **6.26)** and azide **4.21**. The binary reaction mixture was prepared as described in experiment 1 by combining each acetylene (**6.25** or **6.26)** and azide **4.21** to give two reaction mixtures (**6.25/4.21** and **6.26/4.21**). Each mixture was then treated with *Sa*BPL or *Sa*BPL-R122G (final concentration 2 µM). Three controls were also prepared for each mixture using BSA (final concentration 2 µM), water, or Cu_2SO_4 (5 µM). All ten reaction mixtures were incubated at 37°C for 48 h and then analyzed by LC/MS according to general procedure **I** with selective ion monitoring of the target triazoles **6.27** (M+H$^+$ = 471.2398 Da) and **6.28** (M+H$^+$ = 485.2560 Da). The cycloaddition product of triazole **6.27** from biotin acetylene **2.21** and azide **6.25** was identified (see Figure 7) by comparison of the found molecular mass (M+Na$^+$ = 493.2217 Da) and predicted mass (M+Na$^+$ = 493.2222 Da).

Calibration curve for 1.22
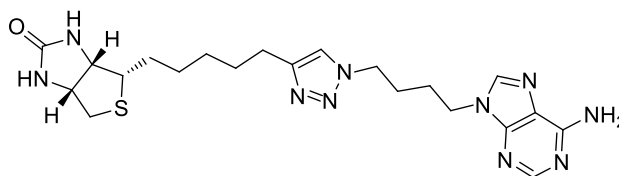
A stock solution of authentic triazole **1.22** was prepared by dissolving it in a mixture of 10% DMSO in Milli-Q water to give a concentration of 25mM. From this stock solution. A series of dilutions was then prepared by treating the stock solution with PBS buffer to give concentrations of 0.00, 0.08, 0.15, 0.30, 0.60, 1.25, 2.50, 5.00, 10.00, 20.00 µM. Each concentration was directly analyzed using LC/MS according to general procedure **I** with selective ion monitoring of the target triazole **1.22** (M+H$^+$ = 471.2398 Da). The presence of triazole was identified by the retention time (6.66 ± 0.18 min) and molecular weights (Δ <5 ppm). The area under the peak on the LC/MS trace was measured and listed in Table 1. The calibration curve was generated by plotting the area under the peak against the corresponding concentration using Graphpad 6.0 as shown in Figure 4.

_____

Calibration curve for 6.11
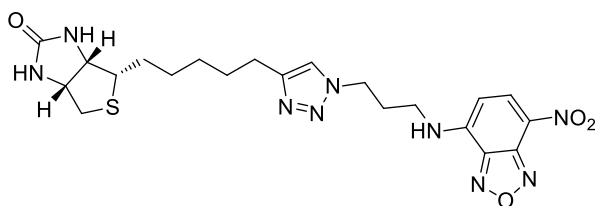
A stock solution of authentic triazole **6.11** was prepared as above and a series of dilutions was then prepared by treating the stock solution with PBS buffer to give concentrations of 0.00, 0.08, 0.15, 0.30, 0.60, 1.25, 2.50, 5.00, 10.00, 20.00 µM . Each concentration was directly analyzed using LC/MS according to general procedure **I** with selective ion monitoring of the target triazole **6.11** (M+H$^+$ = 501.1979 Da). The presence of triazole was identified by the retention time (6.66 ± 0.18 min) and molecular weights (Δ <5 ppm). The area under the peak on the LC/MS trace was measured and listed in Table 2. The calibration curve was generated by plotting the area under the peak against the corresponding concentration using Graphpad 6.0 as shown in Figure 6.

7.8.2 Results

Figure 2: *In situ* click reaction of biotin acetylene **2.21** and azide **4.21** to give triazole **1.22**, as determined by LCMS analysis with detection at 471.2398 mass units.

(A) Authentic sample of 1,4-triazole **1.22**, synthesized by CuAAC of biotin acetylene **2.21** and azide **4.21**, showing a retention time of 7.23 mins. (B) Authentic sample of 1,5-triazole **6.01**, synthesized by Ru catalysed reaction of alkyne **2.21** and azide **4.21**, showing a retention time of 8.19 mins. (C) *In situ* reaction in the presence of wild type SaBPL indicated the formation of **1.22** with a (M + H$^+$) of 471.2396 Da at 7.19 mins (area: 1626726); (D) *In situ* reaction in the absence of enzyme; (E) *In situ* reaction in the presence of BSA in place of BPL; (F) Mass spectra of 1,4-triazole **1.22**.
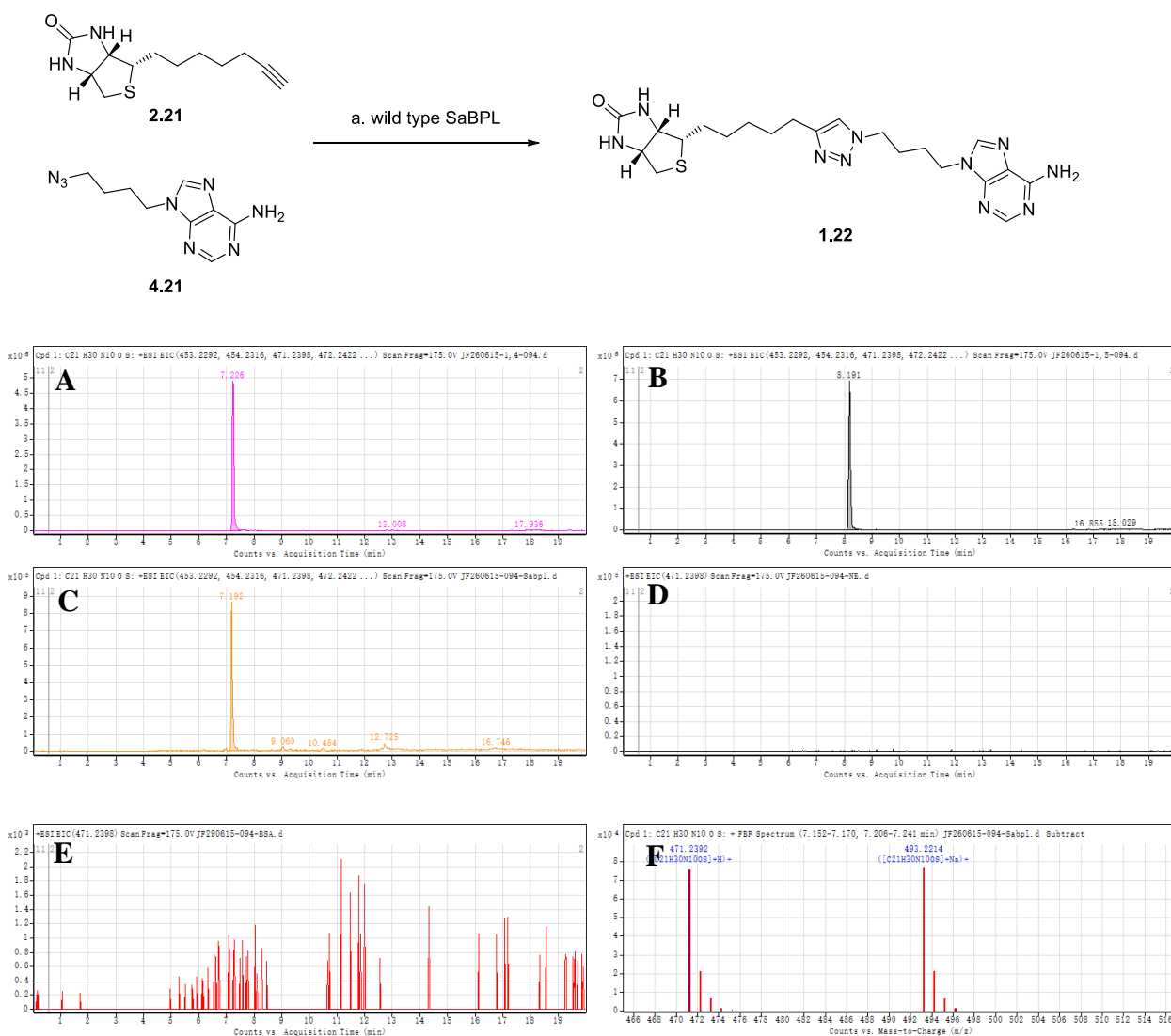
Figure 3: *In situ* click reaction of biotin acetylene **2.21** and azide **4.21** to give triazole **1.22**, as determined by LC/MS analysis with detection at 471.2398 mass units.

(A) Authentic sample of 1,4-triazole **1.22**, synthesized by CuAAC of biotin acetylene **2.21** and azide **4.21**, showing a retention time of 7.23 mins. (B) *In situ* reaction in the presence of *Mtb*BPL showing triazole product formation at 7.21 mins (area: 755753); (C) *In situ* reaction in the presence of *Kp*BPL showing triazole product formation at 7.17 mins (area: 299917); (D) *In situ* reaction in the presence of AcBPL showing no desired triazole product formation; (E) *In situ* reaction in the presence of CaBPL showing no desired triazole product formation; (F) Mass spectra of enzyme generated 1,4-triazole **1.22**.
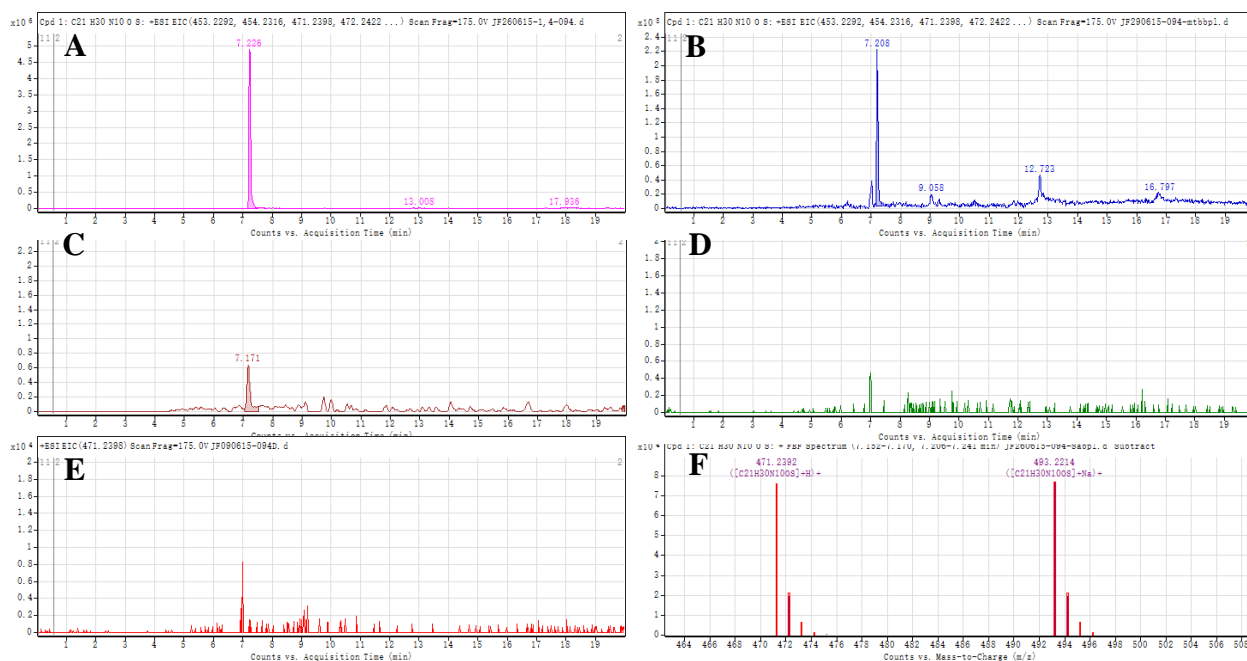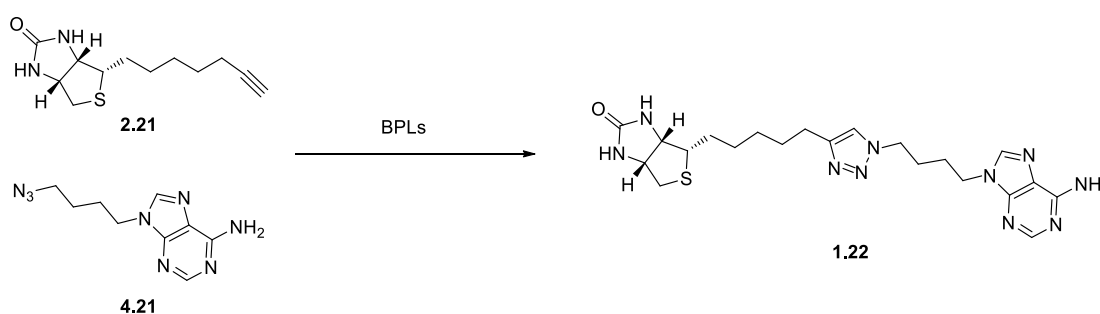
Figure 4: A calibration curve with the best-fit line generated between concentrations of **1.22** and area curve the peak identified by LC/MS, giving $Y = 4.28*10^6 X - 1.05*10^6$ with $R^2 = 0.99$ (Y = area under the curve, X = concentrations of **1.22**).
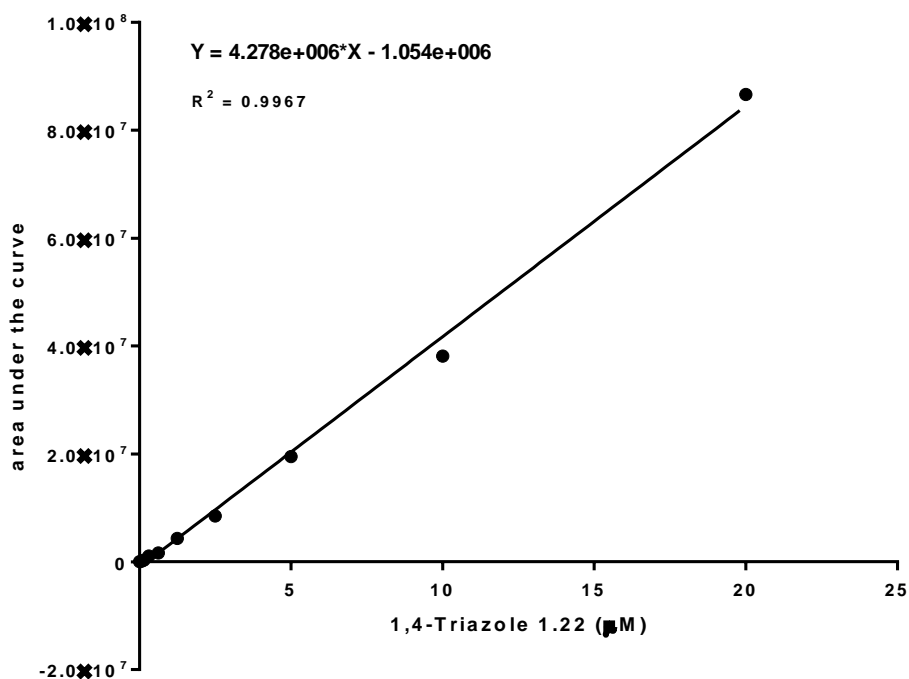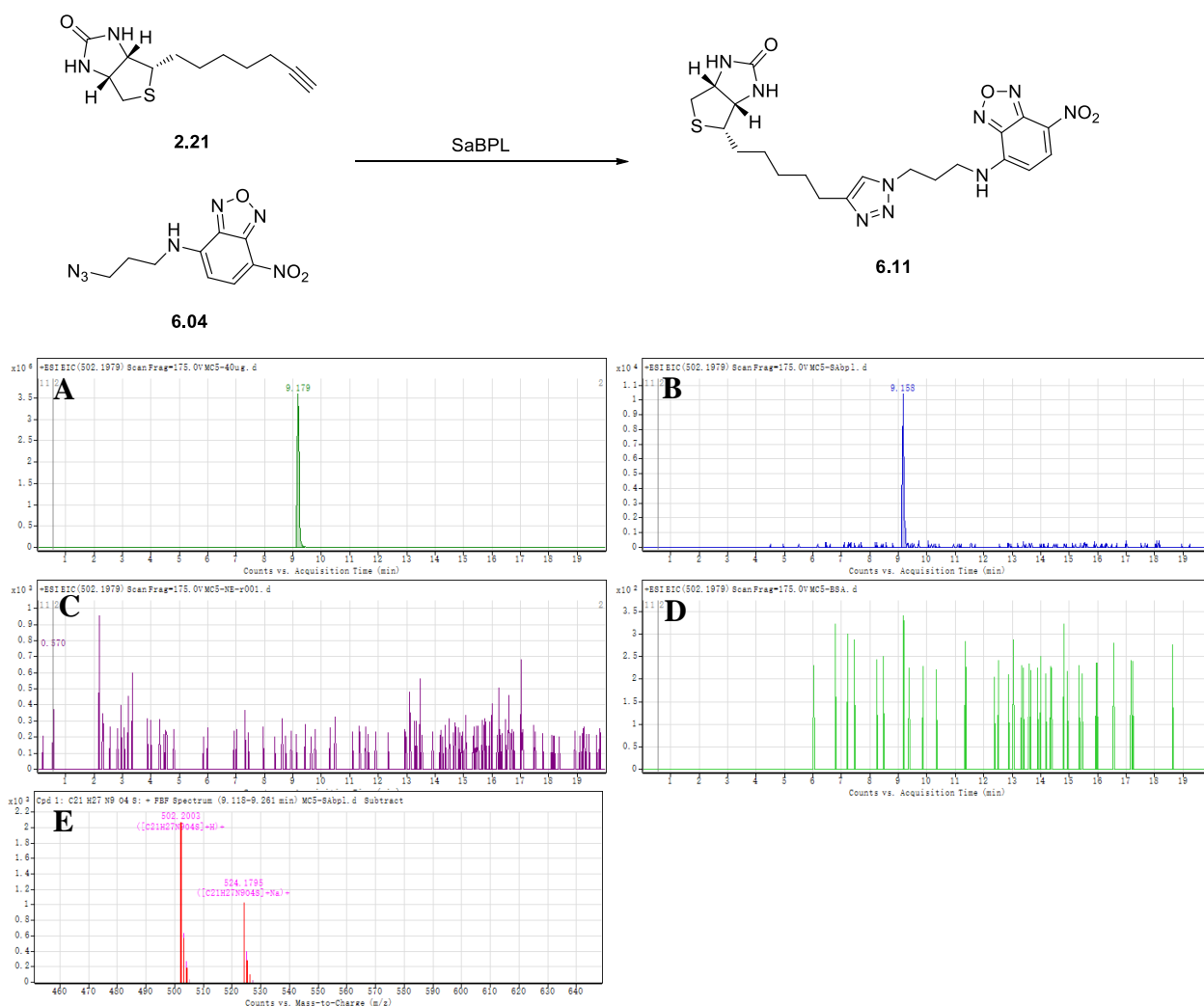

Table 1: Concentrations of **1.22** with the corresponding area under the curve determined by LR/HRMS
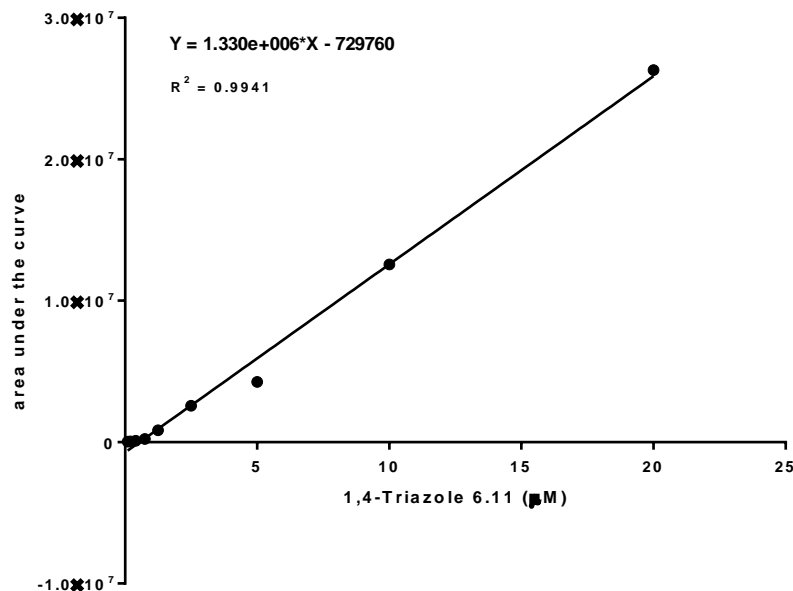
Experiments	1.22 (μM)	area under the curve
1	20.0000	8.664816e+007
2	10.0000	3.811177e+007
3	5.0000	1.950502e+007
4	2.5000	8467936.00
5	1.2500	4338513.00
6	0.6250	1633396.00
7	0.3125	1082988.00
8	0.1500	311904.00
9	0.0750	114180.10
*Sa*BPL	0.6	1626726
*Mtb*BPL	0.4	755753
*Kp*BPL	0.3	299917

Figure 5: *In situ* click reaction of biotin acetylene **2.21** and azide **6.04** to give triazole **6.11**, as determined by LC/MS analysis with detection at 502.1979 mass units.

(A) Authentic sample of 1,4-triazole **6.11** synthesized by CuAAC of acetylene **2.21** and azide **6.04**, showing a retention time of 9.18 mins. (B) *In situ* reaction in the presence of *Sa*BPL showing triazole product formation at 9.16 mins (area: 89706); (C) *In situ* reaction in the absence of enzyme; (D) *In situ* reaction in the presence of BSA instead of BPL; (E) Mass spectra of *Sa*BPL generated triazole **6.11**.

_____

Figure 6: A calibration curve with the best-fit line generated between concentrations of **6.11** and area under the peak identified by LC/MS, giving $Y = 1.33*10^6X - 0.73*10^6$ with $R^2 =$ 0.99 (Y = area under the curve, X = concentrations of **6.11**).


Table 2: Concentrations of **6.11** with the corresponding area under the curve determined by LR/HRMS

| Experiments	6.11 (μM)	area under the curve
1	20.0000	2.629851e+007
2	10.0000	1.255675e+007
3	5.0000	4252110.00
4	2.5000	2568965.00
5	1.2500	834867.00
6	0.7500	223564.00
7	0.4000	96354.00
8	0.2000	52135.00
9	0.1000	26345.00
*Sa***BPL**	0.6	89706

Figure 7: *In situ* click reaction of biotin acetylene **6.25** and azide **4.21** to give triazole **6.27**, as determined by LC/MS analysis with detection at 471.2398 mass units.

(A) *In situ* reaction in the presence of *Sa*BPL showing triazole product formation at 8.86 mins; (B) *In situ* reaction in the presence of *Sa*BPL-R122G showing triazole product formation at 8.85 mins; (C) *In situ* reaction in the absence of enzyme; (D) *In situ* reaction in the presence of Cu$_2$SO$_4$; (E) *In situ* reaction in the presence of BSA instead of BPL; (F) Mass spectra of SaBPL generated triazole **6.27**.
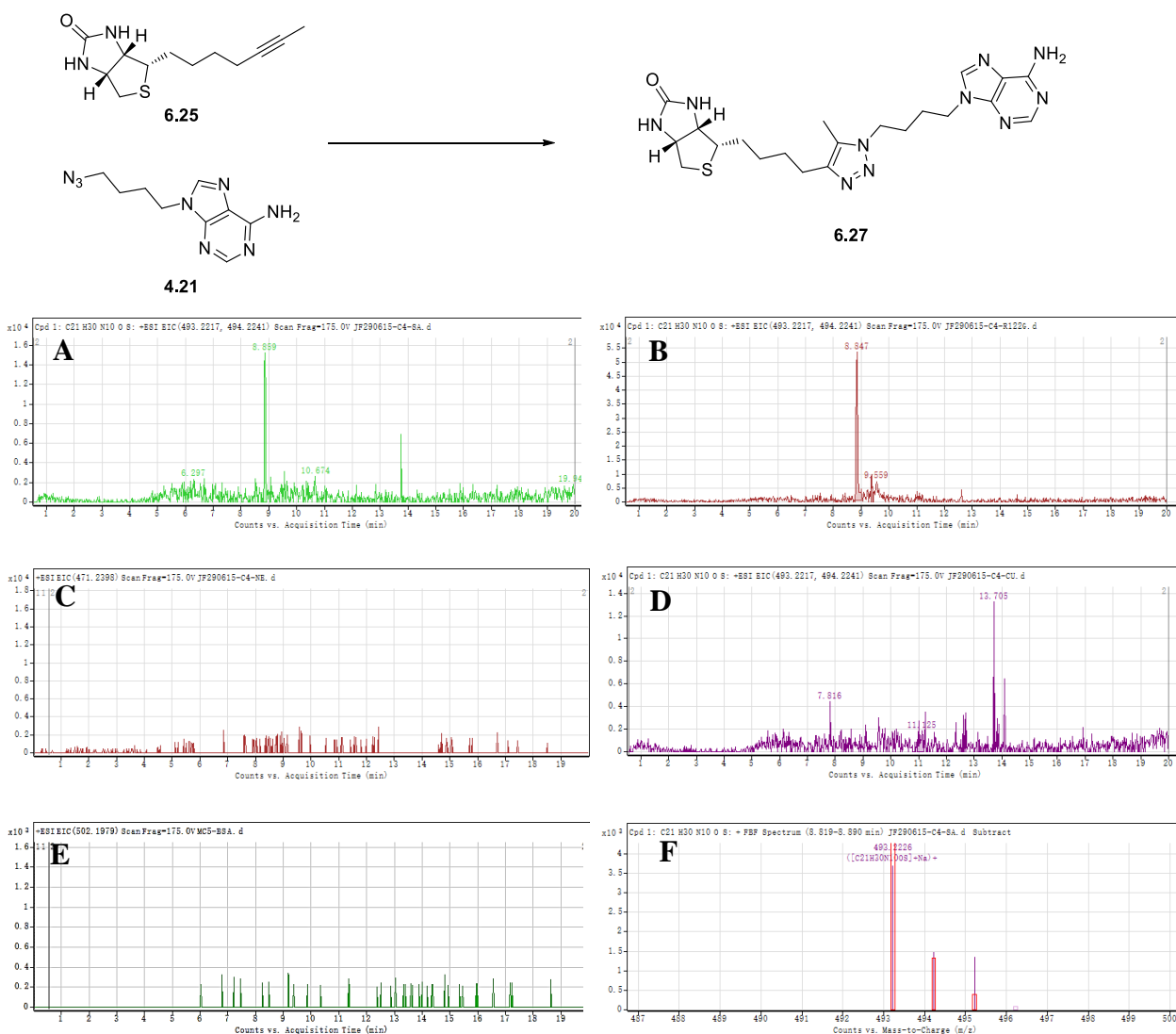
Figure 8: *In situ* click reaction of biotin acetylene **6.26** and azide **4.21** to give triazole **6.28**, as determined by LC/MS analysis with detection at 485.2554 mass units.

(A) *In situ* reaction in the presence of wide type of *Sa*BPL; (B) *In situ* reaction in the presence of *Sa*BPL-R122G; (C) *In situ* reaction in the presence of Cu$_2$SO$_4$; (D) *In situ* reaction in the presence of BSA instead of BPL; (E) *In situ* reaction in the absence of enzyme;
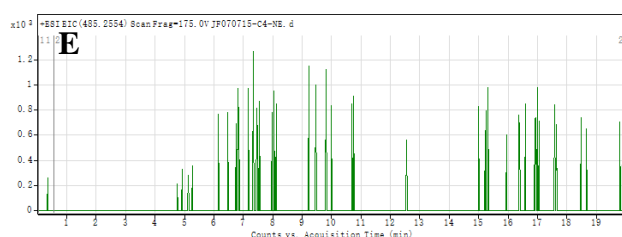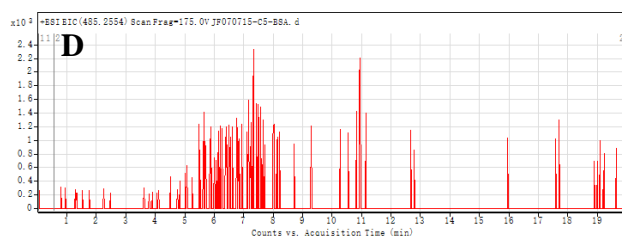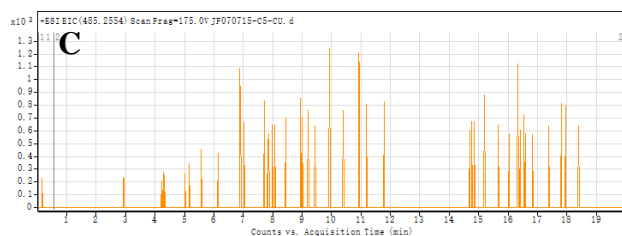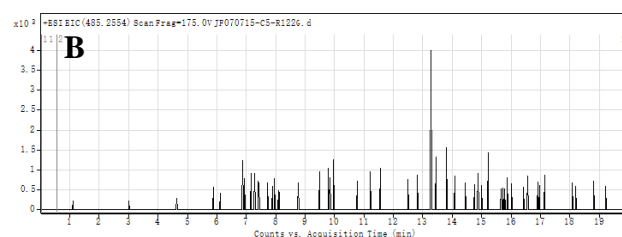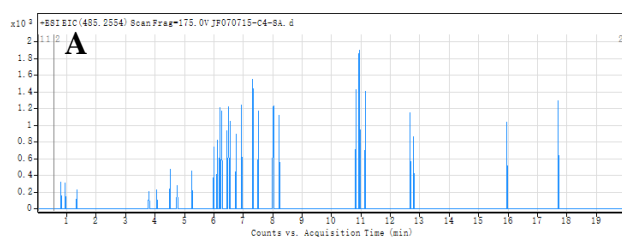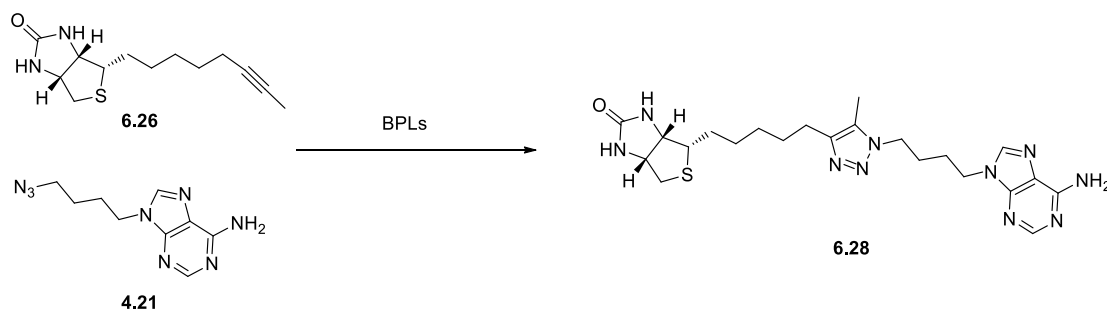
7.8.3 Synthetic chemistry methods

(3a*S*,6a*R*)-4-[5-[1-[4-(6-aminopurin-9-yl)butyl]triazol-4-yl]pentyl]-1,3,3a,4,6,6a-hexahydrothieno[3,4-*d*]imidazol-2-one 1.22
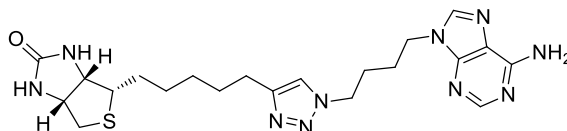
Biotin acetylene **221** (31 mg, 0.13 mmol) was reacted with alkyl adenine **4.21** (36 mg, 0.14 mmol) and Cu nanopowder (2 mg, 0.026 mmol) using General Procedure **A1**. The crude material was purified by flash chromatography on silica eluting with 8% MeOH in DCM to give a crystalline white solid (46 mg, 73%). ^{1}H NMR was consistent with literature.[8]

^{1}H NMR (600 MHz; DMSO-*d6*): δ 8.12 (1H, s, Ar**H**), 8.11 (1H, s, Ar**H**), 7.86 (1H, s, Ar^{tri}**H**), 7.20 (2H, bs, Ar**NH₂**), 6.52 (1H, bs, C(O)N**H**), 6.40 (1H, bs, C(O)N**H**), 4.34-4.38 (3H, m, ArN^{tri}**CH₂**, NH**CH**), 4.34-4.38 (3H, m, Ar^{ad}**CH₂**, NH**CH**), 3.12-3.16 (m, 1H, S**CH**), 3.12-3.16 (1H, dd, *J* = 4.8, 12 Hz, S**CH$_a$**), 2.59-2.64 (3H, m, S**CH$_b$**, ArC^{tri}**CH₂**), 1.76-1.80 (4H, m, 2 x **CH₂**), 1.28-1.67 (8H, m, 4 x **CH₂**);

^{13}C NMR (150 MHz; DMSO-*d6*): 162.8, 156.0, 152.4, 149.5, 146.8, 140.8, 121.8, 118.7, 61.2, 59.2, 55.6, 48.5, 42.2, 40.0, 28.8, 28.6, 28.5, 28.3, 27.0, 26.7, 25.1;

LC/MS calcd. for (M + H$^+$) $C_{21}H_{31}N_{10}OS$: requires 471.2398, found 471.2392;

HPLC R$_t$ = 7.17 min.

Preparation of (3a*S*,4*S*,6a*R*)-4-[5-[1-[4-(6-aminopurin-9-yl)butyl]triazol-4-yl]pentyl]-1,3,3a,4,6,6a-hexahydrothieno[3,4-d]imidazol-2-one 6.01
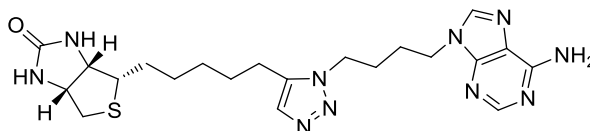

To solution of the biotin acetylene **2.21** (41 mg, 0.17 mmol) and adenine azide **4.21** (47 mg, 0.19 mmol) in 1:1 dry THF/DMF (1 mL) was added Cp*Ru(PPh₃)₂Cl (27 mg, 0.034 mmol) and stirred at 80 ºC under nitrogen atmosphere for 4 h. The reaction mixture was concentrated *in vacuo* and purified by flash chromatography on silica eluting with 7% MeOH in DCM to give a white solid (46 mg, 55%). ^{1}H NMR was consistent with literature.[8]

^{1}H NMR (600 MHz; 1% CD$_3$OD, CDCl$_3$): δ 8.20 (1H, s, Ar**H**), 7.76 (1H, s, Ar**H**), 7.37 (1H, s, Ar^{tri}**H**), 6.14 (1H, bs, C(O)N**H**), 5.58 (1H, bs, C(O)N**H**), 4.47 (1H, dd, *J* = 4.8, 7.8 Hz, NHC**H**), 4.13-4.29 (5H, m, ArC**H$_2$**, ArN^{tri}C**H$_2$**, NHC**H**), 3.08-3.12 (1H, m, SC**H**), 2.88 (1H, dd, *J* = 5.4, 12.9 Hz, SC**H$_b$**), 2.69 (1H, d, *J* = 12.9 Hz, SC**H$_a$**), 1.81-1.89 (2H, m, ArC^{tri}C**H$_2$**), 1.26-1.68 (10H, m, 5 x C**H$_2$**);

^{13}C NMR (150 MHz; DMSO-d^6): 163.9, 155.6, 152.6, 149.4, 140.1, 137.1, 131.7, 118.8, 72.2, 62.0, 59.9, 46.7, 43.0, 40.3, 29.0, 28.7, 28.5, 27.8, 27.0, 26.7, 22.8;

LC/MS calcd. for (M + H) C$_{21}$H$_{31}$N$_{10}$OS: requires 471.2398, found 471.2395;   R$_t$ = 8.19 min.

(3a*S*,4*S*,6a*R*)-4-(5-(1-(3-((7-nitrobenzo[c][1,2,5]oxadiazol-4-yl)amino)propyl)-1*H*-1,2,3-triazol-4-yl)pentyl)tetrahydro-1H-thieno[3,4-*d*]imidazol-2(3*H*)-one 6.11
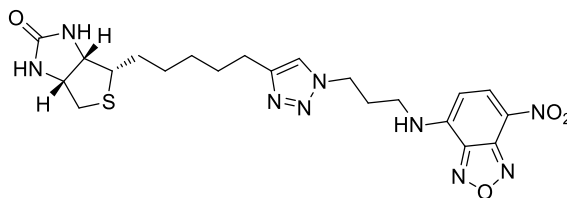

Biotin acetylene **2.21** (50 mg, 0.21 mmol) was reacted with azide **6.04** (62 mg, 0.19 mmol) and Cu nanopowder (2 mg, 0.026 mmol) using General Procedure **A1**. The crude material was purified by flash chromatography on silica gel eluting with 3% MeOH in DCM to give a crystalline white solid (40 mg, 38%).

^{1}H NMR: (500 MHz, DMSO-*d6*) δ 9.49 (1H, s, N**H**), 8.49 (1H, d, *J* = 7.5 Hz, Ar**H**), 7.86 (1H, s, Ar^{tri}**H**)), 6.42 (1H, bs, N**H**), 6.36 (1H, bs, N**H**), 6.35 (1H, d, *J* = 7.5 Hz, Ar**H**), 4.44 (2H, t, *J* = 6.9 Hz, ArN^{tri}C**H$_2$**), 4.35-4.27 (1H, m, NHC**H**), 4.19-4.09 (1H, m, NHC**H**), 3.56-3.43 (2H, m, C**H$_2$**), 3.08 (1H, m, SC**H**), 2.81 (1H, dd, *J* = 12.4, 5.1 Hz, SC**H$_a$**), 2.57 (1H, d, *J* = 12.4 Hz, SC**H$_b$**), 2.57 (2H, m, ArC^{tri}C**H$_2$**), 2.24 (2H, m, C**H$_2$**), 1.65-1.51 (3H, m, C**H$_2$**+CH**H**), 1.49-1.41 (1H, m, C**H**H), 1.35 (4H, m, 2xC**H$_2$**).

^{13}C NMR: (125 MHz, DMSO-*d6*) δ 162.9, 147.1, 125.1, 144.5, 144.2, 137.9, 122.0, 121.0, 99.3, 79.2, 61.2, 59.3, 55.6, 47.0, 28.9, 28.7, 28.5, 28.3, 25.0.

HRMS: calcd for C$_{21}$H$_{28}$N$_9$O$_4$S (M+H$^+$): 502.1985, found 502.1979;

HPLC: R$_t$ = 14.98 min.

_____

N-(3-azidopropyl)-7-nitrobenzo[*c*][1,2,5]oxadiazol-4-amine 6.04
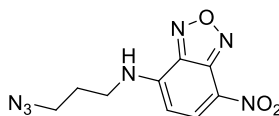
Bromide **6.17** (96 mg, 0.32 mmol) was reacted with sodium azide (24 mg, 0.37 mmol) according to general procedure **B2** and purified by flash chromatography on silica eluting with 30% EtOAc in hexane to yield a yellowish oil (62 mg, 76%).

¹H NMR (500 MHz, CDCl3) δ 8.43 (1H, d, *J* = 8.7 Hz, Ar**H**), 6.93 (1H, br s, N**H**), 6.22 (1H, d, *J* = 8.7 Hz, Ar**H**), 3.67 (2H, dd, *J* = 12.2, 6.0 Hz, C**H₂**), 3.57 (2H, t, J = 6.2 Hz, C**H₂**) and 2.12-2.04 (2H, m, C**H₂**).

¹³C NMR (125 MHz, CDCl3) δ 144.3, 144.2, 143.9, 136.8, 123.6, 98.9, 49.1, 41.7, 27.7.

HRMS calcd. for (M + H⁺) C₉H₉BrN₄NaO₃: 322.9756, found 322.9748

N-(3-bromopropyl)-7-nitrobenzo[*c*][1,2,5]oxadiazol-4-amine 6.17
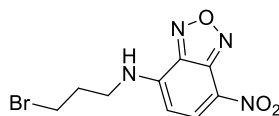
To a stirring solution of 3-bromopropylamine hydrobromide **6.16** (175 mg, 1.00 mmol) in ice-cold MeOH (2 mL) was added NBD-Cl (200 mg, 1.00 mmol) in MeOH (8 mL) dropwise over 1 h. The reaction was gradually allowed to warm to room temperature and stir at that temperature overnight. The mixture was partitioned between water and DCM. The organic phase was separated and the aqueous phase was extracted with DCM (x3). The organics were combined, dried over magnesium sulfate, filtrated and concentrated under reduced pressure. The crude material was purified by flash chromatography on silica eluting with 5% MeOH in DCM to give **6.17** as yellow solid (96 mg, 32%).

¹H NMR (500 MHz, CDCl₃) δ 8.47 (1H, d, *J* = 8.7 Hz, Ar**H**), 6.78 (1H, s, N**H**), 6.30 (1H, d, *J* = 8.7 Hz, Ar**H**), 3.79 (2H, dd, *J* = 13.0, 6.5 Hz, C**H₂**), 3.59 (2H, t, *J* = 6.1 Hz, C**H₂**) and 2.54-2.29 (2H, m, C**H₂**) ppm

¹³C NMR (125 MHz, CDCl3) δ 144.3, 144.1, 143.9, 136.8, 123.8, 99.1, 42.4, 31.0 and 30.2.

HRMS calcd. for (M + Na⁺) C₉H₉BrN₄NaO₃: 322.9756, found 322.9748

HPLC R*t* = 18.11 min.

7.9 References for Chapter 7

(1)   Hartmuth C. Kolb; Michael S. VanNieuwenhze; Sharpless, K. B. *American Chemical Society* **1994**, *94*, 2483-2547.

(2)   Junttila, M. H.; Hormi, O. E. *The Journal of Organic Chemistry* **2004**, *69*, 4816-4820.

(3)   Molander, G. A.; Figueroa, R. *Organic Letters* **2006**, *8*, 75-78.

(4)   Soares da Costa, T. P.; Tieu, W.; Yap, M. Y.; Zvarec, O.; Bell, J. M.; Turnidge, J. D.; Wallace, J. C.; Booker, G. W.; Wilce, M. C.; Abell, A. D. *ACS Medicinal Chemistry Letters* **2012**, *3*, 509-514.

(5)   Hein, J. E.; Tripp, J. C.; Krasnova, L. B.; Sharpless, K. B.; Fokin, V. V. *Angew Chem Int Ed Engl* **2009**, *48*, 8018-21.

(6)   Soares da Costa, T. P.; Tieu, W.; Yap, M. Y.; Pendini, N. R.; Polyak, S. W.; Sejer Pedersen, D.; Morona, R.; Turnidge, J. D.; Wallace, J. C.; Wilce, M. C.; Booker, G. W.; Abell, A. D. *J Biol Chem* **2012**, *287*, 17823-32.

(7)   Worrell, B. T.; Ellery, S. P.; Fokin, V. V. *Angewandte Chemie International Edition in English* **2013**, *52*, 13037-41.

(8)   Tieu, W.; da Costa, T. P. S.; Yap, M. Y.; Keeling, K. L.; Wilce, M. C.; Wallace, J. C.; Booker, G. W.; Polyak, S. W.; Abell, A. D. *Chemical Science* **2013**, *4*, 3533-3537.

(9)   Haddenham, D.; Pasumansky, L.; DeSoto, J.; Eagon, S.; Singaram, B. *The Journal of Organic Chemistry* **2009**, *74*, 1964-1970.

(10)   Winum, J.-Y.; Toupet, L.; Barragan, V.; Dewynter, G.; Montero, J.-L. *Organic Letters* **2001**, *3*, 2241-2243.